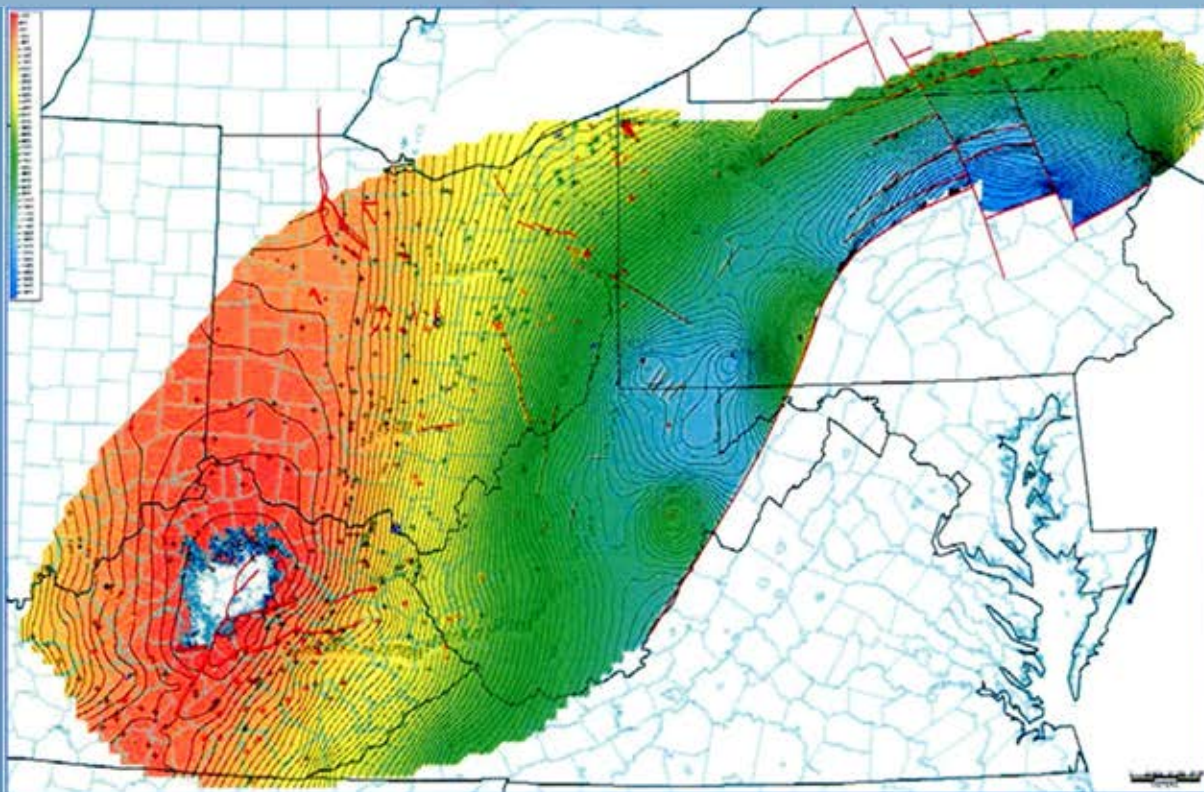# A Geologic Play Book for Utica Shale Appalachian Basin Exploration

FINAL REPORT
April 1, 2012
July 1, 2015

Utica Shale Appalachian Basin Exploration Consortium

A GEOLOGIC PLAY BOOK FOR UTICA SHALE APPALACHIAN BASIN EXPLORATION

FINAL REPORT

Project Start Date: April 1, 2012
Project End Date: March 30, 2014

UTICA SHALE APPALACHIAN BASIN EXPLORATION CONSORTIUM

Editors
Douglas G. Patchen[1] and Kristin M. Carter[2]

Authors
John Hickman[3], Cortland Eble[3], Ronald A. Riley[4], Matthew Erenpreiss[4], Kristin M. Carter[2], John A. Harper[2], Brian Dunst[2], Langhorne "Taury" Smith[5], Michele L. Cooney[5], Daniel Soeder[6], Garrecht Metzger[7], Jessica Moore[8], Michael E. Hohn[8], Susan Pool[8], John Saucer[8], Douglas G. Patchen[1]

With Contributions From
John Barnes[2], Mohammad D. Fakhari[4], David Fike[7], James Leone[9], Thomas Mroz[6], John Repetski[10], Juergen Schieber[11]

[1] West Virginia University Research Corporation
[2] Pennsylvania Geological Survey
[3] Kentucky Geological Survey
[4] Ohio Division of Geological Survey
[5] Smith Stratigraphic LLC
[6] U.S. Department of Energy National Energy Technology Laboratory
[7] Washington University in St. Louis
[8] West Virginia Geological and Economic Survey
[9] New York State Museum
[10] United States Geological Survey
[11] Indiana University

July 1, 2015

CONTENTS

ii

FIGURES

TABLES

LIST OF APPENDICES

EXECUTIVE SUMMARY

This "Geologic Play Book for Utica Shale Appalachian Basin Exploration" (hereafter referred to as the "Utica Shale Play Book Study" or simply "Study") represents the results of a two-year research effort by workers in five different states with the financial support of fifteen oil and gas industry partners. The Study was made possible through a coordinated effort between the Appalachian Basin Oil & Natural Gas Research Consortium (AONGRC) and the West Virginia University Shale Research, Education, Policy and Economic Development Center.

The Study was funded by industry members of the Utica Shale Appalachian Basin Exploration Consortium (the Consortium). The 15 industry members of the Consortium were joined by individuals from four state geological surveys, two universities, one consulting company, the U.S. Geological Survey (USGS) and the Department of Energy's (DOE) National Energy Technology Laboratory (NETL), who collectively comprised the Research Team members of the Consortium.

This play book incorporates and integrates results of research conducted at various granularities, ranging from basin-scale stratigraphy and architecture to the creation of nano-porosity as gas was generated from organic matter in the reservoir. Between these two end members, the research team has mapped the thickness and distribution of the Utica and Point Pleasant formations using well logs; determined favorable reservoir facies through an examination of outcrops, cores and samples at the macroscopic and microscopic scales; identified the source of the total organic carbon (TOC) component in the shales and estimated the maturation level of the TOC; and searched for reservoir porosity utilizing scanning electron microscopy (SEM) technology.

This Study builds on and continues what was learned when AONGRC compiled the Trenton-Black River Play Book. That study examined the stratigraphic interval from the base of the Black River up through the Trenton Limestone and the stratigraphically-equivalent Lexington Limestone. However, it also included an examination of the upper Trenton time-equivalent Point Pleasant Formation that was deposited in a shallow depocenter located between the Trenton Platform to the north, extending from what is now Indiana to New York, and the Lexington Platform to the south, in what is now Kentucky, southwestern West Virginia and western Virginia. Near the end of Trenton time, while relatively clean carbonates were being deposited on the platforms, a mixture of clastic muds and carbonates was being deposited in the intra-platform basin, creating the Logana Shale Member of the Lexington/Trenton Formation, and the younger Point Pleasant Formation above the Lexington/Trenton, which was succeeded by deposition of the darker, but not necessarily more organic-rich Utica Shale.

The Utica Shale Play Book Study had three main objectives: (1) characterize and assess the lithology, source rock geochemistry, stratigraphy, depositional environment(s) and reservoir characteristics of Utica and equivalent rocks in the northern Appalachian basin; (2) define Utica oil and gas fairways by integrating regional mapping work with drilling activity and production tracking efforts; and (3) provide production-based and volumetric Utica resource assessments informed by geologic and geochemical data collected during the course of this Study.

The goals of the Study were accomplished through development of a multi-disciplinary research plan with nine separate tasks, each of which was assigned a team lead in order to streamline project management efforts. To the extent possible, sampling, data collection and related efforts for each task were conducted by the researchers in each state, and then shared with the team leads for compilation and further interpretation. In those instances where a task was particularly broad and/or data intensive, the team lead received support from one or more additional research team members.

Although this play is referred to as the Utica Shale Play, the play is neither "Utica" nor "shale." Drilling tracking activities, bulk mineralogy and carbonate analyses, TOC data, thermal maturity evaluations and stratigraphic correlations all point to an interbedded limestone and organic-rich shale interval in the underlying Point Pleasant Formation as the preferred drilling target. Currently, drilling activity to the Point Pleasant is concentrated in roughly a north-south trend in eastern Ohio, although recent drilling in the north has shifted toward the northeast and eventually nearly west-east in northern Pennsylvania. This pattern of drilling approximates the subsurface strike of the formations while maintaining a fairly consistent depth of drilling – and maturation – pattern. Changes in maturation level as these formations become deeper to the east have resulted in roughly parallel trends of oil, wet gas and dry gas production.

The combination of a relatively shallow reservoir and the potential for liquids production has made this an attractive play. The optimum conditions for liquids production appear to be a combination of depth, reservoir pressure and gas-to-oil ratio that is high enough to drive oil to the wellbore. As operators move eastward in Ohio (or in the current drilling trend in Pennsylvania) into areas of deeper drilling and higher maturation, dry gas is encountered.

Core studies of Ohio samples have determined that the organic-rich Utica Shale has TOC up to 3.5% and an average carbonate content of 25%. This means the clay content is probably in the 70% range, which is very high (perhaps too high for the rock to be hydraulically fractured effectively). The Point Pleasant has TOC up to 4 or 5% and an average carbonate content of approximately 50% within the organic-rich facies and an even higher percentage in the limestone beds. The upper Lexington/Trenton and Logana members have carbonate content values that approximately 70% in their organic-rich facies, with TOC as high as 4 or 5%.

The abundance of fossils present in these rocks indicates an environment that was well oxygenated much of the time. There are delicate trilobites and articulated ostracods that could not have been transported any significant distance. There also are beds composed almost entirely of strophomenid brachiopods, and this sort of monospecific accumulations of fossils is not likely to have been redistributed from some distant area. If they were transported from a different environment they would be more mixed with other fossils. Thus, these fossils likely lived and died in these locations. The silt-sized skeletal debris probably has been reworked; it is of an unknown origin.

The depositional environment of the Point Pleasant Formation, upper Lexington/Trenton Formation and Logana Member is a relatively shallow, probably <100 ft (<30 m) deep, storm-dominated, carbonate shelf that experienced frequent algal blooms. Cross-sections show that there was not much difference in water depth between the organic-rich and organic-poor areas of deposition. The fossils present in the limestone suggest water that was at times shallow, exposed

to sunlight and well oxygenated. The storm-bedding throughout suggests something well above storm wave base. The environment may have been subject to seasonal anoxia due to the frequent algal blooms. A similar depositional model may be invoked for rocks deposited in New York and Pennsylvania, although these were not studied in the same detail.

Petrographic and SEM analyses performed on Utica/Point Pleasant rocks in Ohio, New York and Pennsylvania indicate the existence of little to no matrix porosity. Porosity, where it does exist, is found in the organic matter of these reservoir rocks. If this holds true in the current producing area, the only pores that are likely to be contributing much to hydrocarbon flow are the organic pores that formed during maturation. This makes the Utica very different from other liquids-producing plays, such as the Eagle Ford and the Bakken, which have significant matrix porosity components.

The resource assessment task for this Study was divided into two portions: a probabilistic (USGS-style) assessment to determine technically recoverable unconventional resources, and a volumetric approach to provide a preliminary determination of original in-place hydrocarbon resources for the Utica Shale, Point Pleasant Formation, and Logana Member of the Trenton Limestone. Both approaches evaluate roughly the same play area, which was divided into oil and gas assessment units based on a combination of geological factors and the geographic pattern of predominately oil-producing wells and gas-producing wells in southeastern Ohio, where the greatest concentration of exploration and development has taken place to date.

The probabilistic (USGS-style) resource assessment produced the following results. Please note the study's largest source of production data was the public database from the state of Ohio. In Ohio's way of recordkeeping, production data report NGLs and gas as a single number. Therefore, calculation of gas resource in the oil and the wet gas assessment units includes a significant percentage of natural gas liquids. For this reason, we did not include NGLs in the liquids-to-gas ratio for the gas assessment unit or a NGLs-to-gas ratio for the oil assessment unit. The oil assessment unit was determined to contain technically recoverable volumes of 791 (5%) to 3788 (95%) million barrels of oil (MMbo), with a mean of 1960 MMbo, and 2370 to 17.960 trillion cubic feet (Tcf) gas, with a mean of 8.165 Tcf. The corresponding volumes for the wet gas assessment unit ranged from 24.484 to 106.852 Tcf (mean of 56.427 Tcf). The gas assessment unit contains 228.478 to 1549.586 Tcf gas with projected mean of 717.579 Tcf gas. Together, the entire Utica Shale play contains mean, technically recoverable resources of 1960 MMbo and 782.2 Tcf gas.

Original in-place resources were determined using a volumetric approach. In-place oil and gas resources were determined separately for the Utica Shale, Point Pleasant Formation, and Logana Member of the Trenton Limestone. Original oil-in-place was found to range from 6345 MMbo for the Logana Member to 43,508 MMbo for the Utica Shale with an overall total of 82,903 MMbo for the three units that were evaluated. Original gas-in-place was found to range from 348.5 Tcf for the Logana Member to 1745.8 Tcf for the Point Pleasant Formation with an overall total of 3192.4 Tcf for the three units.

A GEOLOGIC PLAY BOOK FOR UTICA SHALE APPALACHIAN BASIN EXPLORATION

1.0   INTRODUCTION AND PURPOSE

This "Geologic Play Book for Utica Shale Appalachian Basin Exploration" (hereafter referred to as the "Utica Shale Play Book Study" or simply "Study") represents the results of a two-year research effort by workers in five different states with the financial support of fifteen oil and gas industry partners. The Study was made possible through a coordinated effort between the Appalachian Basin Oil & Natural Gas Research Consortium (AONGRC) and the West Virginia University Shale Research, Education, Policy and Economic Development Center.

The Utica Shale Play Book Study was designed to: (1) characterize and assess the lithology, source rock geochemistry, stratigraphy, depositional environment(s) and reservoir characteristics of Utica and equivalent rocks in the northern Appalachian basin; (2) define Utica oil and gas fairways by integrating regional mapping work with drilling activity and production tracking efforts; and (3) provide probabilistic and volumetric Utica resource assessments informed by geologic and geochemical data collected during the course of this Study.

1.1   Research Team

The Utica Shale Play Book Study research team included AONGRC personnel from the Kentucky Geological Survey (KGS; John Hickman and Cortland Eble); the Ohio Division of Geological Survey (ODGS; Ronald Riley, Matthew Erenpreiss and Mohammad Fakhari); the Pennsylvania Geological Survey (PAGS; Kristin Carter, John Harper and Brian Dunst); the West Virginia Geological and Economic Survey (WVGES; Jessica Moore, Michael Hohn, Susan Pool and John Saucer); Smith Stratigraphic LLC (Langhorne "Taury" Smith and Michele Cooney); Washington University in St. Louis (Garrecht Metzger and David Fike); and the U.S. Department of Energy (DOE) National Energy Technology Laboratory (NETL) (Daniel Soeder and Thomas Mroz). John Barnes of PAGS analyzed hundreds of bulk mineralogy samples for the Study, and James Leone of the New York State Museum (NYSM) performed hundreds of Total Organic Carbon analyses (in collaboration with Smith Stratigraphic LLC). John Repetski of the U.S Geological Survey (USGS) contributed important analyses regarding thermal maturity trends in Upper Ordovician rocks based on conodont alteration indices, and Juergen Schieber of Indiana University performed scanning electron microscopy imaging for selected samples (in collaboration with Smith Stratigraphic LLC). Project management was provided by Douglas Patchen of AONGRC.

1.2   Scope of Work

The scope of work for the Utica Shale Play Book Study was divided into nine separate tasks, each of which was assigned a team lead in order to streamline project management efforts. To the extent possible, sampling, data collection and related efforts for each task were conducted by the researchers in each state, and then shared with the team leads for compilation and further

interpretation. In those instances where a task was particularly broad and/or data-intensive, the team lead received support from one or more additional research team members. These nine tasks are shown in Table 1-1.

Table 1-1. Research efforts by task.

Task	Team Lead	Supporting Team Members
1.0 Organization of Existing Data	West Virginia Geological and Economic Survey (WVGES)	---
2.0 Core and Outcrop Descriptions, Petrography, Spectral Gamma-Ray Logging	Ohio Division of Geological Survey (ODGS)	Smith Stratigraphic LLC
3.0 Reservoir Characterization	Pennsylvania Geological Survey (PAGS)	Smith Stratigraphic LLC, U.S. DOE NETL
4.0 Inorganic Geochemistry	Smith Stratigraphic LLC	PAGS, Washington University in St. Louis
5.0 Organic Geochemistry and Petrology	Kentucky Geological Survey (KGS)	USGS, Smith Stratigraphic LLC
6.0 Log Analysis, Stratigraphic Correlation, and Fairway Mapping	KGS	---
7.0 Resource Assessment	WVGES	KGS
8.0 Data, GIS, and Website Management	WVGES	---
9.0 Play Book Compilation and Project Management	Douglas Patchen (AONGRC)	---

While previous Study progress reports were organized relative to these task headings, this final report has been structured differently to provide for more logical development of our research findings. Specifically, the remainder of this introductory chapter provides the details regarding access, organization and management of all data deliverables for the Utica Shale Play Book Study. Chapter 2 provides the results of Utica drilling activity and production tracking efforts. Chapter 3 describes the lithostratigraphy for Utica and equivalent rocks throughout the Study area. Chapter 4 presents the research team's log analysis, correlation and mapping results. Chapter 5 presents the results of the research team's core studies, including interpretations of depositional environments. Chapter 6 includes the results of the team's inorganic geochemistry research efforts, and Chapter 7 presents Utica source rock geochemistry findings and interpretations. Reservoir pore imaging and porosity/permeability data are provided in Chapter 8. Chapter 9 provides the research team's resource assessment results, and Chapter 10 offers the research team's overarching conclusions and implications for development of the Utica play in the northern Appalachian basin, based on data derived from this Study. A comprehensive list of references is included in Chapter 11, and the report appendices are included at the very end of this document.

1.3 Data Deliverables Access, Organization and Management

Data deliverables for the Utica Shale Play Book Study include not only the text, tables, figures and appendices of this final report but also the raw datasets, analyses, and results utilized by the Research Team members. All study-specific data, whether compiled from legacy sources or derived specifically for this work, have been organized and assimilated into a Geographic Information System (GIS) database and interactive mapping application, as well as a searchable Oracle database that is available via the project website. These data may be accessed using the following links/web addresses:

Project Website and Interactive Map:
http://www.wvgs.wvnet.edu/Utica

Appalachian Oil and Natural Gas Research Consortium Website (links to Utica site):
http://aongrc.nrcce.wvu.edu

1.3.1 Interactive Map Application

The Utica Shale Play Book Study's interactive map application utilizes ESRI ArcGIS Server technology and is designed to allow users to visualize geologic data in spatial context (Figure 1-1). Data include the following:

- Wells
  - With Supplemental Data[1]:
    - Digitized Well Logs
    - Scanned Well Logs
    - Source Rock Analyses
    - Total Organic Carbon (TOC) Data
    - Core Photographs
    - Scanning Electron Microscopy (SEM) Images-Data
    - Thin Section Images
    - Thin Section Descriptions
    - All Wells with Data (i.e. a file on the FTP server)
  - With Formation Tops[2]:
    - Upper Ordovician
    - Kope
    - Utica
    - Point Pleasant
    - Lexington/Trenton (includes Logana and Curdsville members)
    - Black River
- Cross-Sections[3]
  - Lines
  - Wells
- Maps[1]
  - Faults

3

- o Kope
- o Utica
- o Point Pleasant
- o Lexington/Trenton (includes Logana and Curdsville members)
- o Black River
- Play Areas
  - o Utica
  - o Ordovician Outcrops

[1] *Data obtained from Utica Shale Project FTP server.*
[2] *Data obtained from Utica Shale Project Petra® file.*
[3]*Data obtained from Trenton-Black River Project.*
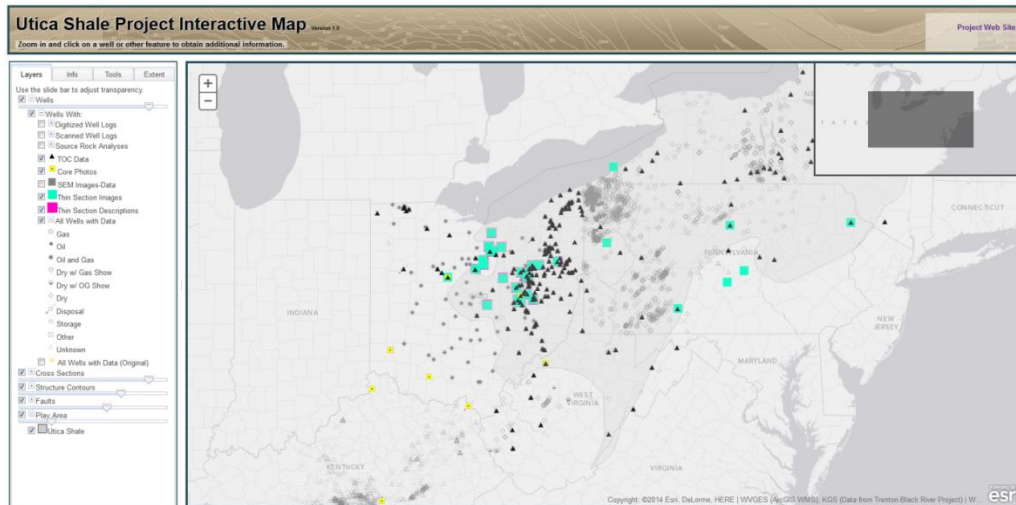
Figure 1-1. Screen-shot display of the Study's secure interactive map application, which was developed using ArcGIS Server. All wells with files or documents are shown along with wells having TOC data, core photos and thin section data.

Selecting a well or area on the map will result in a "Layer Info" window that allows users to see the different data types available for the selection (Figure 1-2). Each data type contains a secure link or links to the project database where the data may be retrieved. Links to the well file document search system and any relevant files or documents are available for "Wells With Supplemental Data" layers (Figure 1-2). Also, links to cross-section images are available for "Cross-Section Line" layers. The application provides the ability to switch base maps as well as basic navigation and print tools.
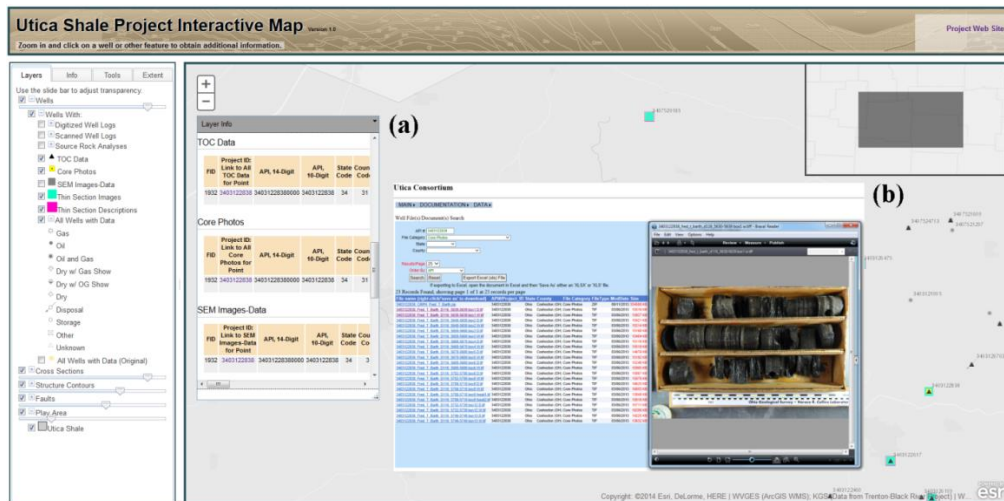
Figure 1-2. Screen-shot display showing the Study's interactive map application. (a) Popup window with additional information, which is accessed by clicking on a well or other feature in the interactive map. (b)) Well file document search system window and a core photo. Search system and files or documents (e.g., core photos) are accessed from the map application using links in the popup window.

1.3.2 Play Book Study Website

The Utica Shale Play Book Study website is the main source of data collected and generated for the project. This website runs on a Microsoft Windows server using IIS 7.0 and SSL encryption.
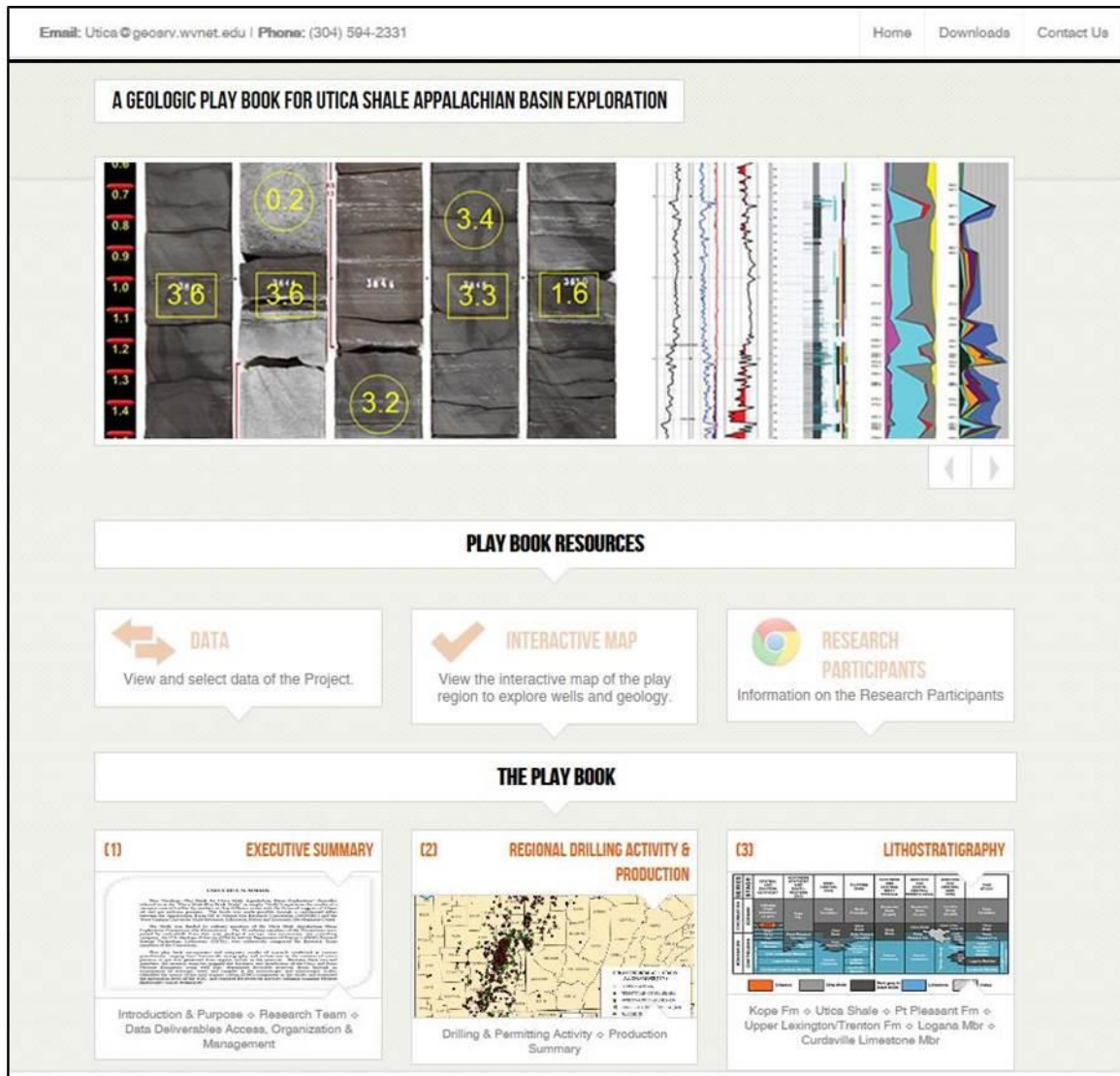
Figure 1-3. Utica project website homepage.

The website contains project information and data under three main categories: "Data", "Interactive Map" (See section 1.3.1 for details) and "The Play Book" (Figure 1-3). Each chapter of the final project report is accessed via its own section of "The Play Book". Links to the corresponding appendices are embedded within the text, enabling users to access related data as they read through the body of the chapter.

Figure 8-3 includes selected photomicrographs for each of the samples listed in Table 8-1, and Appendix 8-A 📕 (PDF, 3.61 MB) includes the entire suite of photomicrographs for samples analyzed for this work. The scale of these images is on the order of tens of μm, and they illustrate the tight nature of the shale matrix in these samples. At this scale, mineral grains are clearly visible, but true pore space (whether phyllosilicate framework, dissolution or organic matter pores) cannot be resolved. In the case of the Utica outcrop samples (Figure 8-3), pyrite grains plucked from some samples (due to either handling during sample collection or weathering at the outcrop) have left polygonal-shaped voids (pop-out holes).

Figure 8-3. Photomicrographs of selected specimens analyzed by PAGS using standard SEM techniques. A - S12-061-003, Utica Shale outcrop, Reedsville exit ramp, Mifflin County, Pennsylvania; B - S13-013-001, top Utica Shale (8504-8513 ft), Hockenberry No. 1 (API#3701990063), Butler County, Pennsylvania; C - S13-014-003, Point Pleasant Formation (3750-3760 ft), Shade Mt. No. 1 (API#3706720001), Juniata County, Pennsylvania; D - S13-015-001, Point Pleasant Formation (13,440-13,450 ft), PA Tr. 163 No. C-1 (API#3710320003), Pike County, Pennsylvania.

API No.	County	Location/Well Name	Sample Depths (ft)	Formation/ Member	Figure No.
3700920034	Bedford/PA	Schellsburg Unit No. 1	7,690	Lexington/Trenton	8-4A
3703520276	Clinton/PA	Commonwealth of PA Tr. 285 No. 1	14,480	Lexington/Trenton	8-4B
3704920049	Erie/PA	PA Dept. of Forests & Waters Block 2 No. 1	4,096	Lexington/Trenton	8-4C
3706720001	Juniata/PA	Shade Mt. No. 1	3,750	Point Pleasant	8-4D
3708720002	Mifflin/PA	Commonwealth of PA Tr. 377 No. 1	5,230	Lexington/Trenton	8-4E
3710320003	Pike/PA	Commonwealth of PA Tr. 163 No. C-1	13,580	Lexington/Trenton	8-4F
3712522278	Washington/PA	Starvaggi No. 1	10,040	Kope	8-4G
NA	Herkimer/NY	74NY5 Mineral Core	170 - 730	Point Pleasant Logana	8-5

NA – not applicable

Table 8-2. Samples analyzed using ion milling and SEM techniques.

Figure 1-4. Within each chapter of the Utica Play Book, links to corresponding appendices are embedded within the text, allowing users to access the referenced data as they read through the chapter.
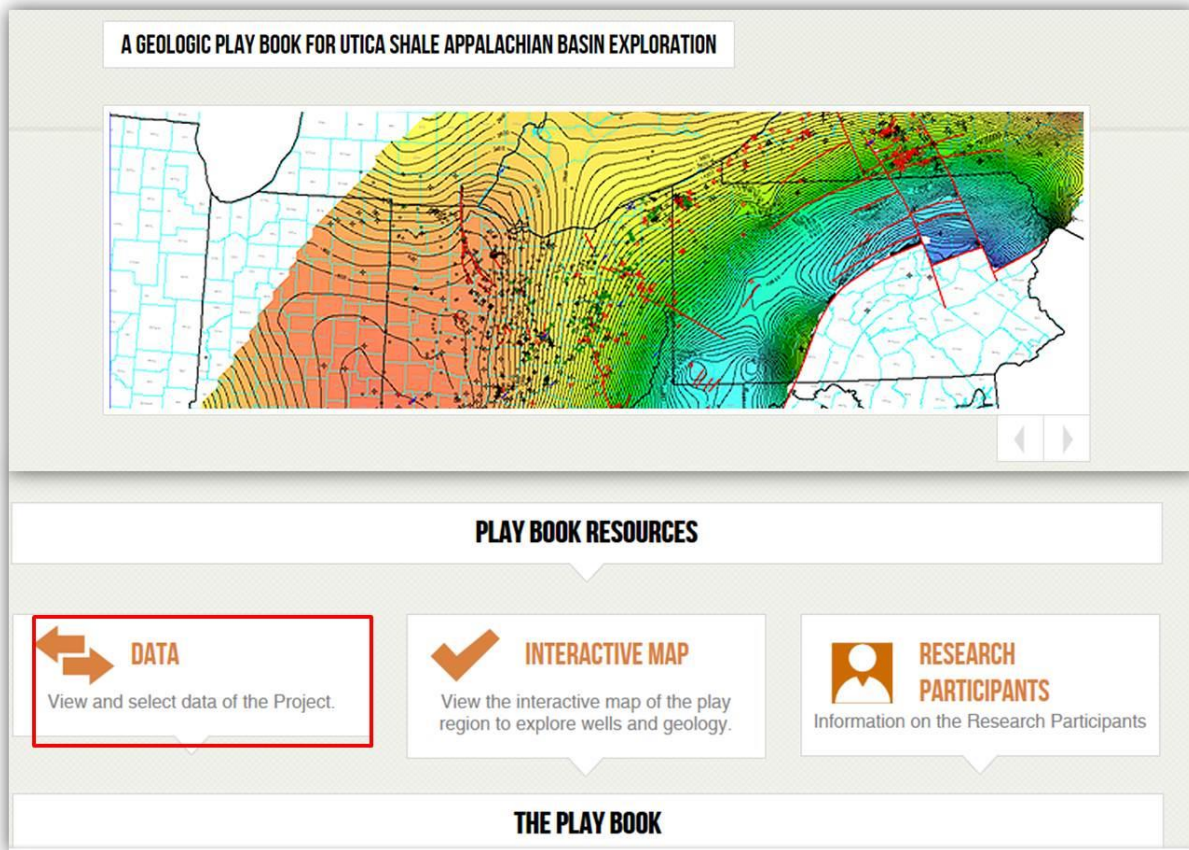
Figure 1-5. Screen-shot display of the Utica project home page with "Data" tab highlighted (http://www.wvgs.wvnet.edu/Utica).

The "Data" section of the website contains all data collected, processed and analyzed during the course of the project's research. Website users may access these data via a well document file search, which links to the project database (Figure 1-5). This document search allows users to create a custom search of the project database. A search may utilize one or more of the following criteria:

- API number
- File category (see Table 1-2 for file category types)
- State
- County

Results of the data search may also be exported to Excel, where the data are able to be further sorted (Figure 1-6). Hyperlinks to the individual files are embedded in the Excel file, which allows users to link back to the project webpage to retrieve the data without performing a duplicate search.

Figure 1-6. Example of a customized Utica database search (Microscopic Organic Analysis, Ohio) with results. The results may also be exported to an Excel file, which allows further sorting of the data. The Excel file also contains links back to each file, which eliminates the need for duplicate searches across multiple work sessions.

1.3.3 Data Management
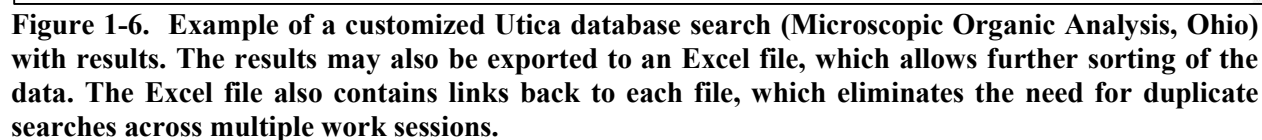
The Consortium database utilizes Oracle 11g technology. The database was initially populated with metadata of the documents uploaded by research team members in fulfillment of the requirements of Task 1 (Organization of Existing Data) and has been periodically updated as new data have become available. This searchable database is now available via the project website (http://www.wvgs.wvnet.edu/utica). All data are organized by API number, as available. If an API number was not available, a Project ID was generated for the well or document.

The folder structure within the Consortium database was initially organized so that each well document file would be classified within a single file category (e.g., Digital Logs, Sample Descriptions, etc.). This file category would serve as the root of the directory folder, with subfolders for each state within the root category. As organization of the data progressed, it became apparent that a given document may contain several data types and would need to be cross-listed within the database. Table 1-2 lists the file categories, abbreviations, and document counts for the database (current as of July 9, 2014).

9

Table 1-2. Consortium file categories, abbreviations and number of files per state. Data categories and counts are current as of July 9, 2014.

FILECATEGORYCODE	FILECATEGORYLONG	KY	NY	OH	PA	WV	TOTAL
BIOSTRAT	Biostratigraphy			12			12
CRPH	Core Photos	146		1046		62	1254
CRPHZ	Core Photos Zipped			5			5
CSP	Crushed Stone Properties (CSP)			1			1
CTDAT	CT Scan Data			11			11
CTIMG	CT Image			220			220
CTIMGZ	CT Zipped Images(CTIMGZ)			9			9
DLOG	Digitized Logs	2	501	170	112	29	814
ELOG	Scanned Logs		1007	31	164	120	1322
FIR	Fluid Inclusion Report			1			1
GEOCHEM	Geo Chem			2			2
ISO	Isotopes	2		10			12
LOGT	Log Tops				2		2
MICP	High Pressure Mercury Injection Porosity (MICP)			12			12
MNRLGY	General Mineralogy (MNRLGY)			8			8
MOA	Microscopic Organic Analysis (MOA)			19			19
OTHR	Other Well Documents		104	27	22		153
RCA	Routine Core Analysis (grain size) (RCA)			8			8
RKMECH	Rock Mechanics			9			9
ROHIST	Ro Histograms			10			10
SEM	Scanning Electron Microscope (SEM)		144	348	444		936
SEMZ	SEM Zipped Images (SEMZ)			5	14		19
SMDS	Sample Descriptions		72	19	1		92
SRA	Source Rock Analyses (SRA)		53	263	12	15	343
TOC	Total Organic Carbon (TOC)		53	260	12	15	340
TRA	Tight Rock Analysis (TRA)			23			23
TSDESC	Thin Section Description			29			29
TSIMG	Thin Section Image			878	53		931
TSIMGZ	Thin Section Zipped Images			7			7
VRR	Vitrinite Reflectance Report			59	17		76
XRD	X-Ray Defraction (XRD)		10	138	68	13	229
XRF	X-Ray Fluorescence (XRF)			6			6

Due to the necessity of cross-listing a single document file under several categories, a naming convention was devised that would support multiple classifications. Each well or document file is first named according to API number (10- or 14-digit). If an API number is unavailable (e.g., outcrop sections, water wells, etc.), the file is given an internal Project ID by the following convention:

Naming Convention: 2-digit state code/3-digit county code/5-character identifier

Example: 37027_OC12 (Pennsylvania, Butler County, Outcrop Sample 12)

For all other wells, the file naming convention leads with the API number. The leading API number/Project ID is then followed by the code for the file category or categories under which the data are classified. For a standard file containing information on a single well or sample, the following naming convention is used:

Naming Convention: API number or Project ID_File Type Code(s)_Optional Description

Example: 34003636910000_SRA_TOC_BP_Chemical_Plant_Well_4.xls

As of July 9, 2014, there were 5696 files organized under this naming convention. In addition to these files, there were an additional 35 files that contain data for multiple wells. These files, which are often final results of data analyzed by service companies or consultants, can contain results for many different wells or samples. For these document types, the following naming convention is used:

Naming Convention: 2-digit state code/000/MLTPL_File Type Codes_Optional Description

Example: 34000MLTPL_SRA_TOC_XRD_OvertonEnergy.pdf

Individual wells contained in the file are stored in a second table, which is linked by the file name, allowing the user to search by any of the individual API numbers/Project IDs contained within the multiple well file.

As the data collected, generated, and interpreted by the research team became finalized, new file categories were created and populated with project results. In addition, a general file with all header data was created, allowing users to import project wells into various subsurface mapping programs. For convenience when downloading multiple image files (e.g., thin-section images, core photographs or SEM images), additional zipped folders that contain all the images have been created. The resultant files are very large, but allow users to retrieve all images without having to download large numbers of individual image files.

2.0   REGIONAL DRILLING ACTIVITY AND PRODUCTION

The application of horizontal drilling combined with multi-staged hydraulic fracturing has resulted in a drilling boom for unconventional gas and oil across the United States. This technology has stimulated drilling activity and production in the Appalachian basin for Devonian shales (most notably the Marcellus, but also the Geneseo/Burket and Rhinestreet shales), as well as the Upper Ordovician black shale interval, which includes the Utica Shale, Point Pleasant Formation, undifferentiated Lexington Limestone (=upper Trenton Formation), and Logana Member (Figure

2-1). Preliminary production data and resource assessments of the Upper Ordovician black shale interval in the region has generated much optimism and drilling activity for this rapidly growing unconventional oil and gas play. Initial daily production rates and Estimated Ultimate Recoveries (EURs) in this report were obtained from company presentations. Sources of permitting and drilling activity included PAGS, WVGES and the Ohio Division of Oil and Gas Resources Management (DOGRM). Production data for Ohio also were obtained from DOGRM (Appendix 2-A). All numbers in the following sections related to well activity and production are current as of May 1, 2014.
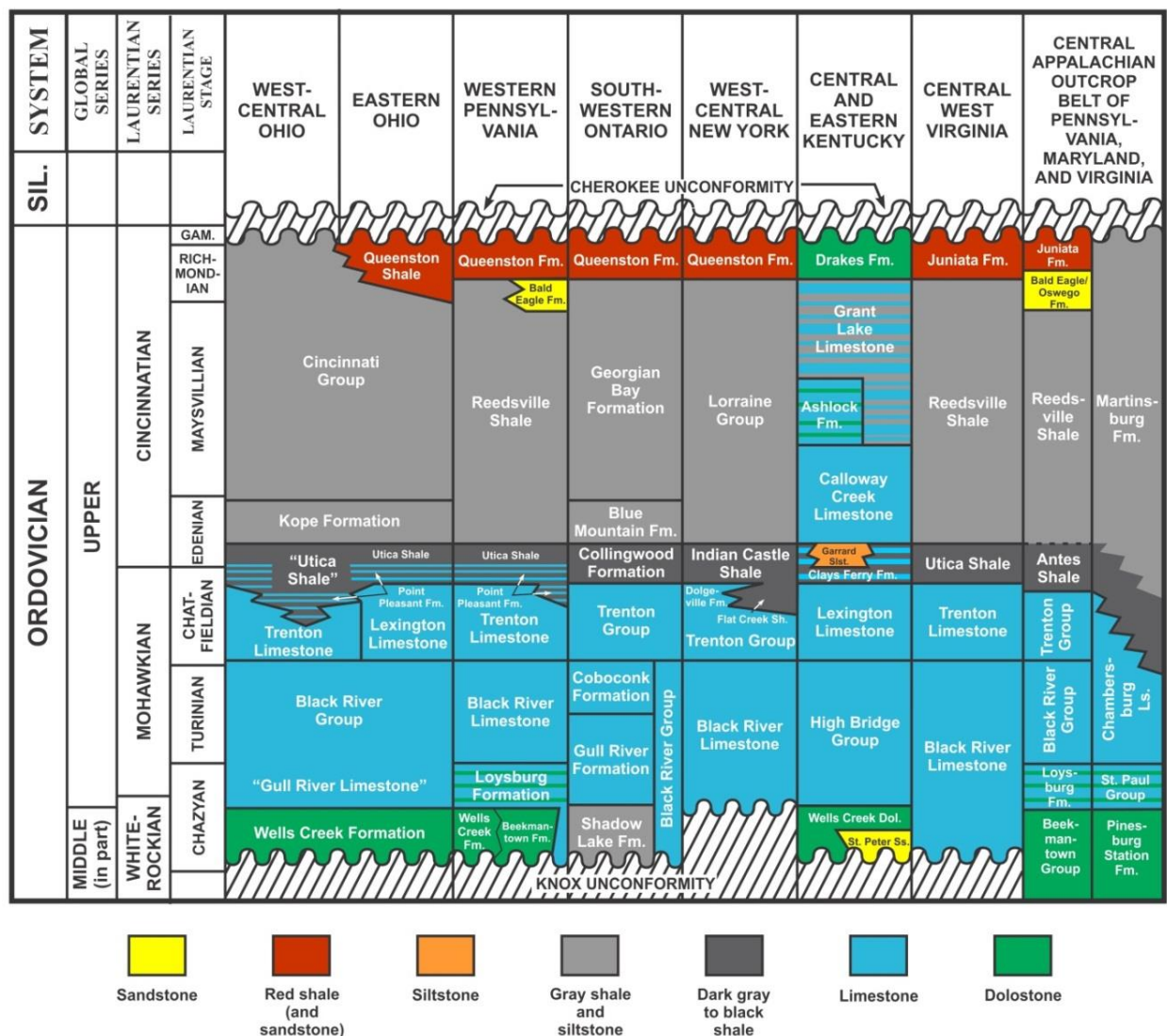
Figure 2-1. Regional correlation chart of Upper Ordovician strata for the Utica Shale Play Book Study.

2.1   Drilling and Permitting Activity

Approximately 1470 permits have been issued to drill horizontal wells to the Upper Ordovician Utica/Point Pleasant horizon, mainly in Ohio, but with approximately 245 in western Pennsylvania and 11 in the northern panhandle counties of West Virginia (Figure 2-2). Although operators for 562 of these permitted wells reportedly have yet to begin drilling, approximately 466

wells are reported as completed or producing, and another 425 are currently reported as drilling or recently drilled. Only 15 wells have been reported as being plugged. Oil, condensate and natural gas liquids (NGLs) are driving production growth.   As midstream operations (pipelines, fractionation and gas processing plants) continue to expand, additional drilled wells are being placed into production mode.

Drilling has extended the Utica/Point Pleasant play from the core area in Carroll, Harrison and Columbiana counties, Ohio to Tioga County, Pennsylvania in the northeast; Washington County, Ohio in the south; Licking County, Ohio in the west; and Ashtabula County, Ohio in the north. The current trend in drilling reflects the subsurface structure of the reservoir – a north-south trend in Ohio, swinging to northeast-southwest to the north, and then to east-west in Pennsylvania. Thus far, drilling has been concentrated in the liquids-rich area of eastern Ohio, with no horizontal Utica/Point Pleasant wells drilled in either Kentucky or New York. Increased drilling and production in southern Ohio may eventually extend the play into northern Kentucky. Although horizontal drilling is permitted in New York, there is a moratorium on hydraulic fracturing jobs using more than 80,000 gallons of water. This, in conjunction with the fact that towns can now use zoning ordinances to individually ban drilling activity within their township limits, has restricted the completion of Utica shale gas wells in the state of New York.

Chesapeake Energy is by far the biggest player in the trend, with Gulfport a distant second (Figure 2-3). Chesapeake has received permits to drill 683 wells (46% of all permits issued), of which 246 are producing or completed and only four have been plugged. Other companies in the play have been issued an additional 791 Utica/Point Pleasant permits, resulting in 220 producing or completed wells and only 15 dry holes; 377 reportedly have yet to be drilled, with the remaining 178 still being drilled or awaiting completion.
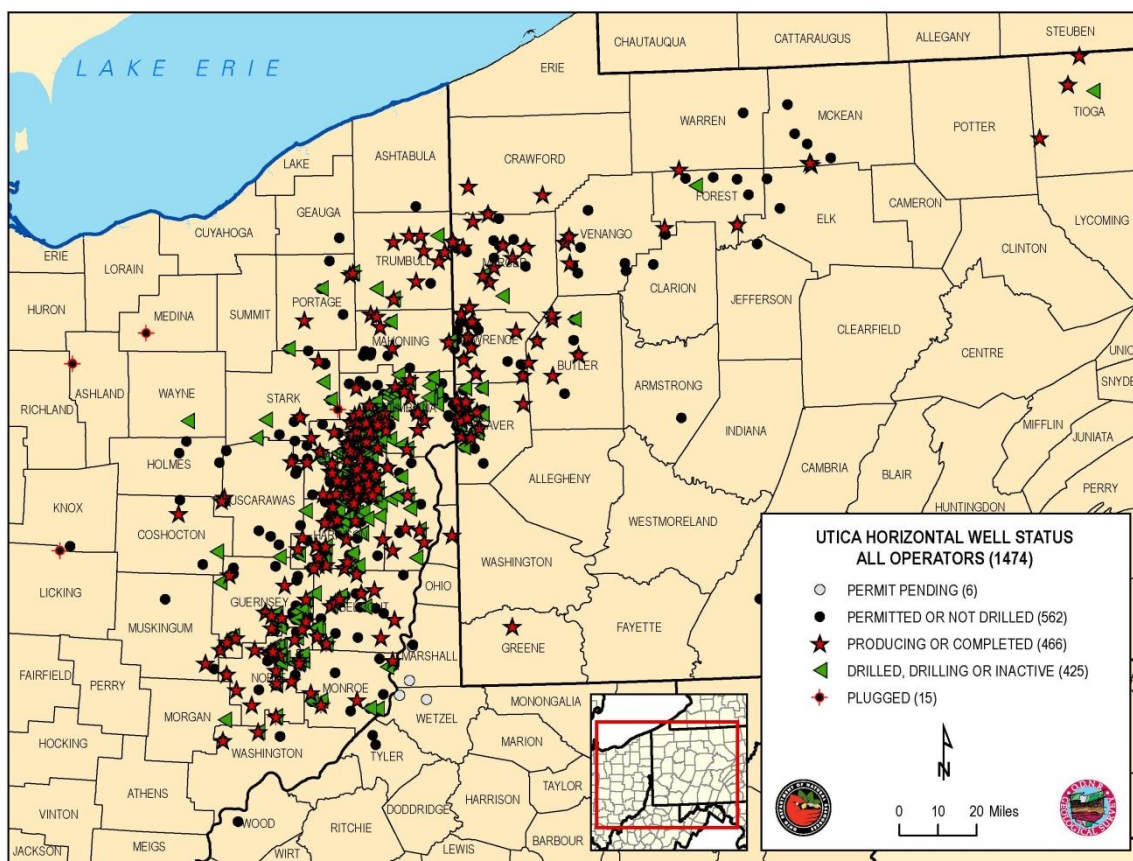
Figure 2-2. Drilling activity associated with the Utica/Point Pleasant play in the Study area. Data supplied by the DOGRM, PAGS and WVGES.
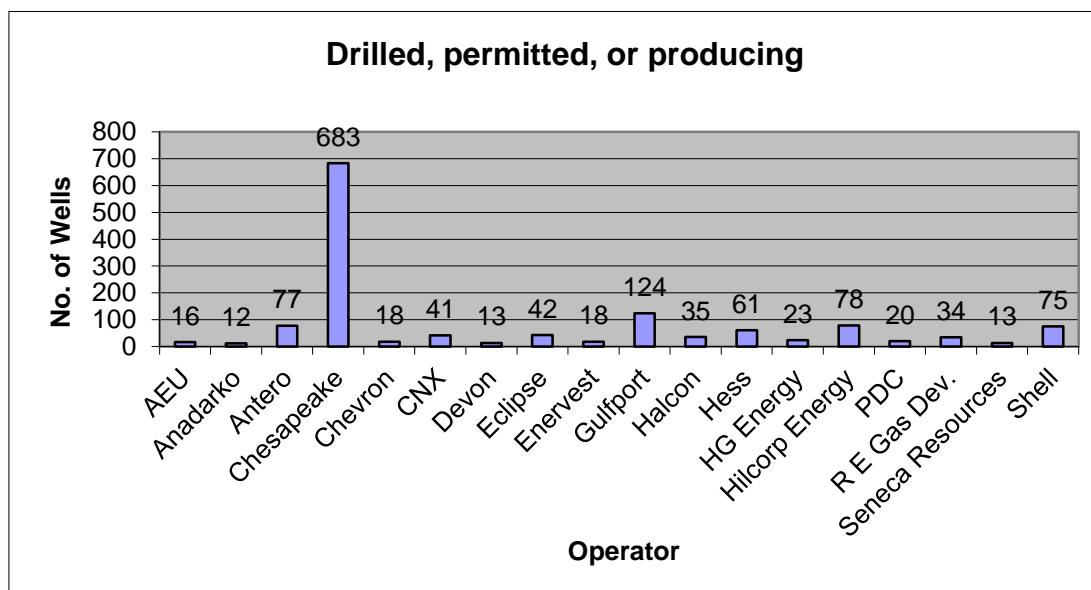
Figure 2-3. Utica/Point Pleasant well statistics by operator.

As industry extended infrastructure, production increased. The 2013 production reported by Chesapeake was 2,078,570 barrels (bbl) oil and 57.7 billion cubic feet (Bcf) gas from 217

14

producing wells (Appendix 2-A). This is up from 418,538 bbl oil and 12.6 Bcf gas for 2011 and 2012 combined. EURs are in the 5 to 10 billion cubic feet equivalent (Bcfe) range in the wet gas area (Chesapeake presentation, 2013). Chesapeake has concentrated in the core area of Carroll, Harrison and Columbiana counties, but has drilled wells as far east as Beaver County, Pennsylvania, as far north as Geauga County, Ohio, as far south as Guernsey County, Ohio, and to the westernmost corner of Tuscarawas County, Ohio.

Gulfport has procured 124 permits to drill, mainly in Harrison, Guernsey and Belmont counties, Ohio, and has 37 wells reported as producing. Their wells in the liquid-rich area have an average horizontal length of 7175 feet (ft), with 25 hydraulic fracturing (frac) stages, and an average initial production (IP) of 2,780 barrels of oil equivalent per day (boe/d) (Gulfport presentation, 2013). Oil, gas and NGLs comprise 33%, 37%, and 29% of this total, respectively. One well, the Shugert 1-12h (API#34013206570000), is in the dry gas window and tested 30.3 million cubic feet of gas per day (MMcfg/d) with no liquids. The 2013 production was up to 675,097 bbl oil and 19.2 Bcf gas from 39 wells, compared to 63,167 bbl oil and 767 million cubic feet (MMcf) gas from 2012. Gulfport has estimated EURs of 3.1 to 3.9 million barrels of oil equivalent (MMboe) for wet gas wells and 1.0 to 1.5 MMboe for condensate wells (Gulfport presentation, 2014). Gulfport has been examining completion methods to eliminate the 30-60 day resting period that commonly follows hydraulic fracturing. This process of resting wells before going into production allows the formation to absorb the frac fluids. Recent slickwater hydraulic fracture completions with no resting periods on the Wagner, Lyon and Clay wells have shown no noticeable decrease in productivity versus using gel and resting wells. Gulfport postulates that the residue left behind from the gel may be closing off the micropores and inhibiting hydrocarbon flow. Slickwater treatment may eliminate the need for the resting period, which could put wells into production up to 60 days earlier.

Antero has 77 permits to drill Utica/Point Pleasant horizontal wells in Monroe and Noble counties, Ohio. All but 20 have been drilled, with 19 producers, 36 drilled or drilling and two dry holes reported to date. Based on IP data, seven of their producing wells are among the top 10 producing wells in Ohio, averaging 5632 boe/d (Antero press release, 2013). The Yontz 1H (API#34111243620000) had an initial rate of 8879 boe/d on a 24-hour test, making it the highest IP in the region. All of Antero's wells have produced gas, condensate, and NGLs: 57% of the production is liquids. The 2013 production was 215,627 bbl oil and 10 Bcf gas from 19 wells. This was significantly up from the 2012 production of 25,522 bbl oil and 37.7 MMcf gas.

Hess has 63 permitted wells concentrated in the southeastern Ohio counties of Harrison, Belmont, Guernsey and Noble. Of these, 19 are reported as producing, 17 are reported as drilled or drilling, and 27 have not been drilled. Initial test rates for nine wells range from 1211 boe/d with 65% liquids to 2519 boe/d with 52% liquids (Hess presentation, 2014). The 2013 production was 27,470 bbl oil and 2.9 Bcf gas for 13 wells. Only 560 bbl oil and 922.9 MMcf gas were produced in 2012.

Rex Energy has been active in Carroll, Noble and Guernsey counties, Ohio, and Lawrence and Butler counties, Pennsylvania, with a total of 37 permitted wells. Of these, 15 are reported as completed or producing and nine are drilled or drilling. The Carroll County wells average a five-day sales rate of 1479 boe/d with 71% liquids (Rex Energy presentation, 2014). The wells in Guernsey and Noble counties have a five-day average sales rate of 1886 boe/d with 60% liquids.

The 2013 production was 180,308 bbl oil and 4.1 Bcf gas for 12 wells, compared to only 12,879 bbl oil and 159 MMcf gas for 2012.

Shell Appalachia has concentrated their efforts in the dry gas area in Pennsylvania – from Lawrence County eastward to Tioga County – and has permitted 75 Utica/Point Pleasant horizontal wells. Of these, 18 are reported as completed, two are drilled or drilling, and 55 are not drilled. There are no annual production data available for these wells. IP data are available for five wells and range from 1.4 to 5.3 MMcf gas.

Magnum Hunter has called the Utica/Point Pleasant potentially the best shale play in the continental United States, and sold their acreage in the Eagle Ford play to concentrate specifically on the Utica/Point Pleasant play. They have nine permitted wells, of which two are producing or completed, two are drilled or drilling, one is plugged and four are not drilled. They drilled the first horizontal well in Washington County, Ohio, in April 2013 on the Farley pad, designed to accommodate 10 horizontal wells. Their Stalder pad, in Monroe County, has been designed for 18 horizontal wells, 10 for the Marcellus Shale and eight targeting the deeper Utica/Point Pleasant interval. The first well drilled on the Stalder pad (API#34111243850100) tested at a peak rate of 32.5 MMcfg/d (Magnum Hunter presentation, 2014). For 2013, Magnum Hunter had produced 5,162 bbl oil for four wells.

Enervest has permitted 18 wells in Guernsey, Tuscarawas, Carroll, Stark and Jefferson counties in eastern Ohio. Of these, three are producing or completed, one is drilled and 14 are not drilled. The Frank 2-H well (API#34151257350000) in Stark County reported initial rates of 870 boe/d (1.2 MMcfg/d, 360 Mbbl/d oil, and 312 Mbbl/d NGLs). The Cairns 5H well (API#34019220930000) in Carroll County had an IP of 1690 boe/d (2.2 MMcfg/d, 729 Mbbl/d oil, and 587 Mbbl/d NGLs). Cumulative production for 2012 was 32,546 bbl oil and 160 MMcf gas. This oil production decreased to 31,835 bbl oil and gas production increased to 290.8 MMcf gas for 2013.

CNX (Consol Energy) has permitted 41 Utica/Point Pleasant wells in seven counties in eastern Ohio. They have 13 wells reported as completed or producing, 17 wells as drilled or drilling, and 11 not drilled. Their exploration strategy has been to target four overlapping stacked shale plays within their acreage position covering portions of eastern Ohio, southwestern Pennsylvania and northern West Virginia. These include the Ordovician-age Utica/Point Pleasant interval, and the Devonian-age Marcellus, Geneseo/Burket and Rhinestreet shales. The Monroe County, Ohio, area has special appeal because of the potential dual pay in Marcellus at approximately 5700 ft and the deeper Utica/Point Pleasant at projected depths of approximately 10,200 ft. Cumulative production for CNX's wells was 10,015 bbl oil and 9.9 MMcf gas in 2012. The cumulative production for 2013 was 14,163 bbl oil and 412.6 MMcf gas.

PDC Energy has permitted 20 wells in the Utica/Point Pleasant play in southeastern Ohio. They have 11 completed or producing wells, eight drilled and one not drilled. Their activity is focused in Guernsey, Washington and Morgan counties along the southern end of the play area. Significant producing wells in Guernsey County include the Onega-Commissioners 14-25 H (API#34059242110100), which had an IP of 1796 boe/d (79% liquids); the Stiers 3-well pad (API#s 34059242420000, 34059242430000 and 34059242440000), which had a combined initial production of 1268 Boe/d (79% liquids); and the Detweiler #42-3H (API#34059242920000) with

2197 boe/d (75% liquids) (PDC presentation, 2014). To the south in Washington County, the Garvin 1-H well (API#34167297210100) had an IP of 1530 boe/d (54% liquids). PDC reported cumulative production of 2120 bbl oil and 10.6 MMcf gas in 2012. The cumulative production for 2013 increased to 204,524 bbl oil and 982.6 MMcf gas. PDC has noted that flowback management of Utica/Point Pleasant wells is critical to the success of this unconventional resource play (PDC presentation, 2014). Preliminary data indicate that applying back pressure during initial flowback can significantly increase reserves and economics of Utica/Point Pleasant wells. Their initial performance results demonstrated longer-term productivity and a lower decline rate in wells simply by decreasing the choke size.

Other companies who have drilled or are actively leasing and permitting Utica/Point Pleasant wells in the basin include Anadarko, Atlas Noble, American Energy, BP America, Carrizo, Chevron, Devon Energy, Eclipse, EQT, Halcon, HG Energy, Hilcorp Energy and XTO Energy, Inc. (XTO). Of particular note is American Energy, a new player that has raised nearly $3 billion to lease and drill Utica/Point Pleasant wells in eastern Ohio. Recent lease acquisitions by American Energy include 24,000 acres (ac) acquired from Shell, 74,000 ac from Hess and 30,000 ac from XTO. They have acquired about 260,000 ac in the play area and announced that they plan to drill 1600 wells during the next decade.

2.2   Production Summary

Annual and quarterly production data reported to DOGRM have shown a marked increase over the past three years (Table 2-1). In 2011, the cumulative annual production was approximately 46,000 bbl oil and 2.5 Bcf gas from nine producing wells, which, incidentally, represented only 1% of the total oil production and 3.5% of the gas produced in Ohio. In 2012, 87 Utica/Point Pleasant wells yielded approximately 635,000 Bbl oil and 12.8 Bcf gas, which represented 12% of the total oil and 16% of the total gas produced in the state. A significant increase was observed in 2013, with just over 3.6 MMbbl oil and 100 Bcf gas produced from 352 wells. These volumes represent 45% of the total oil and 58% of the total gas produced in Ohio. The total reported cumulative production for the Utica/Point Pleasant from 2011 through 2013 in Ohio was approximately 4.3 MMbbl oil and 115.3 Bcf gas. Production numbers are expected to continue increasing in the upcoming years as mid-stream operations expand outward, infrastructure continues to be developed and additional drilling continues.

A bubble map of cumulative production per well was constructed using third and fourth quarter 2013 production data (Figure 2-4). Gas production was converted to boe and added to the barrels of oil produced to determine cumulative production per well in barrels of oil equivalent (boe). A conversion factor of 6000 standard cubic feet gas (sfcg) to 1 bbl oil was used for this purpose. Approximately 15.5 million boe (2,771,784 bbl oil and 76.7 Bcf gas) were produced during the third and fourth quarters of 2013 (Figure 2-4, Appendix 2-A). A northeast-southwest trend of higher production is seen extending through Columbiana, Carroll, Harrison, Belmont, Noble and Monroe counties. The ten best wells produced more than 200,000 boe during this time. All 10 wells were operated by Gulfport Energy or Antero Resources in Monroe and Belmont counties. Higher pressures in this region are thought to be a factor in producing these higher rates. The best producing well during the third and fourth quarter of 2013 was the Gulfport 1-14H Stutzman well (API#34013206650100) in Belmont County, which produced 345,514 boe.
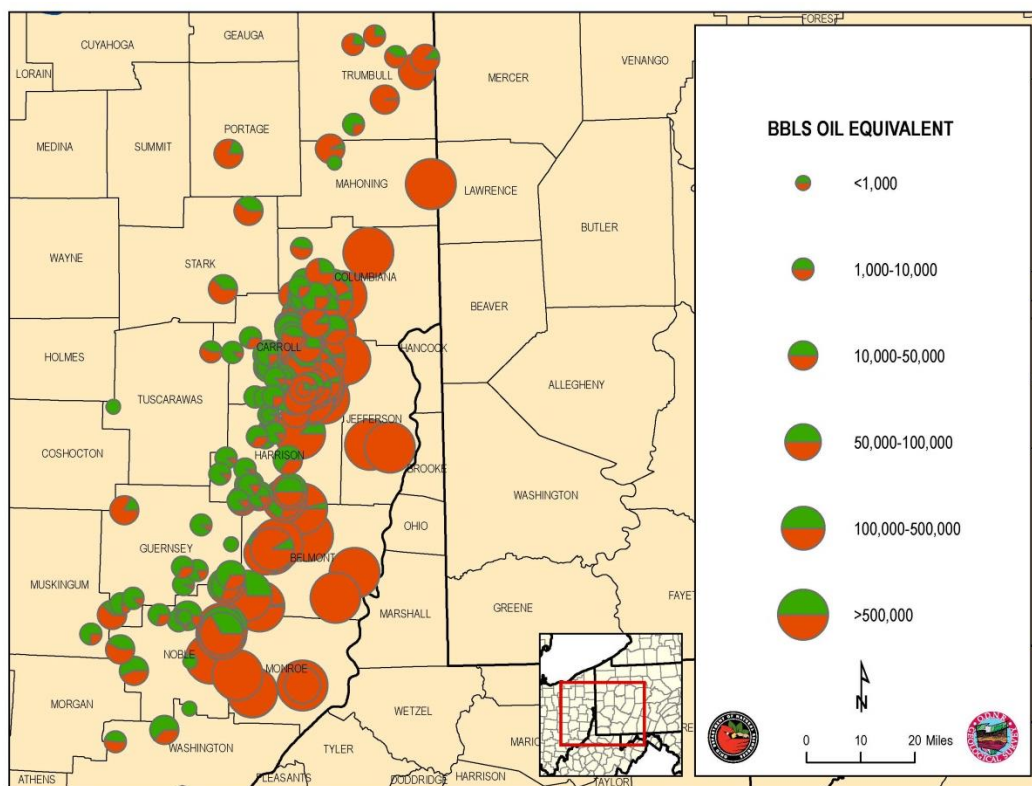
Figure 2-4. Bubble map of combined third and fourth quarter 2013 production data (boe) in Ohio. Gas has been converted to boe using 1 barrel of oil equals 6000 scfg.

Results have been less encouraging to the north and west of these areas. Trumbull County has shown lower producing rates (Figure 2-4, Appendix 2-A). These lower production rates are consistent with recent announcements by BP and Halcon that they are terminating Utica drilling in Trumbull County. Thus far, drilling farther west in the updip portion of the oil window also has produced less encouraging results, as evidenced by nonproductive Devon wells drilled in Coshocton, Knox, Medina, Wayne, and Ashland counties. Clearly, the economic producing extents of this play are still being developed.

A gas-to-oil ratio (GOR) map was constructed using the combined third and fourth quarter 2013 production data for 359 wells in Ohio (Figure 2-5). A northeast-southwest trend separating the oil window from the gas window is visible using a GOR of 20,000 standard cubic feet gas per barrel oil (scfg/bo). A GOR map used in conjunction with bitumen reflectance and RockEval mapping from this Study may help to better refine the oil and gas window in this unconventional shale play.

Table 2-1. Summary of Utica/Point Pleasant production compared to conventional production for 2011 through 2013 in Ohio. Note: Gas includes NGLs.

	Utica/Point Pleasant Production			Conventional Production		
Year	Oil (Barrels)	Gas (Mcf)	No. of Wells	Oil (Barrels)	Gas (Mcf)	No. of Wells
2011	46,326	2,561,524	9	4,809,451	70,728,314	50,192
2012	635,896	12,836,662	87	4,665,167	65,777,332	51,407
2013	3,677,742	100,119,054	359	8,088,599	171,658,608	48,828
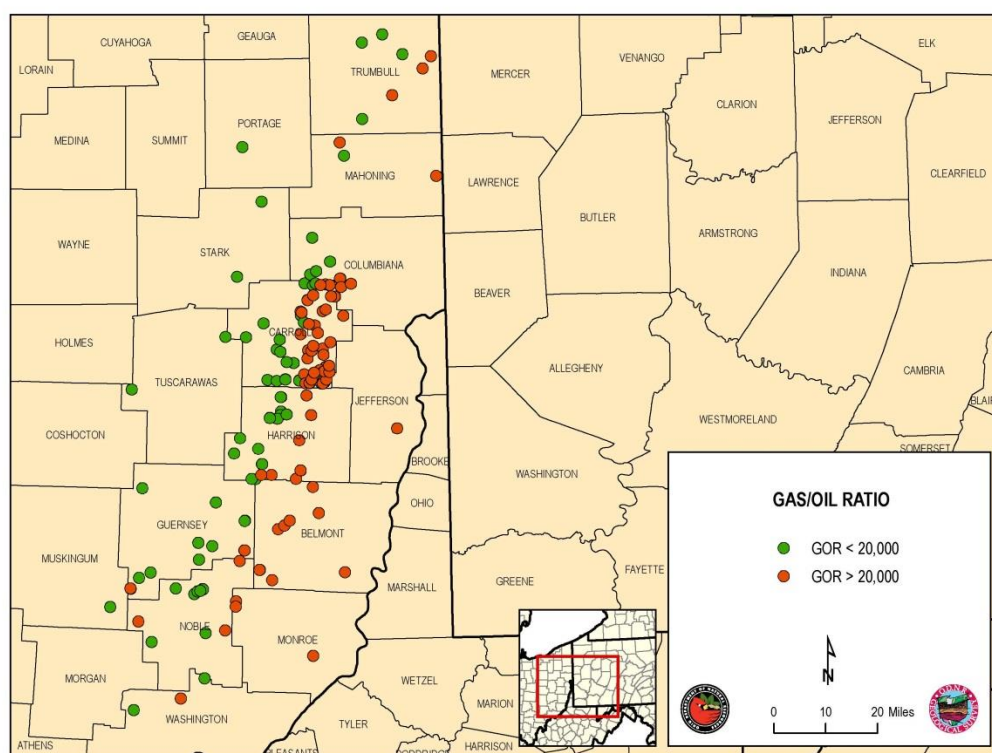
Figure 2-5. GOR map of Ohio using a cutoff of 20,000 scfg/bo. A delineation of the gas to oil window is evident trending northeast-southwest through eastern Ohio.

3.0   LITHOSTRATIGRAPHY

The focus of this particular task is the geology and stratigraphy of the early Late Ordovician strata of the Appalachian basin. These strata include the Kope Formation, Utica Shale, Point Pleasant Formation and Lexington/Trenton Formation (Figure 3-1). Trenton and Lexington are both formal formation names that have been applied to the same interval of rock. Therefore, in keeping with the previously published Trenton/Black River study (Patchen and others, 2006), we are designating this stratigraphic interval the Lexington/Trenton Formation. In some parts of the Study area, it is possible to differentiate individual members of the Lexington/Trenton based on their organic-rich or carbonate-rich but organic-poor characteristics. Formal names have been applied to these members in Kentucky, two of which will be used throughout the report – the basal Curdsville Member (organic-poor) and Logana Member (organic-rich) above. The section between the Logana Member and the Point Pleasant Formation is referred to informally in this

Study as the upper member of the Lexington/Trenton Formation. Of all these Late Ordovician strata, the most productive hydrocarbon source rocks tend to be the Point Pleasant Formation and the upper and Logana members of the Lexington/Trenton Formation. Brief descriptions of each unit's lithostratigraphy are provided below. Detailed Utica/Point Pleasant and equivalent outcrop descriptions have been prepared by each state and are available in Appendix 3-A.
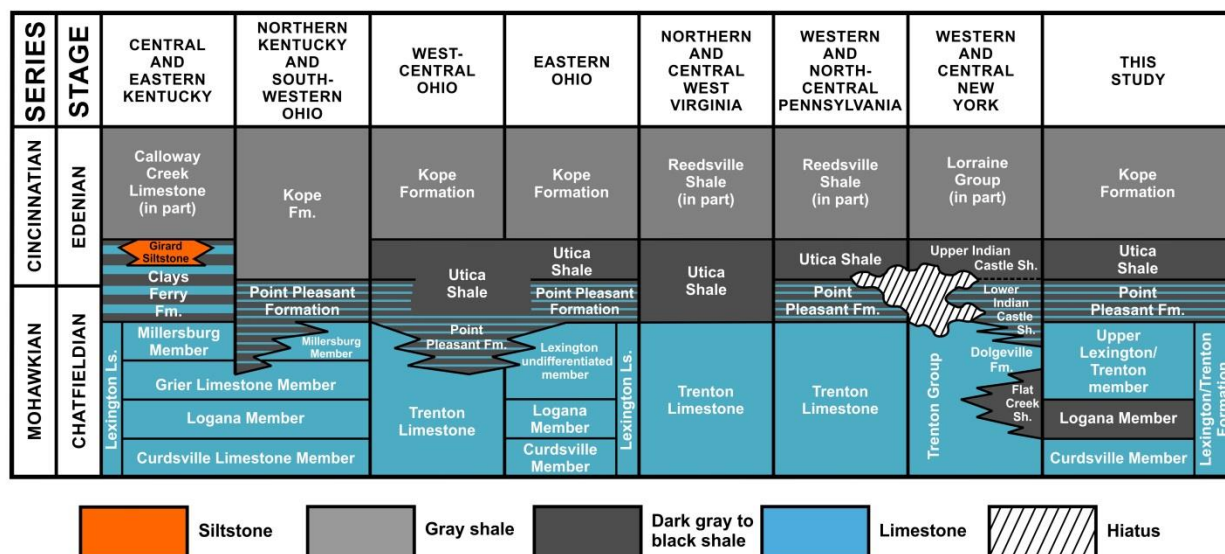
Figure 3-1. Correlation chart for early Late Ordovician strata evaluated by the Utica Shale Play Book Study.

3.1 Kope Formation

The name Kope Formation is used in the Study for the organic-poor shale and siltstone unit above the Utica Shale. It is equivalent to the lower portion of the Calloway Creek Limestone of Kentucky, Lorraine Group of New York, and Reedsville Shale of Pennsylvania and West Virginia (Figure 3-1). The Kope is composed of interbedded shale (about 60 to 80%), limestone (20 to 40%), and minor siltstone; within the Study area it ranges in thickness from about 40 to 1600 ft. The shale commonly occurs in beds 2- to 5-ft thick and is generally very sparsely fossiliferous. Most of the limestone is fossiliferous and commonly occurs in even beds 2- to 6- inches (in) thick that are in places grouped into sets several ft thick. The limestone beds commonly have sharp contacts with the shale beds (McDowell, 1986).

3.2 Utica Shale

For the purposes of this Study, the name Utica Shale is used for all the strata between the Kope and Point Pleasant formations (Figure 3-1). In Kentucky, this interval is equivalent to the upper Clays Ferry Formation, whereas in New York it is called upper Indian Castle Shale. In outcrop in the Appalachian fold belt, the Antes Shale and Martinsburg Formation occupy the stratigraphic level of the Utica. The Utica consists of interbedded dark fissile shale and limey shale (10 to 60% calcite) beds. These beds tend to be bioturbated, and can be fossiliferous in part (Smith, 2013). The Utica Shale pinches out to the south in southern Ohio and West Virginia, but extends to the southwest of the Study area along the "Sebree Trough" (Kolata and others, 2001), roughly coinciding with the Kentucky/Indiana border. The Utica thickens to the northeast to approximately 400 ft in east-central New York.

3.3   Point Pleasant Formation

The Point Pleasant Formation consists of all of the interbedded limestones and black shales between the Utica Shale and the top of the Lexington/Trenton Formation (Figure 3-1). This interval, where it exists, is equivalent to the lower Clays Ferry Formation of Kentucky and the lower Indian Castle Shale of New York. It extends northward beneath the Utica Shale and is comprised of interbedded, fossiliferous limestone, shale and minor siltstone. The limestone and shale occur in roughly equal amounts, whereas the siltstone accounts for only a small percentage of the unit. Within the Study area, this unit ranges in thickness from 0 ft in the northwest to about 240 ft in northern Pennsylvania. The Point Pleasant and Utica intertongue in part with the Lexington/Trenton Formation (Luft, 1972; McDowell, 1986).

3.4   Upper Lexington/Trenton Formation

The upper Lexington/Trenton Formation is equivalent to the Millersburg and Grier Limestone members (undifferentiated) of the Lexington Limestone of Kentucky and the Dolgeville Formation of New York (Figure 3-1). It consists of nodular and irregularly bedded fossiliferous limestone and shale in the upper part of the Lexington Limestone. The limestone consists of very abundant whole and broken fossils in a silt- and clay-sized carbonate matrix. Bryozoans, brachiopods, mollusks and trilobite fragments are particularly abundant, and stromatoporoids and colonial corals are present in some zones. Evidence of bioturbation is common. The limestones were deposited in the infralittoral zone where light, aeration, circulation and the availability of nutrients were at an optimum to foster life (McDowell, 1986).

3.5   Logana Member

The Logana Member is equivalent to the Flat Creek Shale of New York, which is the lowest formation within New York's Utica Group (Figure 3-1). It consists of interbedded calcisiltite and shale, and coquinoid limestone consisting of closely packed shells of the brachiopod *Dalmanella sulcata* (McDowell, 1986). The calcisiltite is generally in even or broadly lenticular beds 0.2- to 0.3-ft thick and is mostly unfossiliferous. The member is about 30-ft thick in western Ohio, and thickens to approximately 220 ft in central New York. The Logana was deposited during the culmination of the initial transgression of Lexington/Trenton time (McDowell, 1986).

3.6   Curdsville Limestone Member

The Curdsville Limestone Member, the basal member of the Lexington/Trenton Formation, consists of 20 to more than 450 ft of bioclastic calcarenite, which is sandy and chert-bearing in part; silicified fossils are common. Near the top of the member, the limestone becomes irregularly bedded, finer grained and more fossiliferous.   MacQuown (1967) identified several thin, discontinuous bentonites in the Curdsville. The Curdsville was deposited in shallow, turbulent water during the initial transgression of the Lexington sea. The member is present throughout the outcrop area. The Curdsville conformably overlies the Middle Ordovician Black River Formation (McDowell, 1986).

4.0 SUBSURFACE MAPPING AND CORRELATION THROUGH GEOPHYSICAL LOG ANALYSIS

4.1 Methods

As the team lead on this task, KGS prepared well-based stratigraphic interpretations within an IHS Petra® software database system. The Petra® project database contains location and header information on 10,416 wells across the five-state Study area and the bordering regions of Indiana, Michigan and southern Ontario, Canada (Figure 4-1), more than 8000 of which are Lexington/Trenton or deeper penetrations. Geophysical well logs have been loaded into the Petra® project for 1978 wells (Figure 4-2). Of these, the vast majority are from digital Log ASCII Standard (LAS) files, which have facilitated log-based correlations and calculations.
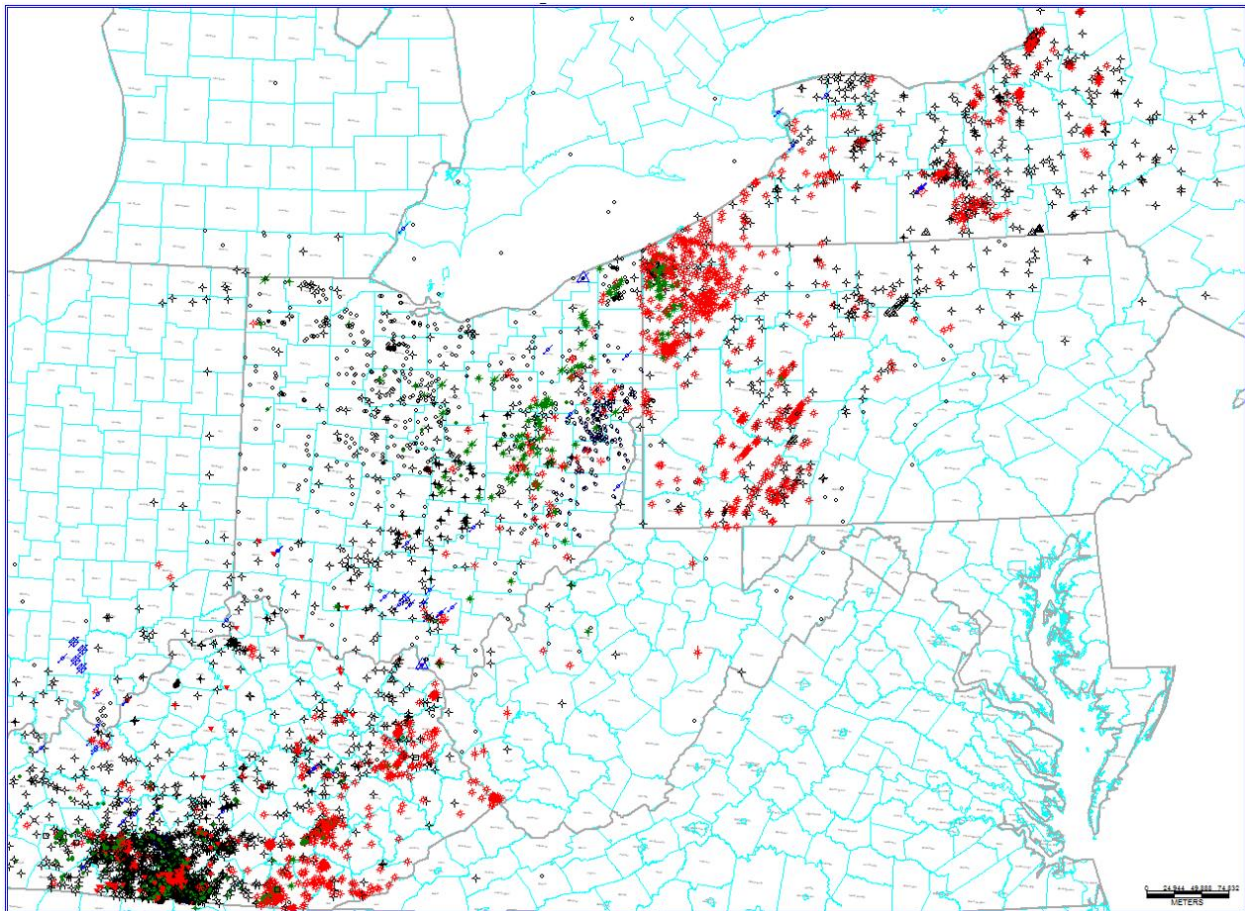
Figure 4-1. Map of 10,416 well locations consulted or otherwise utilized by the Utica Shale Play Book Study.
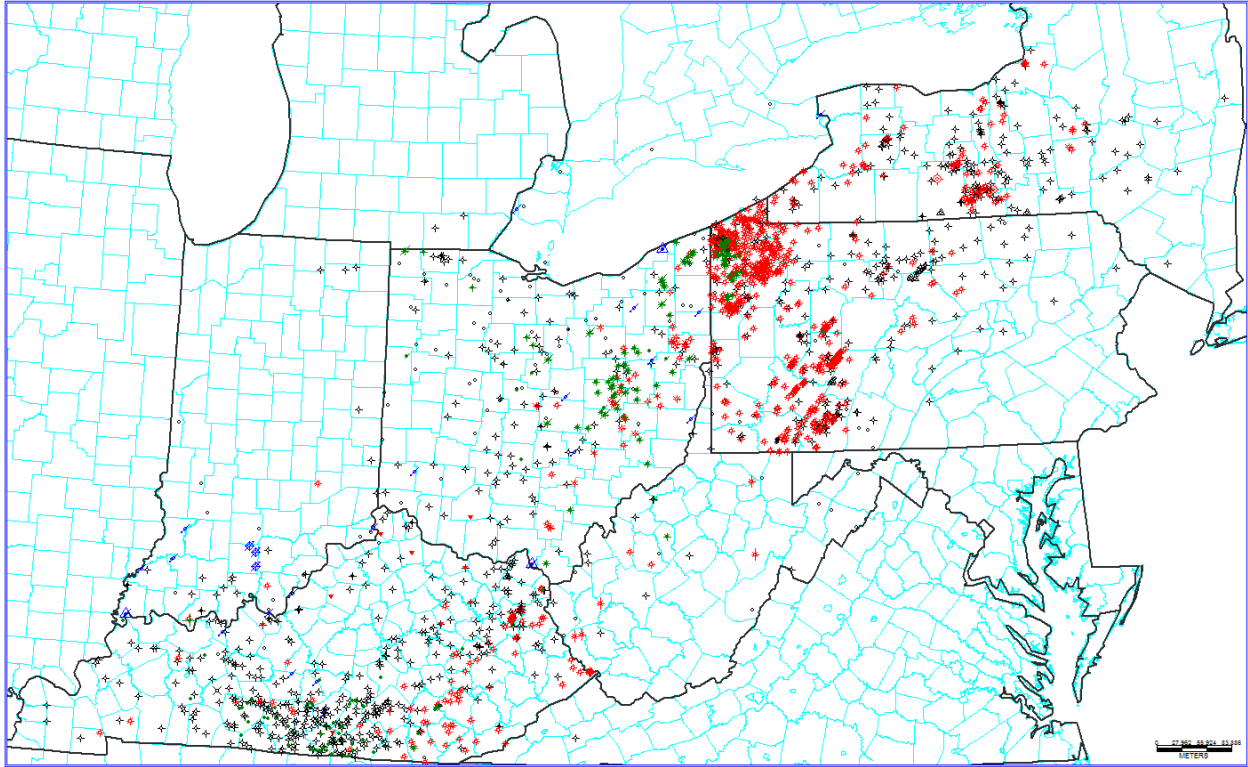
Figure 4-2. Map of project wells in the Study area with geophysical well logs (1978) loaded into Petra® for mapping purposes.

As part of this Study, KGS extended well-log-based stratigraphic interpretations for the Kope Formation, Utica Shale, Point Pleasant Formation, upper Lexington/Trenton Formation and Logana and Curdsville members of the Lexington/Trenton Formation (see Figure 3-1) established in the Trenton/Black River project (Patchen and others, 2006). In addition, KGS researchers studied the Upper Ordovician stratigraphy on outcrops in the Maysville, Kentucky, area in order to better understand depositional and facies characteristics of the Utica and Point Pleasant formations. A type-log for the log character of the researched units is presented in Figure 4-3.
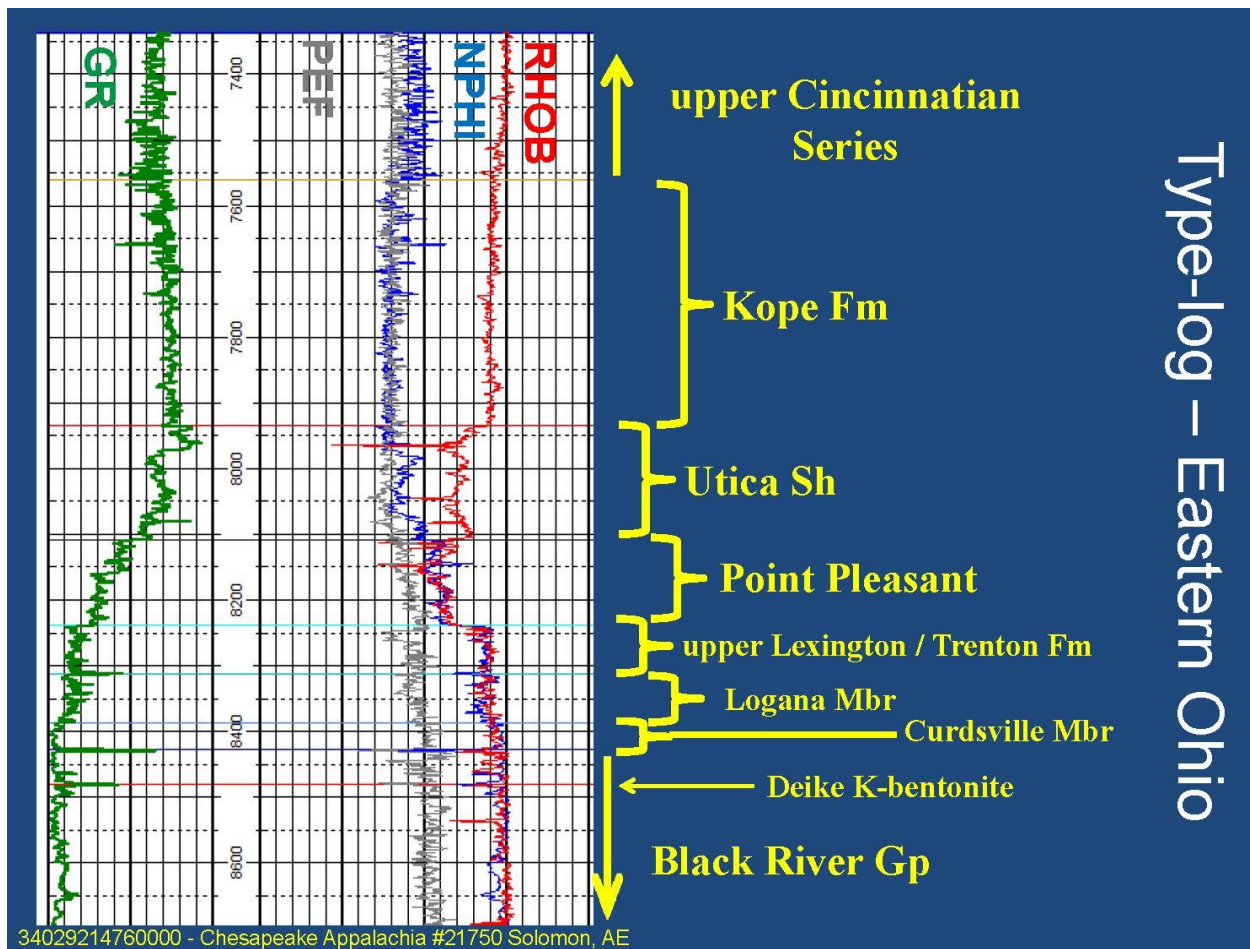
Figure 4-3. Geophysical type-log for the researched units in the Study area.

4.2   Results

The following maps (Figures 4-4 through 4-16) illustrate the results of the stratigraphic correlations for this Study, including both structure and annotated isopach maps. All structure maps display elevations in ft relative to mean sea level (MSL), with bold red lines representing major fault zones that were active in the Ordovician (Patchen and others, 2006).

24
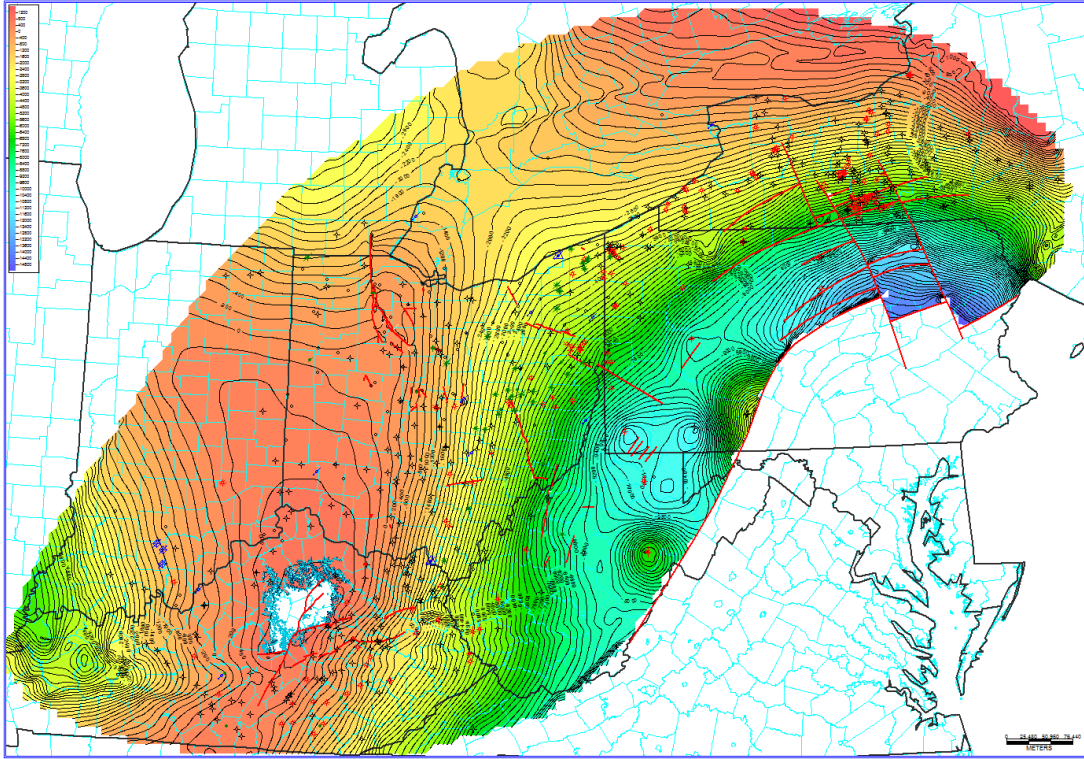
Figure 4-4. Structure map on top of the Kope Formation. Elevation in ft MSL with a 200-ft contour interval.
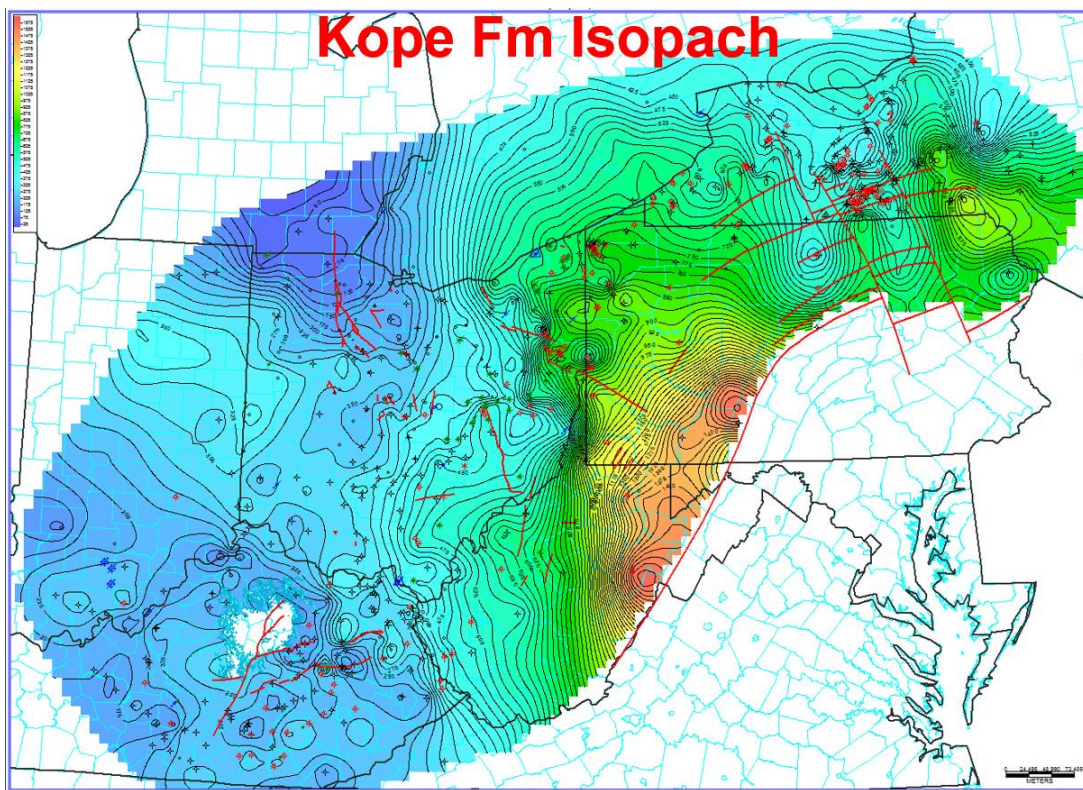
Figure 4-5. Isopach map of the Kope Formation. Thickness in ft with a 25-ft contour interval.

25
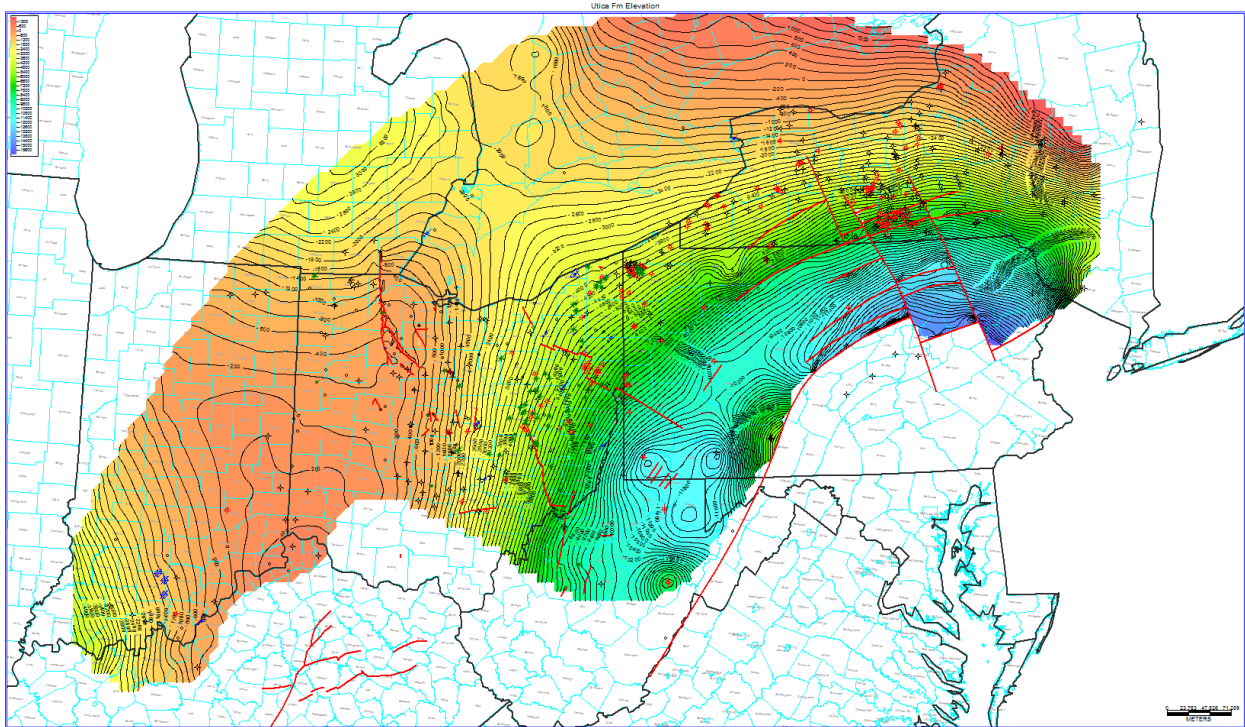
Figure 4-6. Areal extent and structure map on top of the Utica Shale. Elevation in ft MSL with a 200-ft contour interval.
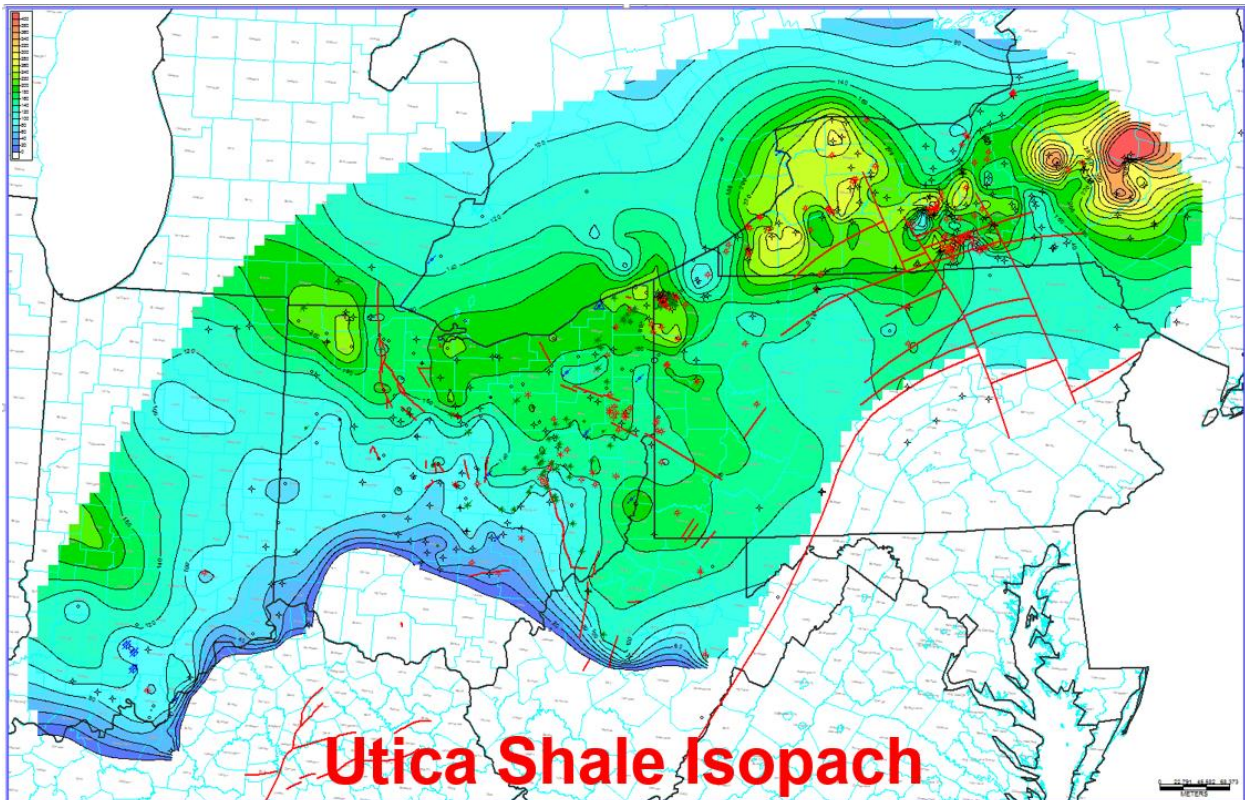
Figure 4-7. Isopach map of the Utica Shale. Thickness in ft with a 20-ft contour interval.

26
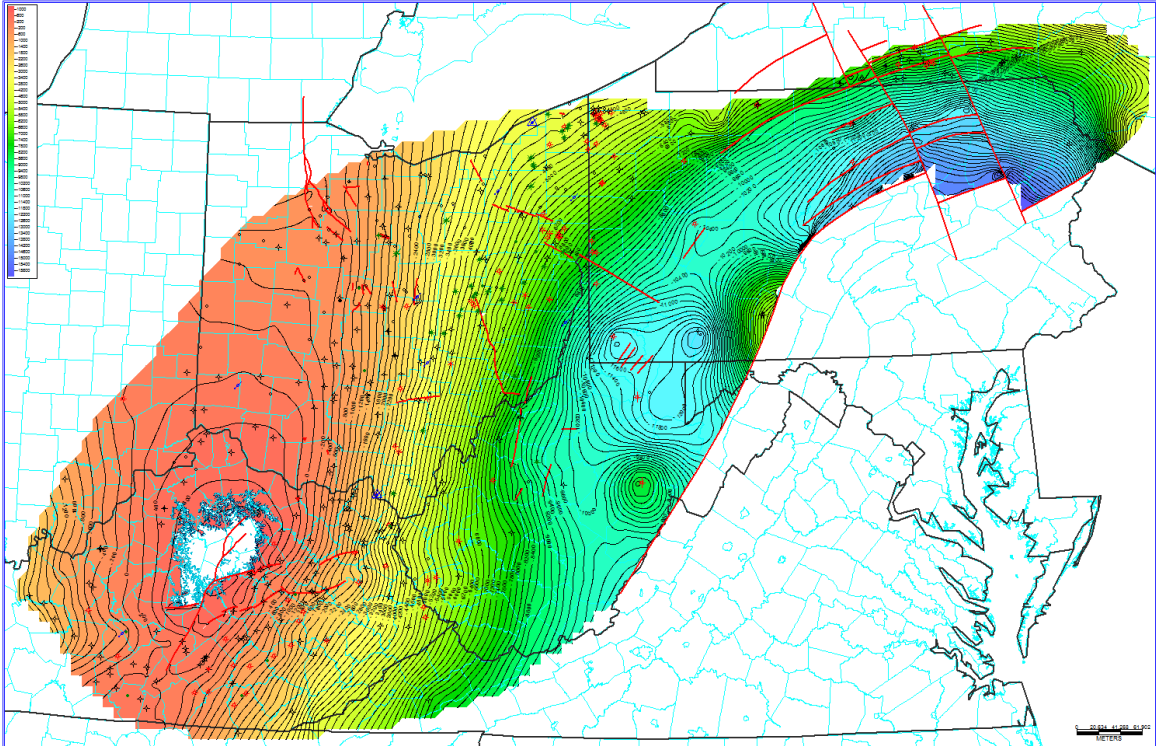
Figure 4-8. Areal extent and structure map on top of the Point Pleasant Formation. Elevation in ft MSL with a 200-ft contour interval.
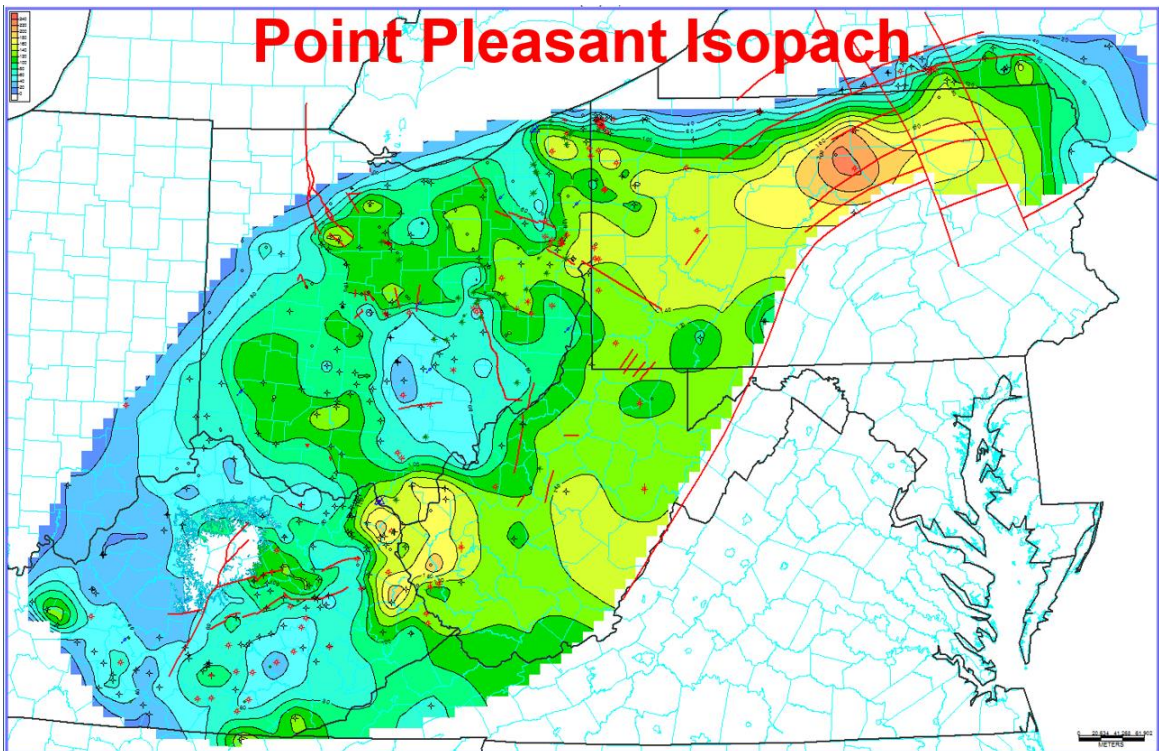
Figure 4-9. Isopach map of the Point Pleasant Formation. Thickness in ft with a 20-ft contour interval.
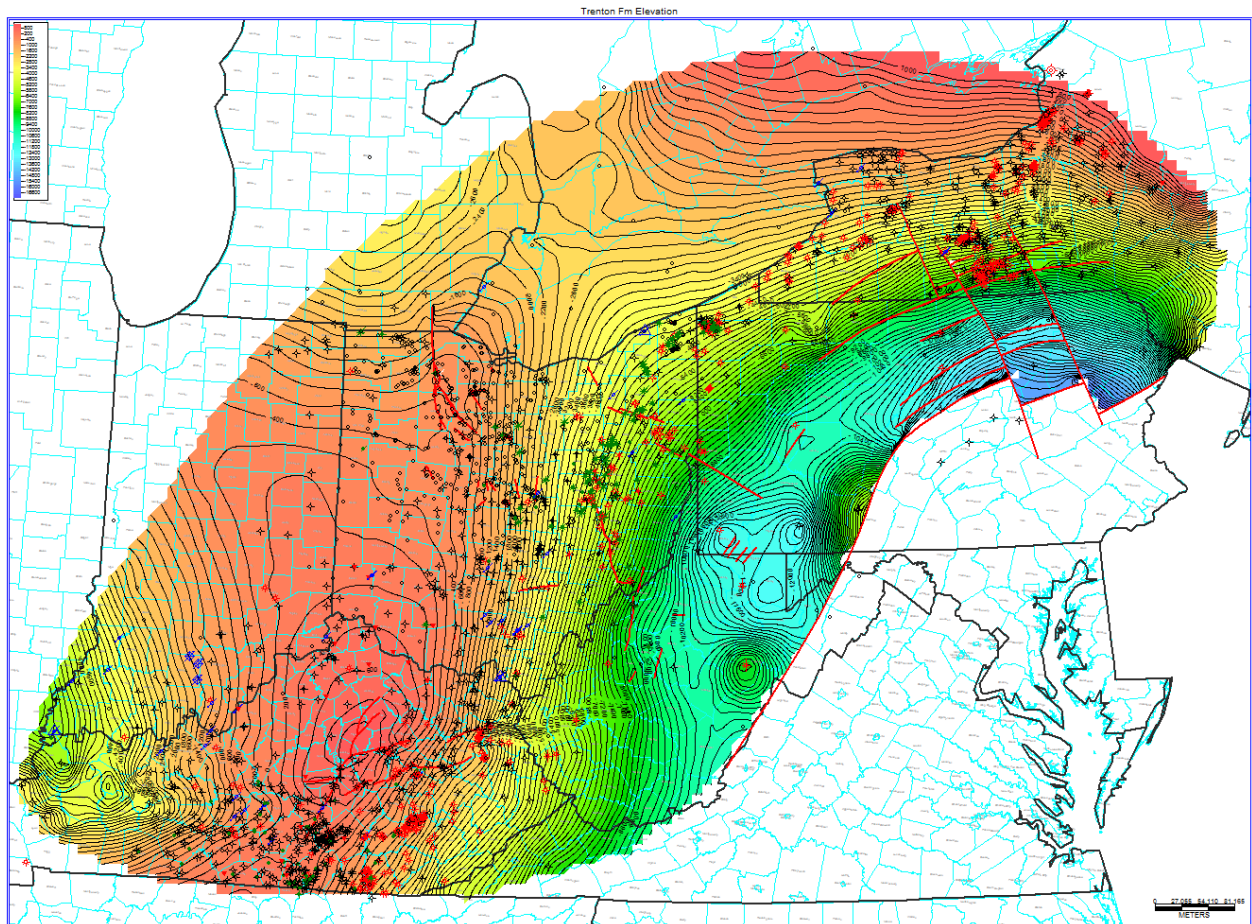
Figure 4-10. Structure map on top of the Lexington/Trenton Formation. Elevation in ft MSL with a 200-ft contour interval.
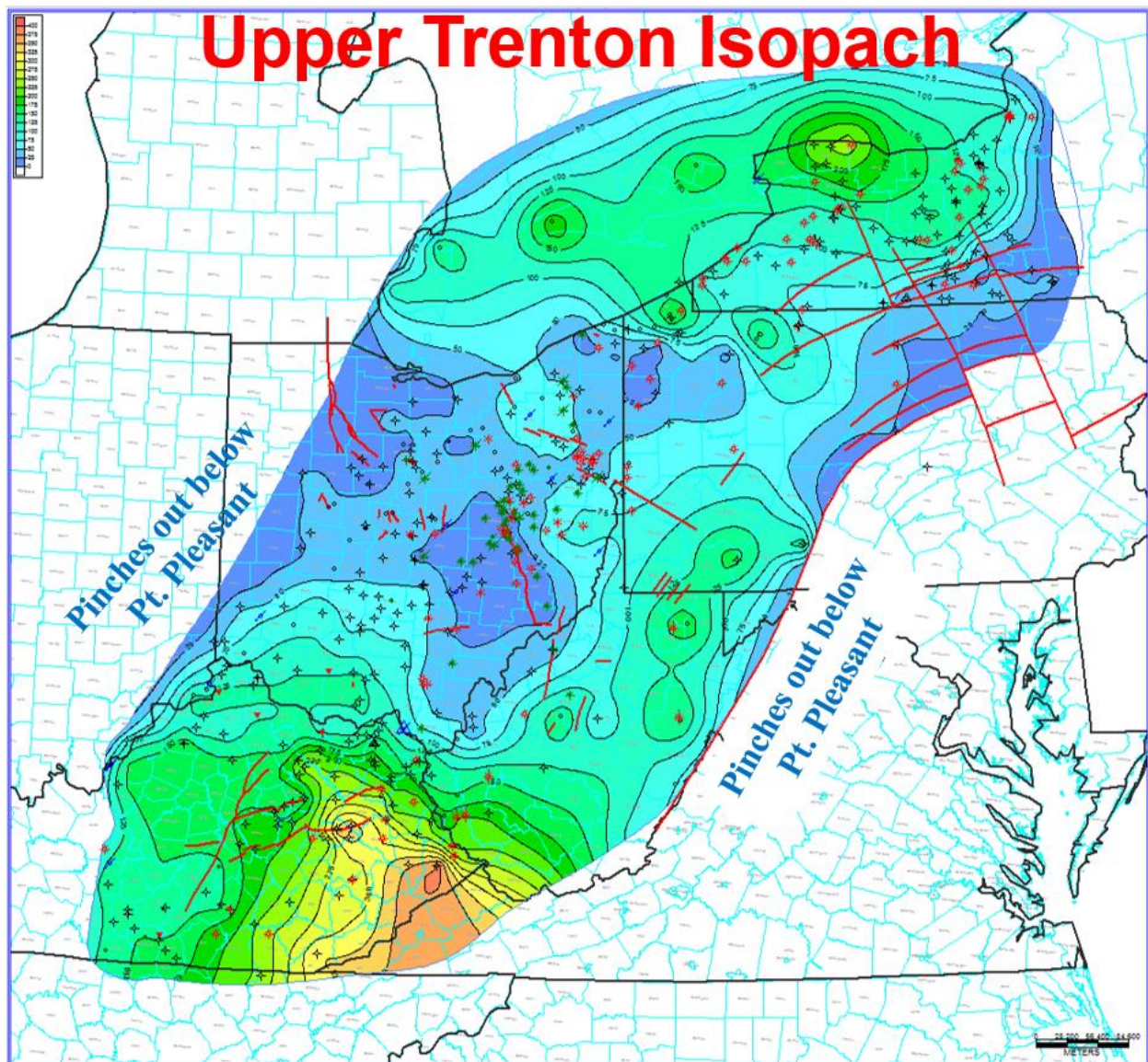
Figure 4-11. **Isopach map of the upper Lexington/Trenton Formation (above the Logana Member). Thickness in ft with a 25-ft contour interval.**
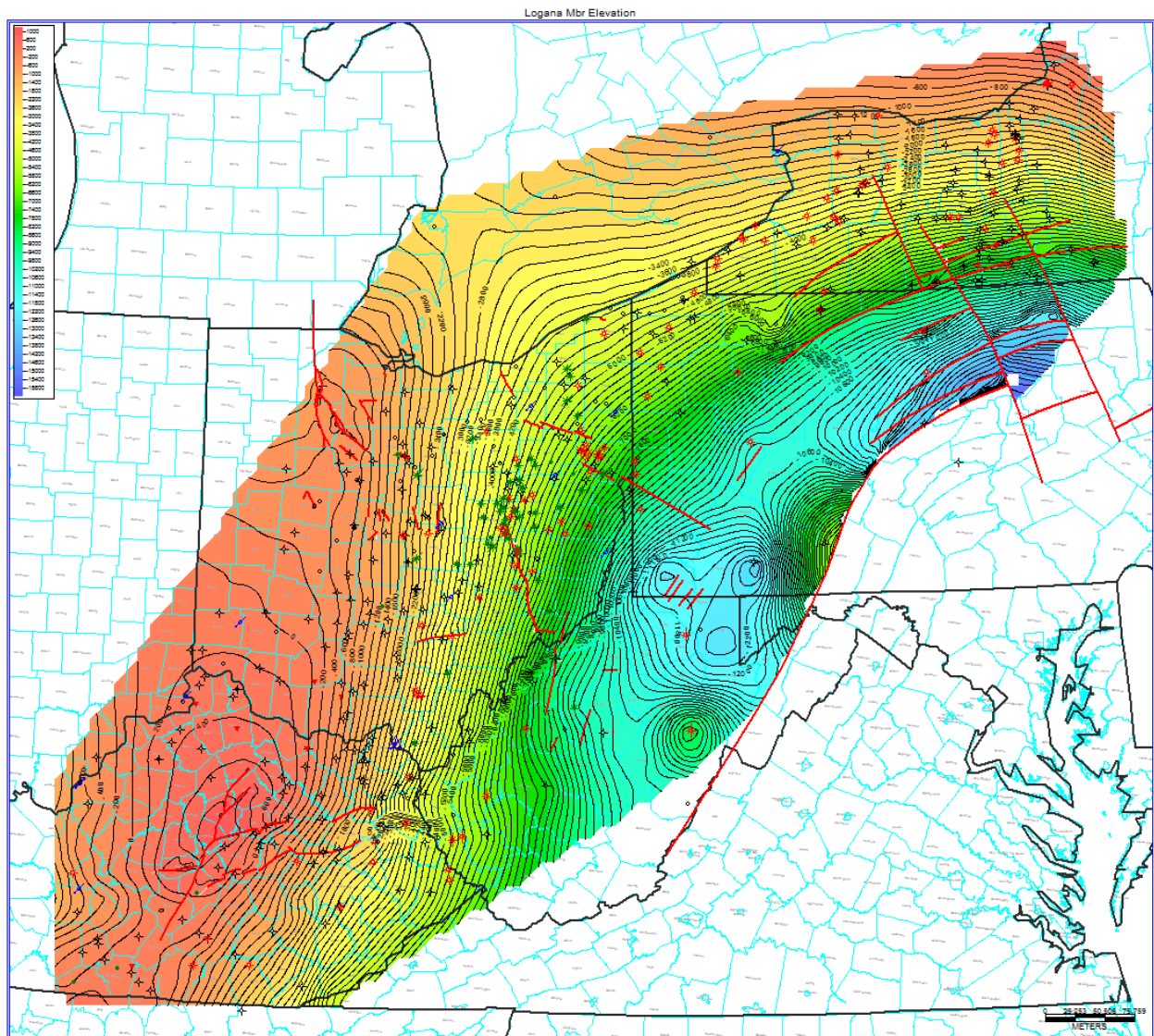
Figure 4-12. Structure map on top of the Logana Member of the Lexington/Trenton Formation. Elevation in ft MSL with a 200-ft contour interval.
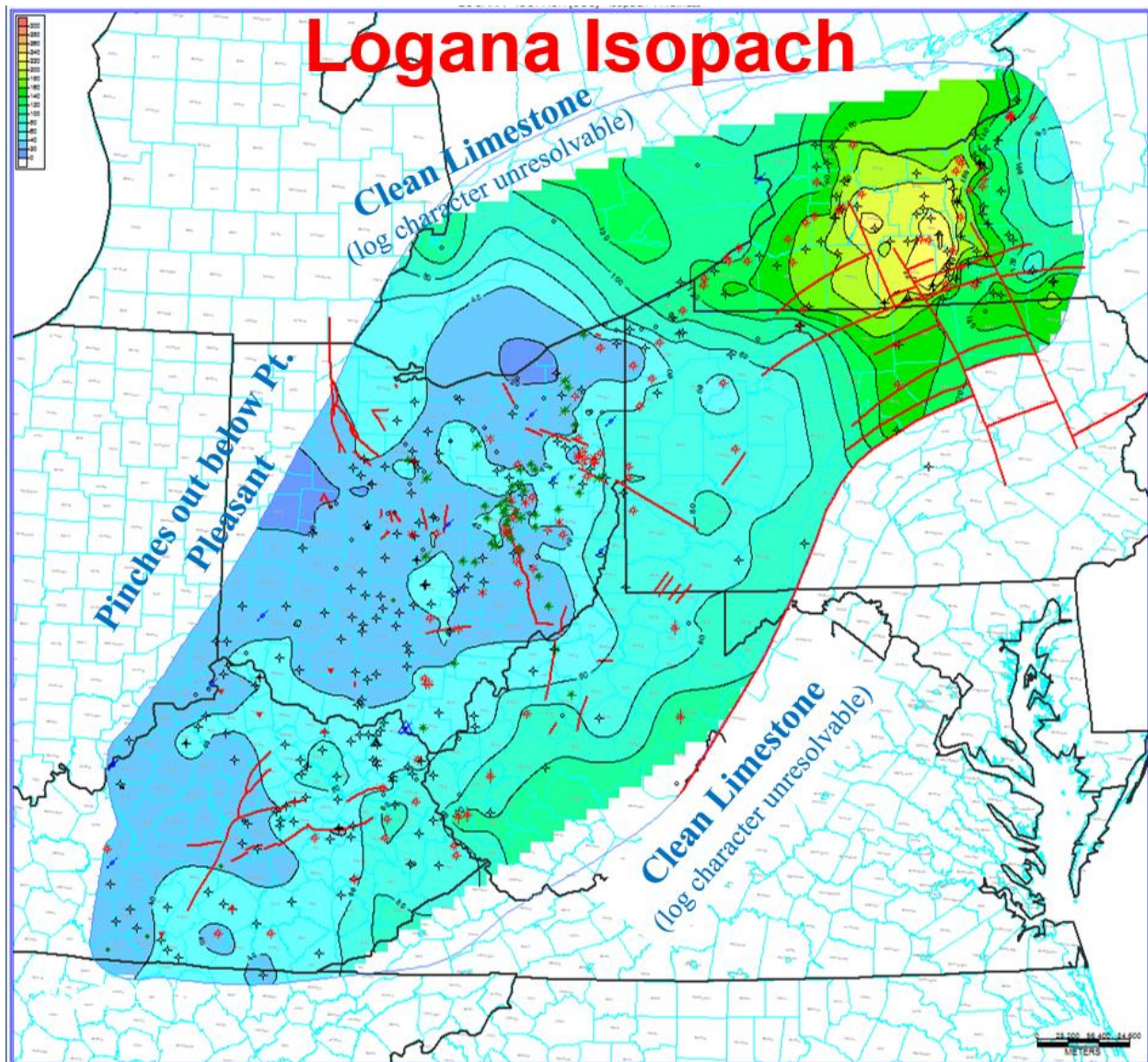
Figure 4-13. Isopach map of the Logana Member of the Lexington/Trenton Formation. Thickness in ft with a 20-ft contour interval.
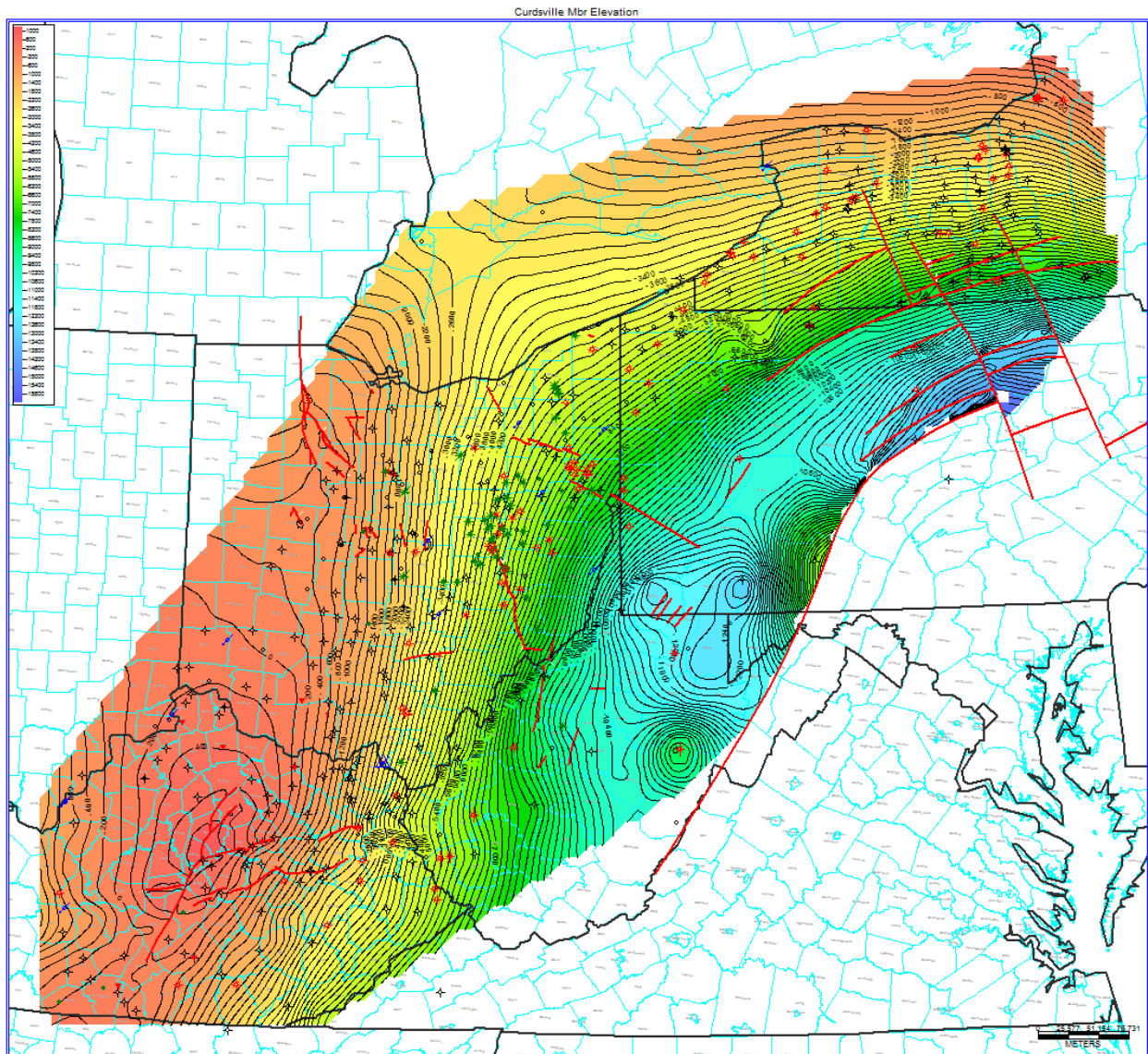
Figure 4-14. Structure map on top of the Curdsville Member of the Lexington/Trenton Formation. Elevation in ft MSL with a 200-ft contour interval.
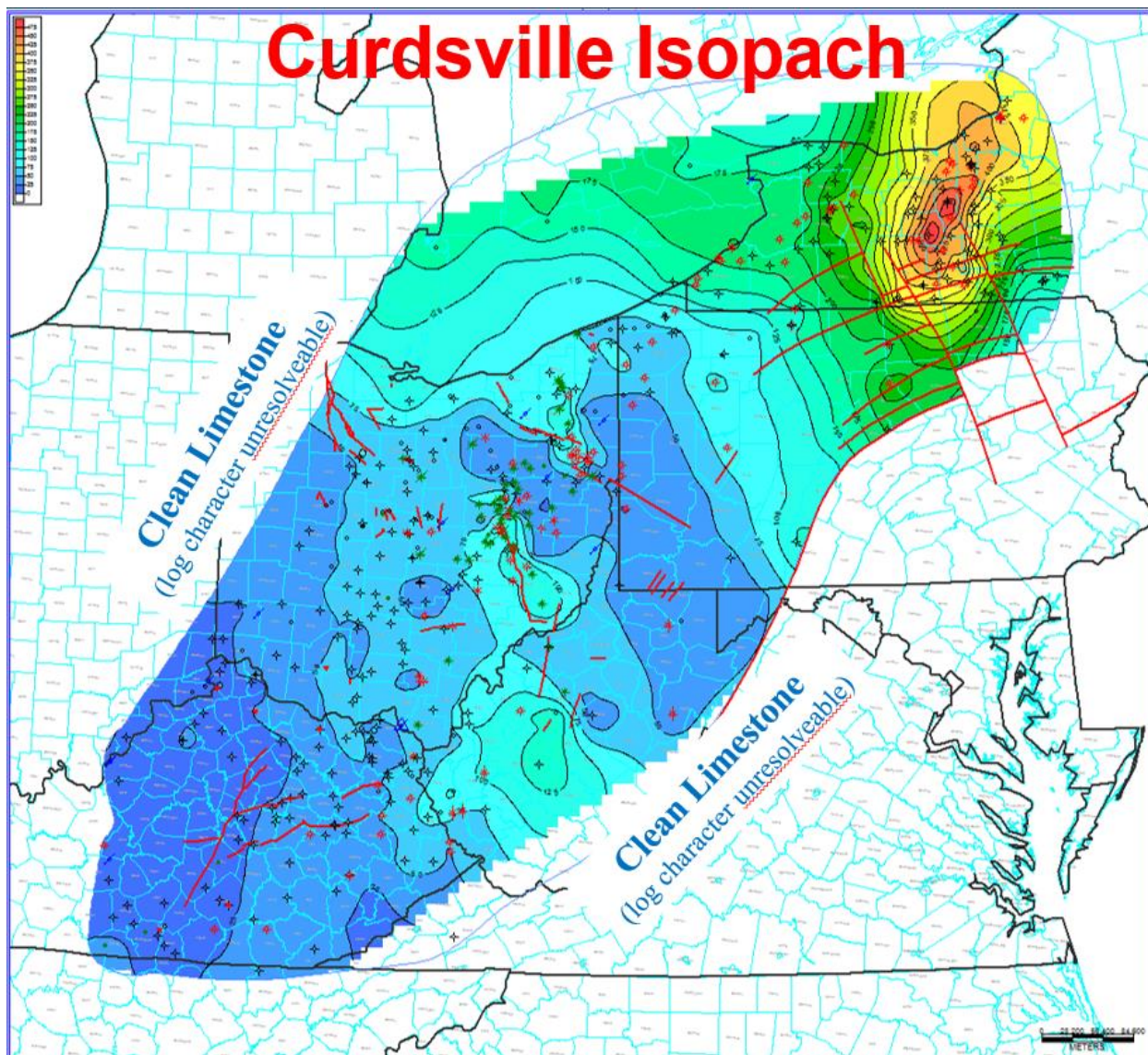
Figure 4-15. Isopach map of the Curdsville Member of the Lexington/Trenton Formation. Thickness in ft with a 25-ft contour interval.
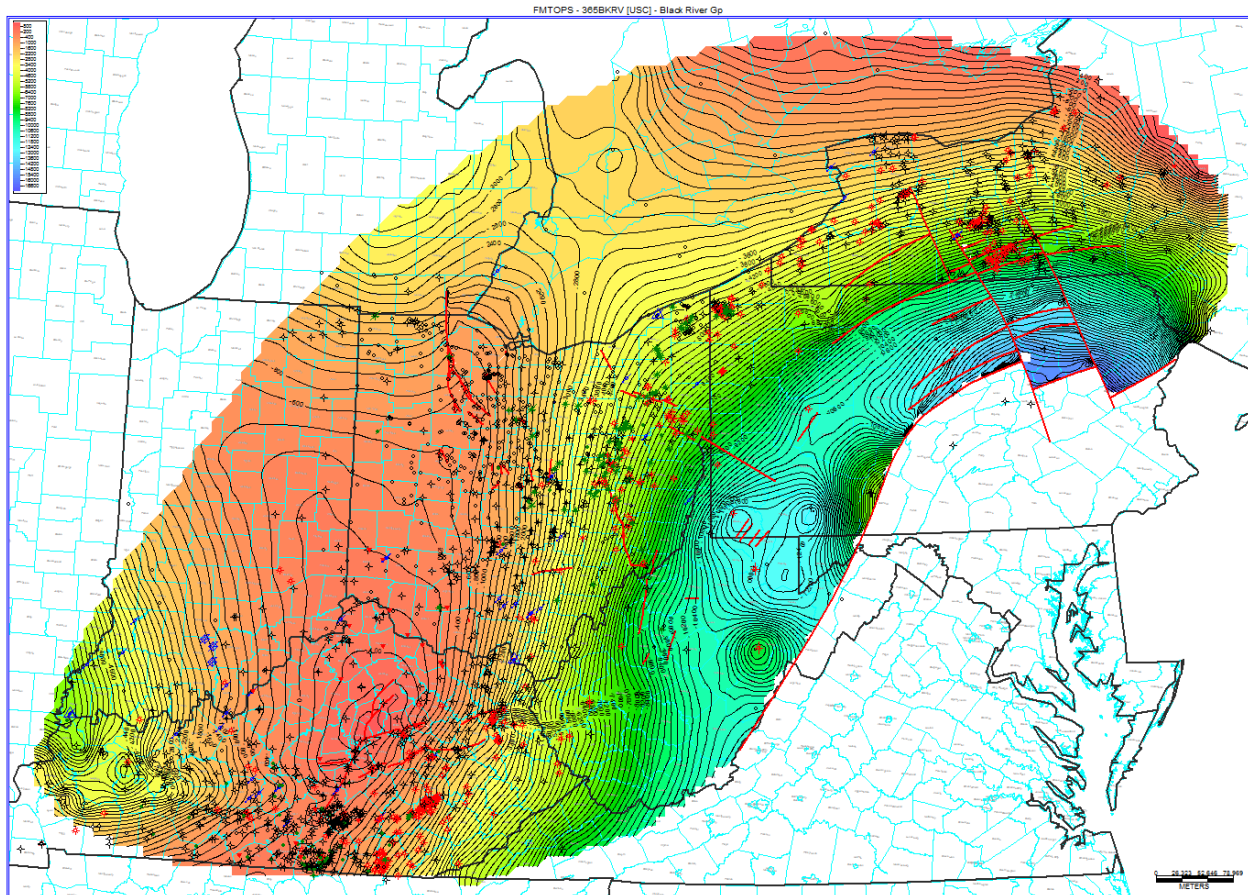
Figure 4-16. Structure map on top of the Middle Ordovician Black River Formation. Elevation in ft MSL with a 200-ft contour interval.

In addition to interpreting traditional stratigraphic tops from geophysical well logs, we have interpreted Upper Ordovician stratigraphy for three continuous cores from Kentucky (Figure 4-18). To aid in interpretation, the Upper Ordovician intervals of two of these (C-209 in Montgomery County and C-316 in Pulaski County) were photographed wet, in 10-ft intervals (Figure 4-19).

Figure 4-17. Map of the locations of three continuous cores from Kentucky that were described, photographed and sampled for stratigraphic correlation and source rock potential analysis.
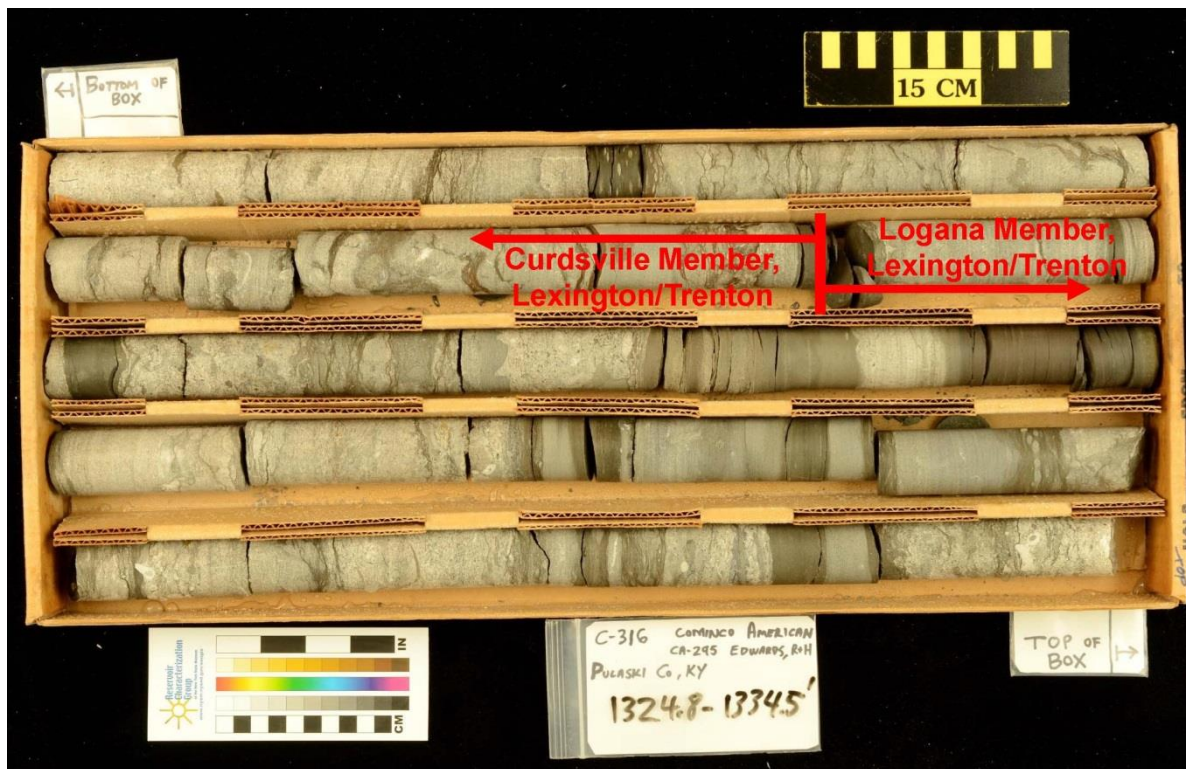
Figure 4-18. Photograph of the Cominco American 1 Edwards R&H core (C-316) in Pulaski County, Kentucky.   The stratigraphic break between the Logana and Curdsville members of the Lexington/Trenton Formation is shown in red.

5.0   CORE STUDIES

Various core studies core studies were conducted by members of the research team in order to document, describe, and interpret the lithology and gamma-ray (GR) character of Utica/Point Pleasant reservoir rocks throughout the Study area. In addition, this work included an evaluation of sedimentary features associated with Utica/Point Pleasant and equivalent rocks, and sought to refine the stratigraphy of the Utica/Point Pleasant interval in central Ohio.

5.1   High-Resolution Core Photography and Spectral Gamma-Ray Logging

5.1.1 Introduction

A key element for potential production from Upper Ordovician shales, as with any shale play, is TOC. High-resolution photography and spectral gamma-ray (SGR) core logging not only facilitates core descriptions but also provides an opportunity to link wireline log data to rock analytical data such as TOC. Using this approach may help identify a proxy for predicting TOC and/or better constrain chronologic stratigraphy. The method of using GR, SGR and density data as proxies for TOC has been performed for other shales in the Appalachian basin (including the Marcellus Shale), and in other basins such as the Alberta of Western Canada (Lunig and Kolonic, 2003).

5.1.2 Materials and Methods

As team lead for this particular task, ODGS reviewed available data on the Upper Ordovician section in Ohio, including core, rock cuttings, paper geophysical logs, LAS files and source rock analyses. ODGS recorded 761 cutting suites, 193 wells with TOC analyses, 68 wells with downhole SGR logs, 58 wells with LAS files and 48 cores. A series of location maps was generated for each data type to determine its geographic coverage across the state. We used these maps to determine where additional data needed to be collected to augment the existing dataset for this task.

Although cuttings samples were available from 761 wells, once the availability of preferred logs (i.e., GR, SGR and density run post-1990) was taken into consideration, only cuttings from 15 wells were chosen for TOC analysis. In addition, three rock cores were chosen for analysis. Data from these 18 well locations were added to the legacy database that contained TOC data for 193 wells, resulting in a TOC data count of 211 Ohio wells. Combining these data with data from wells in other states, and additional data that became public during the term of the Study, resulted in a grand total of 382 wells with TOC data.

Core sampling was imperative for this work because it provided the most accurate depth values for TOC analysis to incorporate into LAS logs. The cores chosen by ODGS were strictly based on geographic location, additional available data and overall condition, with little priority given to age and/or availability of modern logs because the core could be scanned as part of the present work. Prior to any sampling or scanning, high-resolution photographs were taken using a Nikon D700 camera. This provided a permanent visual record of the core in its initial condition. Each photo image file was named based on the core footage, box number and whether the core was wet or dry.

Once a core had been photographed and archived, it was scanned using the Core Lab SGL-300 Spectral Gamma Logger (SGL-300). The SGL-300 is owned by The Ohio State University's Subsurface Energy Materials Characterization & Analysis Laboratory (SEMCAL) and is housed at the ODGS Horace R. Collins Laboratory (HRC). It scans core at high resolution and creates LAS geophysical logs of GR, uranium-free gamma-ray (UFREE and KTh), potassium (POTA), uranium (URAN), thorium (THOR) and bulk density (RHOB). These logs allow geologists to accurately correlate core with other physical data. The SGL-300 is calibrated daily to a set of standards to ensure the production of accurate and consistent data that can be directly compared to all other core scans.

Core is scanned continuously from bottom to top at a rate of 6 in per minute when gathering SGR data and 3 in per minute when measuring RHOB. Information for each data type is recorded every inch, but in order for the SGL to create a "geophysical log-like curve," each data point is based on a progressing average of the previous 6 in of scanned core. In a single day, the maximum length of core that can be scanned is either 300 ft for SGR or 150 ft for RHOB. Cores in excess of these lengths require multiple days of scanning, which also requires recalibration and stitching together numerous LAS output files. To accommodate a seamless LAS merge, each subsequent scan began by rescanning the last 10 ft of core from the previous day. A total of 14 cores (eight from Ohio, three from West Virginia, two from Kentucky and one from New York) were photographed, scanned and converted to LAS files. No Pennsylvania core samples were available for this task.

To supplement the core scans, an additional 92 downhole geophysical logs were digitized using Neuralog software. This provided a total of 162 LAS files, 124 of which include TOC data. The TOC data were manually entered as a unique curve to each corresponding LAS file and were limited to wells that had 15 or more TOC data points. When adding TOC data that originated from well cuttings to an LAS file, a midpoint of the cuttings sample interval was chosen as its corresponding depth. However, TOC data derived from core could be added to the LAS file at their exact footage. This combined dataset was imported into the Landmark GeoGraphix® software and displayed in crossplots for further analysis.

Correlations were made to analyze multiple aspects of the collected data, including which element is driving the overall radioactivity; how core SGR scans relate to downhole SGR; if GR, POTA, URAN and/or THOR relate to TOC; and what, if any, relationships exist among different facies deposited during Lexington/Trenton-to-Point Pleasant time (Patchen and others, 2006). We evaluated linear trends in data and refer to a correlation coefficient 'r'. These correlations are presented in the Section 5.1.5 below.

5.1.3 High-Resolution Core Photography

ODGS completed the task of taking high-resolution photographs of core from the Upper Ordovician interval (including Kope, Utica, Point Pleasant, Upper Lexington/Trenton, Logana and Curdsville) in Ohio and equivalent core intervals from West Virginia, Kentucky and New York. Photographs were taken using a ceiling-mounted, full-frame, Digital Single Lens Reflex (DSLR) camera with an Auto Focus AF-S 24 – 70mm f/2.8 G ED lens. All photographs were exposed using color corrected 6000K light softboxes, creating consistent white balance. This consistency allows for a display of true colors that can be helpful when comparing core. When possible, both

wet and dry photographs were taken for each core box to capture better detail. Fourteen cores were photographed for this task (Table 5-1). Core locations span approximately 600 miles (mi) across the Study area, from east-central Kentucky through Ohio, West Virginia and into central New York (Figure 5-1).

Table 5-1. List of cores photographed and scanned with the SGL-300.

Core #	Name	State	County	Footage	Size (in)
3446	Todhunter	OH	Butler	27 – 381	2 ¼; Full Diameter
860	V. Apple	OH	Butler	67 – 693	2 ¼; Full Diameter/slabs
2535	Howerton	OH	Clermont	19 – 349	2 ¼; Full Diameter
2536	Sky Valley RC	OH	Clermont	21 – 319	2 ¼; Full Diameter
3003	Fred T. Barth	OH	Coshocton	5630 – 5749	3 ⅜; Full Diameter
2626	J. Goins	OH	Highland	600 – 1310	2 ¼; Full Diameter
3372	Prudential	OH	Marion	389 – 1604	2 ¼; Full Diameter
3409	Aristech	OH	Scioto	2734 – 3373	2 ¼; Full Diameter
254	Lost River	WV	Hardy	27 – 100	2 ¼; Full Diameter
256	Lost River	WV	Hardy	17 – 70	2 ¼; Full Diameter
768	Power Oil	WV	Wood	9417 – 9665	2 ¼; ⅓ Slab
139	Bender CG&E	KY	Boone	36 – 284	2 ¼; Full Diameter
209	M. Burchell	KY	Montgomery	20 – 904	2 ¼; Full Diameter
74NY5	Mineral Core	NY	Herkimer	21 – 763	2 ¼; ½ Slab

Figure 5-1. Regional map of Utica/Point Pleasant well locations for which cores were scanned and photographed. Facies map of Trenton/Point Pleasant time from Patchen and others (2006).

38
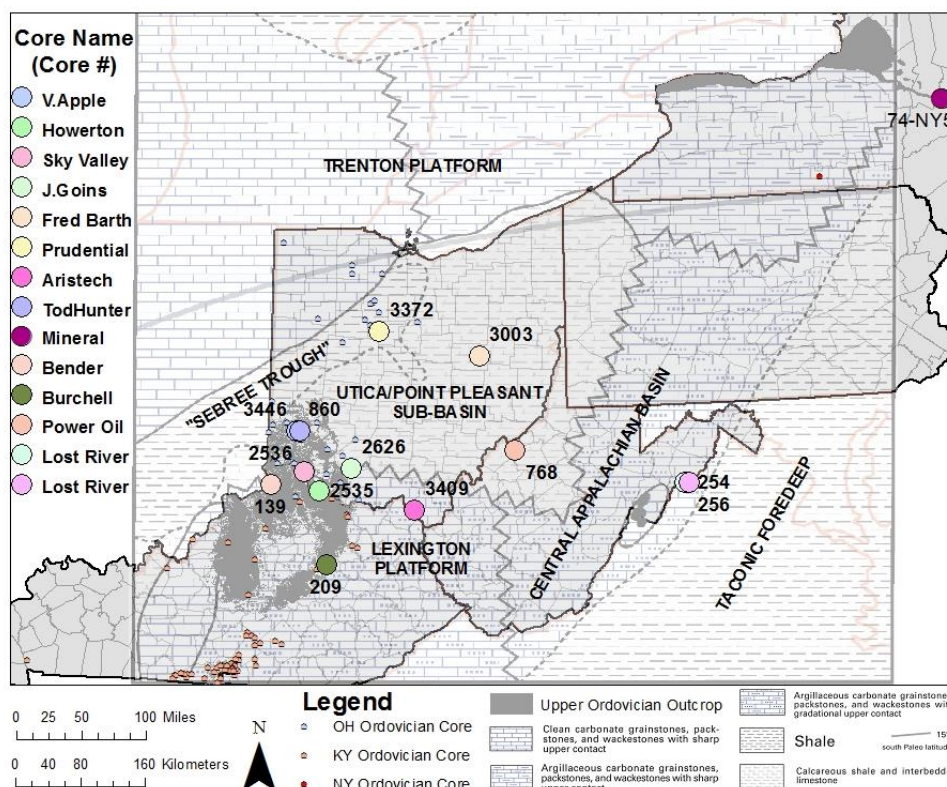
5.1.4 SGR Core Scan Results

5.1.4.1 *Kentucky*

The Bender CG&E No. 1 (#139) well is located in Boone County on the margin between the Lexington Platform and the Utica/Point Pleasant sub-basin (Figure 5-1). This well is approximately 25 mi southwest of the Sky Valley well and 40 mi from the Howerton well. There were many aspects of this core that made it difficult to collect good data and perform accurate correlations. Prior to scanning, a significant portion of this core needed to be organized, depth-checked and oriented correctly. Various intervals of this core were missing, most notably the bentonite beds (Millbrig and Diecke) in the Black River. Once the core was organized, it was scanned with surprisingly good results. The core scan matched well with the downhole logs, which include the bentonite marker beds, allowing for a reasonable correlation to the Ohio Howerton core scan. The best correlation was made using the URAN curve and to a lesser extent the GR, POTA and THOR curves. Even so, potassium was still the most influential element with respect to increasing GR readings. The scanned core data were merged with TOC data, which facilitated further data analysis.

The M. Burchell well (#209) is located in Montgomery County, farther south on the Lexington Platform (Figure 5-1). The SGR scan produced reasonable data because the core is in great condition, has good depth markings, and is largely intact. After creating the LAS file and adding TOC data, a reasonable correlation was made with the Bender well, which is about 75 mi to the northwest of the Burchell well. The intensity of GR in this core seemed to be affected mostly by potassium and, in some instances, uranium above the Kope. The TOC relationships are discussed further below.

5.1.4.2 *Ohio*

All but one of the Ohio cores containing Late Ordovician shale were located in the western half of the state. The Fred Barth No. 3 (#3003; Figure 5-1) is that exception, located in Coshocton County, just west of current Utica drilling activity. The Ohio cores were selected for scanning based on availability of additional data (e.g., TOC, wireline logs), location regarding facies and overall condition, which ultimately facilitated the correlation of these wells across the basin. There are two scans from cores in Butler County, two from Clermont, one from Coshocton, one from Highland, one from Marion and one from Scioto.

The Butler County wells were mainly chosen based mainly on their locations in the Utica/Point Pleasant sub-basin, close to the eastern edge of the "Sebree Trough." The "Sebree Trough" is a narrow northeast-southwest-trending feature described by many as a clastic-filled depression, extending from western Kentucky through southeast Indiana into northwestern Ohio (Patchen and others, 2006). Both cores are relatively shallow and include only the Kope Formation. Core from the Valentine Apple well (#860) is in fair to good condition, but is missing intervals and showed inconsistent depth markings. In spite of this, a realistic LAS file was prepared.

SGR data showed that a majority of the radioactivity was predominantly driven by the percentage of potassium in the Valentine Apple well. However, there were multiple intervals with more than 10 parts per million (ppm) thorium and uranium, which slightly increased GR readings.

Interestingly, the uranium and thorium spikes were cyclical and offset from one another. As uranium increased, thorium would decrease to zero and vice versa.

The second Butler County core (the Todhunter well, #3446) was chosen as a supplement to the Valentine Apple because they are situated only 900 ft apart. Core from this location is in poor condition and was very difficult to scan. There were missing intervals, varying volumes, and inconsistent depth markers, making it nearly impossible to synchronize with the scanner. An LAS file was created, but the accuracy of the data is suspect. In an attempt to salvage this scan, additional correlations and edits were made, but with little success.

Two cores near the Ohio River in Clermont County were selected for scanning, aiding in the correlation with the southern region of the Study area. These Clermont wells, the Howerton (#2535) and Sky Valley Rec Club (#2536), were drilled by ODGS as stratigraphic tests in the early 1980s, and cores cut at these locations are continuous from the Point Pleasant down to the Black River Formation. They straddle the margin between the Lexington Platform and the Utica/Point Pleasant sub-basin (Figure 5-1). This margin line is somewhat tenuous but is based on the overall thickness of the Trenton Limestone (Patchen and others, 2006).

Both cores were in excellent condition and provide a high confidence level in the SGR scans. Each scan started in the Black River, logging multiple bentonite beds (the Millbrig and the Diecke; see Figure 3-1), which provided good stratigraphic markers. The Sky Valley Rec Club well, located on the sub-basin side of the margin, was scanned first and had intriguingly low (near-zero) GR readings throughout the entirety of the log. Little variation in log readings made it difficult to interpret and correlate, but the scan appeared to be accurate when checked against known calibration standards. The scan also was compared to photographs and core descriptions, further confirming the data that indicate a good correlation between GR and increased shale percentage in the Point Pleasant. The scan revealed that the increase of GR in the Point Pleasant was a direct result of the increased potassium percentage.

Scans from the Howerton well, located on the Lexington Platform side of the margin, had considerably different results, showing higher levels of radioactivity and a notable increase of uranium levels in the upper Lexington. Considering that these wells are only 20 mi apart, similar results were expected. This difference in scan data was investigated further by comparing the rocks in cores from these two wells. Overall these cores are very similar, with the only noticeable exceptions being the nearly missing Point Pleasant and the thinner, less radioactively-intense bentonite beds in the Howerton core.

SGR data from the Howerton well were driven mostly by the percentage of potassium, considering that less than five ppm uranium or thorium were detected until the scan reached the upper portions of the upper Lexington/Trenton Formation. In this member, the most uranium detected was just over 10 ppm, but this did not cause a significant change in GR readings. Samples were taken from this core for TOC analyses, which are included in the LAS for this location.

Thirty mi to the northeast of the Howerton well, in Highland County, the J. Goins well (#2626) was selected due to its pristine condition and paleogeographic location in the Utica/Point Pleasant sub-basin (Figure 5-1). There were few to no missing intervals, and the core had not been excessively split or sampled. The LAS file from the scan was compared to the downhole log and

matched almost identically. The natural radioactivity occurring in this well is almost 100% from potassium percentage (Appendix 5-A). There are two small uranium-dominant horizons in the Kope but nothing more. Further data were collected for this well, resulting in a RHOB scan. The smaller diameter of this core presented a unique problem in gathering RHOB data. In order for the scanner to detect a change in density, the core had to be elevated on risers allowing it to sit closer to the cesium source. Overall, the scanned data from this well correlated very well with the nearby Clermont County wells. Core from this well differed in that it included the entire Point Pleasant and Kope intervals, which are not present in either Clermont County core. Samples were taken for TOC analyses, which were studied alongside the spectral/density log.

The Aristech well (#3409) is located approximately 50 mi to the southeast of the J. Goins well on the Lexington Platform (Figure 5-1). This core was in very good condition with few splits or missing pieces, consistent depth markings, and an abundance of supplemental data, including TOC and wireline logs that can be used for evaluation. The LAS file from the scanned core was merged to the downhole LAS file. This merge clearly illustrated that the core scan was about seven feet shallower than the downhole log. This discrepancy is probably caused from mislabeled depths during collection or re-boxing. The original scan depths were maintained when adding the TOC data. Even though this well is located on the Lexington Platform, it encountered about 120 ft of Point Pleasant Formation. Once again, potassium and thorium were the main elements responsible for the increase measure of GR. There were no specific radioactive beds in this core that could be directly linked to an increase in uranium. The uranium content in this core was never measured above six ppm and hardly measured above three ppm. On the other hand, this well displayed some high levels of thorium, with multiple beds measuring contents of 30 ppm or higher. Additional evaluations were completed and are discussed in Section 5.1.5 below.

The Fred Barth No. 3 (#3003) is located approximately 130 mi north of the Aristech well in Coshocton County near the center of the Utica/Point Pleasant basin (Figure 5-1). This core did not produce good SGR results due to its poor condition from over-sampling and missing intervals; approximately 50% of this core was missing when it was donated to the state. Attempts were made to scan the core and correct for missing intervals and changes in volume but with little success. These attempts were made because this is the only core available for study in eastern Ohio close to the current drilling activity. No useful SGR log data have been generated, but photographs were taken to illustrate the organic-rich intervals in this core.

The Prudential well (#3372) is located in Marion County in the northern portion of the "Sebree Trough" (Figure 5-1). This core was a good candidate for SGR scanning because it is a solid core and has modern wireline logs, TOC, X-ray Diffraction (XRD), scanning electron microscopy (SEM) and source rock analysis data. Overall, the scan was successful, but there were some concerns regarding depth, likely due to original mislabeling during core collection and re-boxing. The mislabeled depths resulted in a 20-ft discrepancy between the core scan and downhole logs. As with the previous wells, the GR levels from this core were produced from the increased levels of potassium. Many beds had greater than 30 ppm thorium, and several had uranium levels slightly above 10 ppm, but neither uranium nor thorium caused significant percentage increase in GR. A major problem was still present regarding the TOC data for this well. Even with an understanding of the log discrepancies, there is no way of knowing which depths were used by the five clients who sampled this well for TOC. Therefore, the scanned data cannot be definitively matched with the TOC analyses performed for this well.

5.1.4.3   West Virginia

The Power Oil well (#768) is located in Wood County in the southeast portion of the Utica/Point Pleasant sub-basin (Figure 5-1). Even though the Utica/Point Pleasant interval in this well is thinner than noted in the Aristech well, which is located on the Platform, it is considered to be located in the sub-basin due to the thinning of the overall Lexington/Trenton Formation. The data collected for this well were inconsistent because only a ⅓ slab of the core was available and sections were missing, which challenged the scanner capabilities. The data were converted into an LAS file and merged with the borehole geophysical LAS log and TOC data. Due to missing intervals in the Black River, finding good stratigraphic markers required extensive data manipulation. After several attempts to correct for the missing intervals and inconsistencies, we determined that further data manipulation would not be beneficial for this Study. Consequently, the scanned data were left in their original state, which revealed that the potassium percentage was still the most influential element to GR (Appendix 5-A).

The Lost River cores (#254 and #256) were drilled in 1977 as a part of the Potomac River Watershed Project, Floodwater Retarding Dam No. 27, and are located in the Central Appalachian basin near the Taconic Foredeep (Figure 5-1). Both cores include the Martinsburg Formation (Utica equivalent in part), are less than 100 ft in length, and are in very good condition. The scans were successful in gathering SGR data, but the short length and small shale volume limited their use. No additional data were available for these core locations.

5.1.4.4   New York

The New York Mineral test well (#74NY5) is located in Herkimer County in a deeper-water environment east of the carbonate platform (Figure 5-1). This slabbed core is in excellent condition with no missing intervals, which allowed for the collection of very good data. Overall, the GR was evenly influenced by potassium and uranium with very little amounts of thorium. The relationship, albeit weak, between URAN and GR for this well was not seen in any other well scanned for this task and may be a result of deeper-water deposition. The TOC data were added to the scan and additional correlations were made with Ohio, West Virginia and Kentucky core data.

5.1.5 Discussion

5.1.5.1   Overview

The GR log was the first nuclear well log used in industry and was introduced in the late 1930s (Schlumberger, 1997). This log measures natural radioactivity in API units, and is generally used as a correlation tool. The natural radioactivity in rocks comes from any of three elemental sources, uranium, potassium and/or thorium. Each element emits unique gamma rays with characteristic energy levels that can be measured using a scintillation detector. Knowing the amount of each element in a rock can help determine several features, but only depositional environment and TOC are discussed here. Knowing the origins of these elements and how they react in different environments is essential in determining depositional history.

Uranium-238, the most common isotope of uranium, is naturally occurring in seawater at around three parts per billion (ppb). Disseminated uranium dioxides precipitate out of the seawater onto organic matter by forming organometallic complexes at the sediment-water interface under

anoxic conditions (Swanson, 1960; Lunig and Kolonic, 2003). This implies that rocks with high uranium content may have been slowly deposited in anoxic conditions, allowing for extended time at the sediment-water interface, and consequently may be associated with elevated levels of organic carbon.

In contrast, potassium and thorium do not occur naturally in seawater but are transported there for deposition. Potassium is most commonly found in clays or potassium feldspars. The clay materials associated with potassium are illites and smectites, which are chemically weathered from a parent material.   Thick deposits of clays generally are a result of terrigenous, pelagic or hemipelagic deposition (Bohacs, 1998; Boggs, 2006). Potassium-rich clays are generally not associated with organic matter, but they may amalgamate and can be deposited simultaneously in lower-energy waters. Thorium is often associated with heavy minerals, such as sulfides, oxides and some silicates. These usually originate and weather from igneous parent material and are typically deposited in beach or alluvial environments, sometimes referred to as heavy-mineral placers (Boggs, 2006).   Such environments are higher-energy settings that are generally oxygenated. Because organic matter is subject to oxidation and bacterial decomposition, it is unlikely that thorium and organic carbon would be concurrently deposited.

5.1.5.2   *Correlations*

The compiled dataset, including all SGR core scans, TOC data and downhole geophysical logs, was standardized and imported into the Landmark GeoGraphix® software for further evaluation. Crossplots were generated to analyze the correlations of multiple aspects, including: (1) core scan versus downhole SGR logs; (2) prevalent radioactivity; (3) TOC versus GR, URAN, POTA or THOR; and (4) whether relationships vary among the different facies deposited during Lexington/Trenton-to-Point Pleasant time. All correlation coefficients are provided in Table 5-2, and all crossplots are included in Appendix 5-A. Correlations assessed linear trends and refer to a correlation coefficient 'r', the classification of which is as follows:

- 0.8 to 1.0   or   -0.8 to -1.0   (very strong relationship)
- 0.6 to 0.8   or   -0.6 to -0.8   (strong relationship)
- 0.4 to 0.6   or   -0.4 to -0.6   (moderate relationship)
- 0.2 to 0.4   or   -0.2 to -0.4   (weak relationship)
- 0.0 to 0.2   or   -0.0 to -0.2   (no relationship)

Table 5-2. Correlation coefficients for each crossplot of GR, POTA, URAN, THOR, KTH, TOC and RHOB. * denotes wells that have density crossplots.

Well Name	GR vs POTA	GR vs URAN	GR vs THOR	GR vs KTh	TOC vs GR	TOC vs POTA	TOC vs URAN	TOC vs THOR	TOC vs RHOB
All Wells in Study*	0.588	0.285	0.447	0.981	-0.008	-0.251	0.101	0.122	-0.304
All Core Data (Scanned Core)	0.631	0.307	0.201	0.982	-0.014	-0.260	0.098	0.126	-0.363
Active Area (Eastern OH, Northwestern PA)*	0.879	0.597	0.889	0.961	-0.099	-0.266	0.238	0.201	-0.295
Inactive Area (Western OH, KY, NY, PA, and WV)*	0.597	0.253	0.334	0.998	0.117	-0.246	-0.141	-0.116	-0.252
Bender_KY139	0.483	0.106	0.185	0.995	0.250	0.255	-0.144	0.041	Null
Burchell_KY209	0.464	0.308	0.065	0.993	-0.424	-0.267	-0.069	0.201	Null
Aristech_OH3409	0.853	0.454	0.377	0.999	-0.441	-0.384	-0.149	-0.137	0.092
Power Oil_OH768	0.667	0.126	0.078	0.999	-0.280	-0.335	0.019	-0.195	Null
Mineral_NY74-NY-5	0.250	0.231	0.055	0.987	0.441	-0.153	-0.029	-0.013	Null
Hershberger Devon Data*	0.978	0.957	0.972	0.980	-0.164	-0.199	-0.128	-0.221	-0.714
Chumney Family Devon Data*	0.976	0.865	0.967	0.981	-0.214	-0.328	0.033	-0.273	-0.629
Richman Farms Devon Data*	0.976	0.946	0.963	0.979	-0.019	-0.070	0.069	0.074	-0.734
Georgetown Marine_OH5073 (Sample)*	0.944	0.249	0.908	0.954	-0.345	-0.282	-0.133	-0.567	0.317
Howerton_OH2535	0.626	0.271	0.124	0.995	-0.372	-0.161	0.001	-0.151	Null
J.Goins_OH2626	0.744	0.313	0.134	0.998	-0.231	-0.377	0.416	0.231	Null
Mull Edith_OH3890 (Sample)*	Null	Null	Null	Null	0.317	Null	Null	Null	-0.432
Prudential_OH3372	0.89	0.427	0.289	0.999	-0.579	-0.523	-0.283	-0.268	Null

The first step in our evaluation was to assess the relationship between the SGR core scans generated by the SGL-300 and the downhole SGR logs. The most notable difference between these is the total GR curves. The SGL-300 produces very consistent results because it was calibrated to the same set of standards at a constant gain setting on a daily basis, whereas the downhole logs were collected by different companies using different standards that are calibrated at various gain settings. The gain setting simply increases or decreases the amplitude of the GR signal. The SGL-300 gain is consistently lower than most downhole logs, but the overall signals are the same. Another difference, which is thought to be a product of scintillator resolution, is how well the radioactive elements are recorded. The SGL-300 uses a high-resolution scintillator

that easily differentiates the radioactive gamma characteristics of URAN, POTA and THOR, whereas the scintillators on downhole wireline tools are not as good at separating the unique gamma signals. This is best observed when comparing the GR/POTA, GR/URAN and GR/THOR crossplots from any core scans to the same crossplots from a downhole well log.

The best radioactive correlations from core scans are GR/POTA, which tend to show a strong to very strong relationship, whereas THOR and URAN show a weak to no relationship. Compared to the same GR/POTA, GR/URAN and GR/THOR crossplot correlations from downhole logs, all but one correlation is very strong. These differences need to be considered when using SGR data for further analysis.

Acknowledging that core scans and downhole logs vary in resolution was important when determining which radioactive element was generating GR variations. For this part of our work, only data from the core scans were used. A multi-well analysis on the entire basin demonstrated a decreasing strength in relationship to GR from POTA to URAN to THOR. The POTA had the most consistent influence on GR with an overall core data r-value of 0.631, indicating a strong relationship. This relationship did vary among facies; the strongest occurred in the Utica/Point Pleasant sub-basin, on the Lexington Platform margin, and in the "Sebree Trough." The Prudential well in the northern portion of the "Sebree Trough" had the strongest GR/POTA relationship with an r-value of 0.890. This is likely due to the increased water depth and decreased energy in the sub-basin and trough. The weakest GR/POTA relationships occurred farther down on the Lexington Platform and in New York. The Burchell well in Kentucky had a moderate relationship (r = 0.464), and the New York core had a weak relationship (r = 0.250). The weaker relationship on the Lexington Platform is likely due to increased energy and carbonate percentage. The very low GR/POTA relationship in the New York core is different altogether and may be a result of its clastic source, which is unique to this location.

The basin-wide GR/URAN core data multi-well relationship, although not as significant as GR/POTA, is still interesting. Of the three radioactive elements, uranium has the highest weight percentage influence on the total GR, allowing very small amounts to influence total radioactivity. This could be a factor in the overall weak GR/URAN relationship (r = 0.307) in Upper Ordovician shales. The statistical relationship varies from almost nil (r = 0.126) in the Power Oil well to moderate (r = 0.427) in the Prudential well. There are no prevailing trends among the different facies, but we argue that the deeper, less-oxygenated water in the "Sebree Trough" may play a role in statistical relationships we observed.

The last radioactive element that influences GR is thorium. Based on the results of our work, however, thorium does not play a significant role. This is evidenced by the very weak relationship (r = 0.201) exhibited by our multi-well analysis of core data. Further, most wells evaluated in this task, with the exception of the Prudential, show no relationship, with r-values ranging from 0.055 to 0.134. The Prudential well has a weak GR/THOR relationship (r = 0.289). This may be due to a few beds with higher levels of thorium, but as a rule, only very minor amounts of thorium are present.

5.1.5.3   Relationships with TOC

Initially, all well data collected as part of this task were evaluated together to determine whether a relationship exists between Utica and equivalent GR signatures and TOC, but this

approach provided unexpectedly poor results (Figure 5-2). The multi-well regression produced an r-value of -0.008. In addition to the lack of correlation, the regression line is negative. Generally, we would expect to see TOC increase along with GR. Investigating further, an analysis utilizing only the high-resolution core data still showed no correlation between GR and TOC (r = -0.014). The last evaluation of a potential multi-well GR/TOC relationship used data near the active drilling portion of the play, which includes eastern Ohio counties and northwestern Pennsylvania. Again, a negative correlation was derived (r = -0.099). In fact, there was a weak to no relationship for GR/TOC for all but four wells evaluated in this task. These wells (i.e., the Burchell, Mineral, Aristech and Prudential) displayed a moderate relationship. At this point, the Prudential well was eliminated from consideration due to its questionable core depths. Of the three remaining wells with a moderate GR/TOC relationship, only one had a positive correlation – the New York Mineral Core (r = 0.440). This could be a result of deposition of uranium and organic matter in deeper waters.

**Utica Consortium
All Wells in Study
CGR v TOC**

Active Well Regression Analysis Equations:
y = 66.911476 - 63.743423x   r = -0.424979

Multi-Well Regression Analysis Equations:
y = 131.071472 - 38.092655x   r = -0.008281
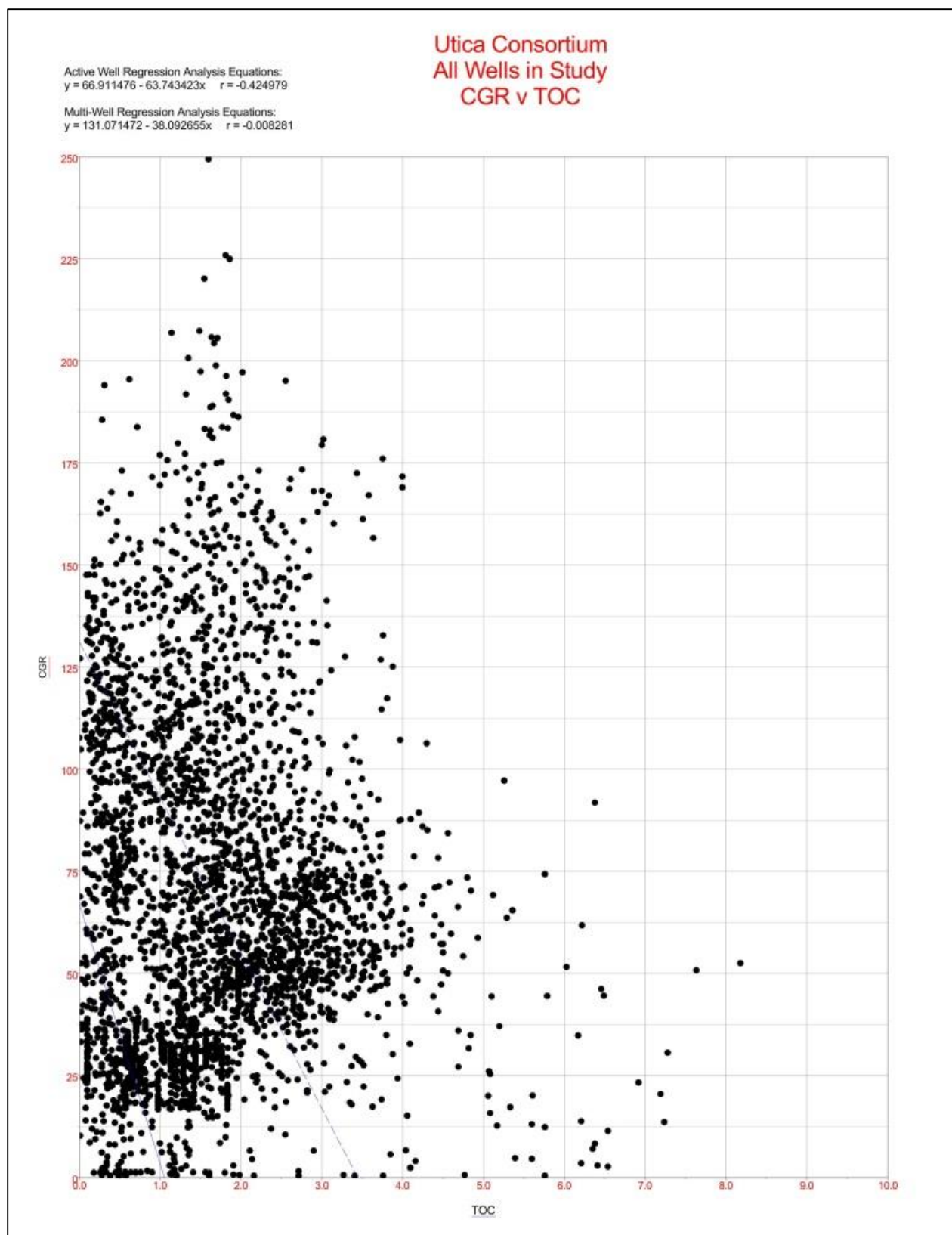
Figure 5-2. Correlation crossplot for core gamma-ray (CGR) and TOC using all wells in the Study.

Considering the GR signature is a composite of three radioactive elements, and no significant relationship was observed between GR and TOC, little correlation was expected when evaluating the relationship of TOC to POTA, URAN or THOR. The overall POTA/TOC relationship was weak (r = -0.251), when using the entire well dataset. An encouraging aspect was the negative regression, which made sense considering potassium has no real depositional relationship to TOC. The relationship was consistently weak even when evaluating only core data, active/inactive drilling areas, facies changes and each formation. Correlations were made for individual wells and varied from no relationship at the Richman Farms well (r = -0.070) to a weak relationship in the Aristech well (r = -0.384).

The URAN/TOC relationship also was weak to nonexistent. The multi-well analysis using all data collected for this task had no relationship (r = 0.101). Similar to the POTA/TOC relationships, no matter how it was tested, the URAN/TOC relationship produced r-values of 0.001 to 0.237. One weak relationship (r = 0.237) came from the active drilling area test. An anomalously high relationship of r = 0.416 was observed from the J. Goins well, indicating a moderate relationship, but this was considered to be an artifact of having too few data points.

The last radioactive element potentially related to TOC was thorium. Little relationship was expected between the two, and the results of our evaluation confirmed this. Using all the wells in the dataset, we observed no relationship (r = 0.122). In fact, only one well (the Georgetown Marine well, which is located in Belmont County, Ohio) showed a moderate relationship. Like the J. Goins anomaly noted above, we have interpreted the relationship reported for the Georgetown Marine well to be a result of a limited dataset.

This work has demonstrated that GR/TOC and/or URAN/TOC relationships only develop in certain shale systems, and the Utica/Point Pleasant system in the Appalachian basin is not one of them. This may be due in part to the high percentage of carbonate present in these rocks. The Utica is described as containing 20% carbonate and the Point Pleasant 60% (Schumacher and others, 2013). Another reason could be position of the redox boundary relative to the sediment-water interface and/or length of depositional anoxic conditions. A number of factors could play a role in the weak relationships of GR, POTA, URAN and THOR to TOC, but suffice to say, none of these support the creation of a proxy for predicting TOC in the Utica Shale play.

5.1.6 RHOB to TOC

Although not part of the original SGR core scanning task, we have investigated the potential relationship of RHOB to TOC, given the disappointing findings of our SGR/TOC statistical evaluations. Bulk density relates to TOC because of the low grain density of organic matter, which can range from 0.95 to 1.6 grams/cubic centimeter (g/cm^3). These are much lower than typical mineral grain densities, which typically vary from 2.5 to 3.0 g/cm^3. The relationship is not constant, however, and can vary greatly with both organic type (Type II vs. Type III) and thermal maturity (Cluff and Holmes, 2013). Other variables that must be considered are amounts of pyrite, formation porosity and mass of organic carbon (Schmoker, 1993). The following are examples gathered in this study to show both the possibility and inconsistency, illustrating the localized analysis that needs to be done when predicting TOC.

When using all well data for this analysis, RHOB/TOC exhibits a weak relationship (r = -0.304). However, when evaluating individual wells, much better relationships were observed.

The best example comes from the Richman Farms well (Medina County, Ohio), which showed a strong RHOB/TOC relationship (r = -0.734). Other well correlations confirm this relationship and are included in Appendix 5-A.

5.1.7 Summary and Conclusions

During shale deposition, several factors play important roles in the preservation of radioactive elements and organic matter. The presence of potassium, uranium and thorium in shales can help determine the depositional environment(s) for the unit, as well as the likelihood that organic matter will be deposited. A good example of this is the Devonian Marcellus Shale, which has a good correlation among GR, uranium signature and TOC measurements (Cluff and Holmes, 2013). Unfortunately, the Upper Ordovician shales in the Appalachian basin do not exhibit this same relationship. The GR intensity for Utica and equivalent rocks is dominated by the presence of potassium, and there is no correlation with the amount of organic matter. Factors that may prevent such a relationship include, but are not limited to, the influence of carbonate material, the lack of available uranium in seawater, or the amount of oxygen in the system. This investigation clearly demonstrates that TOC does not directly correlate to any radioactive material in the Utica/Point Pleasant interval. Other methods may be better gauges for predicting TOC in the Ordovician shales, such as bulk density and/or the Δlog R method (see Meyer and Nederlof, 1984; Passey and others, 1990; and Herron, 1991).

5.2   Core Description

5.2.1 Five Cores from Ohio

Devon Energy kindly provided access to five Ohio cores for description and analysis by Smith Stratigraphic LLC. Core descriptions, logs, core photographs, thin section descriptions and microphotographs, as well as TOC and carbonate content data, were prepared for these locations. The Devon wells are mainly in the western limits of the oil window, west of most of the current drilling activity, but the stratigraphy and rock types present are likely to be the same. Figure 5-3 shows the locations of these five cores.
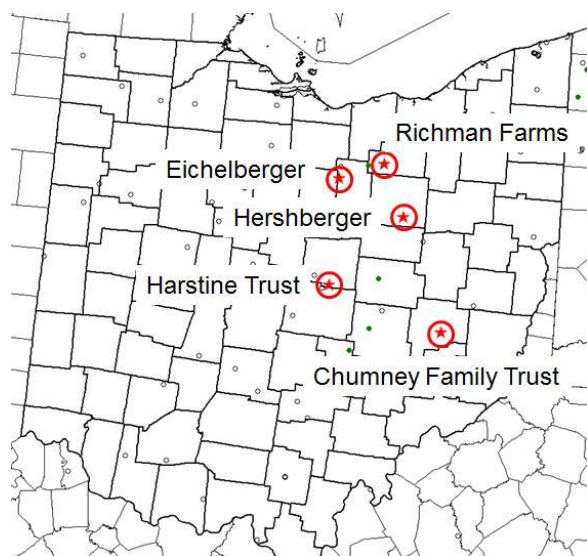
Figure 5-3. Map of Ohio showing the locations of five Devon Energy cores donated for this Study.

5.2.2 Cored Intervals, Nomenclature and Mineral Constituents

Figure 5-4 shows the relationships of the intervals cored in the five Devon Energy wells to the stratigraphic nomenclature used in the Study and by Devon Energy, and to organic-rich and organic-poor zones in the Study area. The Richman Farms, Eichelberger and Harstine Trust cores (Figure 5-5 through 5-7) extend from Kope down into the Curdsville Member of the Lexington/Trenton Formation. The Chumney Family Trust and Hershberger cores (Figures 5-8 and 5-9) are shorter and include mainly the Point Pleasant to Curdsville Member. The following core displays (Figures 5-5 through 5-8) include the logs, measured carbonate content and TOC (at a spacing as low as one per ft), detailed core descriptions done at the cm-scale, and graphical presentations of the relative abundance of various rock constituents from thin sections.
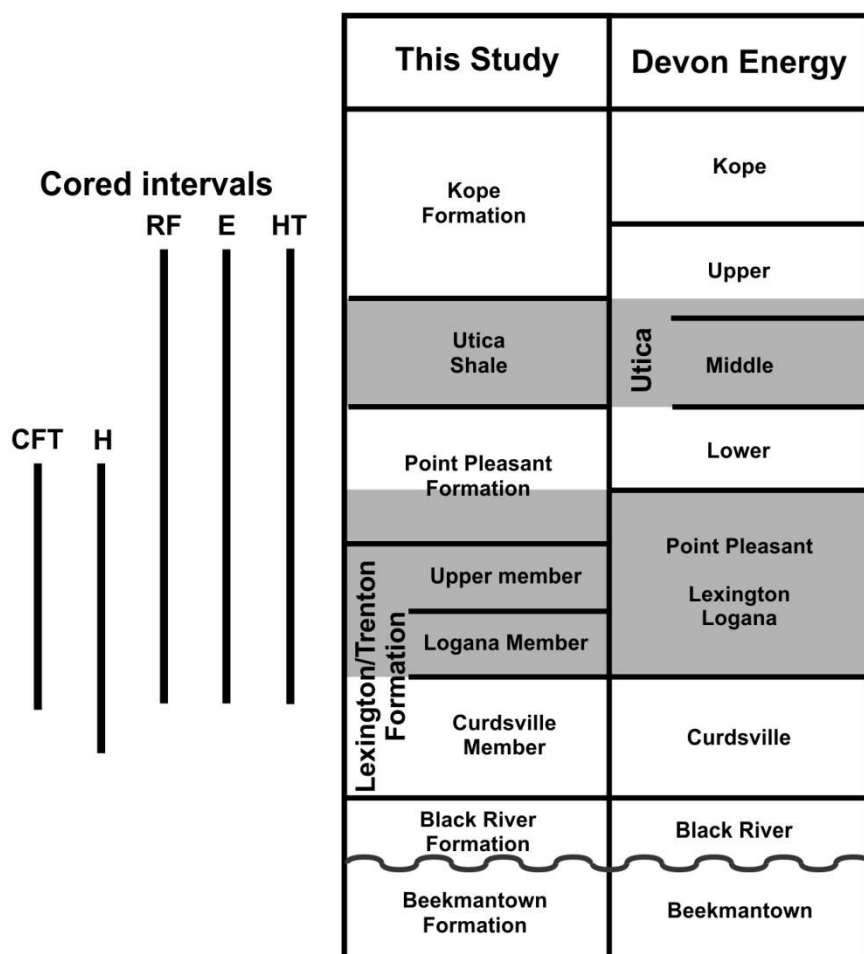
Figure 5-4. Comparison of Late Ordovician lithostratigraphic nomenclature used for this Study with organic-rich and organic-poor zones and cored intervals in five Devon Energy wells in Ohio. Cores include: CFT - Chumney Family Trust; H - Hershberger; RF - Richman Farms; E - Eichelberger; and HT - Harstine Trust).

The organic-rich units in Figure 5-4 are shaded gray. The Kope Formation consists primarily of thin interbeds of gray and black shale. The Utica Shale is a black, organic-rich shale with higher carbonate content than the overlying Kope. The upper part of the Point Pleasant Formation is organic-poor, whereas the lower portion is more organic-rich. The upper Lexington/Trenton

Formation and Logana Member are also organic-rich, whereas the Curdsville Member is organic-poor.
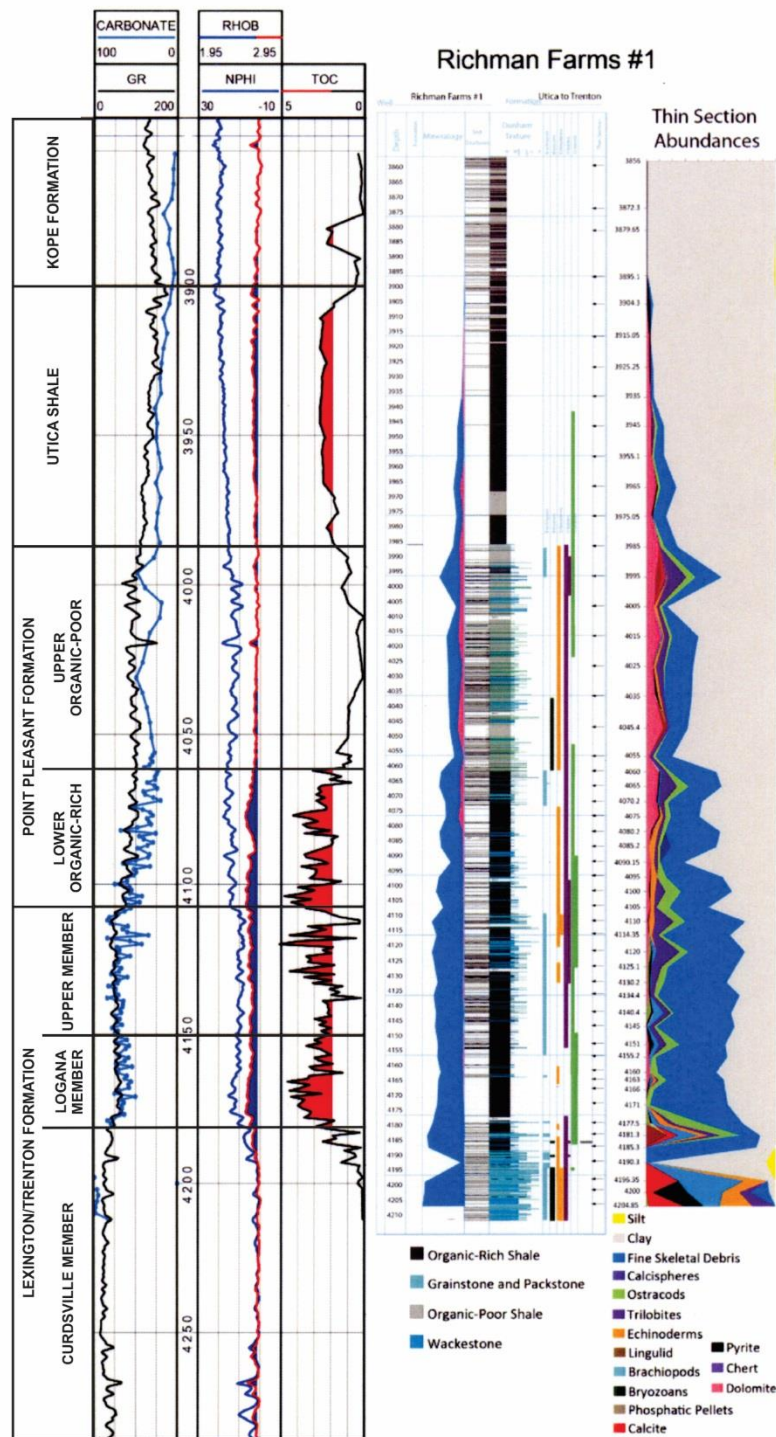
Figure 5-5. Richman Farms No. 1 well with core description logs, carbonate content, TOC and thin section abundance.
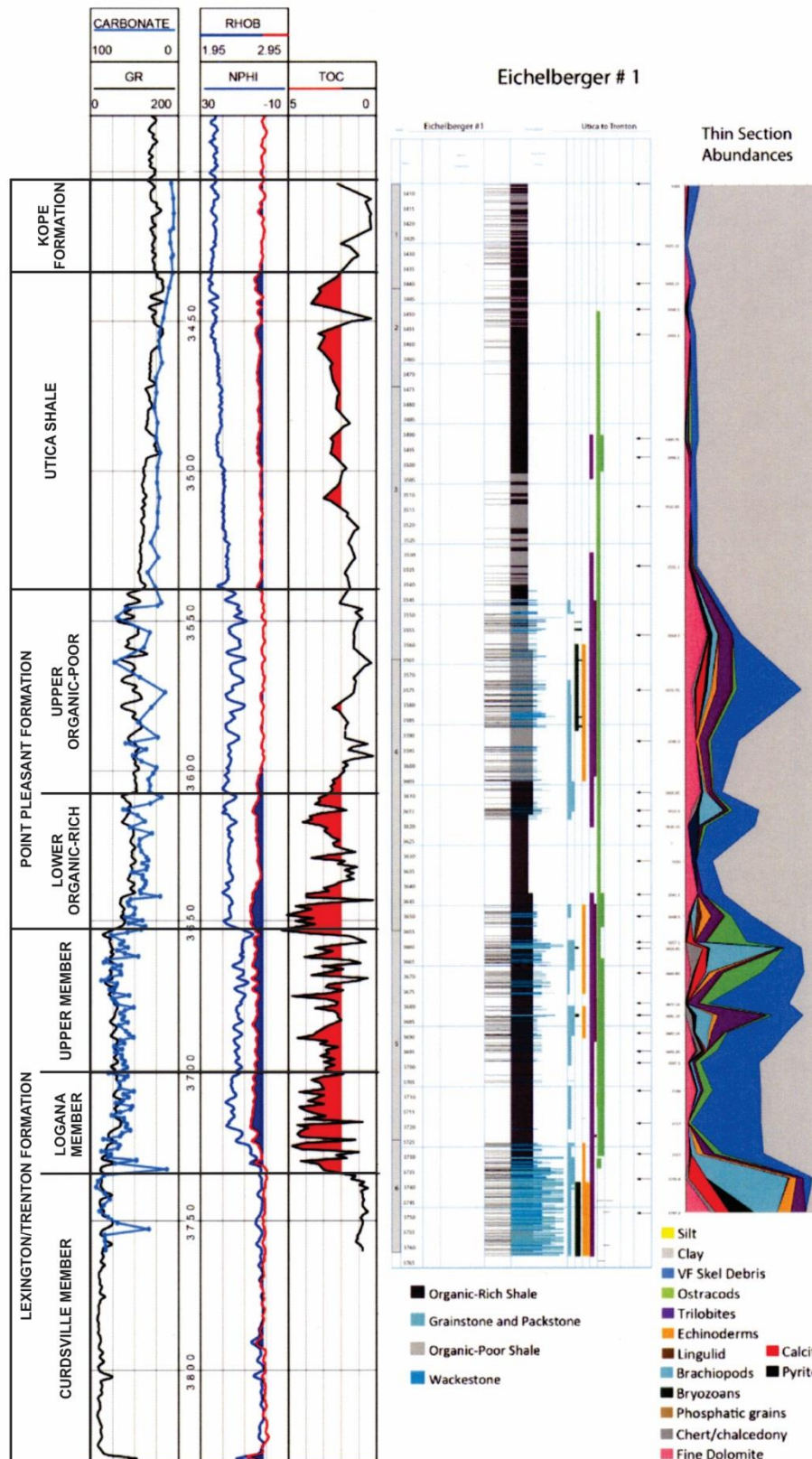
Figure 5-6. Eichelberger No. 1 well with core description, logs, carbonate content, TOC and thin section abundance.

52
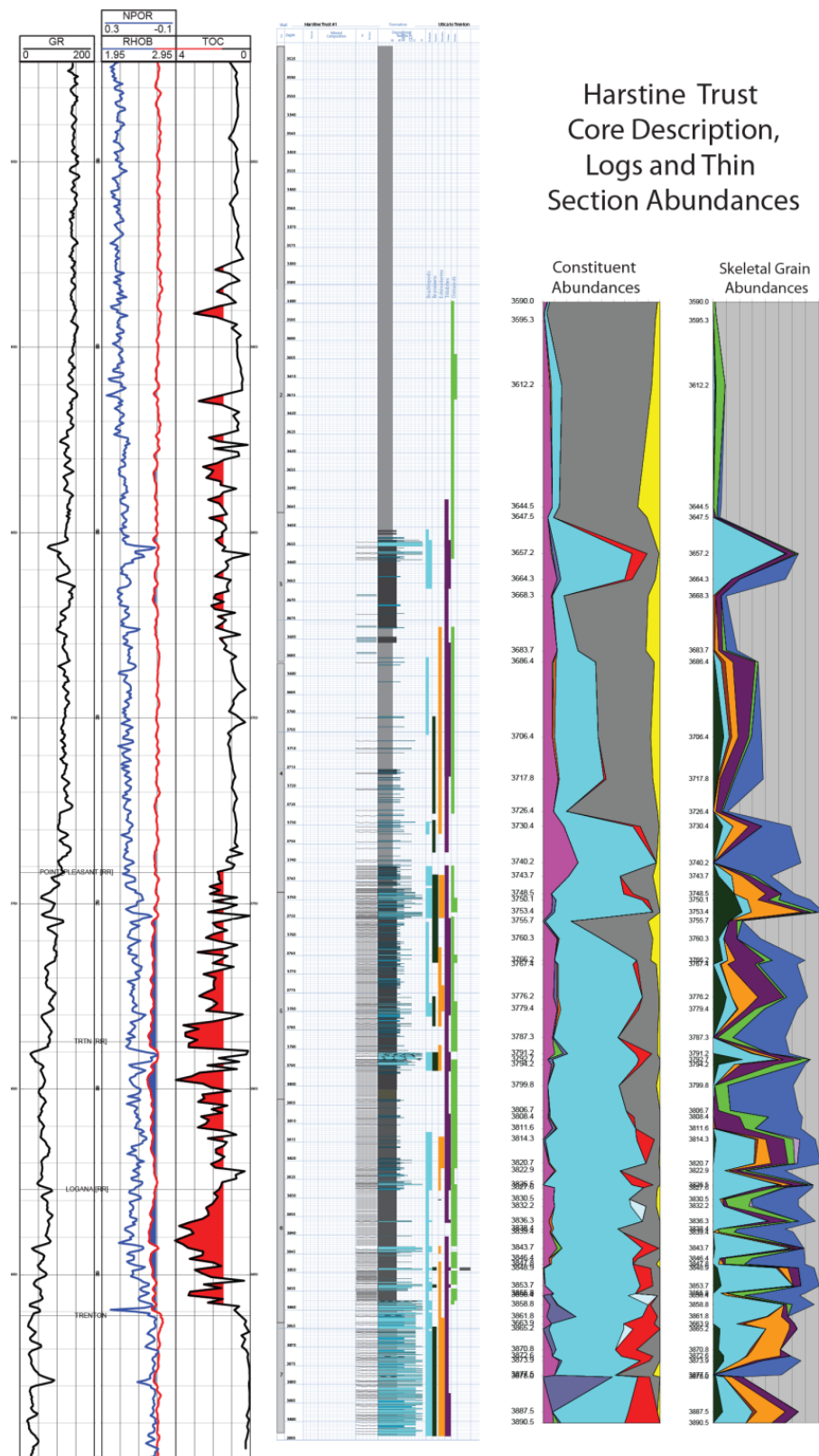
Figure 5-7. Harstine Trust No. 1 well with core description, logs, carbonate content, TOC and thin section abundance.

53

Hershberger #1P
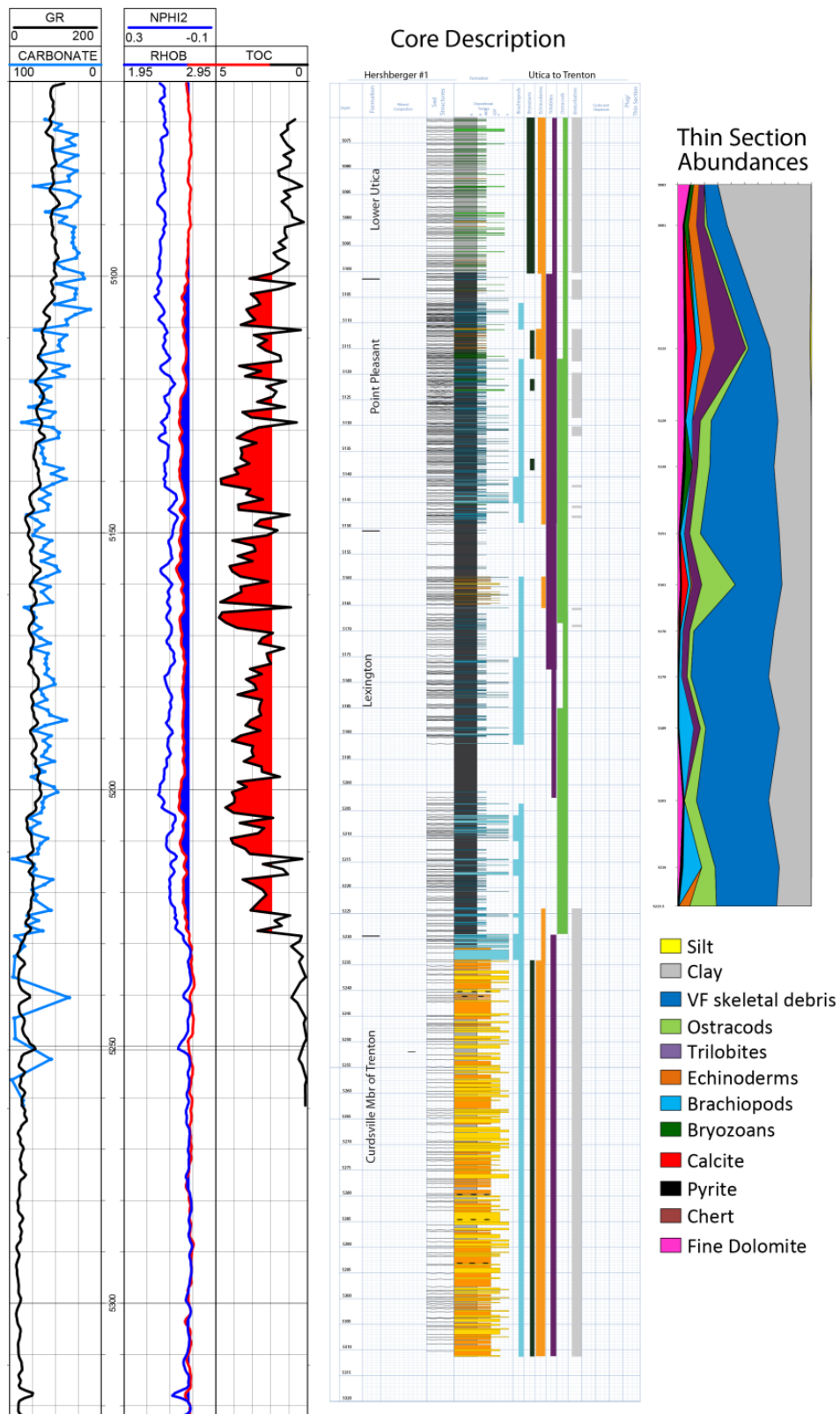
Core Description

Figure 5-8. Hershberger No. 1 well with core description, logs, carbonate content, TOC and thin section abundance.
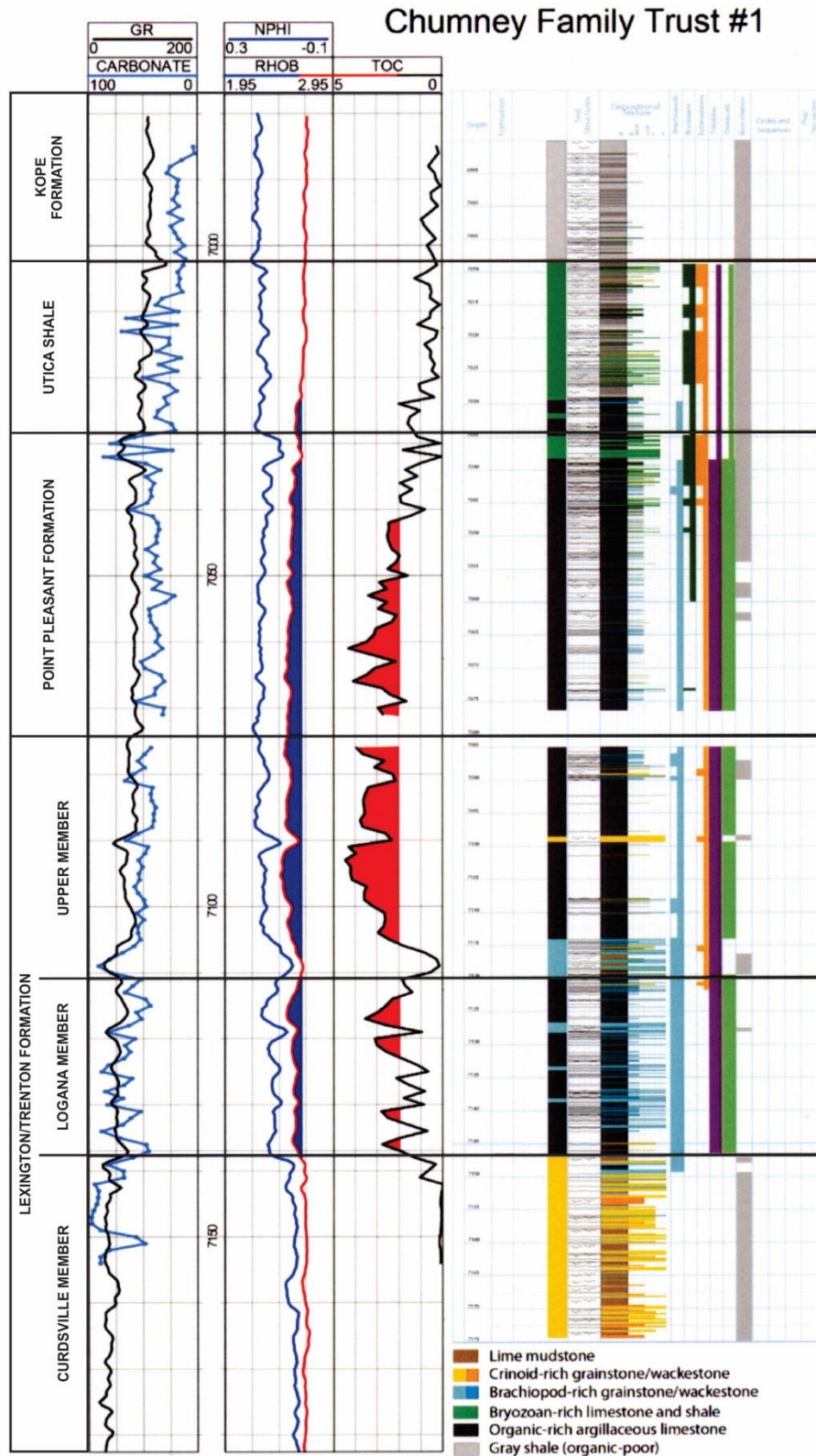
Figure 5-9. Chumney Family Trust No. 1 well with core description, logs, carbonate content and TOC.

5.3   Petrography

The initial step when trying to capture the rock types present in these cores was to make thin sections and describe them in detail. Although it is desirable to make a thin section every foot, or otherwise at a high frequency to capture all the variations, Devon chose a wider spacing for this work to manage costs. Each thin section was described semi-quantitatively using visual estimates of all the constituents present and the estimates entered into a spreadsheet. The rock constituents found include dolomite, very minor diagenetic anhydrite and chert, pyrite, skeletal grains, pellets, calcite, clay and quartz silt. A sample spreadsheet is found in Table 5-3.

Table 5-3. Spreadsheet of data from the Harstine Trust well showing the relative abundance of various rock constituents.

Thin Section Depth	Dolomite	Anhydrite	Chert/Chalcedony	Pyrite	Skeletal	Pellets	Calcite	Clay	Silt	Total	Grain density
3589.95	5	0	0	1	1	0	0	91	2	100	2.73
3595.3	1	0	0	0	2	0	0	93	4	100	2.70
3612.2	6	0	0	1	9	0	0	77	7	100	2.73
3644.5	8	0	0	0	6	0	0	67	19	100	2.70
3647.45	4	0	0	0	5	0	0	80	11	100	2.70
3657.15	7	1	3	0	65	0	13	10	1	100	2.72
3664.34	12	0	3	0	55	0	6	20	4	100	2.72
3668.32	7	0	0	1	10	0	0	72	10	100	2.73
3683.65	12	0	0	0	18	0	0	58	12	100	2.72
3686.35	8	1	0	2	34	0	0	50	5	100	2.76
3706.42	8	0	0	2	37	0	0	45	8	100	2.76
3717.83	13	0	0	1	38	0	2	40	6	100	2.74
3726.35	9	0	0	0	11	0	0	78	2	100	2.71
3730.37	18	0	0	0	59	0	6	16	1	100	2.73
3740.2	30	0	0	0	67	0	0	0	3	100	2.75

Figure 5-10 shows a graphical display of the main constituents from one of the wells plotted with the logs and the measured TOC. One of the more surprising things we discovered was the abundance of finely disseminated dolomite through much of the section in the cores. It averages about 7.5% and is most abundant in the Point Pleasant Formation.

A second spreadsheet was generated for each thin section breaking down the relative abundance of each skeletal grain type. The skeletal grain types include bryozoans, brachiopods, phosphatic lingulid brachiopods, echinoderms, trilobites, ostracods and abundant silt-sized undifferentiated skeletal fragments. A sample of this spreadsheet is shown in Table 5-4.

56
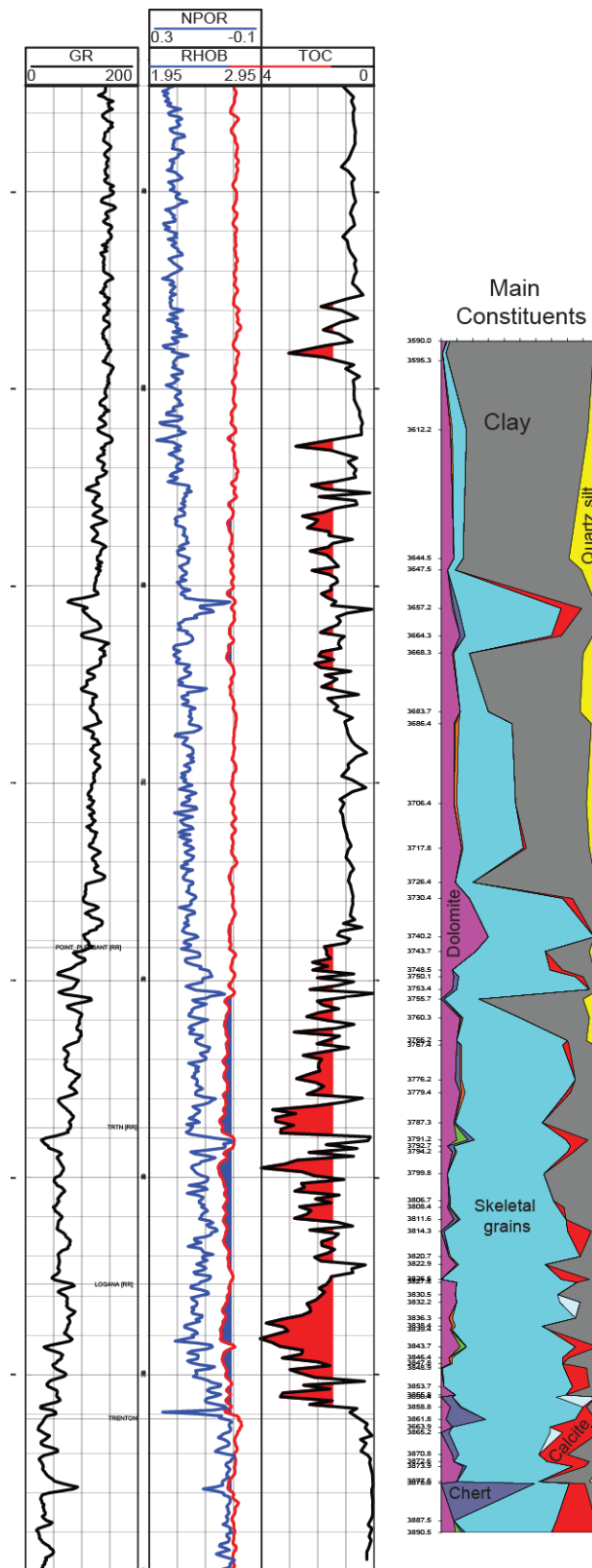
Figure 5-10. Harstine Trust No. 1 well with logs, TOC and plot of main constituents.

57

Table 5-4. Sample spreadsheet of skeletal grain type relative abundance.

Thin section Depth	Bryozoans	Brachiopods	Lingulid Brachiopods	Echinoderms	Trilobites	Ostracods	Bivalves	Undifferentiated
3589.95	0	0	0	0	0	1	0	0
3595.3	0	0	0	0	0	2	0	0
3612.2	0	1	0.5	0.5	0	7	0	0
3644.5	0	0	0	0	0	3	0	3
3647.45	0	0	0	0	2	1	0	2
3657.15	0	55	1	0	7	2	0	0
3664.34	0	14	0	0	6	0	0	35
3668.32	0	0	2	0	4	0	0	4
3683.65	0	0	1	3	3	3	0	8
3686.35	1	5	3	6	17	2	0	0
3706.42	8	4	2	5	8	2	0	8
3717.83	3	0	1	1	10	1	0	22
3726.35	0	0	0	2	4	1	0	4
3730.37	7	8	0	12	10	0	0	22
3740.2	0	0	0	0	0	0	0	67
3743.7	4	10	0	8	6	4	0	12
3748.47	16	0	0	24	12	0	0	10
3750.1	18	8	0	8	8	8	0	24
3753.42	22	7	0	39	6	5	0	5

The abundance of fossils present in these rocks indicates an environment that was well oxygenated much of the time. There are delicate trilobites and articulated ostracods that could not have been transported any significant difference. There also are beds composed almost entirely of strophomenid brachiopods, and this sort of monospecific accumulations of fossils is not likely to have been redistributed from some distant area. If they were transported from a different environment they would be more mixed with other fossils. Thus, these fossils likely lived and died in these locations. The silt-sized skeletal debris probably has been reworked; it is of an unknown origin.

One interesting point is that there are abundant ostracods in the most organic-rich facies in the upper Lexington/Trenton Formation and Logana Member. There also are some trilobites but ostracods are the most abundant. These ostracods may have been planktic as there are a few species of planktic ostracods. They may have fed on the algae near the surface during algal blooms, or perhaps the sea floor was not anoxic during deposition of the organic matter. The presence of some other fossils that are known to be benthic within the organic-rich facies, plus the abundance of storm beds, suggests that the bottom may not have been anoxic, or at least may have endured frequent intervals of being oxygenated.

Figure 5-11 shows a display of the logs with the main mineral constituents and skeletal grain types. This sort of display is helpful for evaluating stratigraphy and depositional environment. As a companion to the results presented here, the FTP site contains more than a thousand thin section photographs from the different cores, the spreadsheets from the petrography and graphic displays of the data.
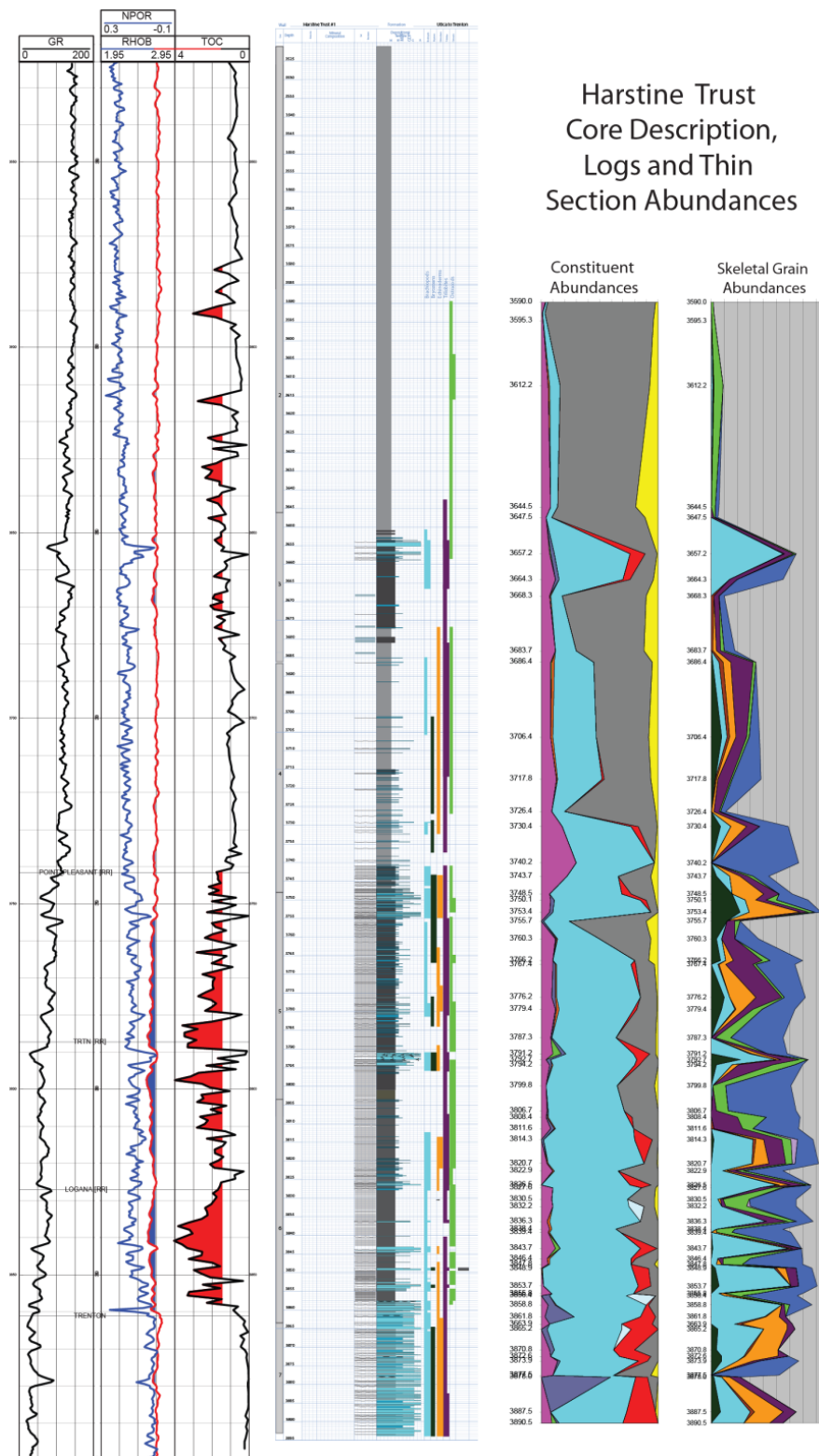
Figure 5-11. Harstine Trust No. 1 well with logs, TOC, core description, main constituents and fossil abundances.

5.3.1 Pore Types

There were no visible pores in any of the thin sections examined from any of these wells. This suggests that in the area studied there is no matrix porosity in the limestone. Any indication of porosity on the logs, therefore, is coming from the presence of organic matter, which has lower density, lower velocity and looks like porosity on the neutron logs. SEM photos of the organic-rich facies revealed little matrix porosity either. This also is the case in New York, where there are very few if any pores other than organic matter pores. If this holds true in the producing area, the only pores that are likely to be contributing much to hydrocarbon flow are the organic matter pores that formed during maturation. This would make the Utica very different from other liquids-producing plays, such as the Eagle Ford and the Bakken, which have a significant matrix porosity component.

5.3.2 Sedimentary Features

Key sedimentary features present in the cores that help understand the depositional environment include laminations, scour surfaces, burrows and apparent unconformities.

5.3.2.1 *Laminations*

There are laminations throughout almost all of the organic-rich shales and also in the clay-rich, organic-poor shales. The laminations were probably produced by moving currents rather than variations in suspended load. Schieber and others (2007) showed in flume experiments that laminations in shales can form due to migrating clay ripples on the sea floor. Because the sediments were 85% water when they were deposited, they compact significantly and any inclined cross laminations eventually will look like flat, planar laminations after compaction. Figure 5-12 shows a photograph with laminations that clearly look like ripple cross laminations down lapping to right. Figure 5-13 shows laminations in an organic-rich shale that clearly appear to have been produced by moving currents overlying a scour surface.

Figure 5-12. Thin section photomicrograph from the Richman Farms well showing ripple cross lamination overlying scour surface from Richman Farms well.
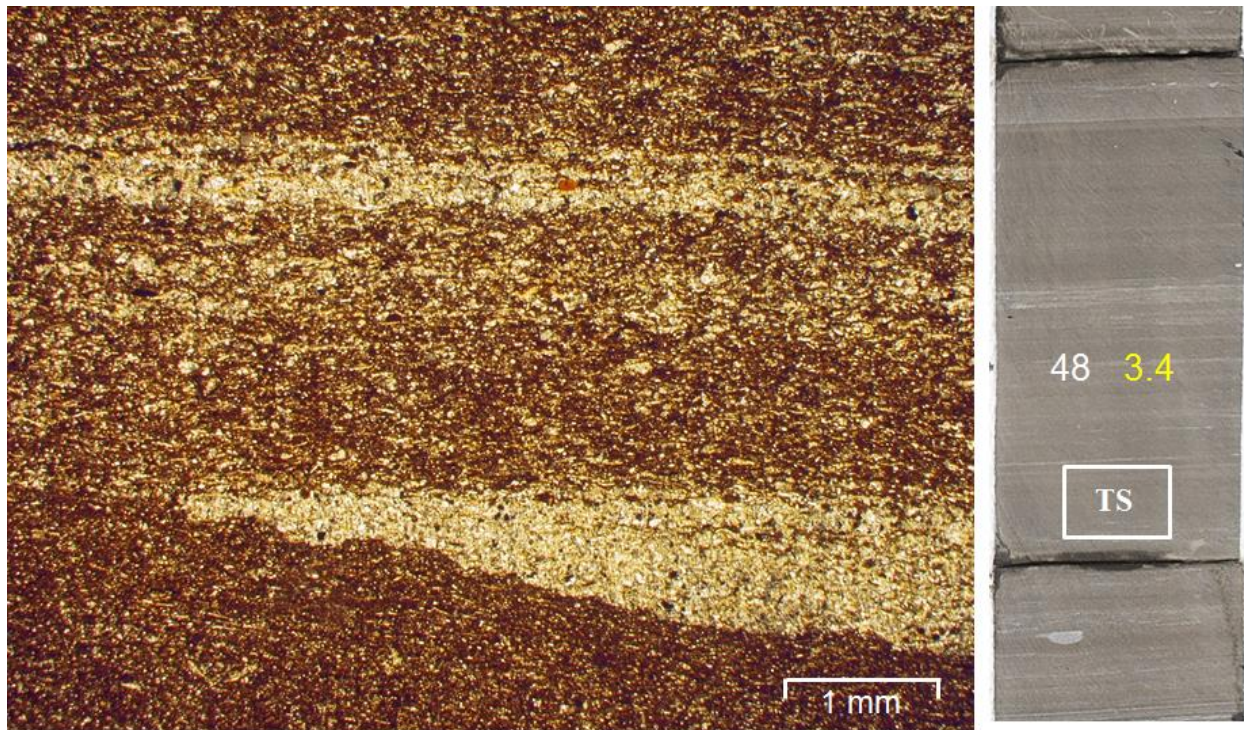
Figure 5-13. Thin section photomicrograph showing scour surface at base of slightly coarser bed in organic-rich shale.

5.3.2.2   Scour Surfaces

Scour surfaces are present throughout the studied interval from the Kope Formation to the Curdsville Member. They typically occur on top of finer shale facies and below coarser, grainier beds. These scour surfaces are surfaces of erosion that form due to an increase in energy. Given their frequency, which is sometimes down at the millimeter (mm)-scale, and definitely at the centimeter (cm)-scale, they probably are evidence of a storm-dominated shelf environment. This means that the organic-rich faces were being deposited and preserved in an environment that was being hit with frequent storms. Figure 5-13 shows a scour surface at the base of the grainier bed. Figure 5-14 shows an interval at the base of the organic-rich Point Pleasant and top of the upper Lexington/Trenton Formation composed of tens or hundreds of scour surfaces and probable storm beds.

5.3.2.3   Burrows

Burrows are common throughout much of the cored section. In some cases they are readily apparent in the slabbed cores, are approximately one-cm wide, and probably are *Planolites* or *Thallasinoides*. There also are some *Chondrites* burrows in the Trenton Formation, and there may be some very fine micron- (μm-) scale burrows in the organic-rich shale itself.
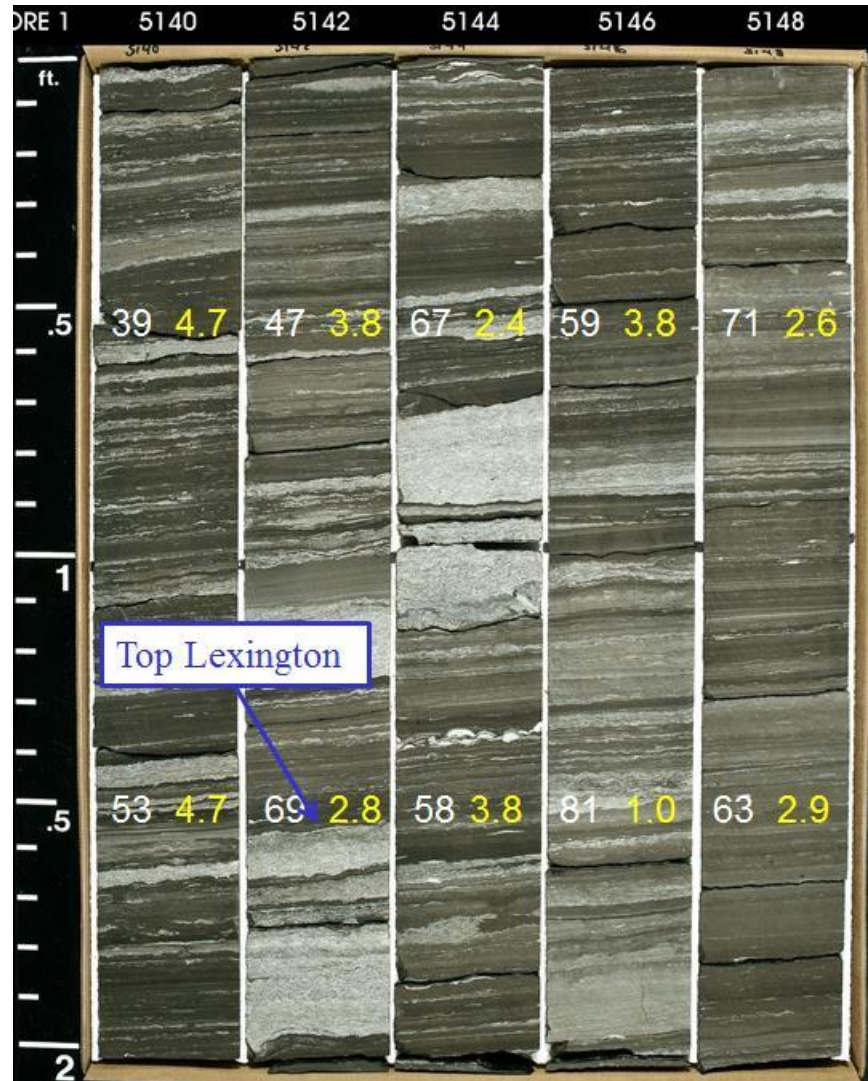
Figure 5-14. Scour surfaces and storm beds in organic-rich shale and limestone of the Point Pleasant and upper Lexington/Trenton formations. White numbers are carbonate content, and yellow numbers are TOC values. "Top Lexington" indicates top of the upper Lexington/Trenton Formation.

5.3.2.4   *Unconformities*

There are several horizons within the cored intervals that appear to be unconformities. Two can be recognized in core by the presence of undulose surfaces: one is at the top of the upper Lexington/Trenton Formation, which is in the middle of the organic-rich zone (Figure 5-6); the other is at the top of the Point Pleasant Formation (Figure 5-15). There also are two log markers that look like sequence boundaries at the top of the lower, organic-poor Utica that can be recognized on logs and correlated for long distances. There are others throughout the section. For example, Figure 5-16 shows a surface from the top of the Point Pleasant Formation, and Figure 5-17 shows a surface from the top of the upper Lexington/Trenton Formation.
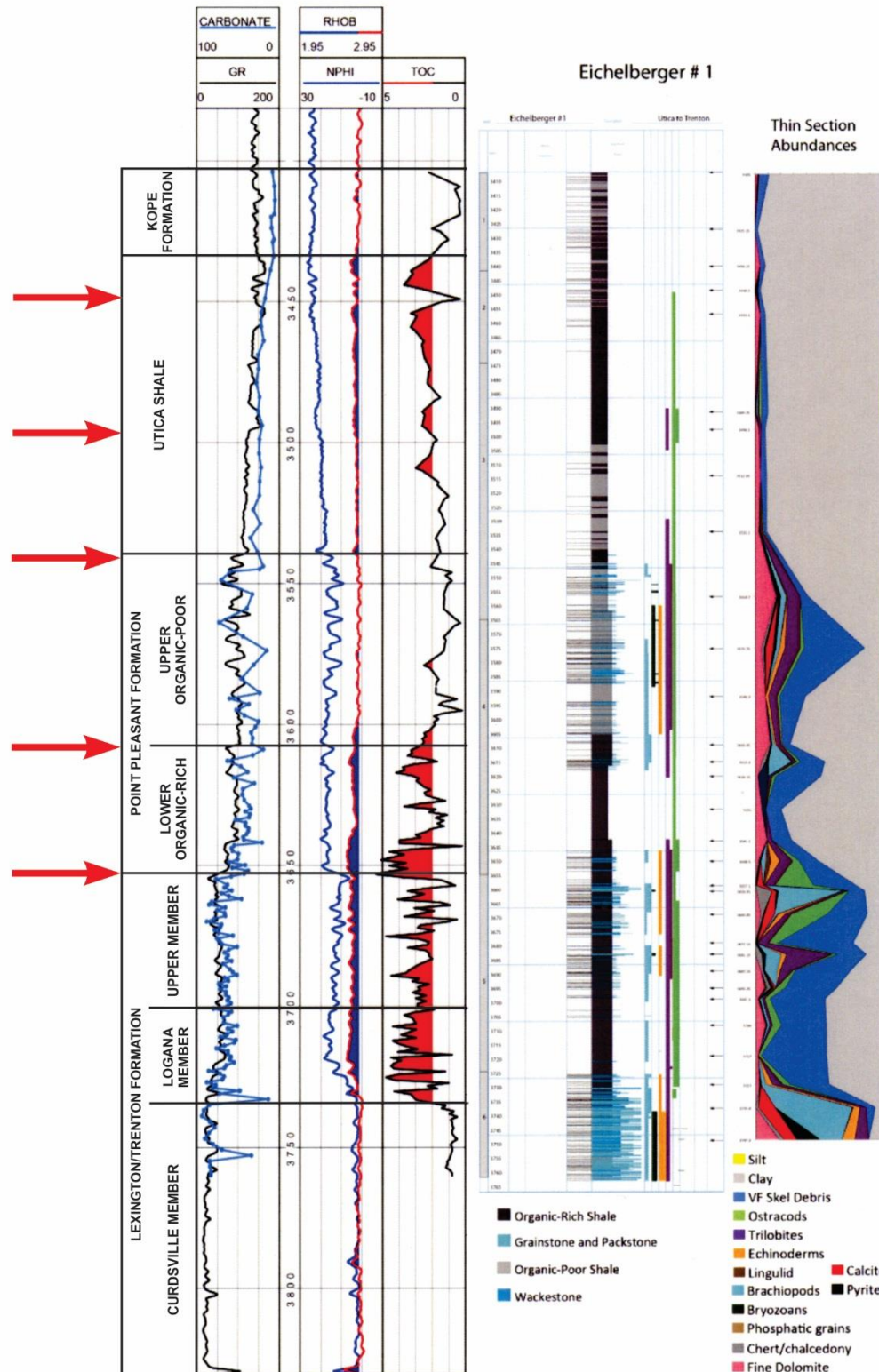
Figure 5-15. Logs, core description and thin section abundance from the Eichelberger No. 1 well. Red arrows indicate possible unconformities in the Utica/Point Pleasant interval. These look like surfaces in the logs and, in some cases, in the cores as well.

63

Figure 5-16. Photograph of a portion of the Eichelberger No. 1 core with logs, core description and thin section abundance for comparison. The undulose surface occurs in the top of Point Pleasant Formation. This surface was also found in the Harstine Trust well core.

Figure 5-17. Photograph of a portion of the Harstine Trust core showing an erosion surface at the top of the upper Lexington/Trenton Formation with organic-rich facies above and below.

5.4 Sedimentology, Stratigraphy and TOC

5.4.1 Kope Formation

The Kope Formation is composed of gray shale and cm- to decimeter (dm)-scale interbedded black and gray shale at the base (Figure 5-18). The black shale can have TOC up to 3%. There are several tens of these black-gray couplets in each of the cores studied, with a sharp boundary below each gray bed and a slightly burrowed, gradational contact with the overlying black shales.
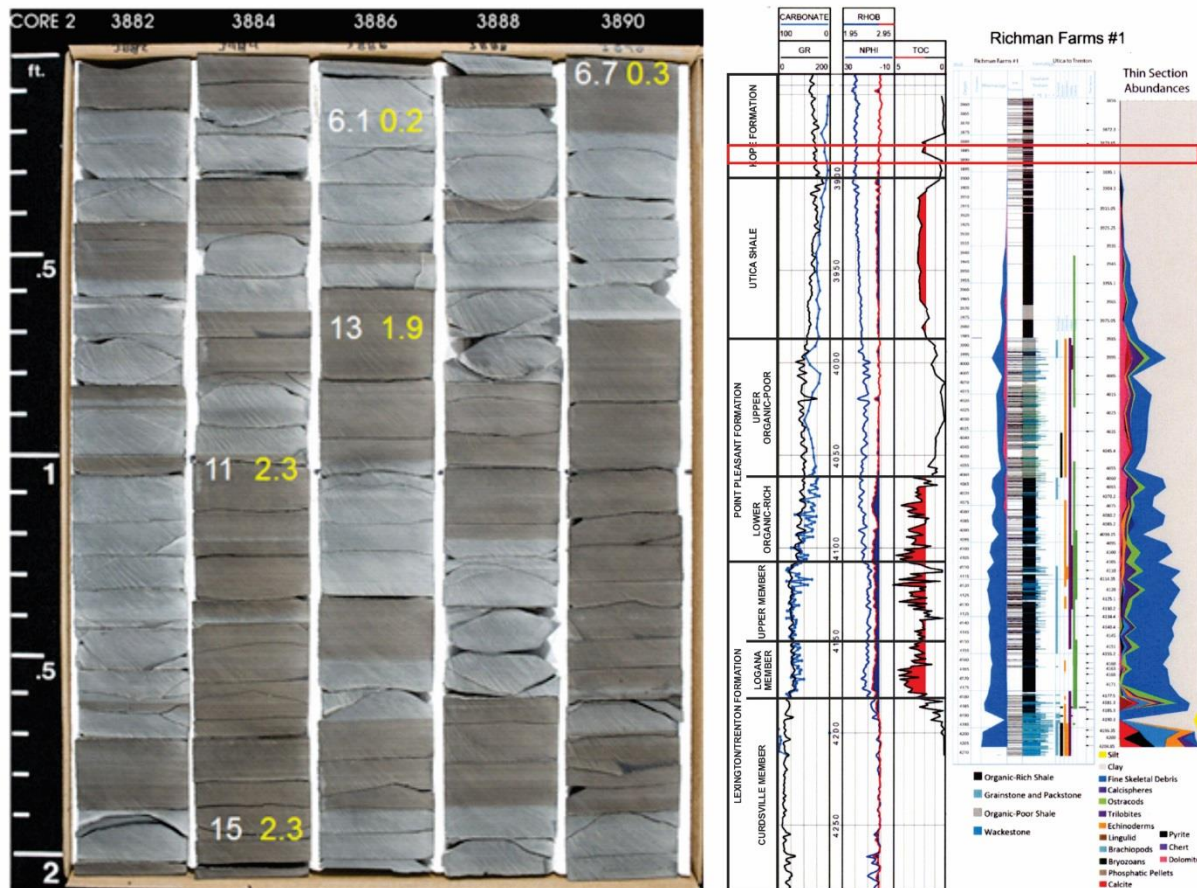
Figure 5-18. Photograph of core of the Kope Formation from the Richman Farms No. 1 well showing thin beds of alternating black and gray shale. Gray units fluoresce. White numbers are carbonate content, and yellow numbers are TOC values.

5.4.2 Utica Shale

The Utica Shale is composed of calcareous black shale with TOC up to 3.5% (Figure 5-19). It typically has carbonate content of approximately 25%, which is higher than the Kope Formation but lower than the underlying organic-rich carbonate facies (Point Pleasant and Lexington/Trenton formations).   It is laminated with very few of the storm beds found in the underlying units. The basal part of this portion of the Utica contains some brachiopod-bearing carbonate beds, as observed in the Harstine Trust core, which is to the south.
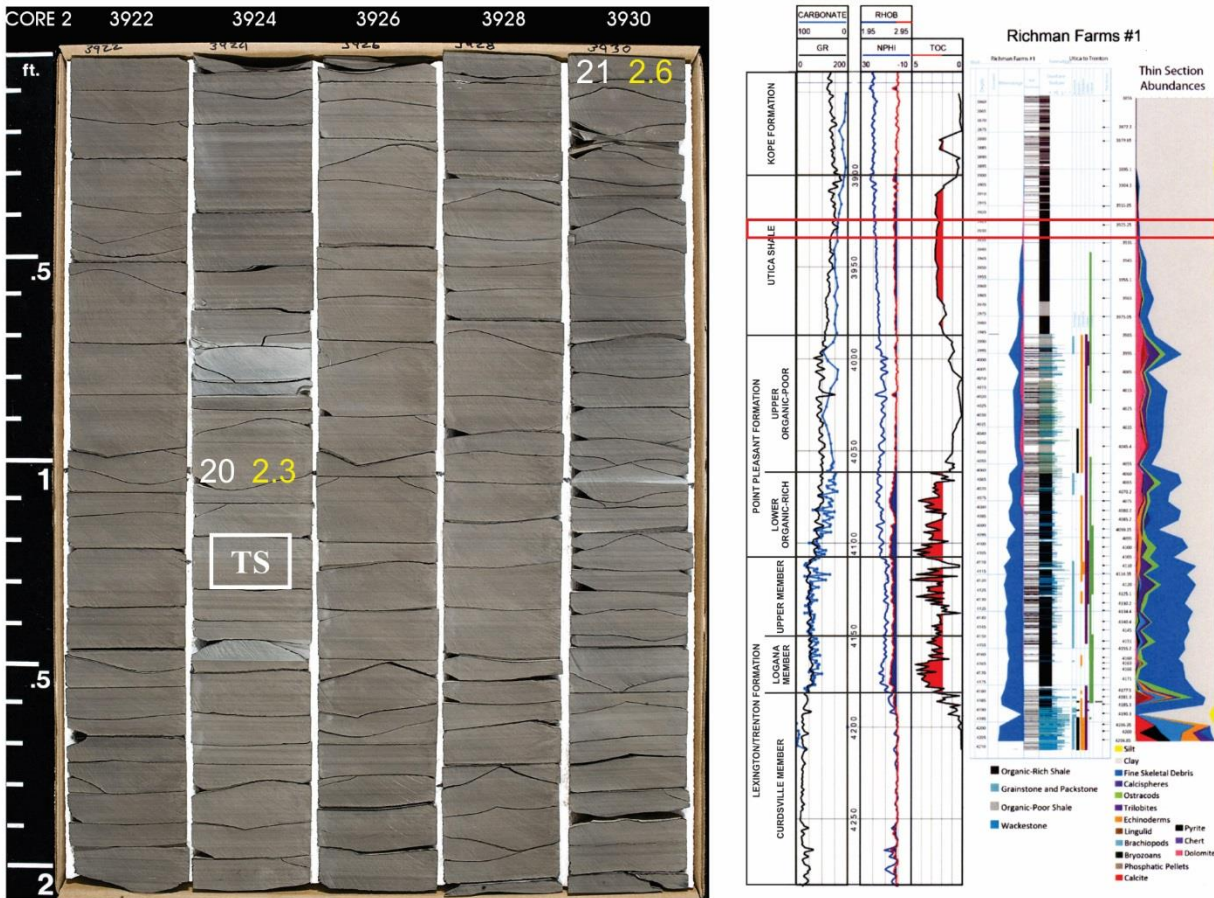
Figure 5-19. Photograph of core of the Utica Shale from the Richman Farms No. 1 well showing laminated black calcareous shale. White numbers are carbonate content, and the yellow numbers are TOC values.

5.4.3 Upper Organic-Poor Point Pleasant Formation

The Upper Organic-poor Point Pleasant Formation is an organic-poor gray shale with abundant thin carbonate beds containing common *Prasopora* bryozoans (Figure 5-20). TOC is generally low (most samples <1%). This interval is considered to be primarily non-reservoir. It has abundant storm beds and a more diverse, open marine fauna.
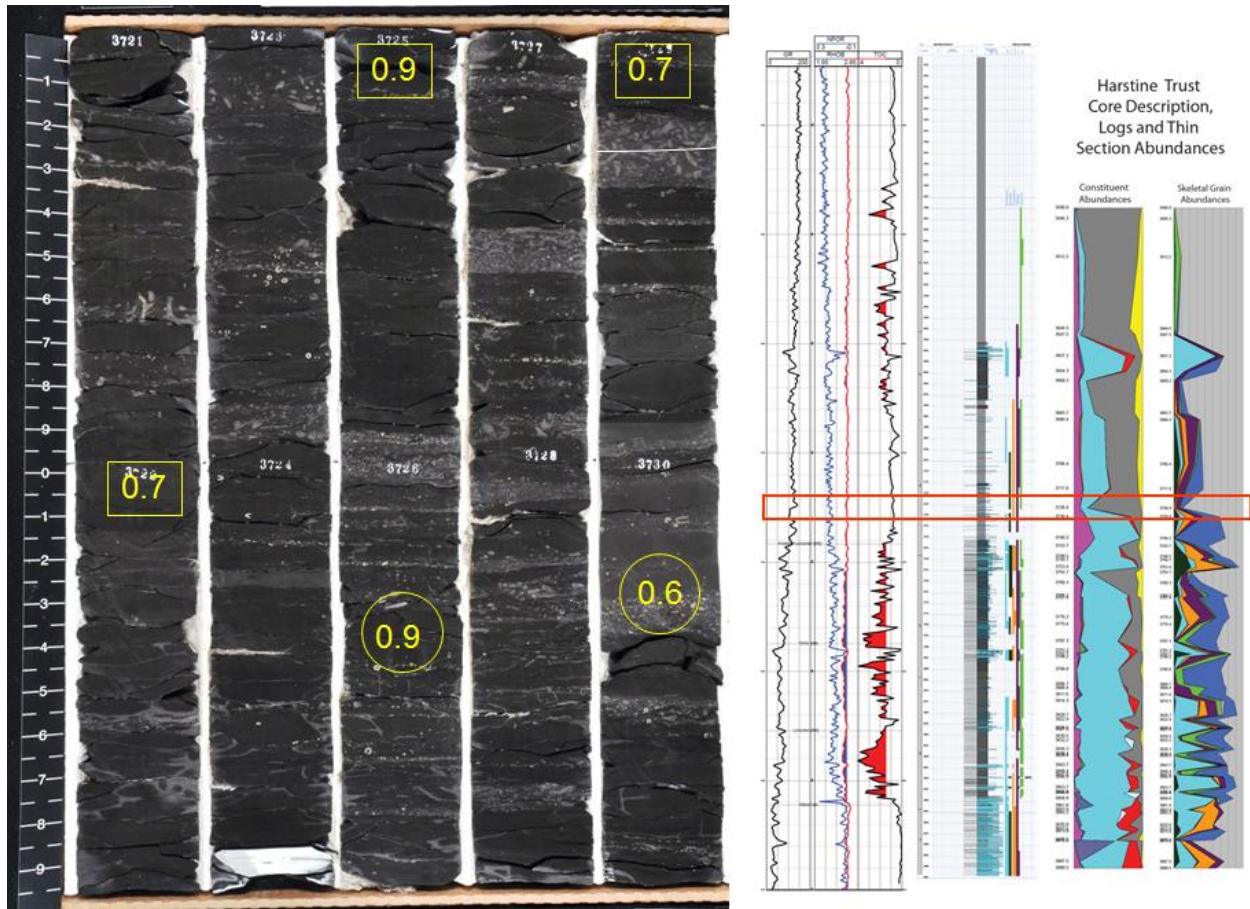
Figure 5-20. Photograph of core of the upper Point Pleasant Formation from the Harstine Trust well. Large visible fossils are mainly *Prasopora* bryozoans and large crinoids. Yellow numbers are TOC values.

5.4.4 Lower Organic-Rich Point Pleasant Formation

The Point Pleasant Formation is an organic-rich calcareous shale with some limestone beds. The organic-rich units have roughly 40-60% carbonate content with TOC up to 4 or 5%. This interval is apparently the target for drilling in most of the wells that have been drilled to date. There is a limestone at the top of the unit that is commonly picked as the top, but there is some organic-rich shale just above it. The Point Pleasant has abundant storm beds and clearly is a storm-influenced formation and also has common burrows, even in the organic-rich facies.
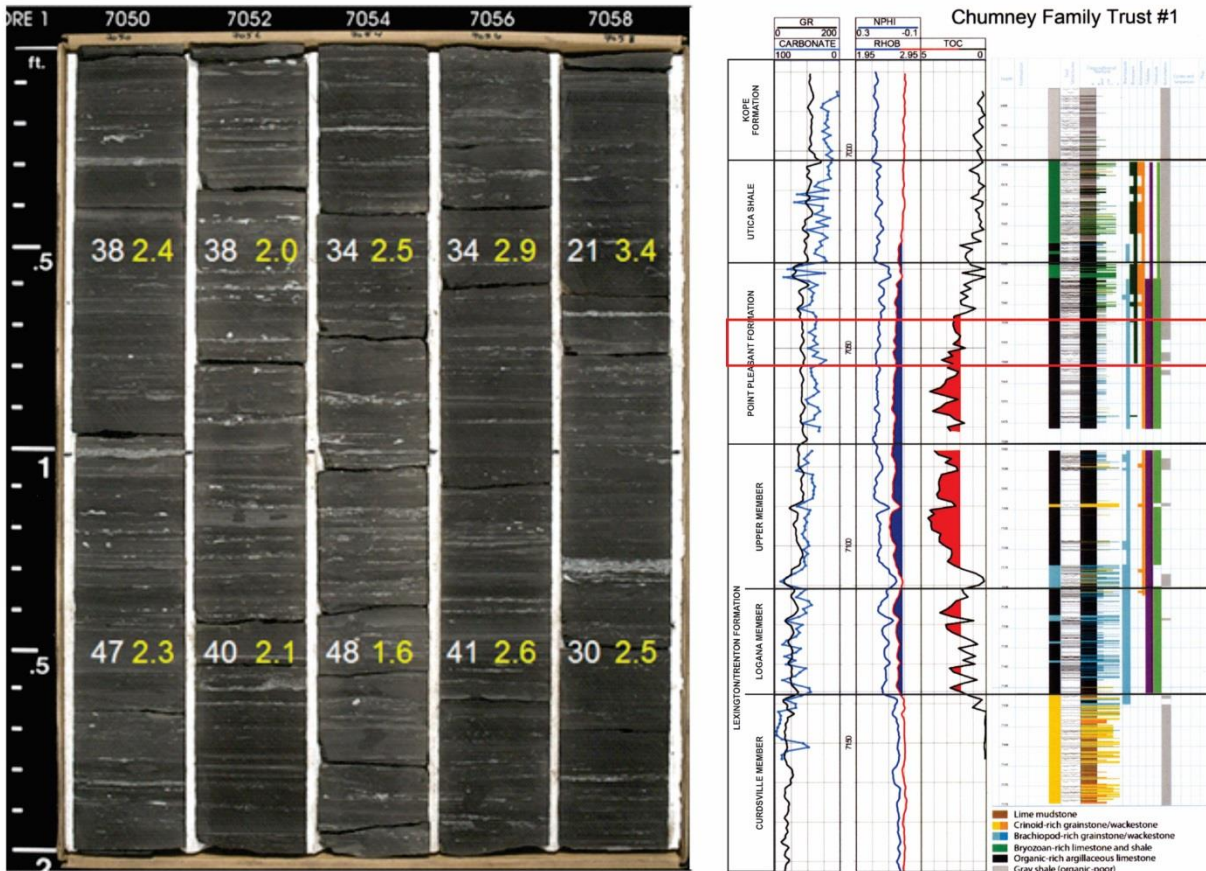
Figure 5-21. Photograph of core of the Point Pleasant Formation from the Chumney Family Trust No. 1 well showing storm beds in organic-rich black shale. White numbers are carbonate content, and yellow numbers are TOC values.

5.4.5 Upper Lexington/Trenton Formation

The upper Lexington/Trenton Formation appears to be capped by an unconformity in most wells and is more of an argillaceous limestone with limestone beds more common. The boundary at the top of the Lexington/Trenton looks like an exposure surface or sequence boundary in several of the cores (see Figure 5-17). In some areas it is less organic-rich than the Point Pleasant Formation, and in other areas it has some of the highest TOC values in the interval. TOC varies with the limestone shale cycles but can be as high as 4 or 5%. Figure 5-22 shows a core from just below the top of the upper Lexington/Trenton Formation that has abundant lighter colored limestone interbedded with a darker, organic-rich facies with up to 5.1% TOC. The interval just above and just below the sequence boundary at the top of the Lexington commonly has the highest values. The most common fossils in the organic-rich facies are ostracods, which may be planktonic, and trilobites. Bryozoans and crinoids become more common at the top of the Lexington/Trenton.
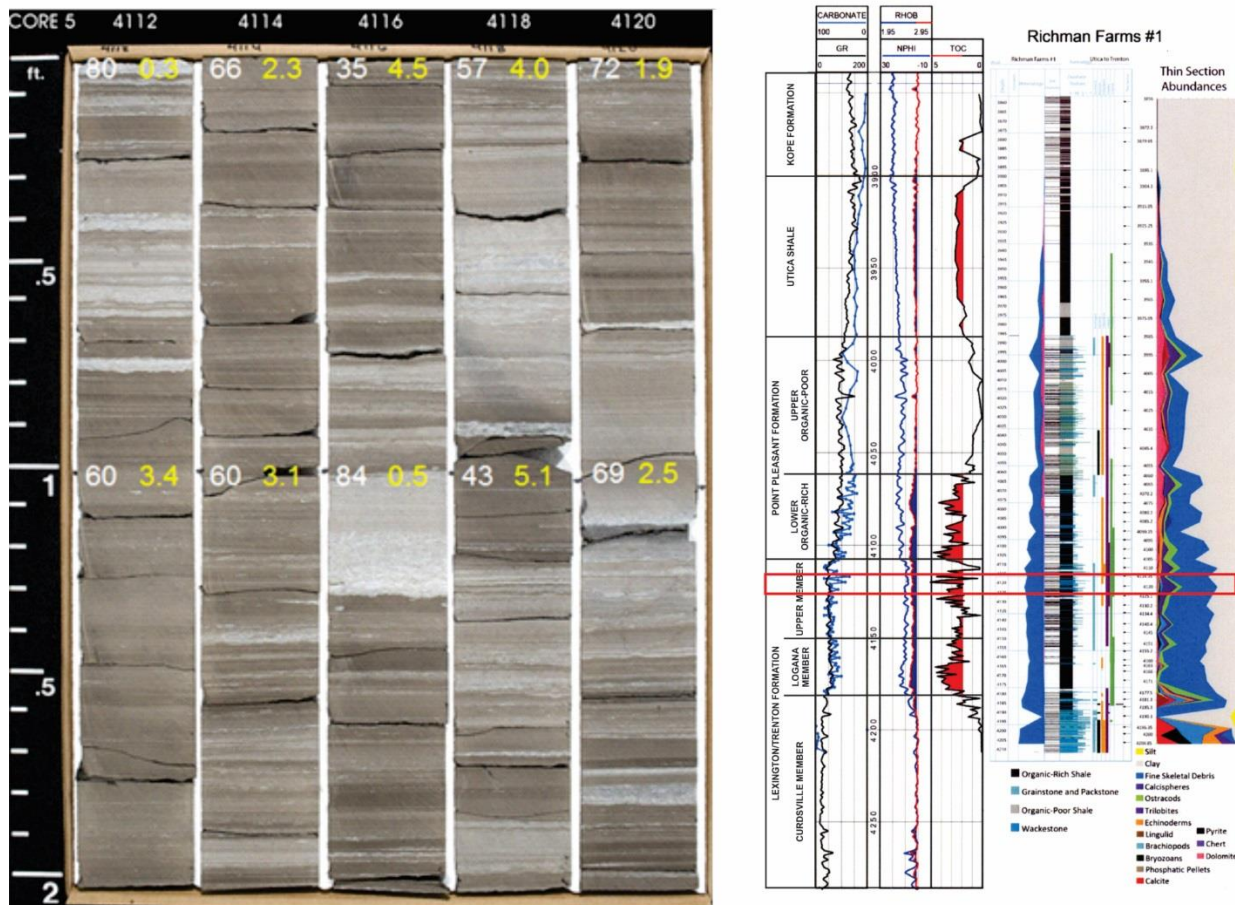
Figure 5-22. Photograph of core of the upper Lexington/Trenton Formation from the Richman Farms No. 1 well showing abundant limestone beds with low TOC, interbedded with organic-rich facies with TOC up to 5%. White numbers are carbonate content, and yellow numbers are TOC values.

5.4.6 Logana Member of the Lexington/Trenton Formation

The Logana Member of the Lexington/Trenton Formation is an organic-rich argillaceous limestone with TOC up to 5% and carbonate content consistently greater than 70%. It is laminated and has few limestone beds in the top and some well-developed, laterally extensive, brachiopod-rich beds at the base. These brachiopod rudstones are composed almost entirely of what appears to be a single species of brachiopod – some kinds of strophomenid. These brachiopod rudstones are interbedded with high-TOC organic-rich facies (Figure 5-23). The most common fossils in the organic-rich facies are ostracods that may be planktic in origin.
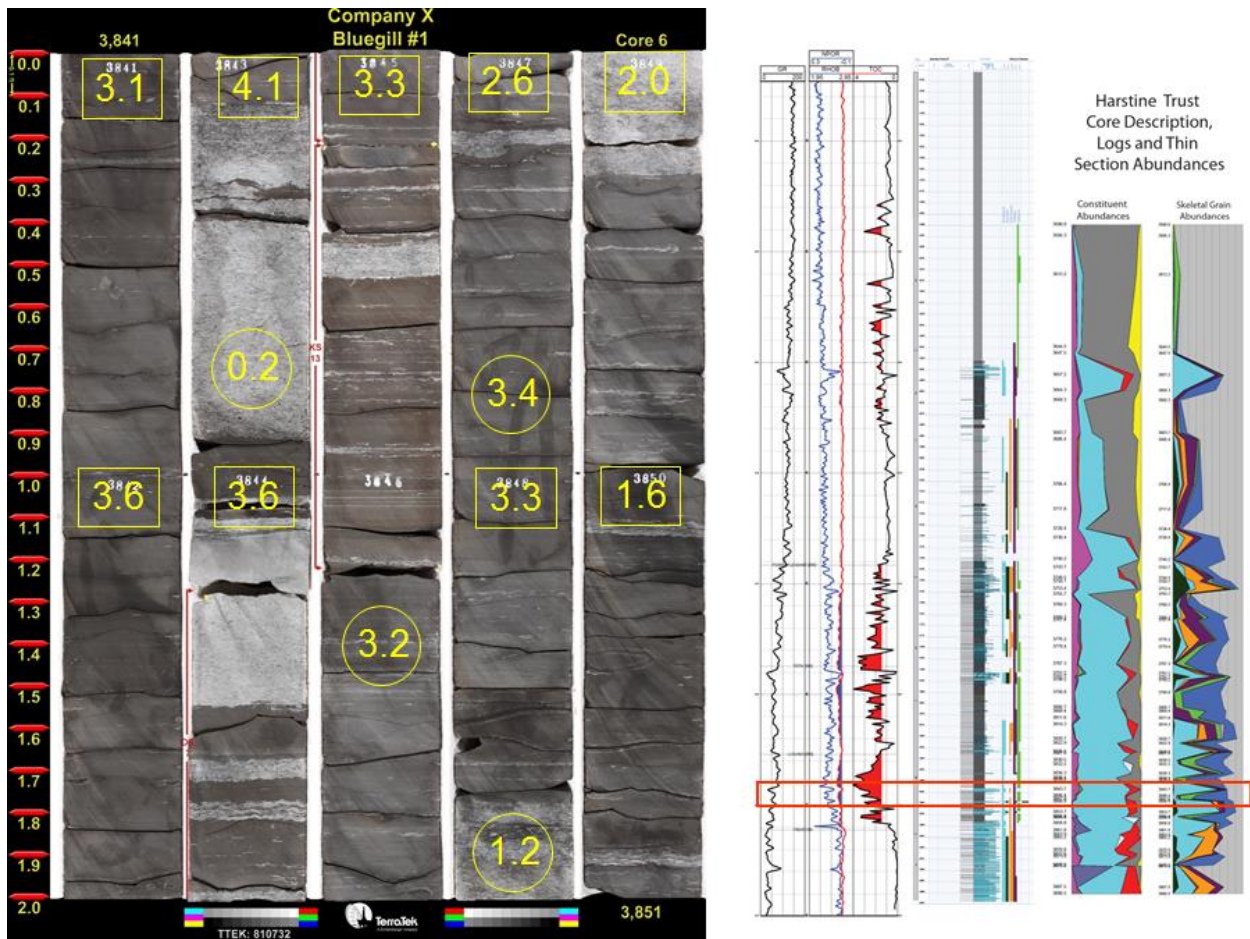
Figure 5-23. Photograph of core of the Logana Member of the Lexington/Trenton Formation in the Harstine Trust well showing interbedded organic-rich, argillaceous limestone and organic-poor, brachiopod rudstone. Yellow numbers are TOC values.

5.4.7 Curdsville Member of the Lexington/Trenton Formation

The Curdsville Member of the Lexington/Trenton Formation is a more typical Lexington/Trenton lithology with fossiliferous limestones and thin gray shale partings, and with little or no TOC in the shaly partings. There is a diverse marine assemblage including bryozoans, echinoderms, trilobites and brachiopods. It was deposited in a shallow marine environment. Figure 5-24 shows some typical Curdsville strata.
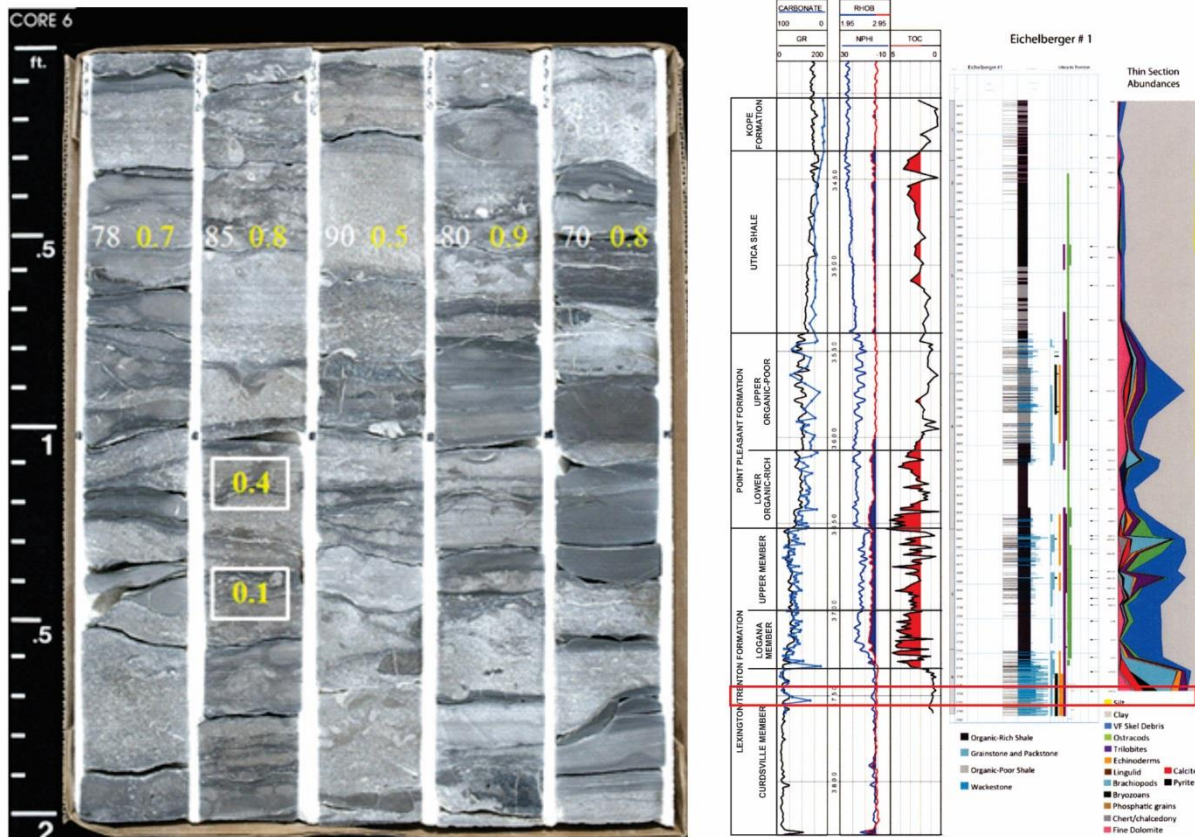
Figure 5-24. Photograph of core of the Curdsville Member of the Lexington/Trenton Formation in the Eichelberger No. 1 well showing interbedded shale with lime grainstone and packstone. Yellow numbers are TOC values.

5.4.8 Correlation

Figure 5-25 illustrates a north-south correlation of four of the cored wells. It shows a very layer-cake stratigraphy, although the units thin slightly and becomes more carbonate-rich and less organic-rich to the south. At least eight cycles can be correlated through all of the wells. The red lines are possible sequence boundaries picked at log markers that in some cases can be linked to possible erosion surfaces in the core.
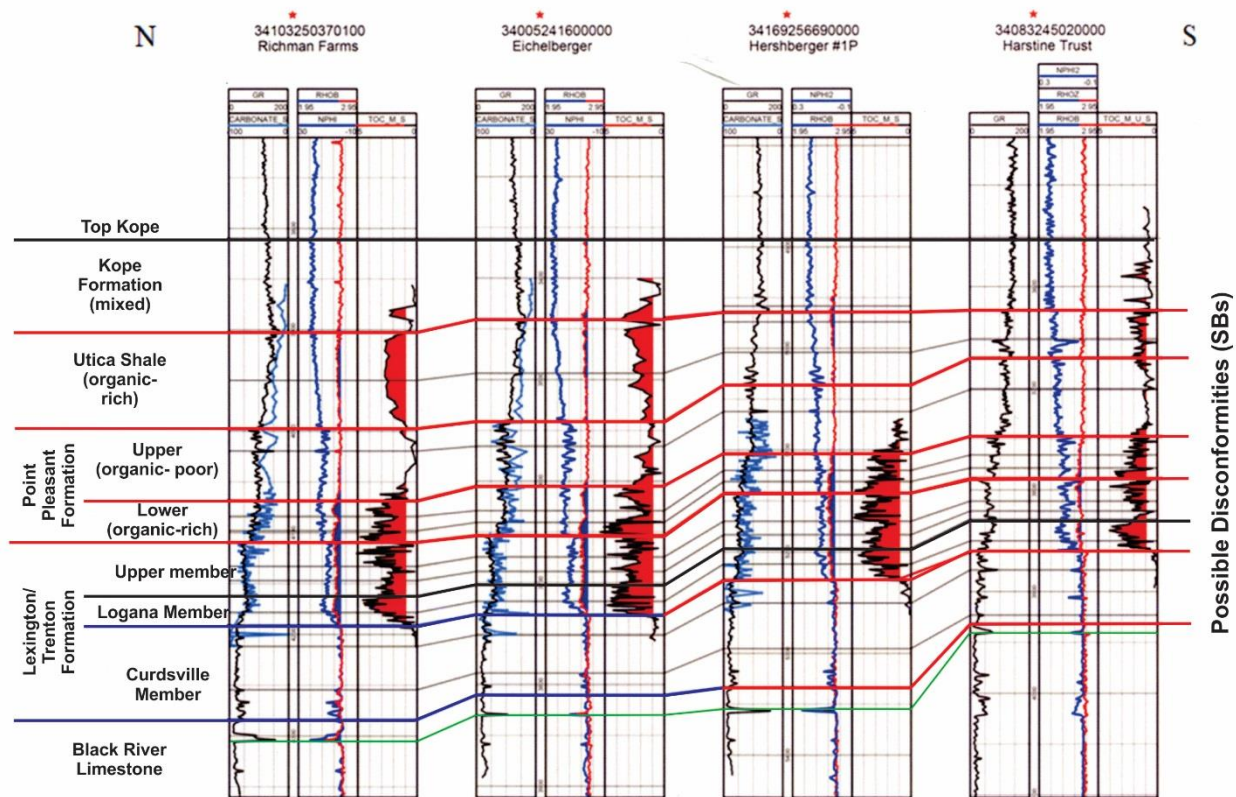
Figure 5-25. Correlation of four of the cored Devon Energy wells. See Figure 5-3 for core location map.

Figure 5-26 shows a correlation that continues farther south tying the cored wells to some non-cored wells in southern Ohio. The thicknesses do not change much, but the TOC content has decreased and the carbonate content has increased.
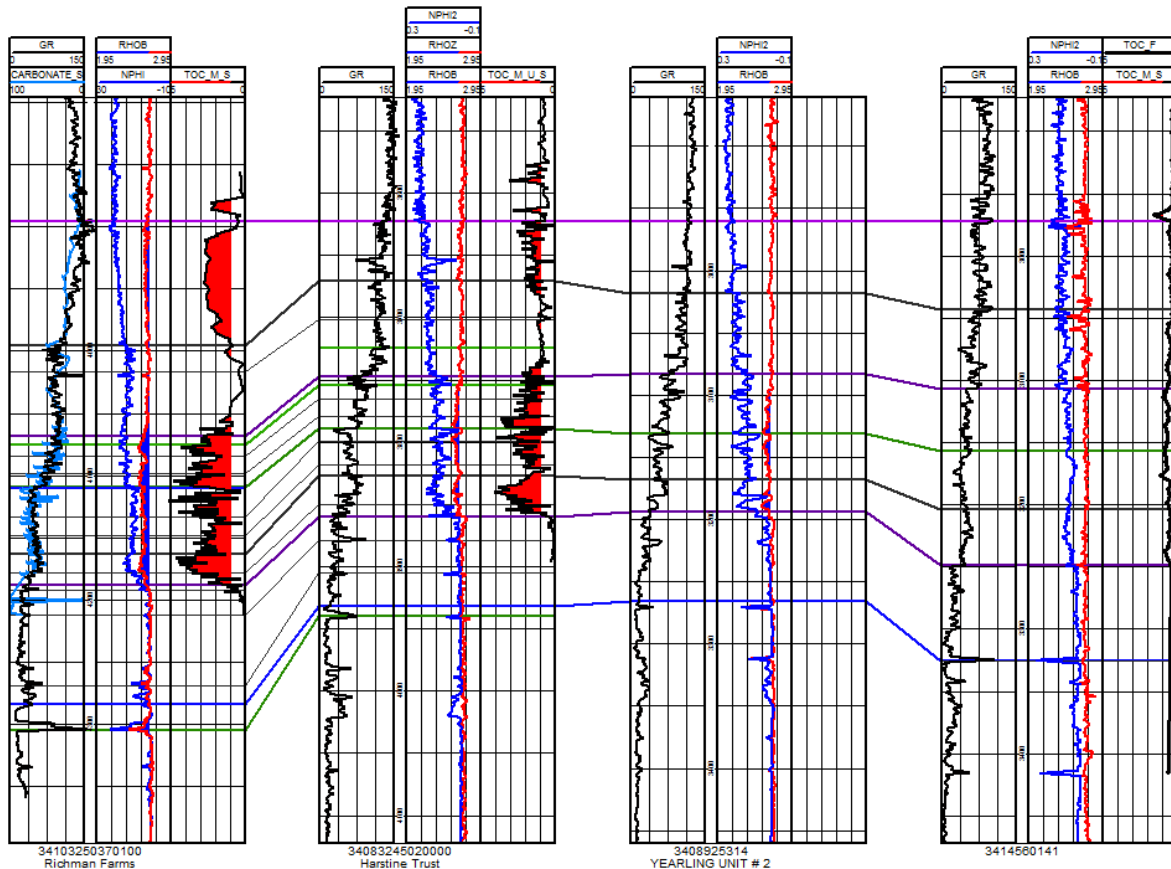
Figure 5-26. North-south correlation from northern OH to southern Ohio. Limestone content based on GR log is higher although the section is still shaly.

5.5   Depositional Environment

The depositional environment of the Point Pleasant Formation, upper Lexington/Trenton Formation and Logana Member is a relatively shallow, probably <100 ft (<30 meters [m] deep, storm-dominated, carbonate shelf that experienced frequent algal blooms. Cross-sections show that there was not much difference in water depth between the organic-rich and organic-poor areas of deposition. The fossils present in the limestone suggest water that was at times shallow, exposed to sunlight and well oxygenated. The storm-bedding throughout suggests something well above storm wave base. The environment may have been subject to seasonal anoxia due to the frequent algal blooms. In New York and Pennsylvania, which were not studied in the same detail, a similar depositional model may be invoked.

6.0   INORGANIC GEOCHEMISTRY

The research team evaluated the inorganic geochemistry of Utica Shale and equivalent rocks by conducting bulk mineralogy, carbonate content and inorganic carbon isotope testing on rock core and cuttings samples.   Bulk mineralogy was determined using XRD and SEM techniques, with the results categorized in three main groupings – quartz plus feldspar, carbonate and clay minerals.   Carbonate content was further evaluated using insoluble-residue analysis to determine how relative amounts of carbonate minerals (calcite and dolomite) may vary throughout the Utica interval.   Carbon isotope tests were performed to evaluate the chronostratigraphic relationships of Late Ordovician strata across the Study area.

6.1   Bulk Mineralogy

The Consortium website provides access to bulk mineralogy results for more than 1200 samples collected at dozens of well locations throughout the Study area.   A majority of these (i.e., 930) were specifically analyzed for the current Study (Appendix 6-A).   The remaining bulk mineralogy data (i.e., 299 samples taken from 78 cores) represent legacy XRD analyses from Ohio, and are not discussed herein.

6.1.1 X-ray Diffraction

6.1.1.1   Materials and Methods

PAGS was the team lead on bulk mineralogy testing performed for the Study.   Accordingly, PAGS purchased and installed new XRD equipment for this project in June 2013.   The equipment includes a computed tomography (CT) stage (Figure 6-1A) and a multi-sample changer (Figure 6-1B).   The multi-sample changer was heavily used by John Barnes, the PAGS geochemist who performed the XRD work between July 2013 and April 2014.

PAGS obtained outcrop samples of Utica-equivalent rocks from 18 outcrops in central Pennsylvania during the field season of 2012.   In addition, we collected drill cutting samples from both survey repositories and newer well locations donated by Consortium partners for 28 wells in the Study area, including five wells in New York, six wells in Ohio and 17 wells in Pennsylvania. The locations of the outcrops and wells are shown in Figure 6-2 and additional details are given in Table 6-1.

The mineral compositions of 930 samples representing all 18 outcrops and 28 drill holes were determined using X-ray powder diffraction. The analyses were run using a PANalytical Empyrean X-ray diffractometer. The samples were loaded in 16-mm-diameter back-packed sample holders that were mounted in a sample spinner. The results were interpreted using PANalytical HighScore Plus software and the ICDD PDF-4 database. Replicate analyses of 55 samples, representing both outcrops and drill holes, were run as a test of precision.
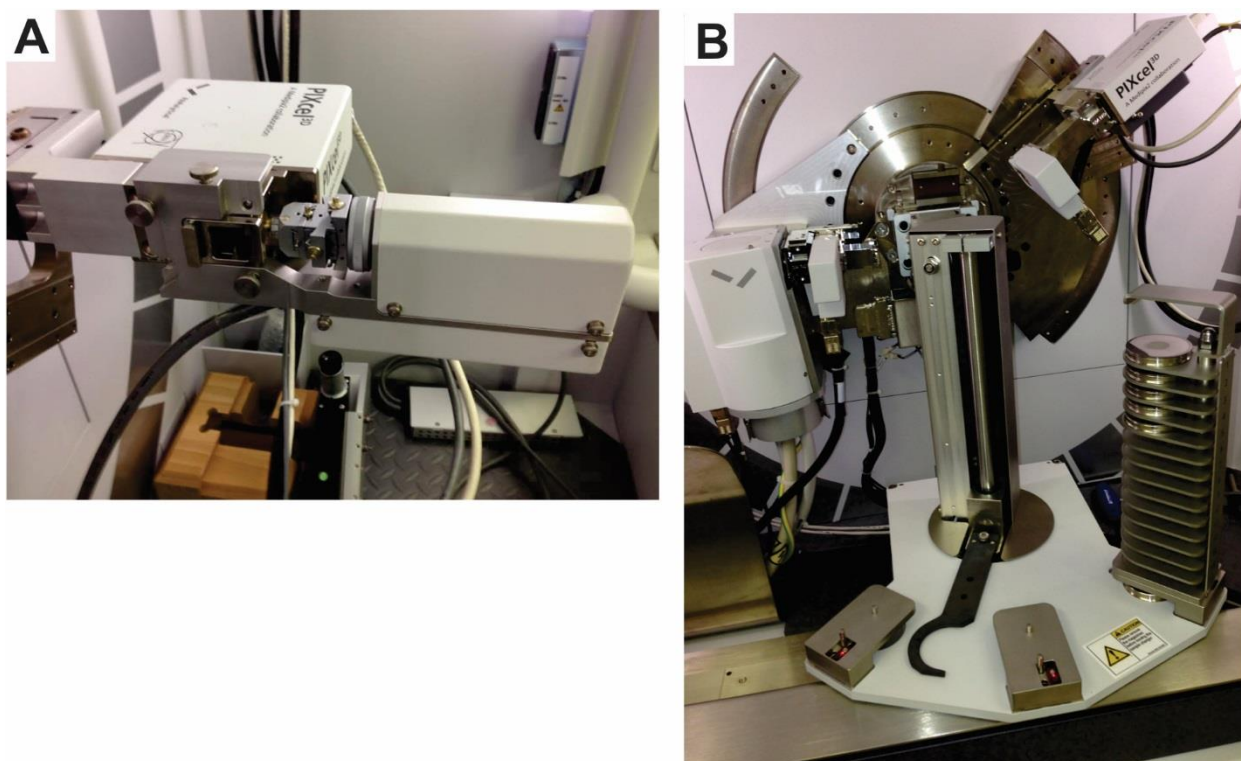
Figure 6-1. Photographs of the XRD equipment at the PAGS laboratory in Middletown, PA. A - CT stage used to measure sample density. B - XRD equipped with multi-sample changer.
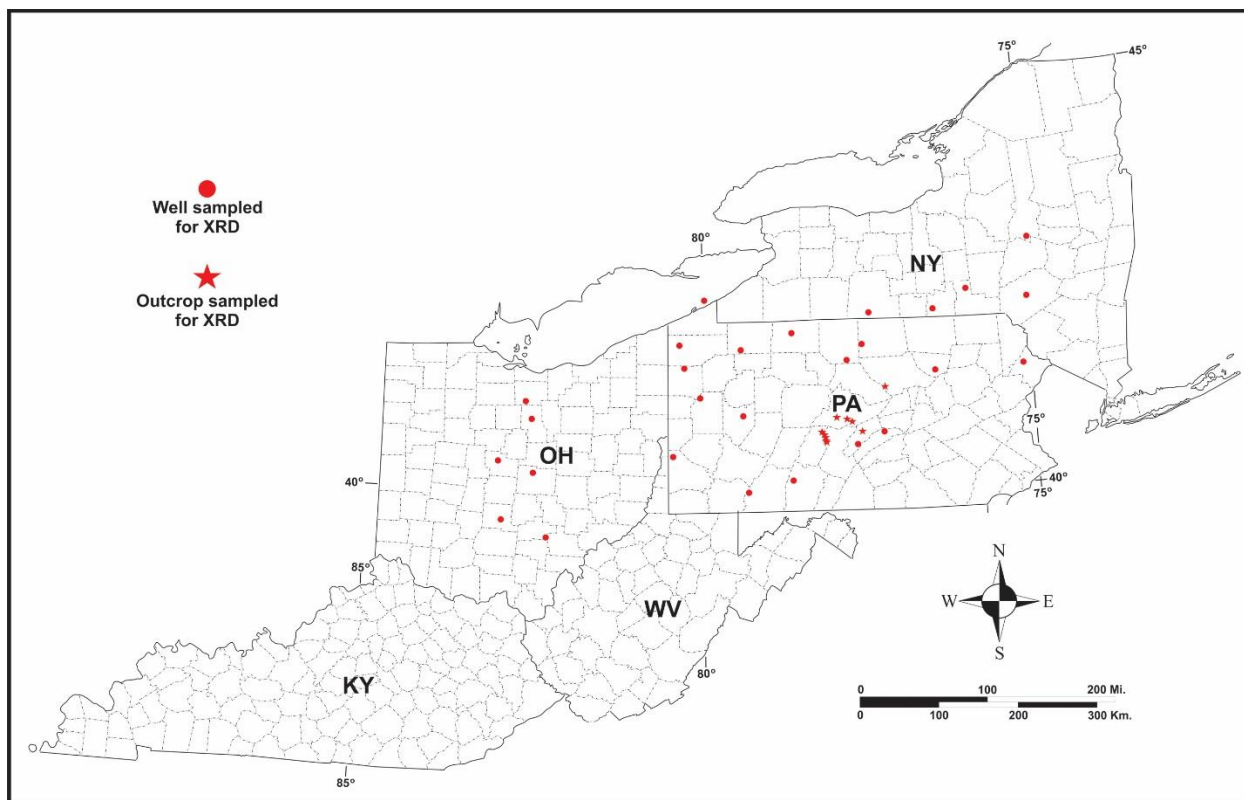
Figure 6-2. Location map of outcrops and wells sampled for XRD analysis as part of the Study. See Table 6-1 for details.

75

Two different methods of calculating semi-quantitative results were attempted before it was determined that one was clearly superior to the other for this set of samples. The initial attempt to obtain semi-quantitative results used the Reference Intensity Ratio (RIR) method. According to this method, quantities of minerals in a mixture are determined by comparing the intensities of each mineral's most intense diffraction peaks to each other and to the published ratios of their most intense peaks to the most intense peak of the stable mineral corundum (Al_2O_3). This method can sometimes work for minerals that have relatively consistent simple chemical compositions and molecular structures, such as quartz and calcite. The replicate analyses for this Study, however, clearly showed that it yielded unsatisfactory results because the method is strongly affected by which polytypes of layered silicate minerals (e.g., muscovite) are present. Knowing exactly which polytype of such a mineral is present is very difficult to determine in a timely way for scans of mixtures of minerals, especially in a project that involves hundreds of samples.

Even as this comparative analysis of XRD interpretive methods was being performed, PAGS prepared 24 grain mount thin sections for petrographic analysis in an effort to: (1) better estimate bulk clay mineralogy composition in selected Utica and equivalent samples from Pennsylvania, and (2) investigate whether the RIR method was on the right track in interpreting clay mineralogy percentages. Comparison of the petrographic analyses derived from this sample set with their corresponding XRD mineralogy results indicated that there is no direct correspondence between these approaches. The thin section photomicrographs and data derived from this particular effort are included in Appendix 6-B.

A second attempt to obtain semi-quantitative results was made using the Rietveld method, a more sophisticated method that uses the whole X-ray pattern, not just its most intense peaks, to find agreement between observed patterns and the published crystal structure data of the minerals through least-squares analyses. Quantities are then calculated based on these analyses. This method can take into account such factors as preferred orientation and peak shape that can present problems in dealing with layered silicate minerals. The HighScore Plus software enabled the programming of an automated Rietveld procedure that took these factors into account, and that was able to provide a level of precision sufficient for dividing the minerals into the major categories reported herein for classifying the lithologies that were encountered.

Table 6-1. Location of samples that have undergone XRD analysis.

API No.	State	County	Location/Well Name	Sample Depths (ft)	Number of Samples
NA	PA	Various	Outcrops in central PA	NA	18
3100705087	NY	Broome	Richards No. 1	7400-7940	25
3102504214	NY	Delaware	Campbell No. 1	7400-8300	19
3104303993	NY	Herkimer	Skranko No. 1	1550-2950	26
3110103924	NY	Steuben	Olin No. 1	9500-10,010	20
3110723883	NY	Tioga	Beach No. 1	10,000-10,700	35
3404120253	OH	Delaware	Weed No. 1	1650-1960	29
3407323283	OH	Hocking	Sunday Creek Coal Co. No. 3-S	4450-4790	33
3407720028	OH	Huron	Newmeyer No. 1	2568-2935	32
3408926065	OH	Licking	Rowe-Grube Unit No. 1-3613	3300-3570	27
3412920089	OH	Pickaway	Clutts George & Sue No. 1	1590-1960	37
3413920608	OH	Richland	Joseph Kruso No. 1	3210-3520	29
3700521201	PA	Armstrong	Martin No. 1	11,750-12,020	30
3700920034	PA	Bedford	Schellsburg Unit No. 1	7300-7700	40
3701990063	PA	Butler	Hockenberry No. 1	8404-8902	46
3702720001	PA	Centre	Long No. 1	13,800-14,250	2
3703520276	PA	Clinton	Commonwealth of PA Tr. 285 No. 1	14,000-14,500	49
3703920007	PA	Crawford	Kardosh No. 1	5870-6280	44
3704920049	PA	Erie	PA Dept. of Forests & Waters Block 2 No. 1	3705-4096	37
3706720001	PA	Juniata	Shade Mt. No. 1	3650-3900	25
3708333511	PA	McKean	Say No. 1	9000-9200	20
3708520116	PA	Mercer	Fleck No. 1	6650-7200	57
3708720002	PA	Mifflin	Commonwealth of PA Tr. 377 No. 1	5050-5350	20
3710320003	PA	Pike	Commonwealth of PA Tr. 163 No. C-1	13,400-13,600	18
3711120045	PA	Somerset	Svetz No. 1	15,000-15,170	16
3711320002	PA	Sullivan	Dieffenbach No. 2951	16,050-16,450	3
3711720181	PA	Tioga	Marshlands No. 2	11,660-12,130	46
3712320150	PA	Warren	Shaw No. 1	8047-8376	48
3712522278	PA	Washington	Starvaggi No. 1	10,030-11,010	99
				Total Samples	**930**

6.1.1.2   Results

As XRD analyses were interpreted, data were assigned to three categories – quartz plus feldspar, carbonate and clay minerals. PAGS plotted the data for these three categories for all of the wells in which more than three intervals were sampled. The plots reflect changes in mineralogy with depth. Displaying the mineralogy results in this manner facilitates the interpretation (or in many cases, confirmation of past interpretation) of Utica and other formation tops (e.g., Figure 6-3). It should be pointed out, however, that the XRD plots are based on drill cuttings obtained from intervals within each well, and interpretations based on them without reference to geophysical logs of the same intervals may result in inconsistent or inaccurate correlations. A complete set of these data plots, as well as of the data spreadsheets used to develop them, is provided in Appendix 6-A.
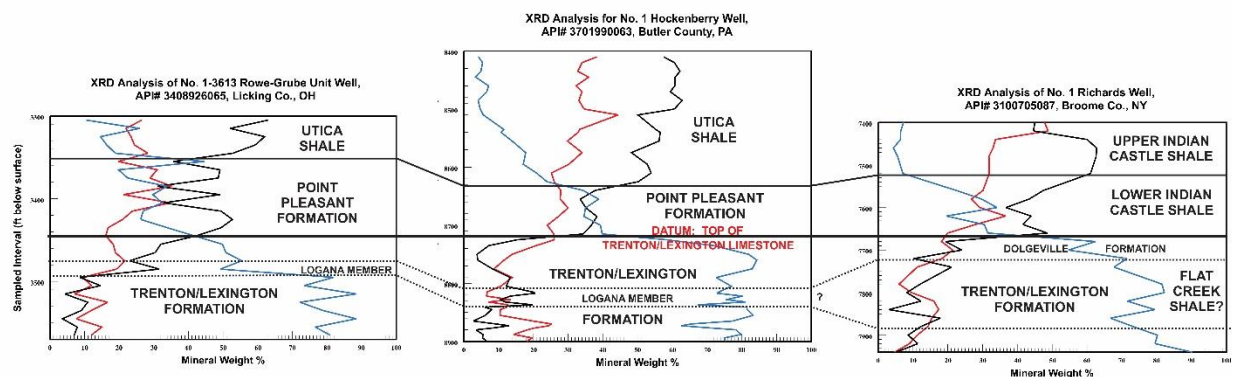
Figure 6-3. Mineral fraction (weight %) versus sample depth (ft) for selected samples in, from left to right, Ohio, Pennsylvania and New York, and their possible use in stratigraphic correlation. Deflections in clay and carbonate mineral percentages may be used to mark the boundaries between the Utica Shale and Point Pleasant Formation (where they both exist), as well as clearly identify the underlying Trenton/Lexington Formation. A small deflection in the clay and carbonate fractions within the Lexington/Trenton Formation possibly identifies the Logana Member and equivalent Flat Creek Shale of New York.

6.1.2   SEM – Energy-Dispersive Spectroscopy

6.1.2.1   Methods

PAGS used SEM imaging in conjunction with energy-dispersive spectroscopy (EDS) techniques to further evaluate the bulk mineralogy composition of nine rock cuttings samples from three wells in Pennsylvania. The samples were chosen for size (>3 mm in largest diameter) from intervals of these wells determined to contain Utica or Point Pleasant shale. The SEM images and corresponding SEM-EDS analytical data (including graphs, text files and element maps) are included in Appendix 6-C.

6.1.2.2   Results

Analytical data for each sample are provided in three parts: (1) a high-resolution image with a nine-digit file name (e.g., S13-013-001) (see, for example, Figure 6-4); (2) an EDS spectrum, which includes a graph and a text file in which the percentages of the elements are listed (Figures 6-5A and B). The percentages represent the entire area shown in the high-resolution image; and (3) a set of element maps showing the image in subdued form overlain with colored dots that show where the element was detected (Figure 6-6). The maps assist with detecting the distribution of

minerals. For example, the map for sulfur (Figure 6-6A) shows where pyrite grains exist, whereas the map for calcium (Figure 6-6B) probably indicates the distribution of carbonates (but could also represent plagioclase feldspars). For each sample, there are separate maps for the elements that were detected, including aluminum, calcium, iron, potassium, magnesium, sodium, sulfur, silicon and titanium. Oxygen, although present, was not included because it occurs in nearly every mineral in these samples; a plot of oxygen would be meaningless under the circumstances. Another element that is conspicuously absent is carbon. Carbon is difficult to detect with the instrument used unless it is extremely abundant. In addition, there is a peak for calcium that coincides with the main peak for carbon, making detecting carbon in calcite nearly impossible, even though we know it is there.
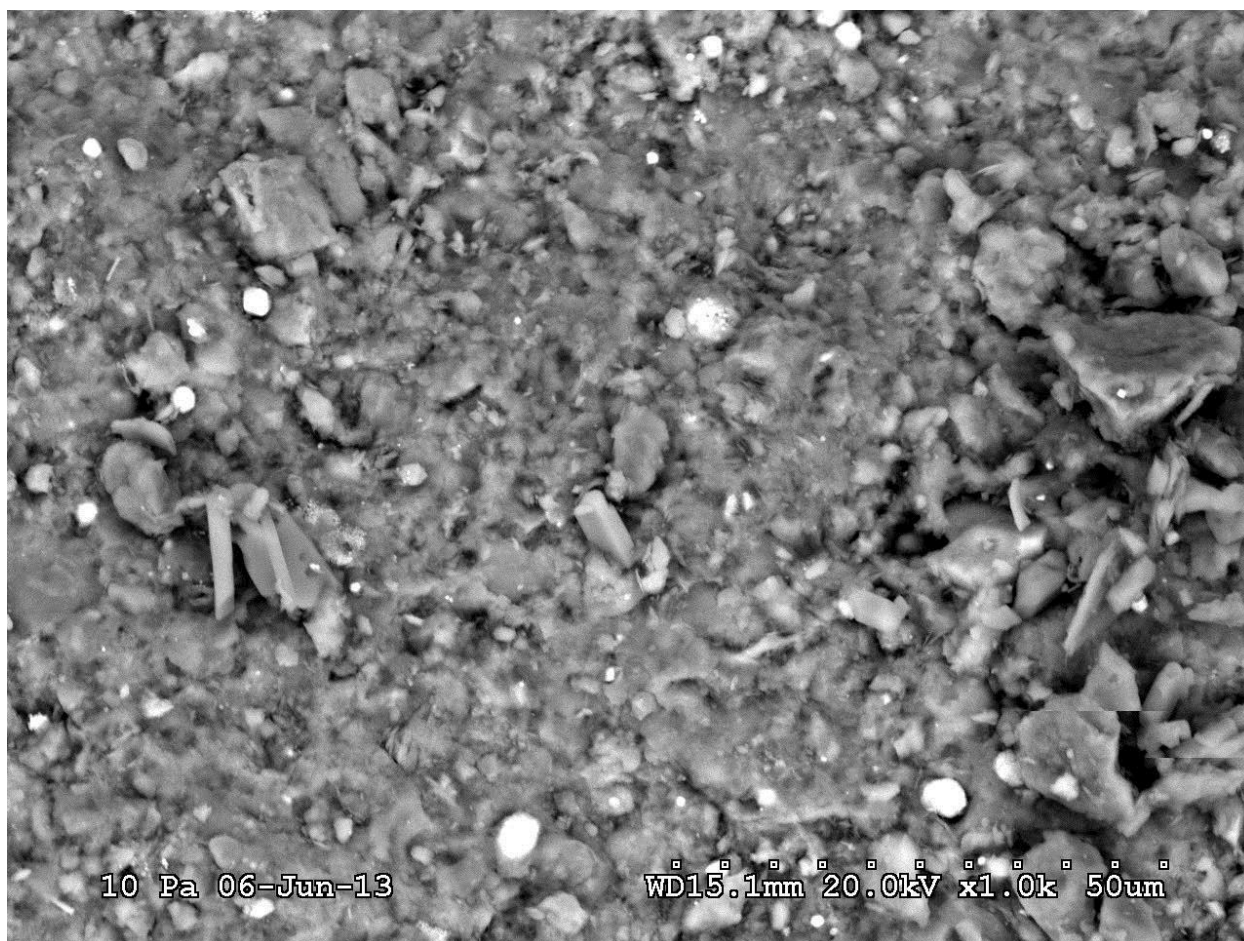
Figure 6-4. High-resolution SEM image of specimen S13-013-001 from sample interval 8504-8513 ft in the Hockenberry No. 1, Butler County, PA.
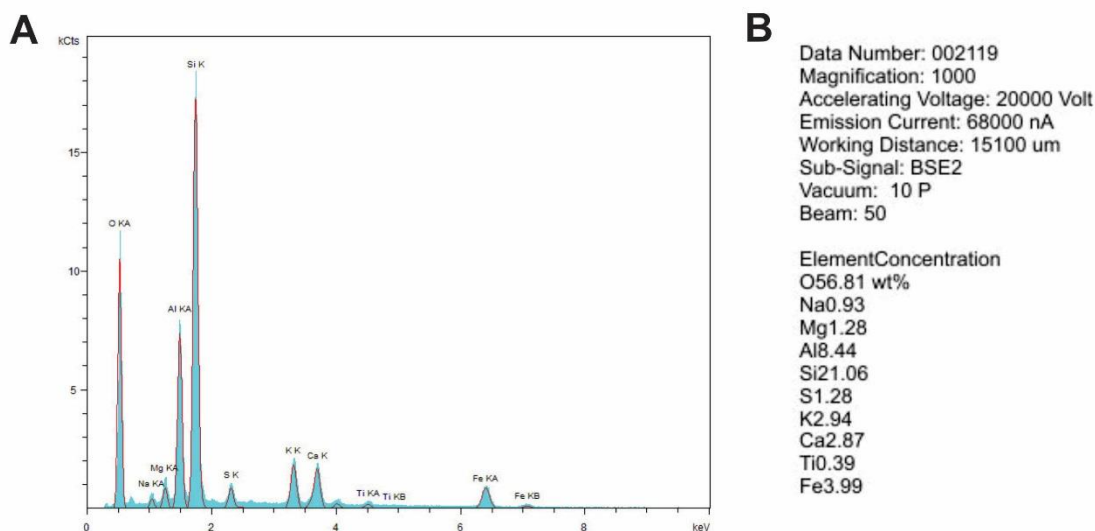
Figure 6-5. Energy-dispersive spectroscopy (EDS) analysis of the sample in Figure 6-4. A – Graph of the elements detected. B – Text file generated to describe the elemental concentrations (weight %) of the primary elements detected in Figure 6-4.
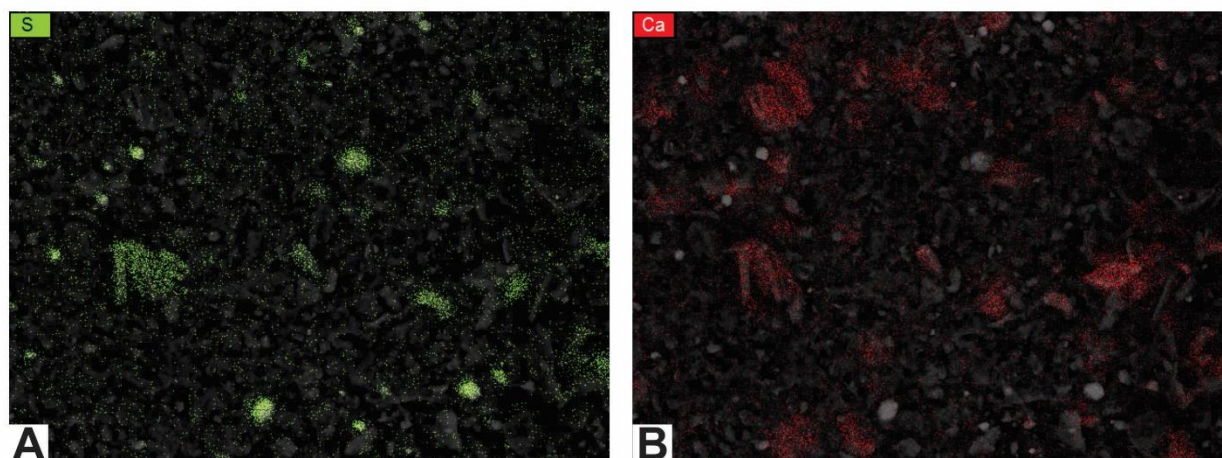
Figure 6-6. Element maps for the image in Figure 6-4 using EDS. A – map of sulfur (green dots); clusters most likely indicate pyrite. B – map of calcium (red dots); clusters most likely indicate calcite or dolomite.

It should be noted that, because these rock fragments do not have perfectly smooth, polished surfaces (i.e., ion milling was not used to process these particular samples), there are places where no element is plotted on the map. Those are areas that were hidden from the detector because of the sample's rough surface. Further, while most of the elements can easily be correlated with specific grains that are visible in the images, some elements show up only as random dots that are sparsely but evenly scattered across a given sample. This likely represents instrument noise and is not a true representation of the present of an element. This is especially noticeable for magnesium and potassium maps in some of these samples.

PAGS also prepared element maps that illustrate multiple elements in contrasting colors (Figure 6-7).   These can be used not only to show the distribution of elements, but also to verify the identity of grains in the SEM photomicrographs. For example, Figures 6-7A and 6-7B provide

maps of silicon and calcium in two wells located at opposite ends of Pennsylvania (Butler and Pike counties). It appears that both samples include grains that are high in calcium and basically devoid of silicon, so these grains should be carbonates rather than plagioclase feldspars. The maps also indicate different calcium contents in these samples, which agrees with the XRD analyses from these wells (total carbonate content in the sampled interval of the Butler County well is 6%, whereas total carbonate content in the sampled interval of the Pike County well is 45%).
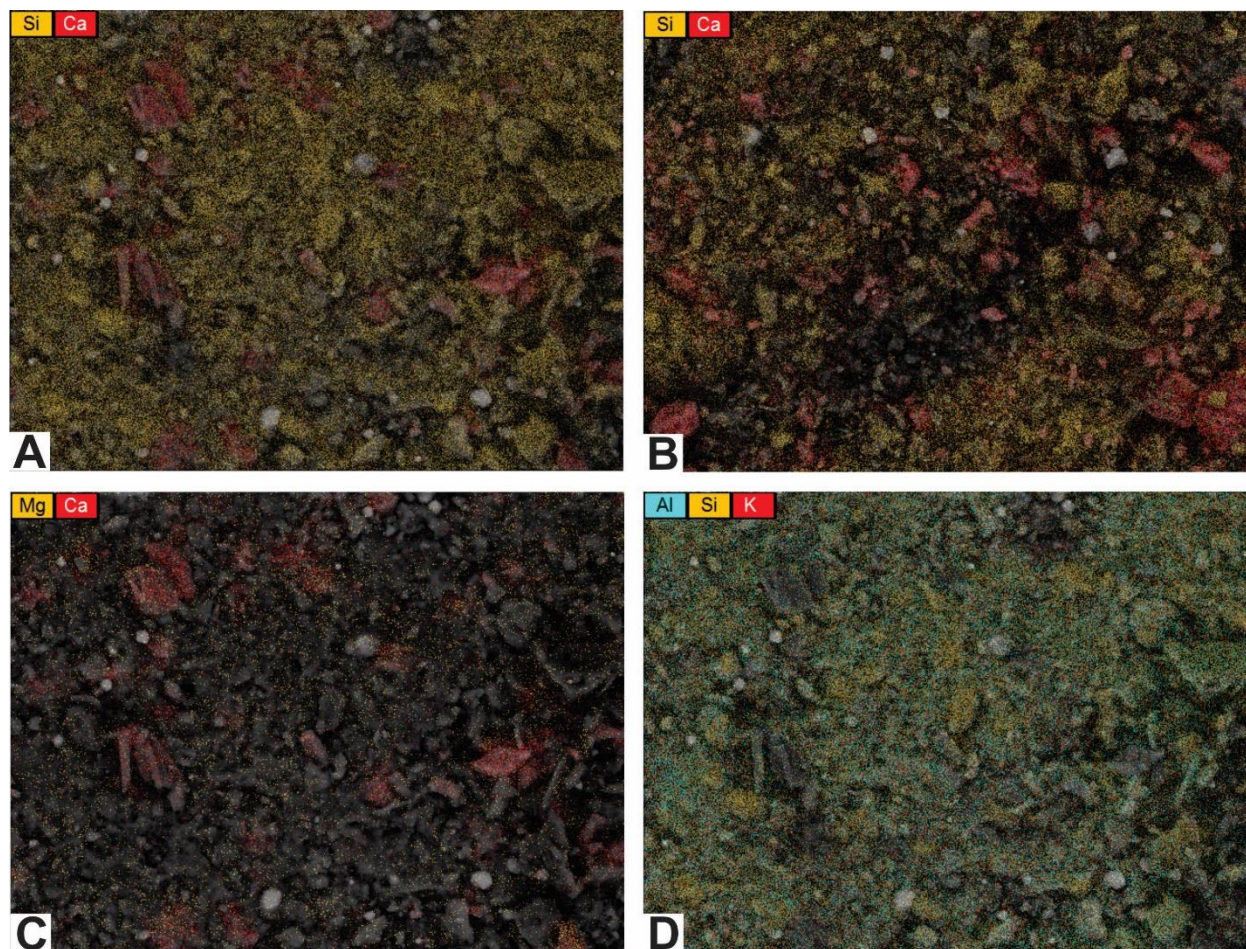
Figure 6-7. Element maps showing distributions of multiple elements. A, C, and D – maps of a rock cuttings sample from a depth of 8504-8513 ft in the Hockenberry No. 1, Butler County, PA. B – map of a rock cuttings sample from a depth of 13,440-13,450 ft in the PA Tract 163 No. 1, Pike County, PA (shown for contrast with A).

Other element maps can be used to detect different minerals. Figure 6-7C is a map of magnesium and calcium in the same Butler County sample as shown in Figure 6-7A. There is very little magnesium in this sample, so the carbonate grains are most likely calcite rather than dolomite. Figure 6-7D is a three-color map of aluminum, silicon and potassium of this same sample. It shows an abundance of each element scattered across the map, suggesting that the majority of this sample is a potassium aluminum silicate. Although the distribution of these elements could indicate clay minerals, k-feldspar, and/or other silicate minerals, the XRD analysis associated with this sample found no k-feldspar present. Therefore, the XRD results are consistent with the interpretation that the matrix in this particular Butler County sample is most likely comprised of one or more clay minerals (e.g., illite).

6.2 Carbonate Content

6.2.1 Methods

NYSM measured rock cuttings and core samples from approximately sixty wells in New York and Ohio for carbonate content using an insoluble-residue analytical procedure. This was accomplished by crushing a sample, weighing the crushed material, acidizing it, putting it in a centrifuge to ensure mixing for three ten-minute periods, drying the sample in an oven and weighing it again. Only the carbonates present (i.e., dolomite and calcite) should be removed by acidizing the sample. The two measured weights for each sample were entered into a formula that is used to calculate the carbonate content. The remaining material (i.e., insoluble residue) would be all non-carbonate constituents – mainly clay with lesser amounts of organic matter, quartz silt and pyrite.

6.2.2 Results and Discussion

When carbonate-content results and TOC measurements were plotted with geophysical logs for a given sample, it became clear that the GR log is mainly driven by carbonate and clay content, rather than TOC content (Figure 6-8). This is unlike the Marcellus Shale play, where GR and TOC track each other very closely. In the Utica Shale and Point Pleasant Formation, the TOC and GR do not track each other for the most part, whereas the carbonate content tracks the GR almost exactly.
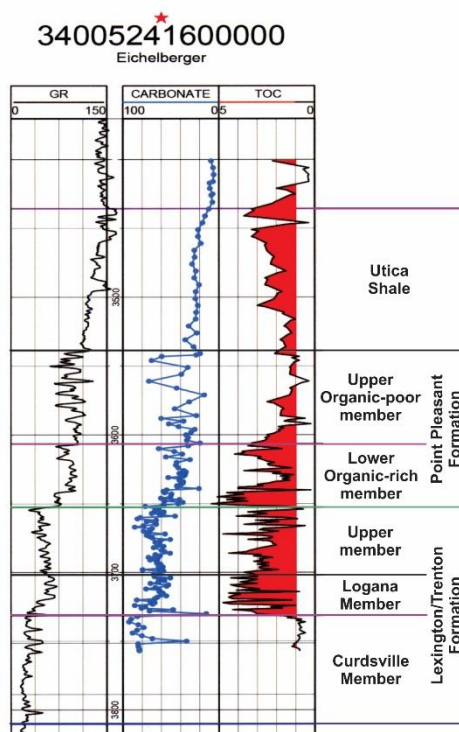
Figure 6-8. GR log, carbonate content and TOC from the Eichelberger No. 1, Ashland County, Ohio.

Figures 6-9 through 6-12 illustrate crossplots of TOC and carbonate content from four cored wells in Ohio. Core descriptions for these locations can be found in Section 5.2. In the absence of matrix porosity, it may be that the best reservoir is where both the TOC and carbonate content

82

are high. Higher carbonate content might lead to a more brittle and "fracable" rock, while high TOC will provide the organic matter porosity necessary for a productive reservoir. If that is the case, the formations plotting along the upper right on these crossplots would be the best potential reservoirs. Alternatively, it may be that some additional porosity can be found between clay particles and that a slightly higher clay (but not too high) content is best. In that case, formations that plot in the upper center on these crossplots would contain better reservoirs (e.g., see upper Lexington/Trenton Formation, Logana Member and Point Pleasant Formation data points on Figure 6-12).

In general, the organic-rich interval is more carbonate-rich in the basal sections of the Utica and more clay-rich upward. Most or all wells drilled in Ohio are targeting the Point Pleasant, which is the organic- and carbonate-rich portion at the base of the organic-rich interval. In the wells studied, the organic-rich shale in the Utica has an average carbonate content of about 25%. This means that the clay content is probably in the 70% range, which is very high (perhaps too high for the rock to be fraced effectively). The Point Pleasant has an average clay content of approximately 50% within the organic-rich facies, and an even greater percentage in the limestone beds. The upper Lexington/Trenton and Logana members have carbonate content values that average about 70% in their organic-rich facies.
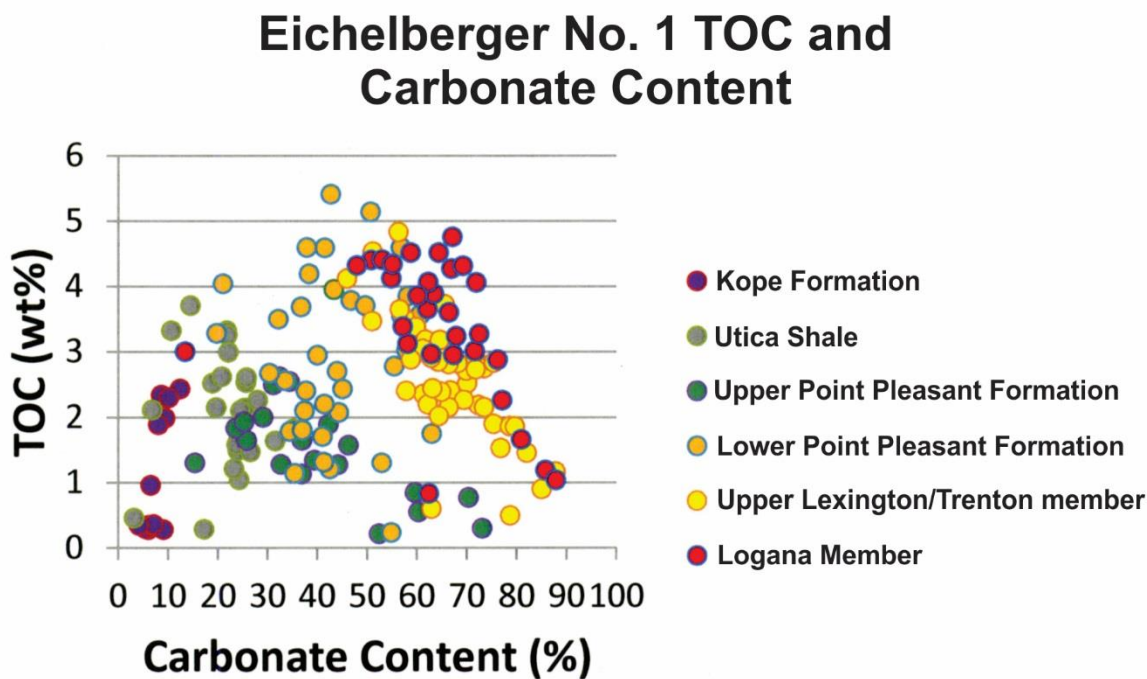
Figure 6-9. Crossplot of TOC and carbonate content from the Eichelberger No. 1 well, Ashland County, Ohio.
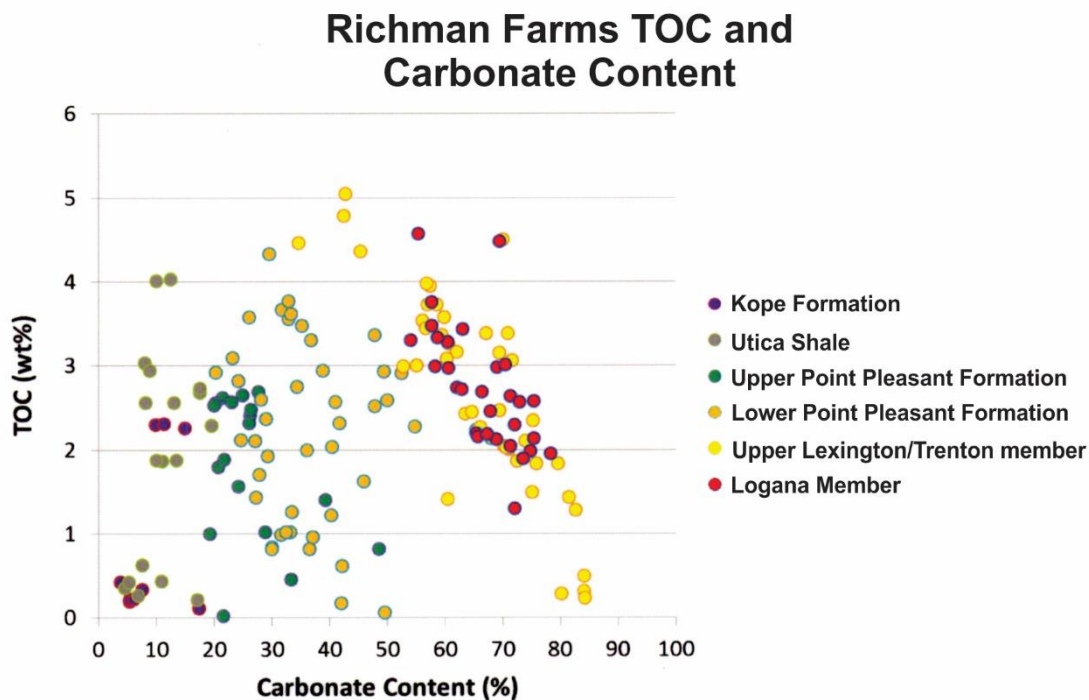
Figure 6-10. Crossplot of TOC and carbonate content from the Richman Farms No. 1 well, Medina County, Ohio.
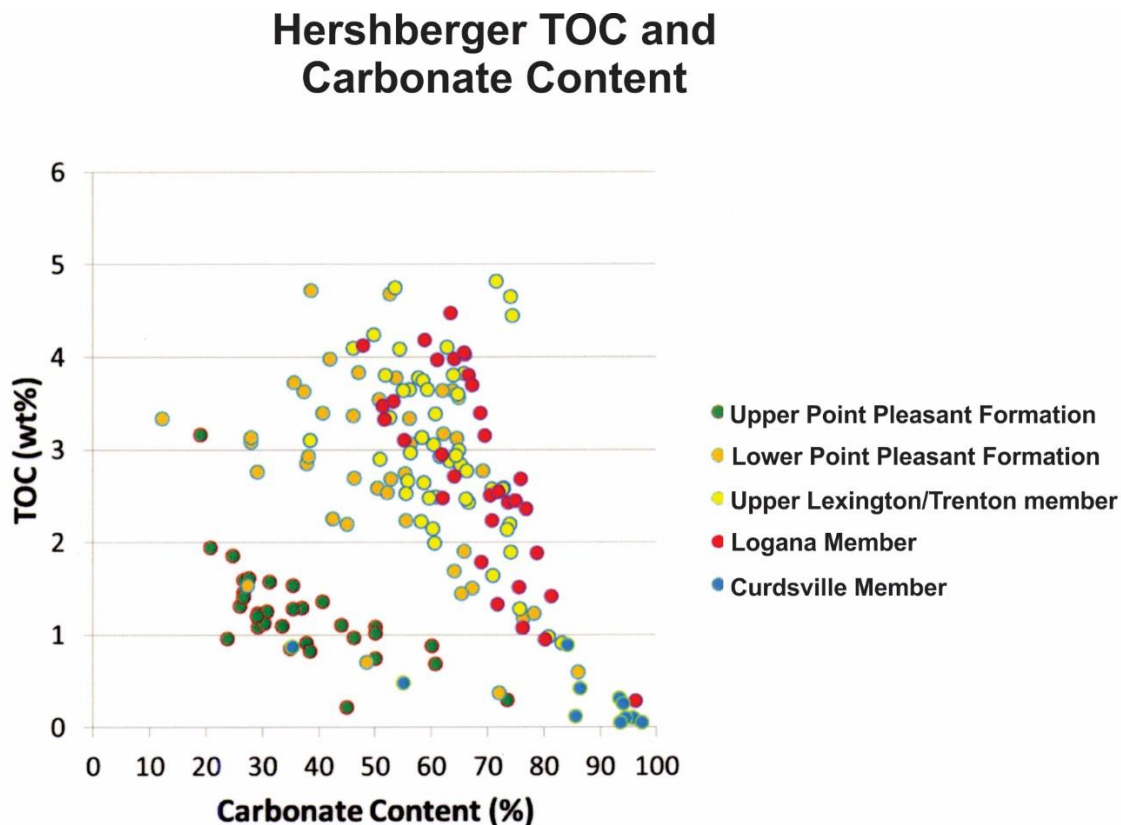
Figure 6-11. Crossplot of TOC and carbonate content from the Hershberger No. 1 well, Wayne County, Ohio.

84
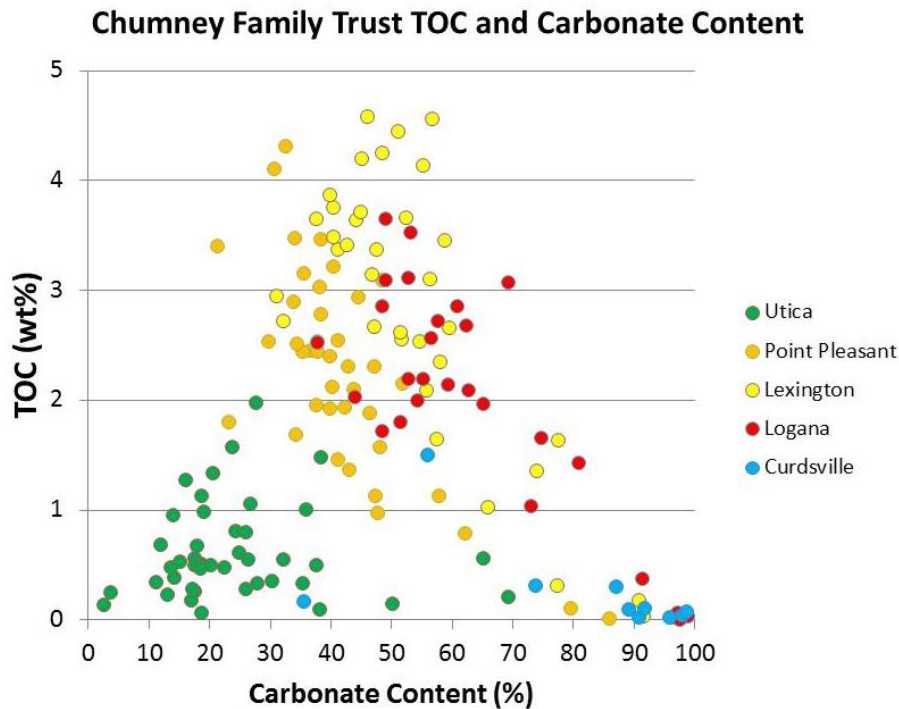
Figure 6-12. Crossplot of TOC and carbonate content from Chumney Family Trust No. 1 well, Guernsey County, Ohio.

Figure 6-13 shows a correlation from Ohio to New York, and Figure 6-14 zooms in on the organic-rich interval. This correlation was confirmed by carbon isotope data (see Section 6.3 below). The organic-rich intervals are time equivalent to each other. See Figure 3-1 for a correlation of the formation names.
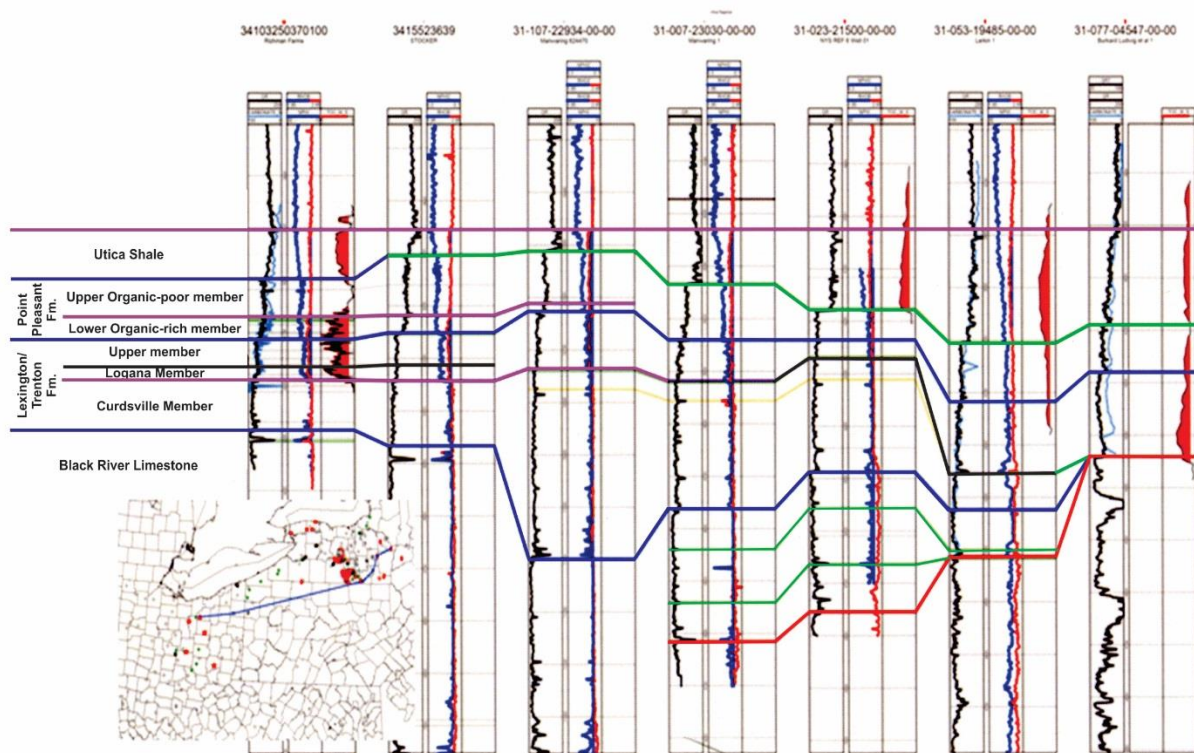
Figure 6-13. Correlation of wells from Ohio to New York from Black River Formation up to Utica Shale. Inset map shows line of section.
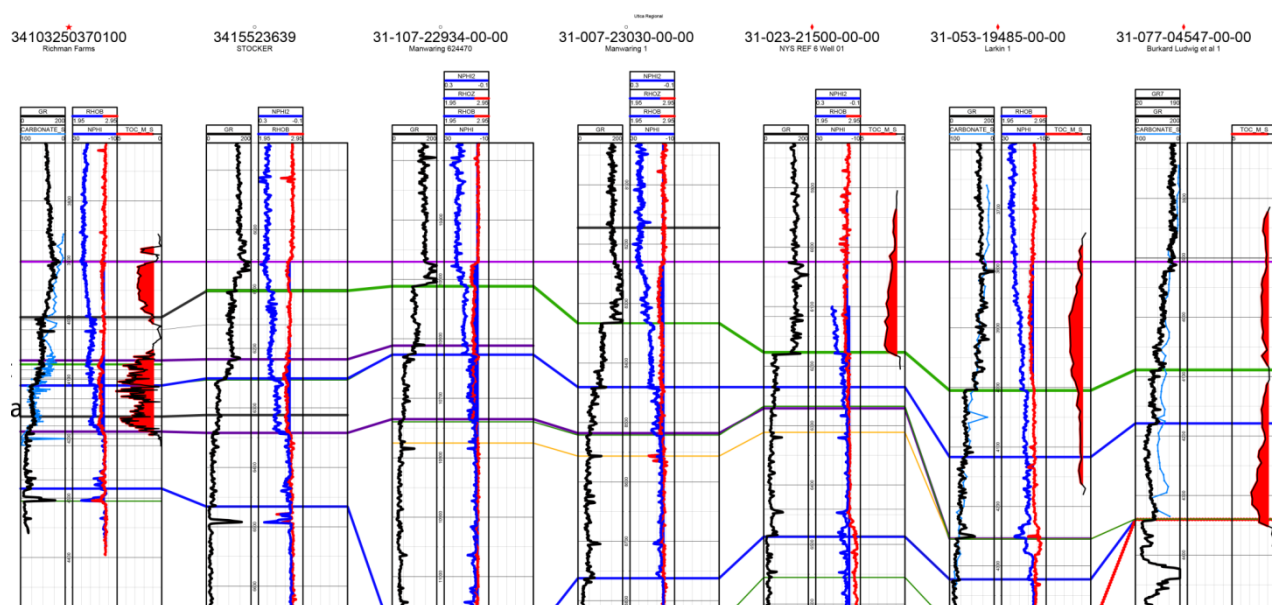
Figure 6-14. Detailed view of organic-rich interval correlated in Figure 6-13. Red-filled curve represents TOC values (%).

Figure 6-15 shows TOC value and carbonate content plotted against well logs from the Skranko No. 1 in Herkimer County, New York, which was drilled into a deep graben where the Utica Shale is extremely thick. The total thickness of organic-rich strata >1% TOC is more than

1300 ft. Figure 6-16 shows a crossplot of TOC value and carbonate content data from rock cuttings collected from this well. At this location, the most organic-rich interval is clearly in the Point Pleasant Formation, which has higher TOC but a low carbonate percentage between 20 and 60% (averages about 40%). Again, the highest TOC intervals have the lowest carbonate content.
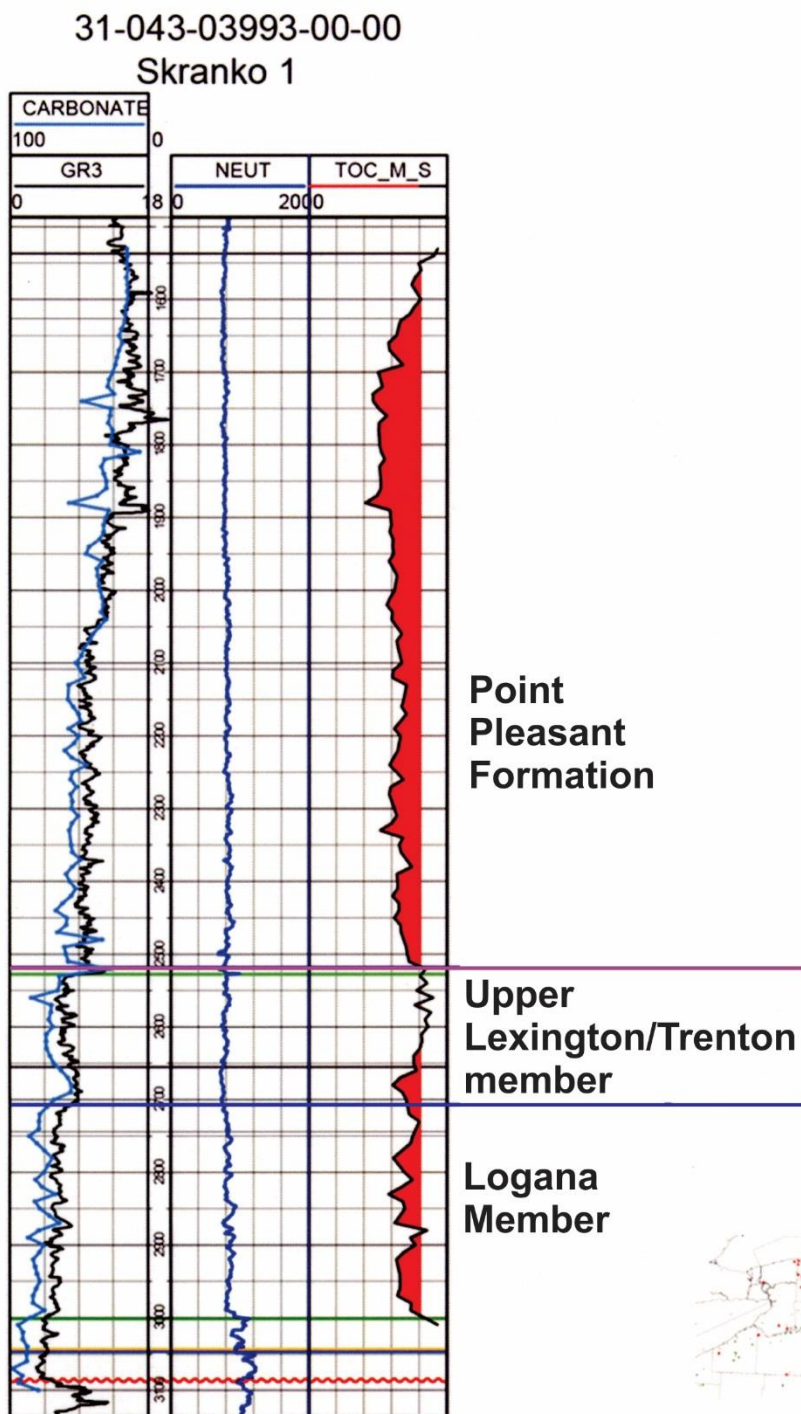
Figure 6-15. GR log, TOC value and carbonate content from the Skranko No. 1 well, which is near the outcrop belt in Herkimer County, New York.
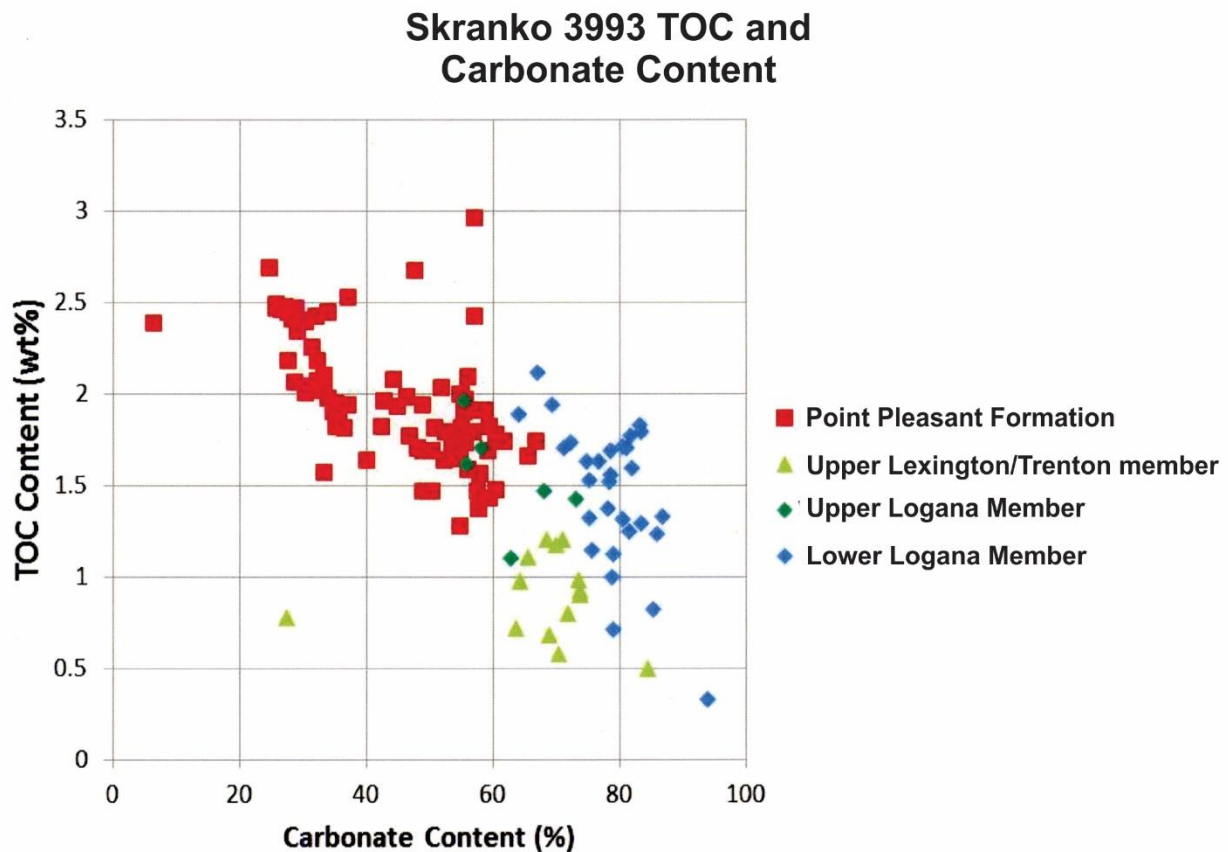
Figure 6-16. Crossplot of TOC value and carbonate content data from the Skranko No. 1 well, Herkimer County, New York.

Figure 6-17 shows well logs and vertical plots of TOC and carbonate content from the Lanzilotta No. 1 well in Delaware County, New York. The GR log follows the carbonate content very closely. In the Lanzilotta well, the most organic-rich interval has shifted to the Logana Member, and it appears that even the upper Lexington/Trenton Formation is somewhat organic-rich. The Point Pleasant Formation, however, is not as organic-rich here. Figure 6-18 is a crossplot of TOC value and carbonate content from rock cuttings from the Lanzilotta No. 1 that confirms that the Logana Member is both the most carbonate- and organic-rich, making it the most likely target in this area.
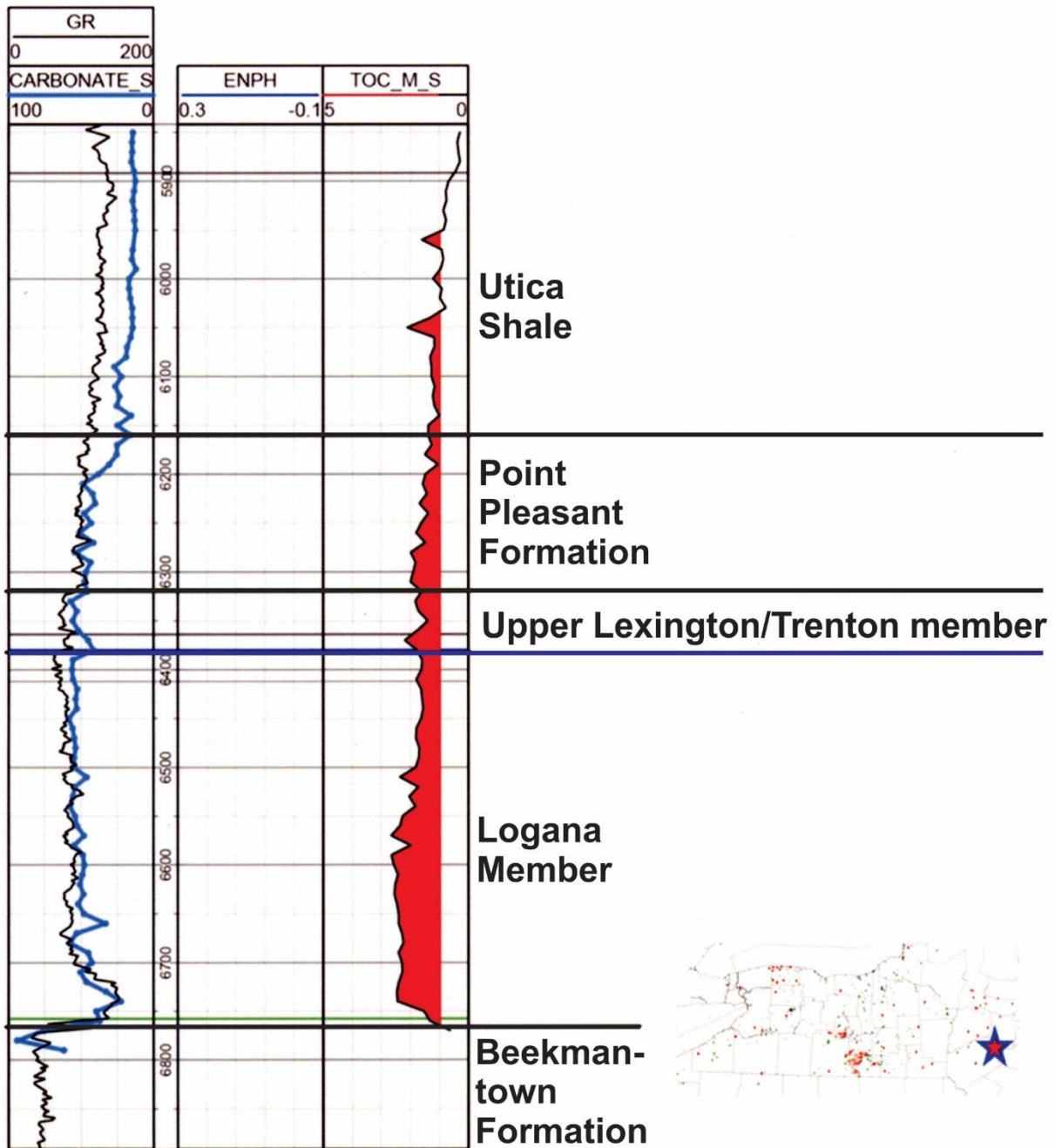
Figure 6-17. GR log, TOC value and carbonate content from the Lanzilotta No. 1 well, Delaware County, New York.
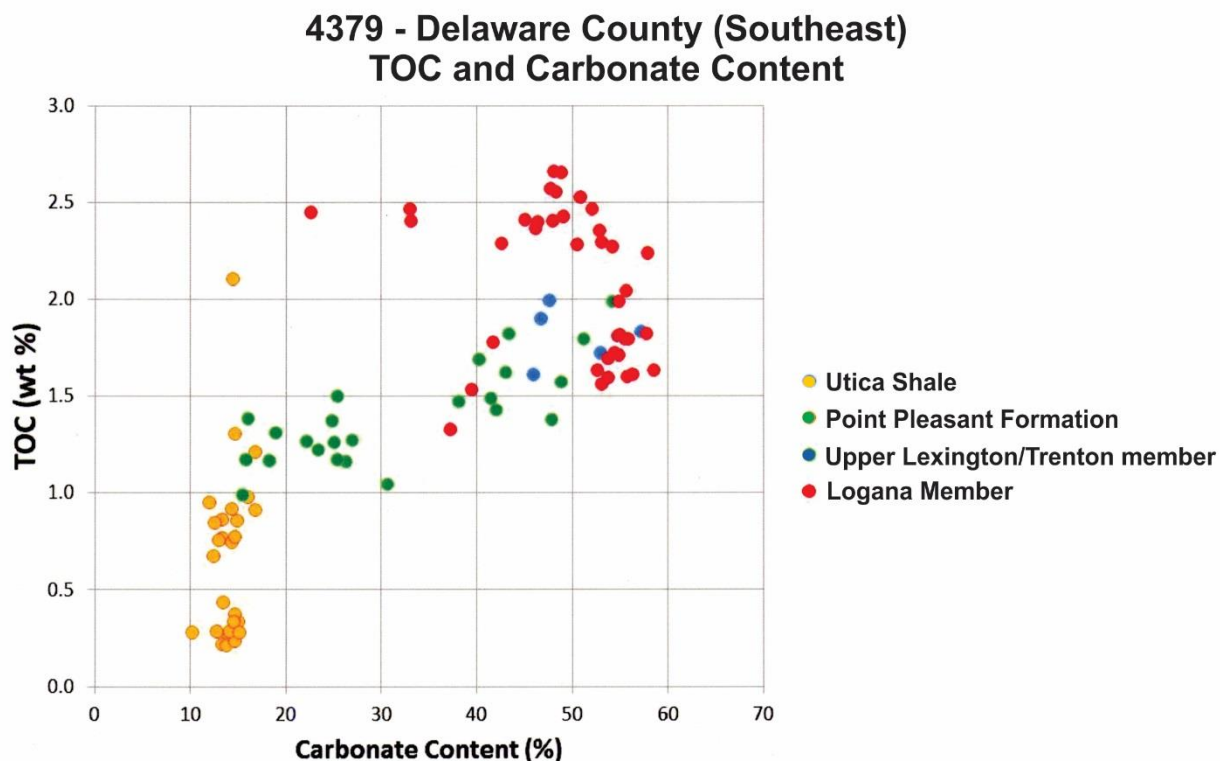
Figure 6-18. Crossplot of TOC value and carbonate content from the Lanzilotta No. 1 well, Delaware County, New York.

6.3 Carbon Isotopes

Carbon isotopes can be used as a chronostratigraphic tool because the isotopic composition of the marine inorganic carbon reservoir ($\delta^{13}C_{DIC}$) changes synchronously across the ocean over time (see Kump and Arthur, 1999, and Metzger and Fike, 2013, for a detailed discussion). There is little isotopic fractionation during carbonate precipitation so that $\delta^{13}C_{carb} \approx \delta^{13}C_{DIC}$. Carbon isotopes are thought to change largely as a function of the global burial flux of organic carbon. The ultimate source of organic carbon produced in the ocean is dissolved inorganic carbon (DIC), and organic carbon is enriched in the lighter isotope, ^{12}C (and therefore has a lower $\delta^{13}C$ value). Buried organic carbon means it does not get oxidized back to DIC and is removed from the ocean. Therefore, when organic-carbon burial is high, $\delta^{13}C_{DIC}$ will increase because organic carbon is enriched in the lighter isotope, ^{12}C. $\delta^{13}C_{carb}$ also can change as a result of the isotopic signature of material DIC being delivered to the ocean. This may be important when the source of carbon being delivered to the ocean changes.

The Late Ordovician Black River, Lexington/Trenton, Point Pleasant and Utica formations were all deposited during the final phase of the Taconic Orogeny, which is characterized by high volcanism and the growth of the Taconic foreland basin. In general, organic matter content increases stratigraphically upward from the Black River to the Lexington/Trenton and Utica, and may represent a globally significant increase in organic carbon burial. This is consistent with positive excursions in $\delta^{13}C_{carb}$ during the study period, but the exact relationship between organic carbon burial and $\delta^{13}C_{carb}$ requires additional constraints on sedimentation rate. The uplift of carbonates in the Taconic highlands to the east of the Taconic foreland basin also may have

90

increased $\delta^{13}C_{carb}$. Future basin history and geochemical work may be able to discriminate between these two mechanisms as a cause of the $\delta^{13}C_{carb}$ excursions.

6.3.1 Methods

Both core and cuttings samples were collected for carbon isotope testing from locations across the Study area (Figure 6-19). Cores were sampled at state geological surveys using hand drills equipped with 1-2 mm carbide drill bits. Mudstone lithologies were targeted in evenly spaced intervals whenever possible, and veins, fossils, burrows, bedding planes, pyritized zones, tempestites and cement-rich zones were avoided altogether. Rock cuttings were collected by J. Garrecht Metzger, Rachel Folkerts and Davey Jones or collected by, and mailed from, companies and state geological surveys. Cuttings were washed in deionized water, when necessary, to remove drilling mud, and then dried in a 70° Celsius (C) oven for 4-24 hours. Cements, fossils, pyrite, metamorphic minerals (e.g., micas), drill bit fragments and other exotic material (e.g., leaves from drill sites) were removed to the extent possible (removal of all secondary material was not possible for very fine-grained samples).
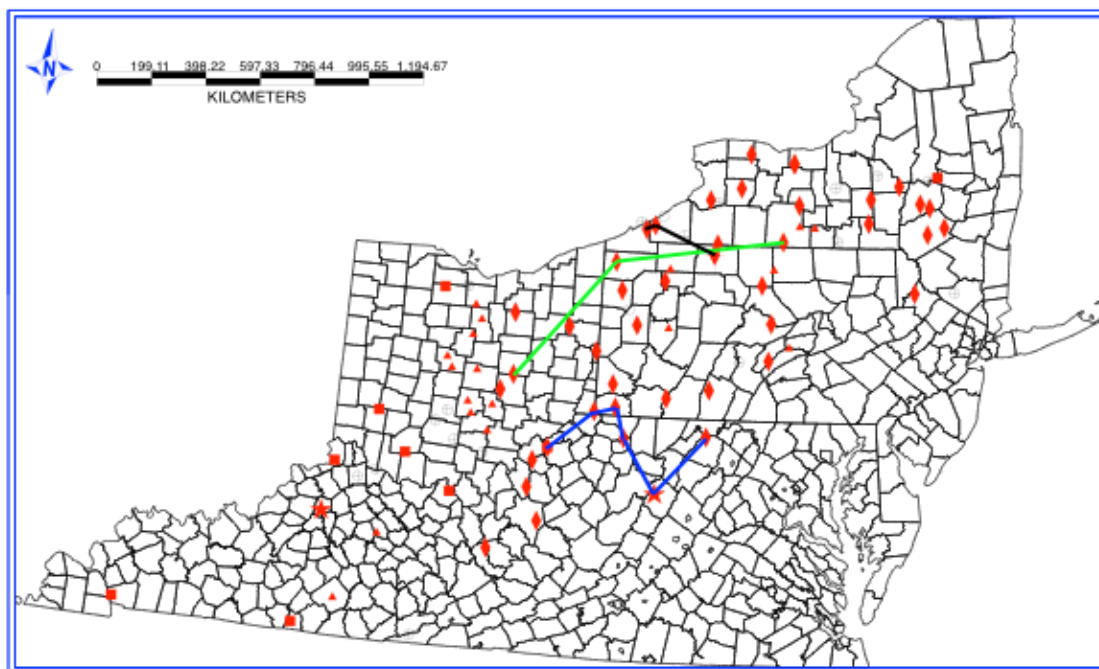
Figure 6-19. Map of sampling locations for carbon isotopes. Cores are identified with red squares, cuttings are red diamonds, and outcrops are red stars. Locations with lithologic and/or TOC and %carbonate data are red triangles. Green line represents the transect for Figure 6-21. Blue line is the transect for Figure 6-22. Black line is the transect for Figure 6-23.

A fraction of each cuttings sample (<1 gram [g]) was selected for analysis based on lithological properties. As color-specific sampling in New York core 74NY5 demonstrated that darker material extracted from mixed dark and light mudstone lithologies better represented the basinwide $\delta^{13}C$ signal (Metzger and others, in press), darker material was isolated in the sampling process whenever possible. Cuttings were crushed using an electric drill equipped with carbide drilling chamber or crushed by hand using a ceramic mortar and pestle.

Carbon and oxygen isotopes were measured on a Thermo Fischer Delta V Plus Isotope Ratio Mass Spectrometer at Washington University in St. Louis. Isotope values are reported in per mil (‰) relative to the Vienna Pee Dee belemnite (VPDB) standard. Isotope values are defined in the following way:

$$\delta^{13}C = (^{13}C/^{12}C_{standard}/^{13}C/^{12}C_{sample} - 1) * 1,000 \text{ in units of per mil (‰)}$$

$$\delta^{18}O = (^{18}O/^{16}O_{standard}/^{18}O/^{16}O_{sample} - 1) * 1,000 \text{ in units of per mil (‰)}$$

All runs contained internal standards calibrated to international standards. A typical standard deviation for replicates of $\delta^{13}C_{carb}$ and $\delta^{18}O_{carb}$ was ~0.1‰. In total, samples from six cores and 51 wells were analyzed (Table 6-2).

Table 6-2. List of core and cuttings samples analyzed for carbon isotopes.

State	Well ID	API	Type	Total # of Samples	U/Tr Samples only
KY	C511	N/A	Core	133	44
KY	T1294	N/A	Core	137	24
NY	03924	3110103924	Cuttings	11	11
NY	03993	3104303993	Cuttings	1	NA
NY	04214	3102404214	Cuttings	2	2
NY	04379	3102504379	Cuttings	9	NA
NY	04547	3107704547	Cuttings	22	NA
NY	09540	3107309540	Cuttings	16	16
NY	09578	3105309578	Cuttings	22	NA
NY	10834	3107710834	Cuttings	11	11
NY	11387	3101311387	Cuttings	77	NA
NY	19485	3105319485	Cuttings	16	6
NY	21500	3102321500	Cuttings	27	27
NY	21703	3110121703	Cuttings	152	87
NY	23158	3101123158	Cuttings	6	0
NY	23551	3102923551	Cuttings	24	0
NY	23829	3110123829	Cuttings	21	21
OH	1365	3404120109	Cuttings	54	NA
OH	1513	3414120014	Cuttings	14	NA
OH	1943	3407720053	Cuttings	20	NA
OH	4135	3414120042	Cuttings	26	NA
OH	4136	3412727130	Cuttings	26	NA
OH	4230	3416320924	Cuttings	14	NA
OH	4245	3404521156	Cuttings	29	NA
OH	5194	3404521249	Cuttings	16	NA
OH	20670	3402920670	Cuttings	118	37
OH	22570	3403122570	Cuttings	83	45
OH	23743	3411723743	Cuttings	27	14
OH	24861	3416924861	Cuttings	80	26
OH	28214	3411928214	Cuttings	65	27
OH	H2626	3407160009	Core	166	66
OH	S2580	3414760840	Core	161	58
OH	W2627	3416560005	Core	156	54

State	Well ID	API	Type	Total # of Samples	U/Tr Samples only
PA	22278	3712522278	Cuttings	100	NA
PA	30138	3705330138	Cuttings	75	NA
PA	90063	3701990063	Cuttings	100	NA
PA	24659 (AKA: EQT 590003)	3705924659	Cuttings	125	NA
PA	KRDSH	3703920007	Cuttings	85	53
PA	LONG	3702720001	Cuttings	113	92
PA	N2F	3708331744	Cuttings	94	56
PA	N972	3710520182	Cuttings	229	122
PA	ORSHK	3704920345	Cuttings	91	55
PA	PASF	3708720002	Cuttings	140	100
PA	PIKE	3710320003	Cuttings	23	23
PA	SHLBG	3700920034	Cuttings	86	42
PA	SVETZ	3711120045	Cuttings	162	6
PA	TMPL	3708520036	Cuttings	98	67
WV	H12	4702700012	Cuttings	244	106
WV	H80	4702900080	Cuttings	93	56
WV	J1366	4703501366	Cuttings	213	99
WV	K3462	4703903462	Cuttings	121	75
WV	M244	4704900244	Cuttings	145	57
WV	M539	4705100539	Cuttings	194	108
WV	M805	4705900805	Cuttings	151	36
WV	W351	4710700351	Cuttings	85	85
WV	WCC	4710700351	Core	48	30
WV	W756	4710700756	Cuttings	149	82
		TOTAL		3813	1453

6.3.2 Results and Discussion

In general, the isotopic intervals of Metzger and others (in press) are identifiable throughout the Study area. Chronostratigraphic correlations were based on $\delta^{13}C_{carb}$, and many of these were geographically consistent with GR logs. Therefore, if $\delta^{13}C_{carb}$ internal boundaries were indistinct in a given well, the corresponding GR logs were used to facilitate correlations. While $\delta^{13}C_{carb}$ results provide new insights into the chronostratigraphic relationships of Late Ordovician strata across the Study area (for example, Figure 6-20, which is confined to New York), some wells contained noisy, uncorrelateable $\delta^{13}C_{carb}$ signals. In general, these were found in wells with grainstone lithologies or high cement contents. Figure 6-21 shows an example of close well spacing with a combination of clear and noisy $\delta^{13}C_{carb}$ signals. This emphasizes that not only should $\delta^{13}C_{carb}$ records be interpreted in conjunction with other credible data (e.g., core descriptions and geophysical logs) but also that $\delta^{13}C_{carb}$ should be sampled from multiple locations within a given region in order to provide the most precise results.
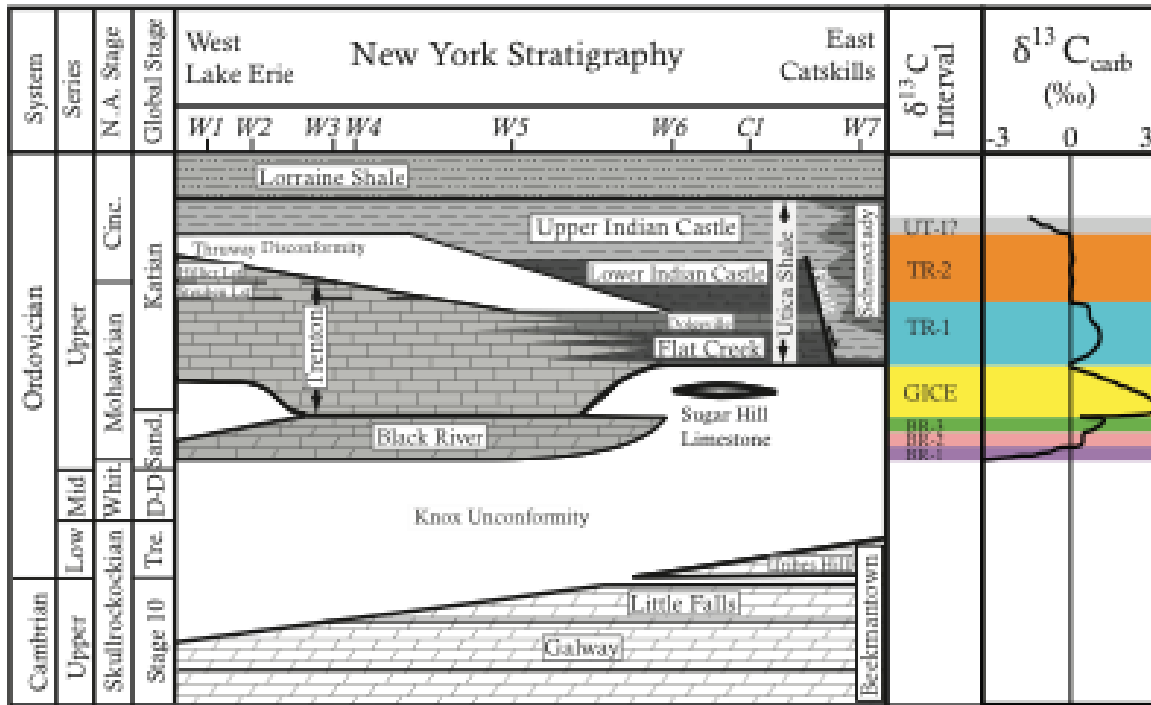
Figure 6-20. Chronostratigraphic relationships of Late Ordovician formations in New York (left) with generalized $\delta^{13}C_{carb}$ intervals and $\delta^{13}C_{carb}$ chemostratigraphic profiles (right). Stage abbreviations are Whit = Whiterockian, Cinc = Cincinnatian, Sand = Sandbian, D-D = Darriwilian to Dapingian, Tre = Tremadocian. New $\delta^{13}C_{carb}$ intervals (BR = Black River Group, TR = Lexington/Trenton Formation, UT = Utica Shale) are named for lowest formation in which they were found. GICE = Guttenberg isotopic carbon excursion. "?" next to UT-1 suggests interval is not suitable for correlation (see discussion). $\delta^{13}C_{carb}$ reference curve with intervals taken from data in this work. Values are in permil (‰) relative to VPDB. Study locations (W1-W7, C1) are shown in their approximate position along the west to east transect. Figure adapted from Metzger and others (in press).
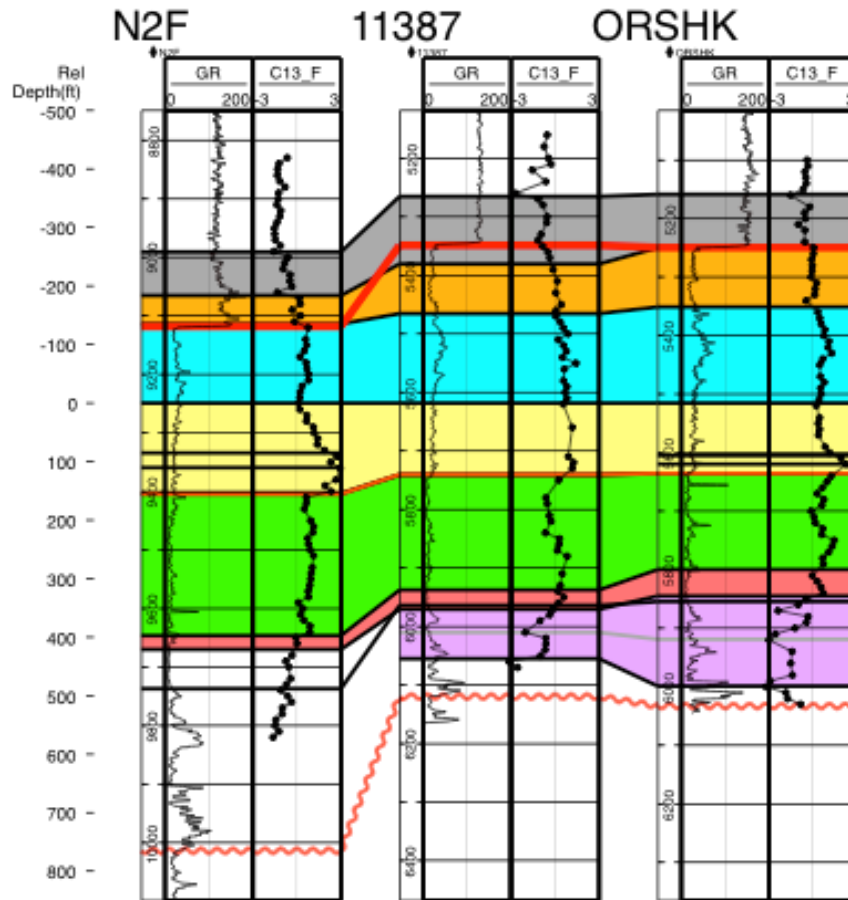
Figure 6-21. Transect of closely spaced wells showing discrepancy in $\delta^{13}C_{carb}$ records over short distances (green line in Figure 6-19). Well N2F best records isotope intervals while 11387 shows signs of significant alteration in GICE (yellow) and BR-3 (green), while well ORSHK shows moderate alteration. Solid red line indicates the top of the Lexington/Trenton Formation. Wavy red line indicates the Knox unconformity.

Figure 6-22 shows a transect across West Virginia, illustrating the shifting sediment depocenter during Ordovician time. Here, the locus of sedimentation shifts from the west during the Black River (purple, red and green intervals) to the east during the early part of the Guttenberg excursion (yellow interval), and back to the west in the upper Guttenberg excursion and interval TR-1 (blue). Because the duration of the Guttenberg excursion is ~500,000 years the sedimentation shift takes place over the course of a few hundred thousand years. This transition is sufficiently rapid that a simple tectonic explanation is difficult to construct. The bi-directional movement (west then back east) adds to the complication. It may be that the change in sedimentation is a response to changing eustatic sea level caused by ice formation or a combination of tectonics and ice. While no direct geologic evidence for ice accumulation in the Ordovician exists prior to the Late Katian, there is geochemical evidence that suggests ice may have been present around the time of the Black River-Trenton transition (Finnegan and others, 2011).
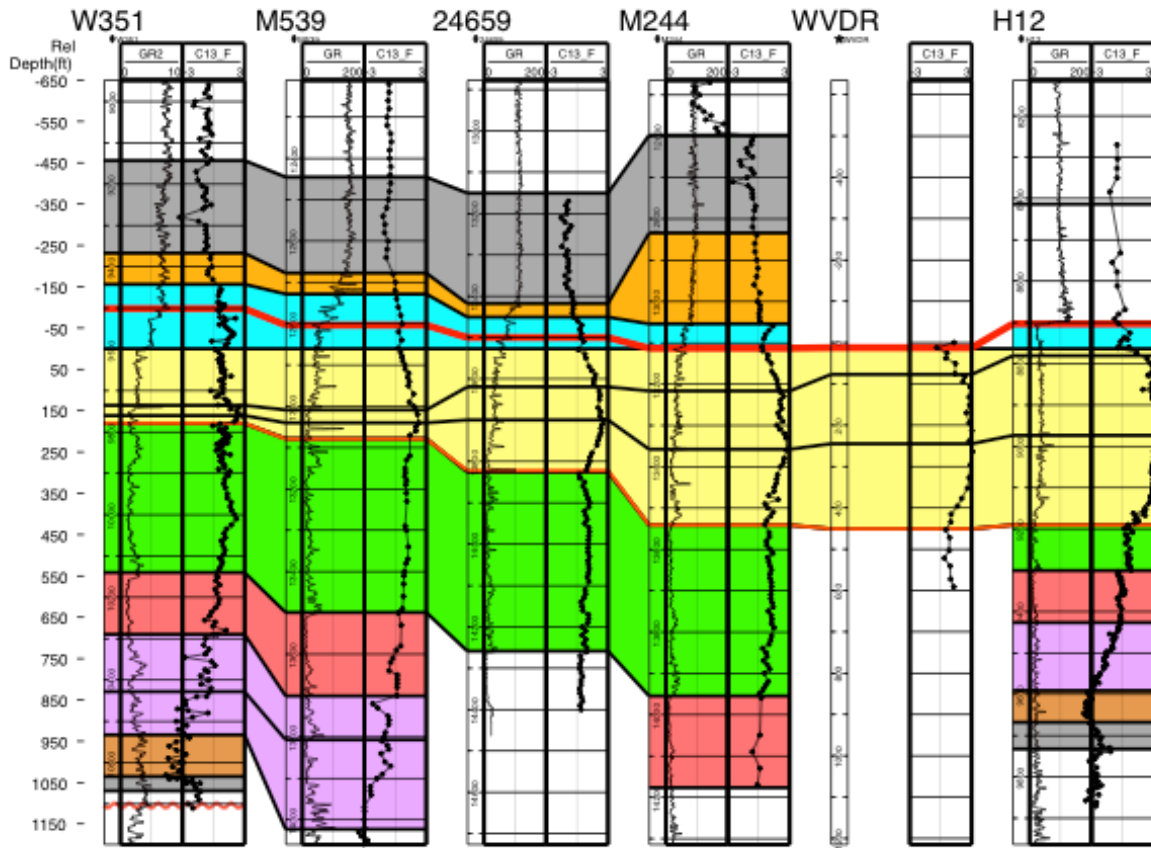
Figure 6-22. Transect across West Virginia and Pennsylvania (blue line in Figure 6-19). Solid red line is the top of Lexington/Trenton, wavy red line is the Knox unconformity. Base of GICE is always found at the top of Black River. Note changing depocenter from west during Black River time, east during the lower GICE, and back to west in the upper GICE, and TR-1. Correlation picks within the GICE are based on peak $\delta^{13}C_{carb}$ values (lower black line within yellow interval) and falling limb of excursion where $\delta^{13}C_{carb} = 2‰$ (upper black line in yellow interval). Transect is flattened on top of GICE excursion. WVDR is an outcrop from Young and others (2005). This outcrop is not thrust-thickened, despite being in the fold and thrust belt, which suggests that at least some of the thick sections seen in the fold and thrust belt are original thicknesses.
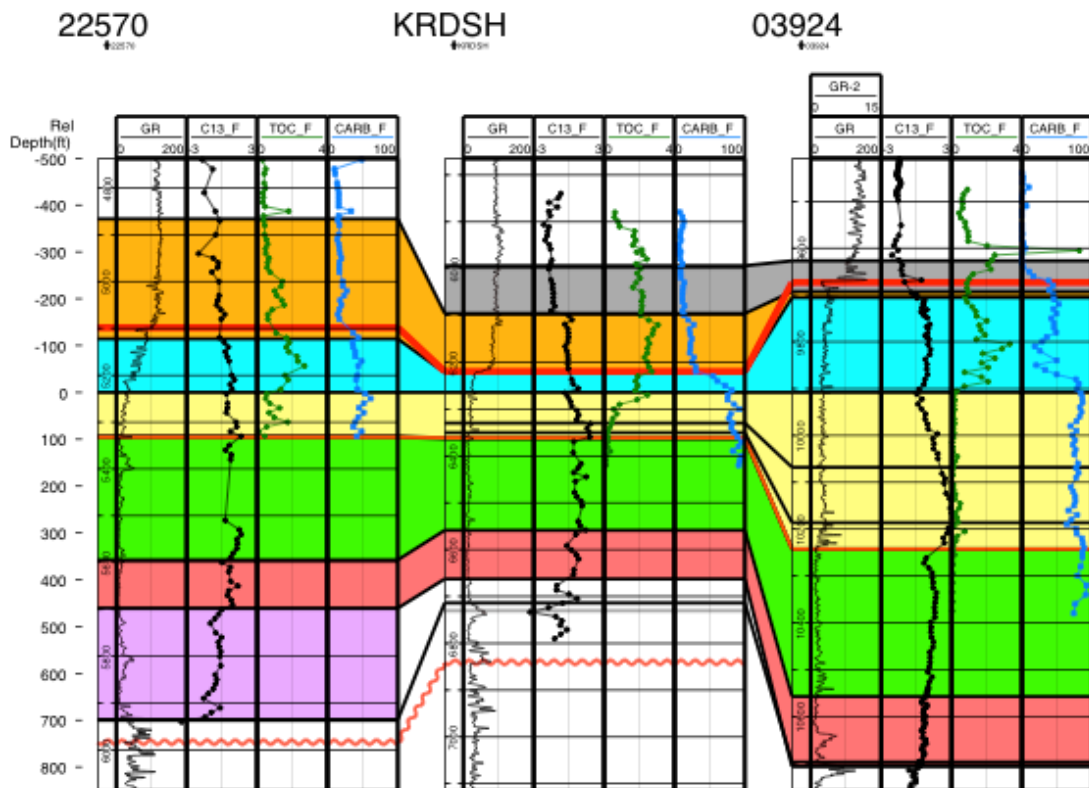
Figure 6-23. Transect across New York and Pennsylvania (black line in Figure 6-19). Relationship between TOC and $\delta^{13}C_{carb}$, where TOC is most often highest in TR-1 (blue) and TR-2 (orange). This is thought to show the time dependence of organic-rich rocks, rather than a specific lithology that traps migrating hydrocarbons. TR-1 includes transitional units between the Lexington/Trenton and Utica Shale.

The remainder of this section presents isopach maps (Figures 6-24 through 6-31) based on the $\delta^{13}C_{carb}$ intervals of Metzger and others (in press). In general, they illustrate a shift in depocenter from West Virginia during Black River time, to New York during the GICE and TR-1 when faulting is initiated in New York, and then onto the carbonate platform in Ohio during TR-2. This could be due to rising sea level from the uppermost GICE interval and above where the sedimentation locus moved shoreward during transgression.
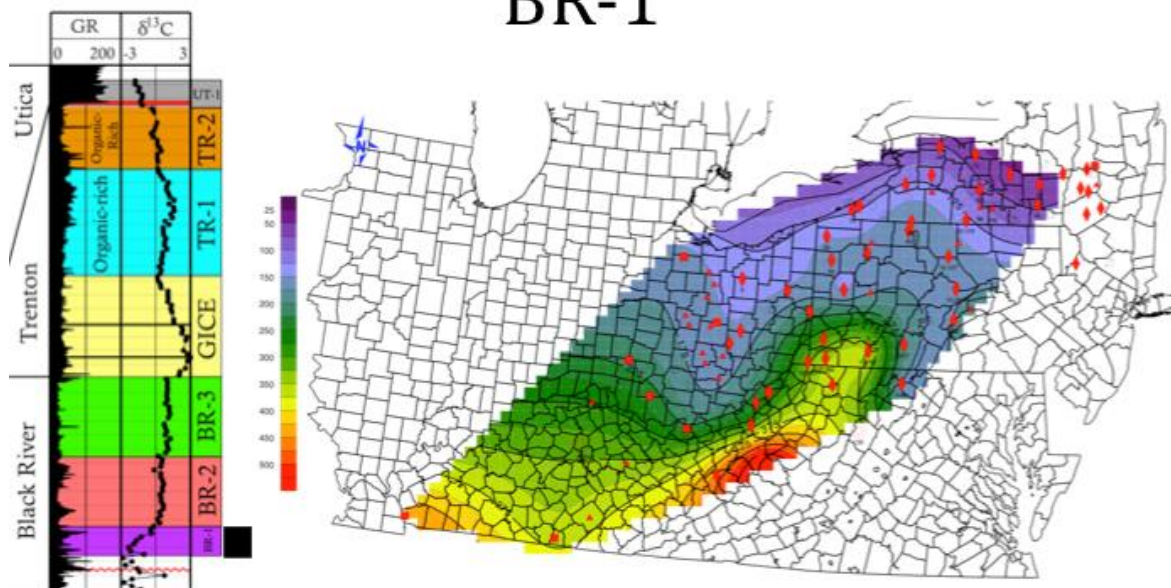
Figure 6-24. Isopach map in ft of $\delta^{13}C_{carb}$ interval BR-1.

Figure 6-25. Isopach map in ft of $\delta^{13}C_{carb}$ interval BR-2.
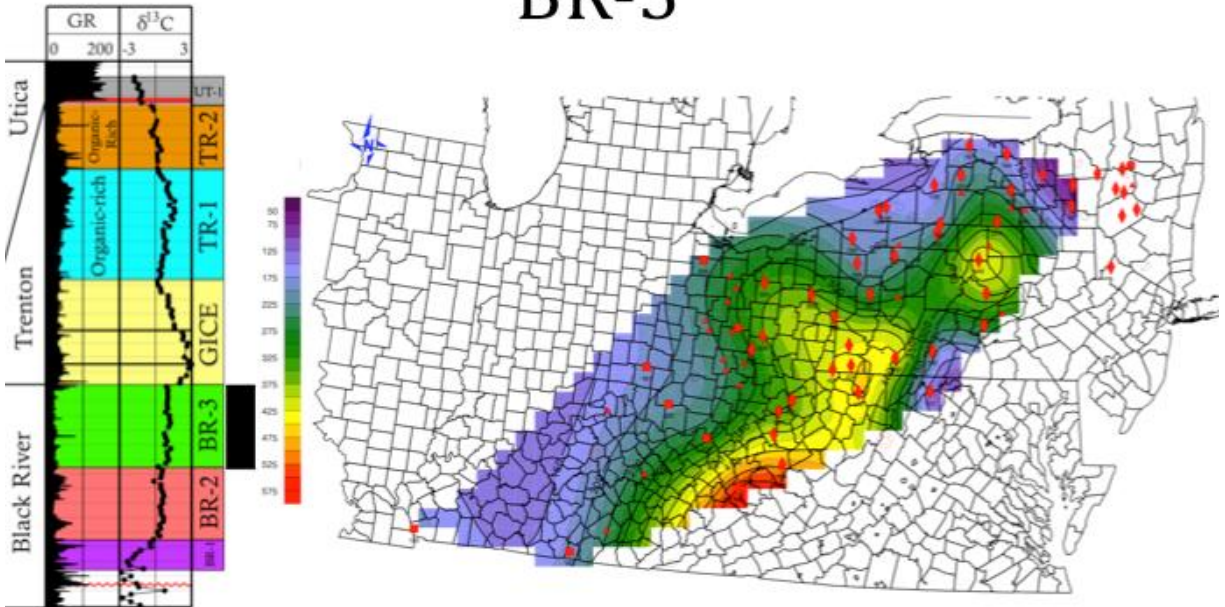
Figure 6-26. Isopach map in ft of $\delta^{13}C_{carb}$ interval BR-3.
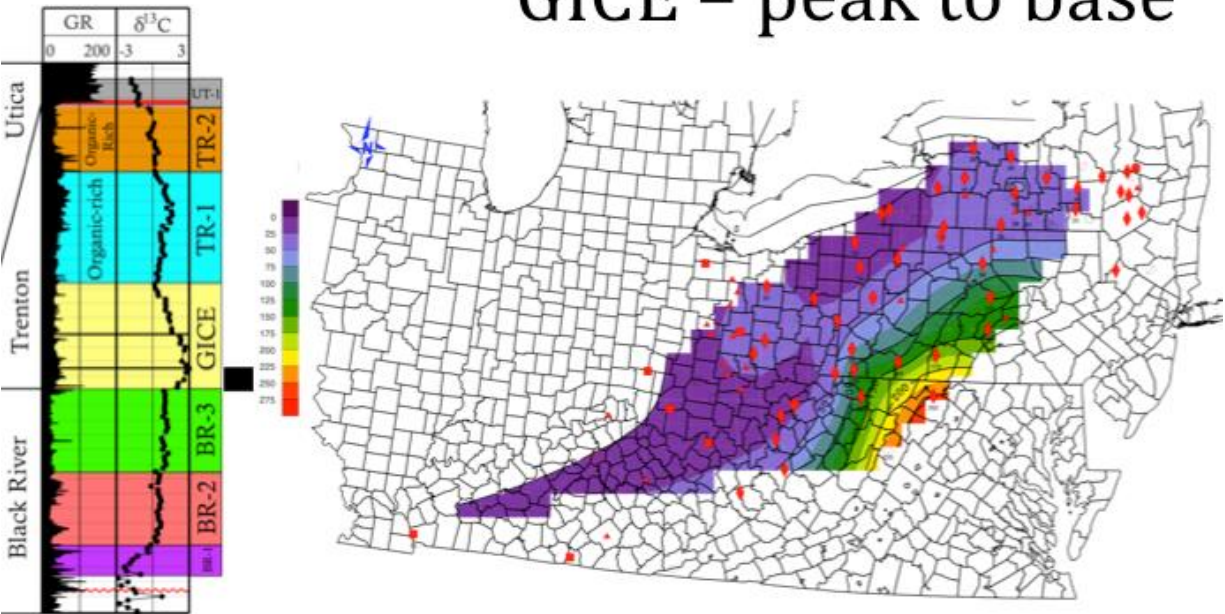
Figure 6-27. Isopach map in ft of $\delta^{13}C_{carb}$ interval GICE peak to base.

Figure 6-28. Isopach map in ft of $\delta^{13}C_{carb}$ interval GICE fall to peak.

Figure 6-29. Isopach map in ft of $\delta^{13}C_{carb}$ interval GICE end to fall.

TR-1
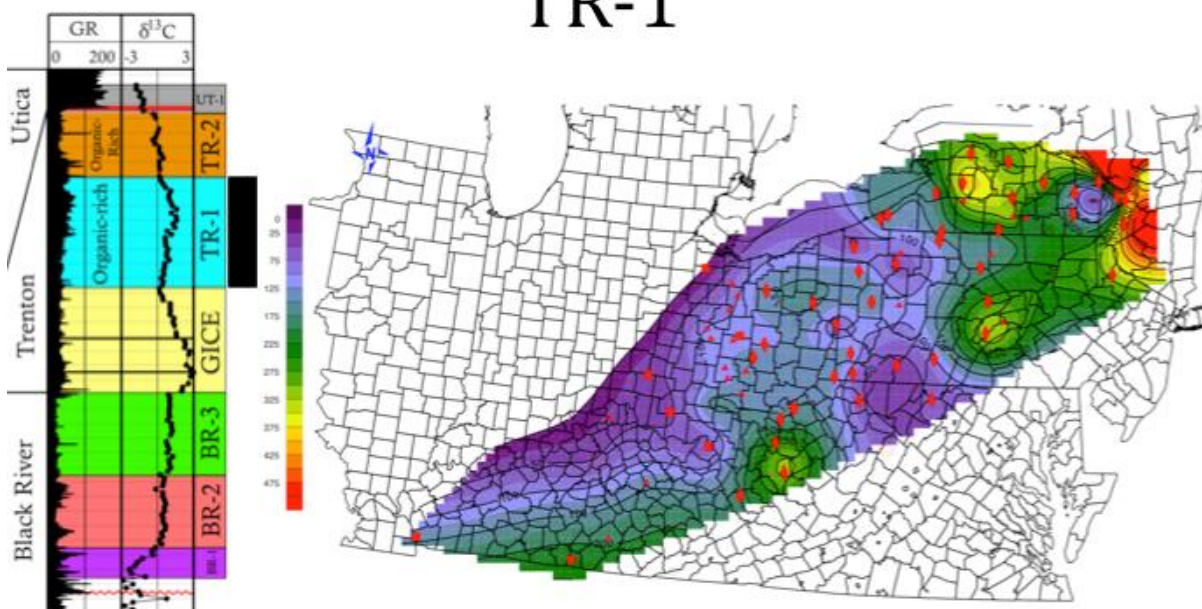
Figure 6-30. Isopach map in ft of $\delta^{13}C_{carb}$ interval TR-1.

TR-2
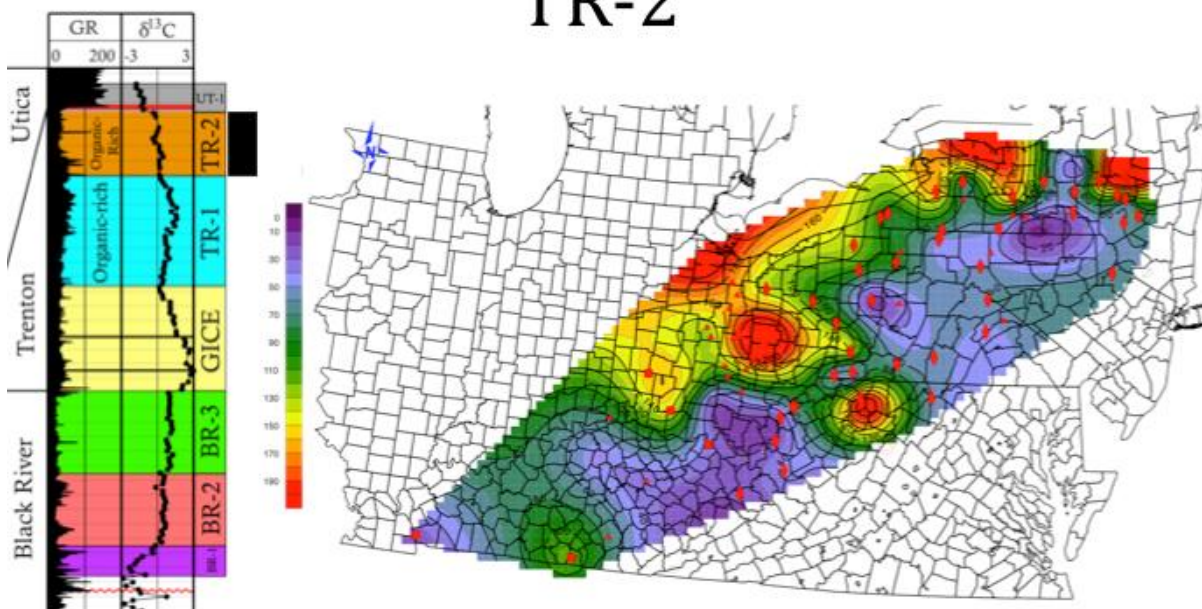
Figure 6-31. Isopach map in ft of $\delta^{13}C_{carb}$ interval TR-2.

Clearly correlatable $\delta^{13}C_{carb}$ signals were captured in all study areas, and $\delta^{13}C_{carb}$ intervals are largely equivalent to those observed in New York (Metzger and others, in press). Signal clarity was lower in cement-rich grainstone lithologies and in areas with low sampling resolution (relative to sedimentation rate). In general, the most organic-rich strata were found in $\delta^{13}C_{carb}$ intervals TR-1 and TR-2, with the former being the most organic-rich of all the $\delta^{13}C_{carb}$ intervals. Interval TR-

1 is found in the strata transitional between the argillaceous carbonates of the Lexington/Trenton Formation and black shales of the Utica and Point Pleasant formations.

7.0   SOURCE ROCK GEOCHEMISTRY

The source rock geochemistry findings reported for this Study incorporate both legacy and newly-generated data for Utica/Point Pleasant and equivalent samples collected in the basin, and include evaluations of organic matter content, quality and thermal maturity. The research team performed TOC analyses, reviewed legacy RockEval data, evaluated organic petrography and performed reflectance and conodont alteration index (CAI) analyses to assess the thermal maturity of these reservoir rocks.

7.1   TOC Analysis

In order to analyze the potential for hydrocarbon production from Late Ordovician strata within the Study area, well cuttings and core samples were analyzed to assess their TOC content. TOC values greater than 1% are interpreted to have the potential for hydrocarbon production, presuming that adequate thermal maturation has occurred (Jarvie, 1991).

7.1.1 Materials and Methods

KGS analyzed 1094 samples from 29 wells for TOC content for this Study using a LECO carbon/sulfur analyzer.   Sample preparation involved pulverizing each shale sample to approximately 60-100 mesh size. Pulverized samples were then analyzed for Total Carbon (TC) utilizing a LECO SC 144 analyzer and Total Inorganic Carbon (TIC) utilizing a UIC coulometer. The TOC value for each sample was calculated by subtracting the Total Inorganic Carbon value from the Total Carbon value:

TC-TIC=TOC

TC on the LECO SC 144 analyzer consisted of weighing between 100 and 400 milligrams (mg) of sample into a sample boat. The sample was combusted at a temperature of 1350°C. The instrument utilizes an Infrared (IR) detector/cell that is calibrated against known reference standards. At that temperature, all forms of carbon are released and detected in gas stream by the IR cell.

TIC on the UIC coulometer consisted of weighing between 50 and 300 mg of the sample into a glass vial. Carbon dioxide gas evolved by dissolution in acid from carbonates in the sample was swept by a gas stream into a coulometer cell. The coulometer cell is filled with a partially aqueous medium containing ethanolamine and a colorimetric indicator. Carbon dioxide is quantitatively absorbed by the solution and reacts with the ethanolamine to form a strong, titratable acid that causes the indicator color to fade. The titration current automatically turns on and electrically generates base to return the solution to its original color (blue).

For wells where insufficient volumes of rock samples were available to accurately perform TOC analysis using the LECO technique (approximately 1 g of well cuttings or core chips),

samples were analyzed using a carbon coulometer at NYSM. A total of 703 well cuttings samples too small for the LECO technique at KGS were shipped to the NYSM for analysis.

In addition to the TOC analyses completed for this Study, the research team also compiled values from existing TOC datasets for inclusion into the database. Numerous oil and gas companies have sampled Upper Ordovician black shale well cuttings and core from ODGS core repository during the past few years to obtain source rock analyses. These companies are required to provide to ODGS a copy of all analyses, which can be held confidential for one year. Many of these analyses are no longer confidential in status, and are now available for public distribution. Because of this data availability, ODGS was able to donate an additional 3054 Upper Ordovician TOC data points to the Study. NYSM also donated an additional 4652 TOC data points for New York wells (including some shallower data) that were collected for other projects. Including these data, the Study has a total of 368 well locations with TOC data (Figure 7-1).
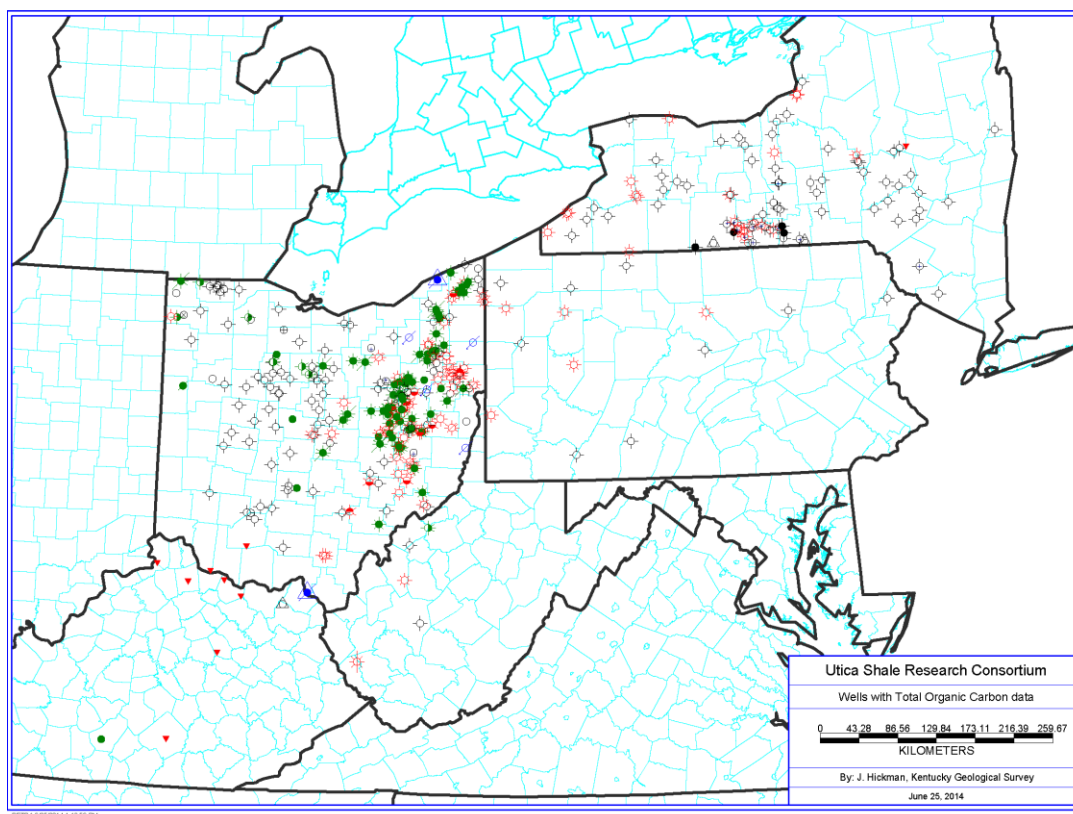
Figure 7-1. Map of wells with TOC data gathered for the Study.

7.1.2 Results

As TOC results began to arrive from the laboratory, it became apparent that the organic carbon content of Utica/Point Pleasant and equivalent rocks is not identifiable by visual inspection (i.e., the "darkness" of samples does not correlate to the organic richness of samples). Many dark-colored shaly beds returned lower TOC percentages than relatively light colored, limestone-rich beds within the same well and stratigraphic unit. Consequently, potential source zones for TOC analysis of rock cuttings can be difficult to target, at least from a sampling perspective. Also, because of the interlayered limestone/shale nature of these formations, all of the studied Upper

Ordovician units have at least some nonorganic beds. Therefore, if only a few samples are taken per well (or if representative proportions of aggregate cutting sets are not used), false negatives are common, yielding low %TOC values from what is actually an organic-rich unit. This can lead to confusing, "bullseye" heavy maps of TOC value when contoured on raw measured data (or even averaged) values alone.

In order to present TOC variability in the most realistic and practical manner, we chose a methodology that displays the highest %TOC encountered in each well at each of the studied horizons. Even so, many of the organic-rich beds (within a larger stratigraphic unit) were quite thin. To account for vertical variations in organic carbon, wells with more than 25 ft of greater than 1% TOC values were highlighted. By using this combination of symbologies, the areas with the highest overall organic content for each unit are easily identified. In the following figures, the maximum TOC value from each well within the specified formation is indicated by colored circles, overlain on generalized isopach grids (darker = thicker). Wells with maximum %TOC values for each stratigraphic unit less than 1% are highlighted in white, 1-2% (source rock threshold) are in yellow, 2-4% are light orange, and values over 4% are in dark orange. Wells with more than 25 ft of sampled strata and with TOC values greater than 1% are highlighted by smaller red circles.
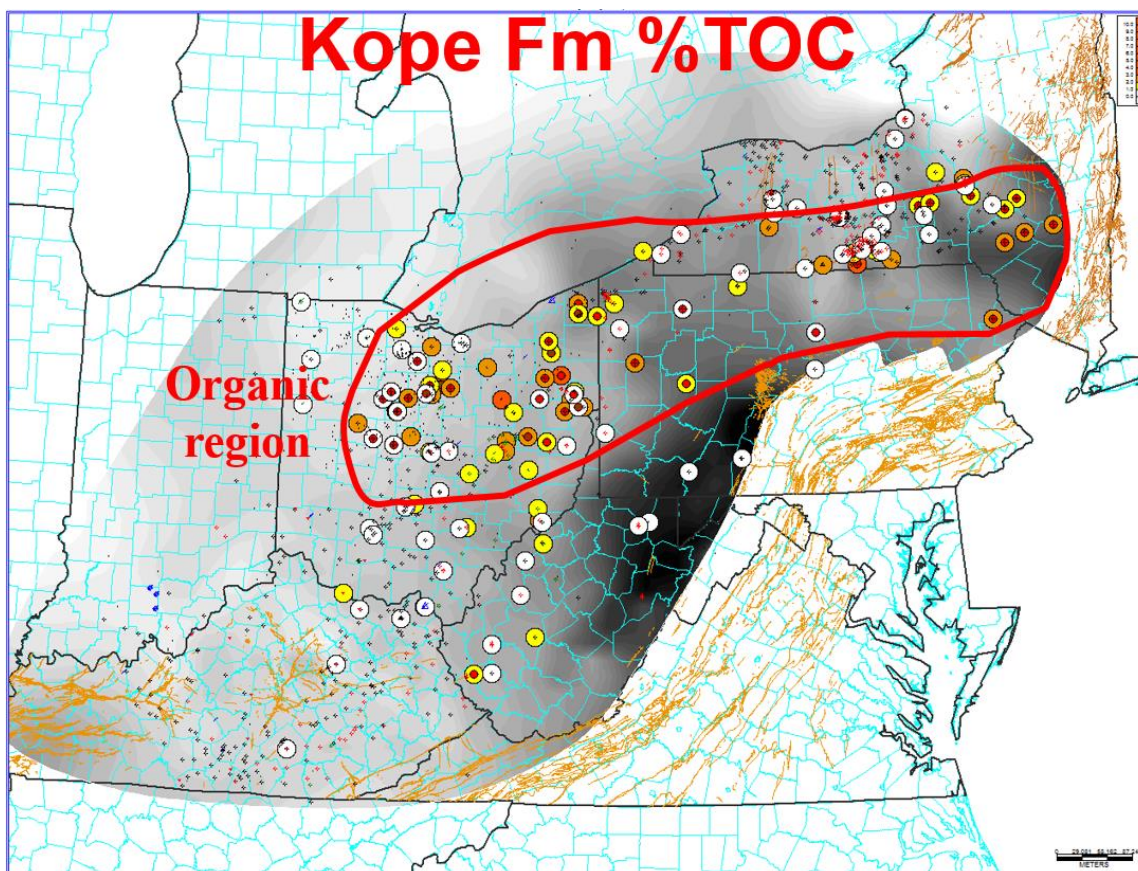
Figure 7-2. Map of maximum TOC (%) measured in the Kope Formation. See text for explanation of symbols and colors.

104
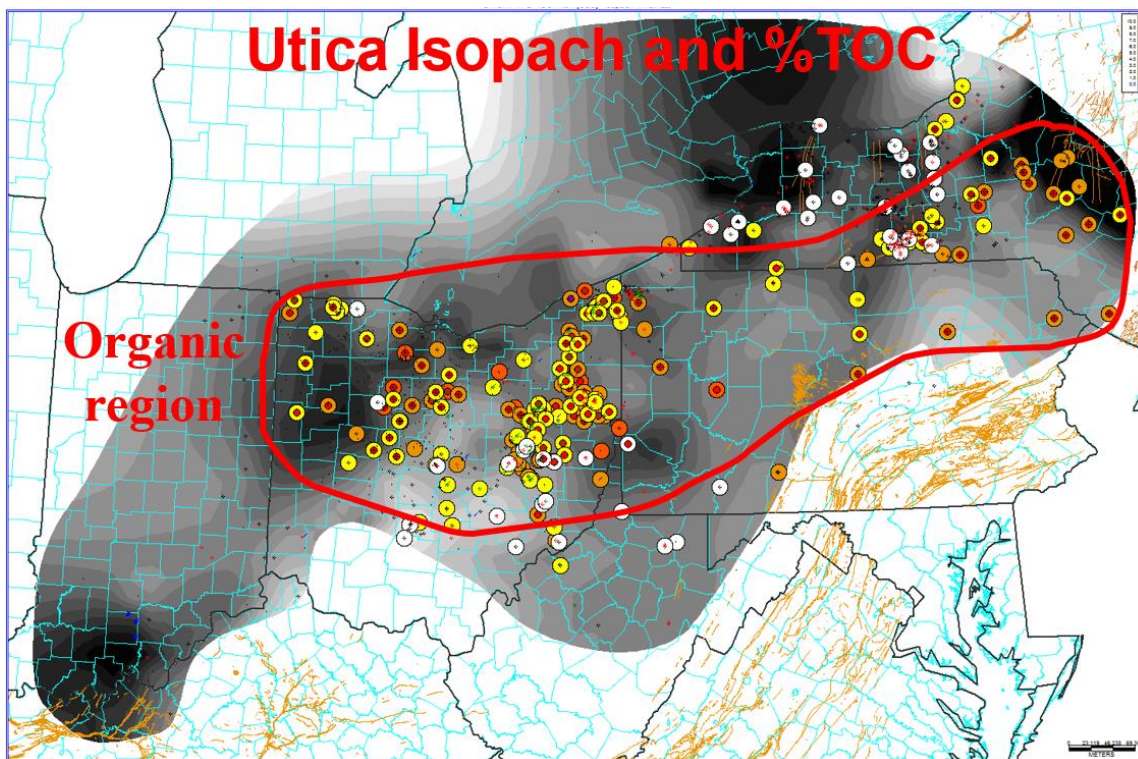
Figure 7-3. Map of maximum TOC (%) measured in the Utica Shale. See text for explanation of symbols and colors.
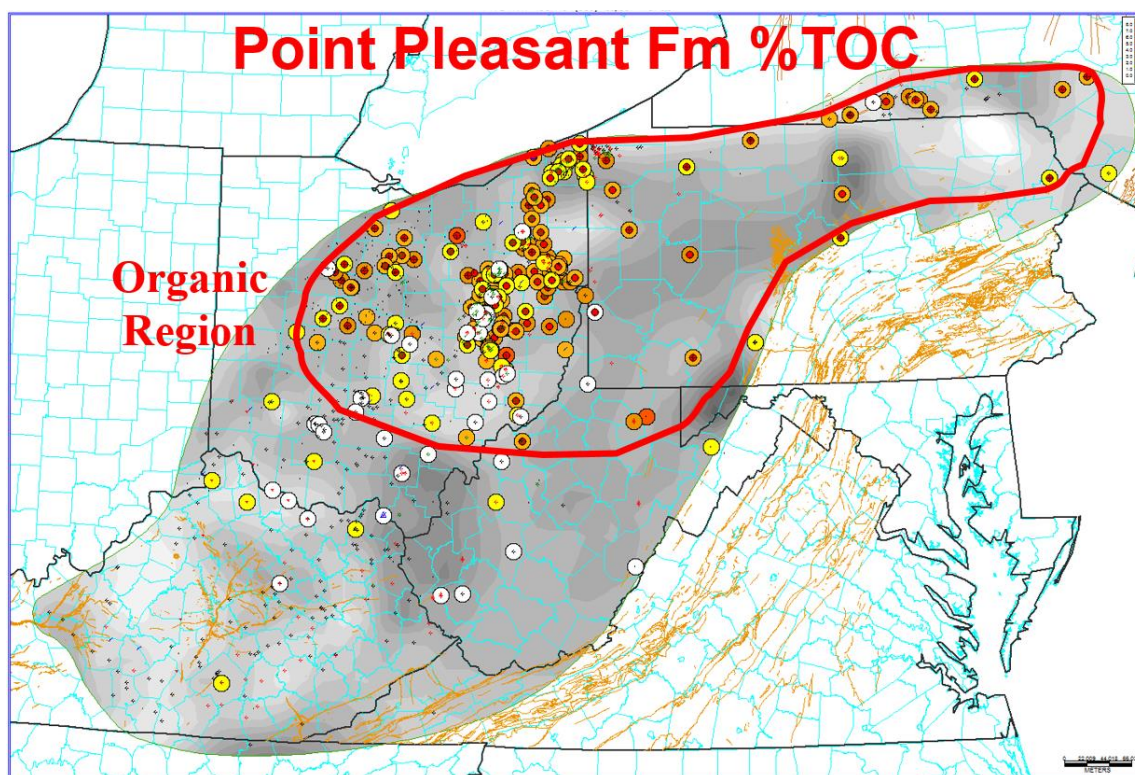
Figure 7-4. Map of maximum TOC (%) measured in the Point Pleasant Formation. See text for explanation of symbols and colors.
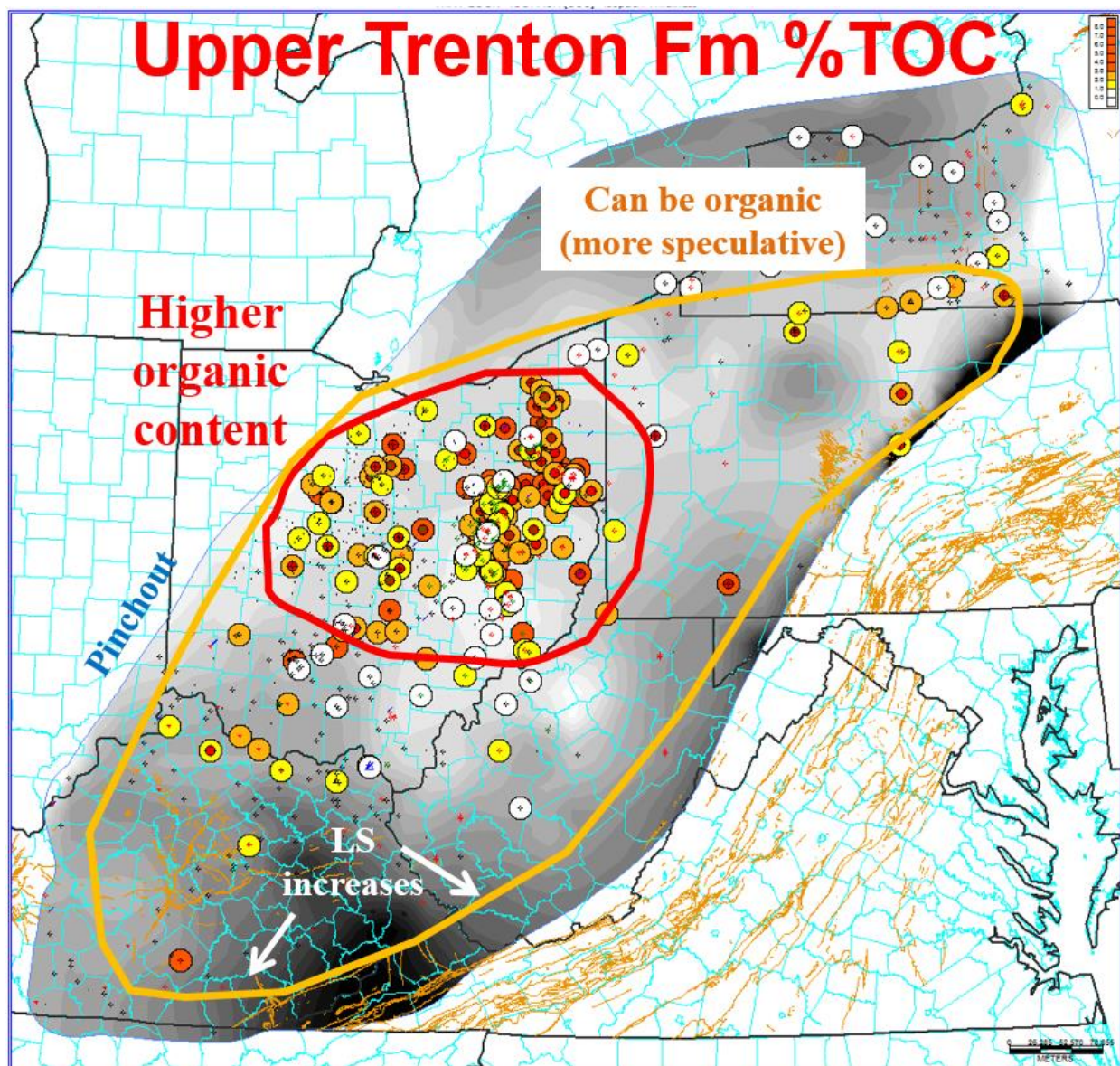
Figure 7-5. Map of maximum TOC (%) measured in the upper Lexington/Trenton Formation interval. See text for explanation of symbols and colors.
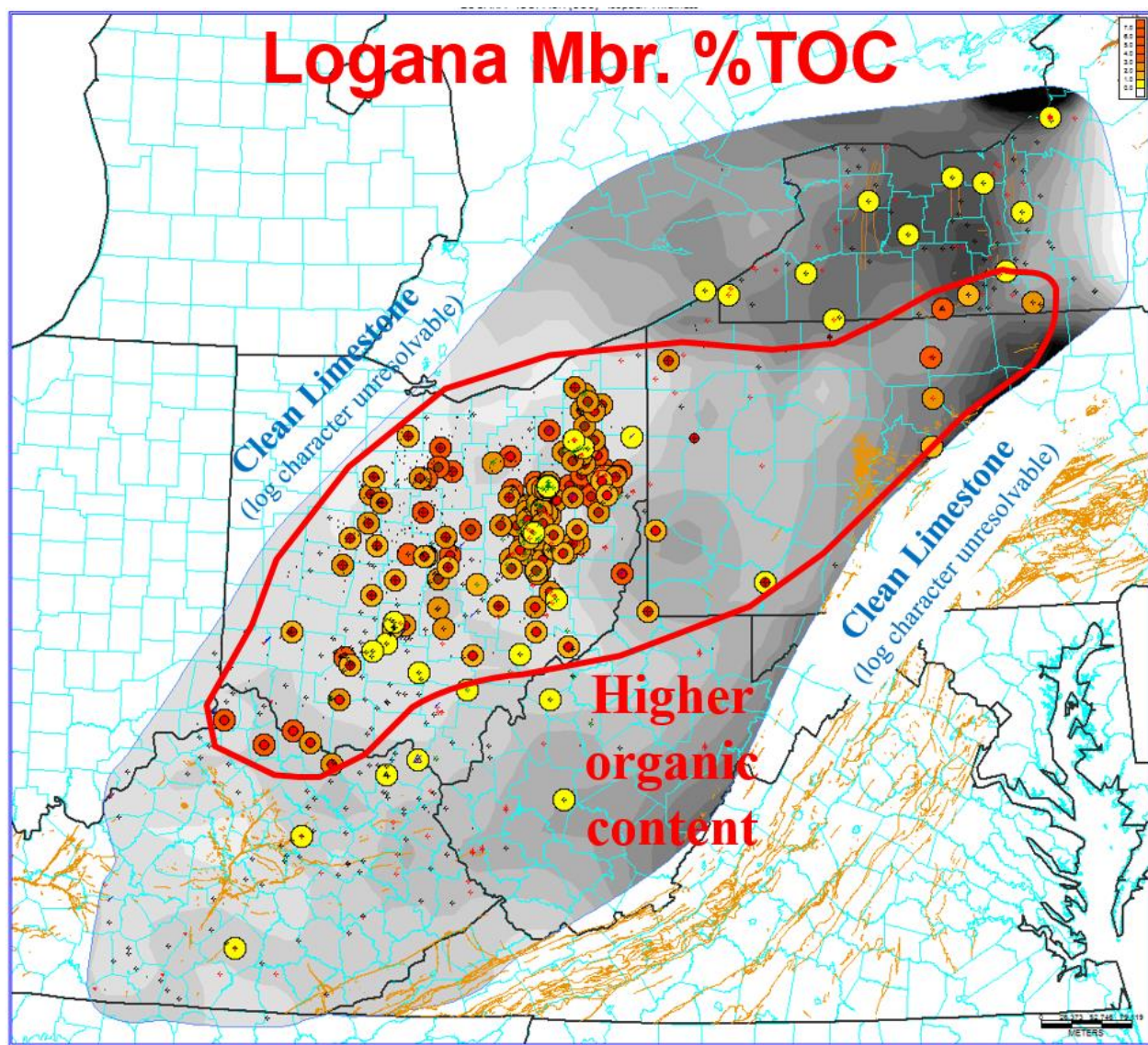
Figure 7-6. Map of maximum TOC (%) measured in the Logana Member of the Lexington/Trenton Formation. See text for explanation of symbols and colors.
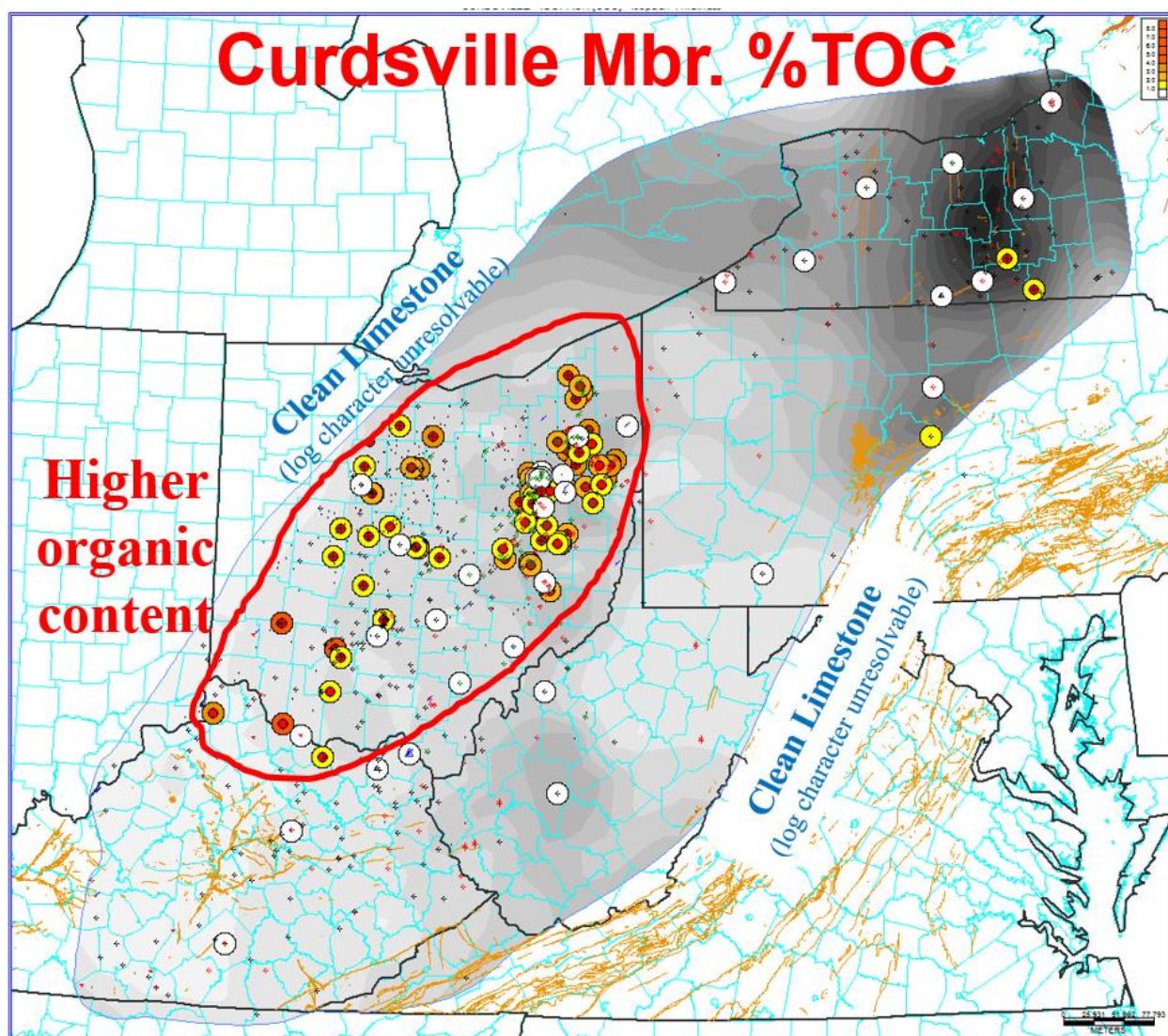
Figure 7-7. **Map of maximum TOC (%) measured in the Curdsville Member of the Lexington/Trenton Formation. See text for explanation of symbols and colors.**

Sampling and analysis for TOC can be time-consuming and raises costs for hydrocarbon source and reservoir characterization efforts. Once the regional TOC data had been compiled for the studied units, numerous data comparisons and crossplots were made in the hopes that a more efficient indicator of TOC could be defined for the Utica Shale play. The one commonly recorded parameter that appears to correlate with TOC abundance is the RHOB log. Although the TOC sampling methods produced some scatter on the crossplots (Figures 7-8 through 7-13), subjective analysis of individual density logs appears to be a reliable method of predicting TOC within the mature region of the play. This correlation appears to be the strongest within the upper Lexington/Trenton Formation and Logana Member, and with slightly less correlation within the more shale-rich Point Pleasant Formation and Utica Shale. The Kope Formation and Curdsville Member displayed little to no correlation between RHOB and TOC.
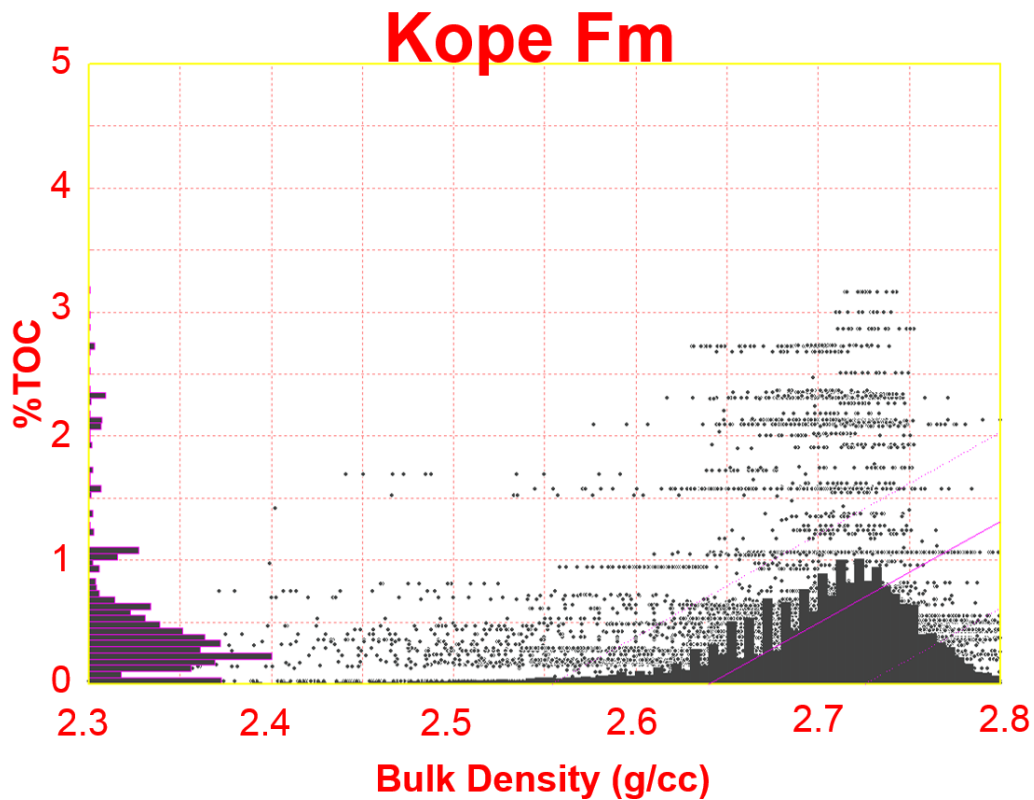
Figure 7-8. Crossplot of RHOB log value vs. sampled %TOC for the Kope Formation.
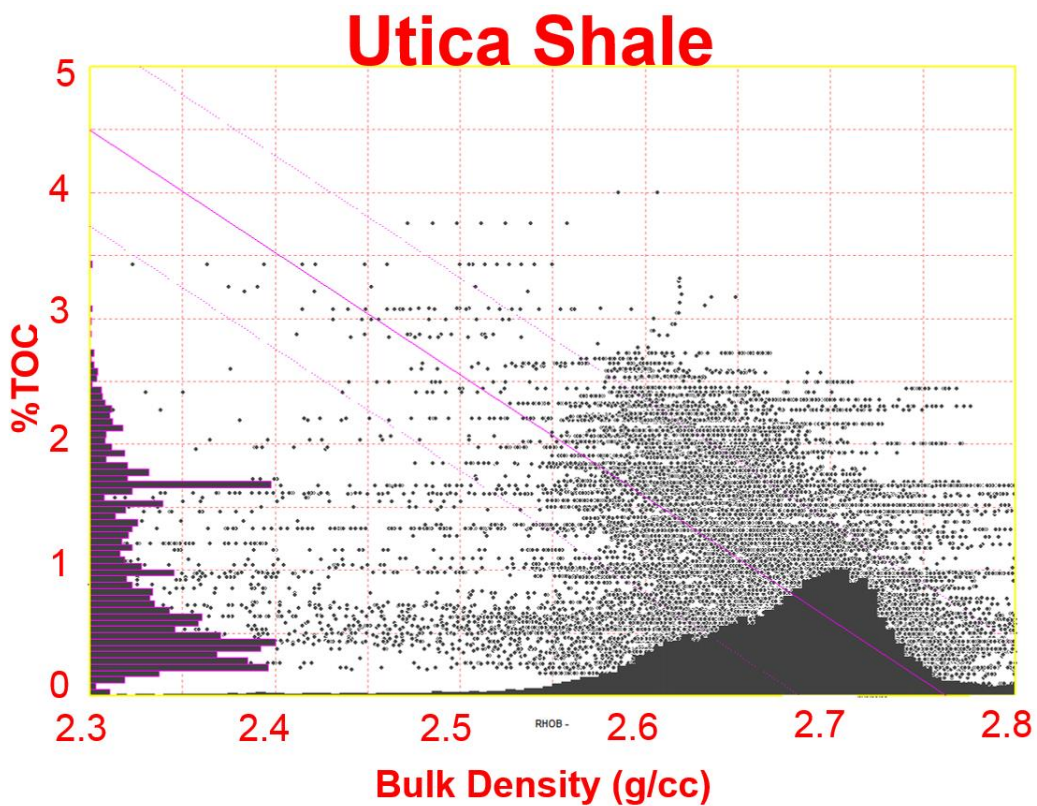
Figure 7-9. Crossplot of RHOB log value vs. sampled %TOC for the Utica Shale.
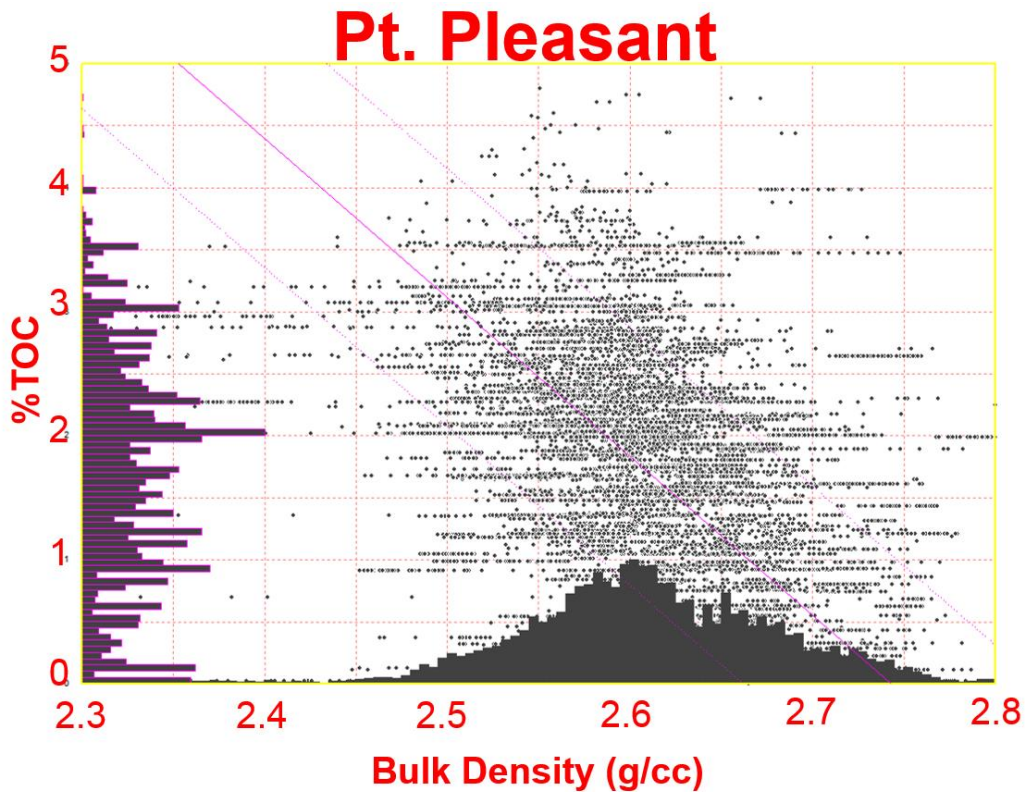
Figure 7-10. Crossplot of RHOB log value vs. sampled %TOC for the Point Pleasant Formation.
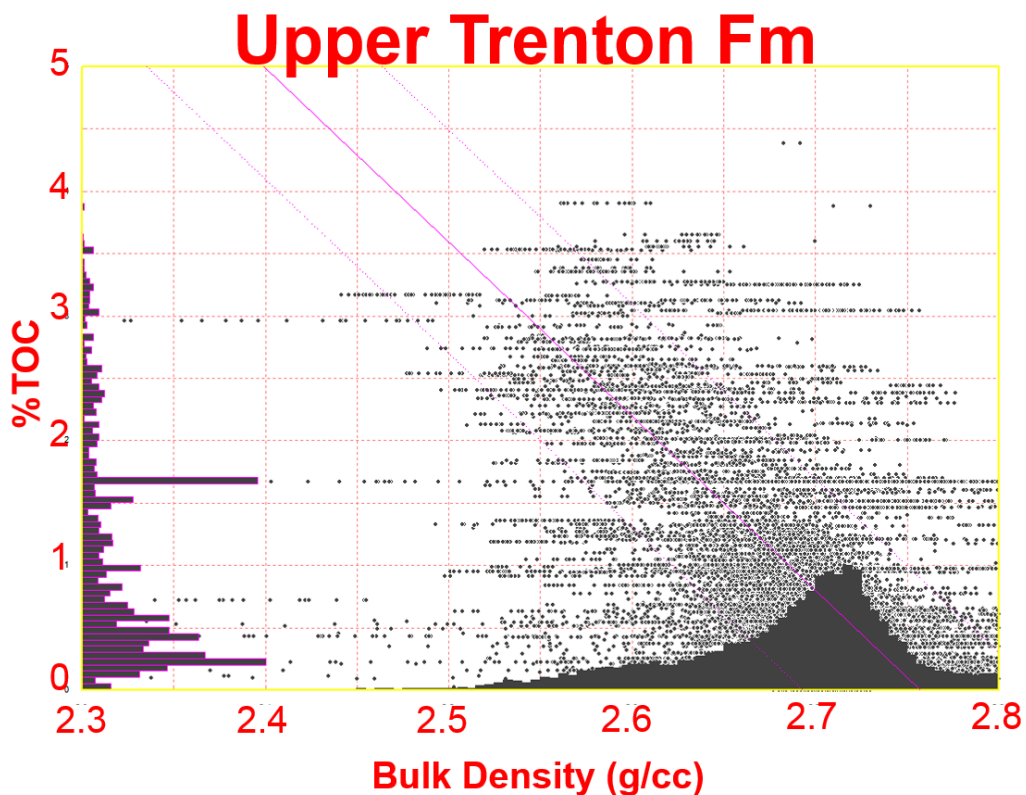
Figure 7-11. Crossplot of RHOB log value vs. sampled %TOC for the upper Lexington/Trenton Formation.
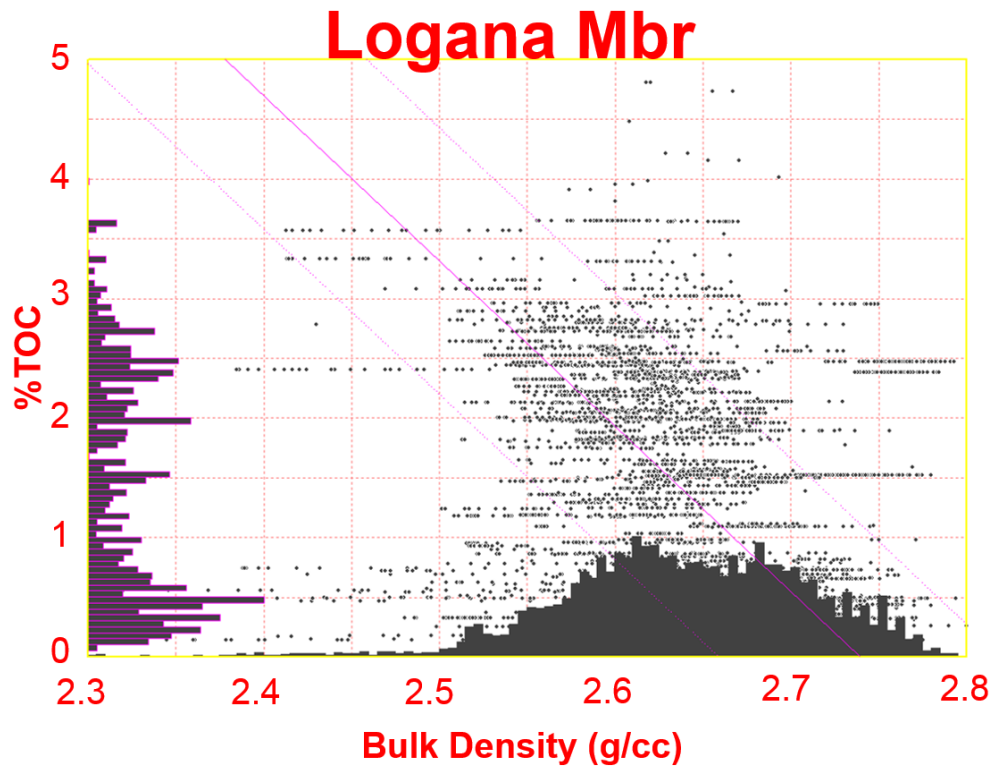
Figure 7-12. Crossplot of RHOB log value vs. sampled %TOC for the Logana Member of the Lexington/Trenton Formation.
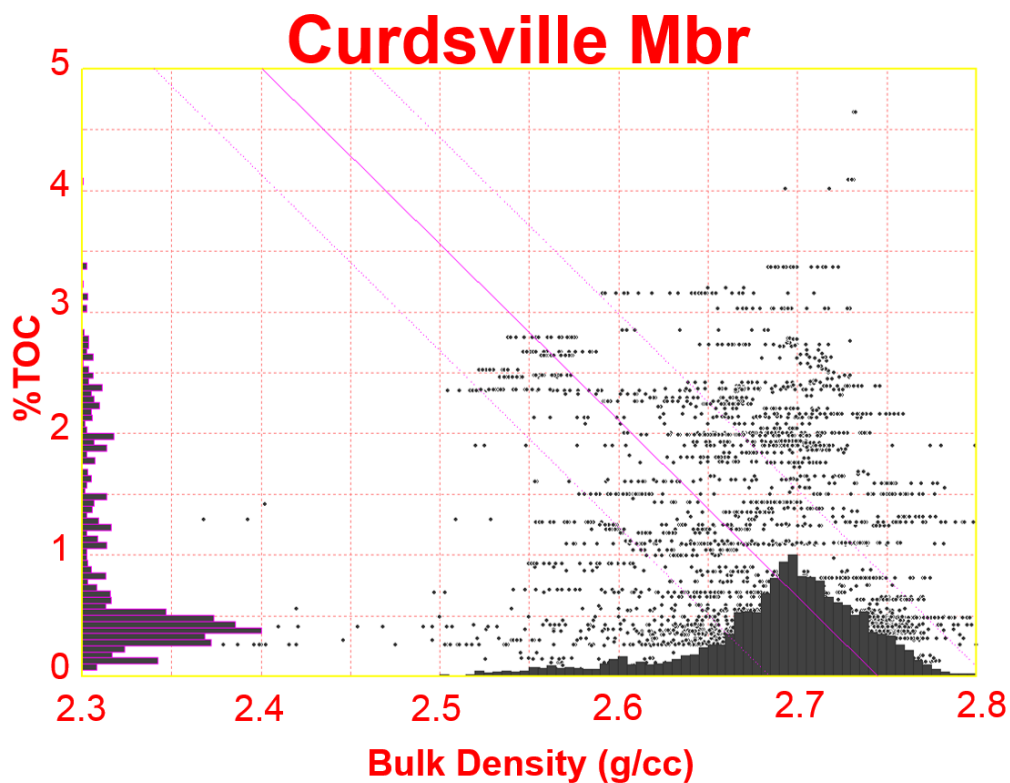
Figure 7-13. Crossplot of RHOB log value vs. sampled %TOC for the Curdsville Member of the Lexington/Trenton Formation.

7.2   RockEval

As part of the compilation of preexisting data for this project, ODGS provided results for 1900 RockEval analyses of Upper Ordovician strata from their sample record inventory. The original scope of this Study included funds for additional RockEval laboratory analyses to augment this existing Ohio dataset. After thorough examination of the legacy data, however, it became apparent that there was a high degree of variability in the RockEval results. This variability was noted both between adjacent wells and even within the same unit of individual wells. The variation appears to be the result of weak or poorly defined S2 peaks on the pyrolysis curves for these units. Whether this is due to the oxidation of older cuttings samples (Peters, 1986), or it is just the nature of the specific organic material within these units, is unclear.

Thermal maturity analyses of bitumen reflectance, as performed by Cortland Eble of KGS (see Section 7.3), were both internally consistent and roughly matched expected maturities based upon the fluid content (oil, wet gas, dry gas, etc.) from initial production reports in the eastern Ohio Utica Play area. Based on these results, the research team decided that the Study would benefit more from additional reflectance analyses, rather than more RockEval tests, so the project budget and scope was modified to reflect this change in focus.

7.3   Organic Petrography and Thermal Maturity

KGS obtained Utica/Point Pleasant samples from Kentucky, Ohio and Pennsylvania exploration wells and examined them petrographically in reflected light to obtain reflectance measurement data (Ro). Of the approximately 350 samples that were prepared and examined, 90 had sufficient bitumen for reflectance analysis, and are discussed herein.

7.3.1 Materials and Methods

Samples from Kentucky and Ohio consisted of core cuttings and core pieces. Samples from Pennsylvania consisted of rock cuttings that had been previously reduced in size to -60 mesh (250 µm maximum particle size). All samples were mixed with epoxy resin and placed into 2.5-, 3.2-, or 3.8-cm diameter phenolic ring form molds, depending on the size of the material. After curing, the samples were ground and polished using 320, 400 and 600 grit papers, 1.0, 0.03 and 0.05 µm alumina slurries, and 0.05-µm colloidal silica. Polished samples were air-dried and placed in a desiccator prior to analysis.

Reflected light analysis was performed on a Zeiss UEM microscope, with a Zeiss epiplan 40X oil immersion objective, and a Hamamastu R928 photomultiplier. The light source for the analysis was supplied by an Osram Xenophot HLX 12V, 100W bulb; Zeiss Immersol oil was used (ne = 1.518, ve = 42). Random reflectance (Ro random) measurements were collected by first calibrating the system using a glass standard of known reflectance. Following this, reflectance measurements were collected particles of bitumen, using a 2-µm diameter measuring spot. In most cases, 30 to 40 measurements were taken for each sample, though this depended on the abundance of bitumen. In some samples, fewer than 30 particles could be identified and measured. The average, maximum, minimum, standard deviation and number of measurements were recorded for each sample.

Fluorescent light was used to assist in the identification of organic components. A Lumen Dynamics 120-watt high pressure metal halide arc lamp was used in conjunction with a Zeiss 09 filter set (450-490 nanometer [nm] excitation, 510 nm beam splitter and 515 nm emission filters). This particular light/filter configuration makes the liptinitic portion of the organic material fluoresce yellow, orange or red, depending on the level of thermal maturity.

7.3.2 Results

7.3.2.1 *Organic Composition of the Utica Shale*

Samples with elevated (>2.0 %) TOC contents typically had the most abundant bitumen. Two principle types of bitumen were observed in the samples – grahamite and epi-impsonite, according to the genetic classification of solid bitumen developed by Jacob (1976). Particles of epi-impsonite were selected for measurement, as they had very smooth surfaces. Particles identified as grahamite had coarse-textured surfaces with lower reflectance. It is probable that some fragments of graptolites were also measured, especially as the typical particle size of the bitumen particles was <10 μm.

Bitumen was found to be a minor organic component in these samples. Instead, amorphous organic matter, referred to as amorphinite (Senftle and others, 1987) in this text, is by far the dominant (<75%, mineral matter free) organic component of nearly all of the samples. Amorphinite appears as an organic coating on (mainly) clay grains, and is identified principally by fluorescence. In lower rank samples (Ro 0.6-0.8%), it has a yellow fluorescence, changing to orange and red in higher rank samples (Ro 1.0-1.5%). It cannot be seen in very high rank samples (Ro >1.5%), as fluorescence becomes negligible, and finally disappears.

The association of well-preserved organic material in fine-grained sediments has been discussed by MacQuaker and others (2010). Organic material is enhanced through entombment in a shale-dominant mineral matrix, which protects and preserves the organic material in an otherwise oxygen-rich depositional environment.

Carbonate minerals (mainly calcite) dominate the inorganic matrix of most samples. Occasionally, grains of calcite were observed to fluoresce brightly. Although the cause of this is unclear, it is possible that these grains may have been impregnated with liquid hydrocarbons (paraffinic oils?). Examples of the types of organic material identified from Utica and equivalent samples are provided in Appendix 7-A.

7.3.2.2 *Bitumen Reflectance and Thermal Maturity*

Ro random reflectance measurements collected for the Study ranged from 0.66% to 2.2%, indicating thermal maturity levels from early oil generation to catagenic gas (Dow, 1977; Figure 7-14).
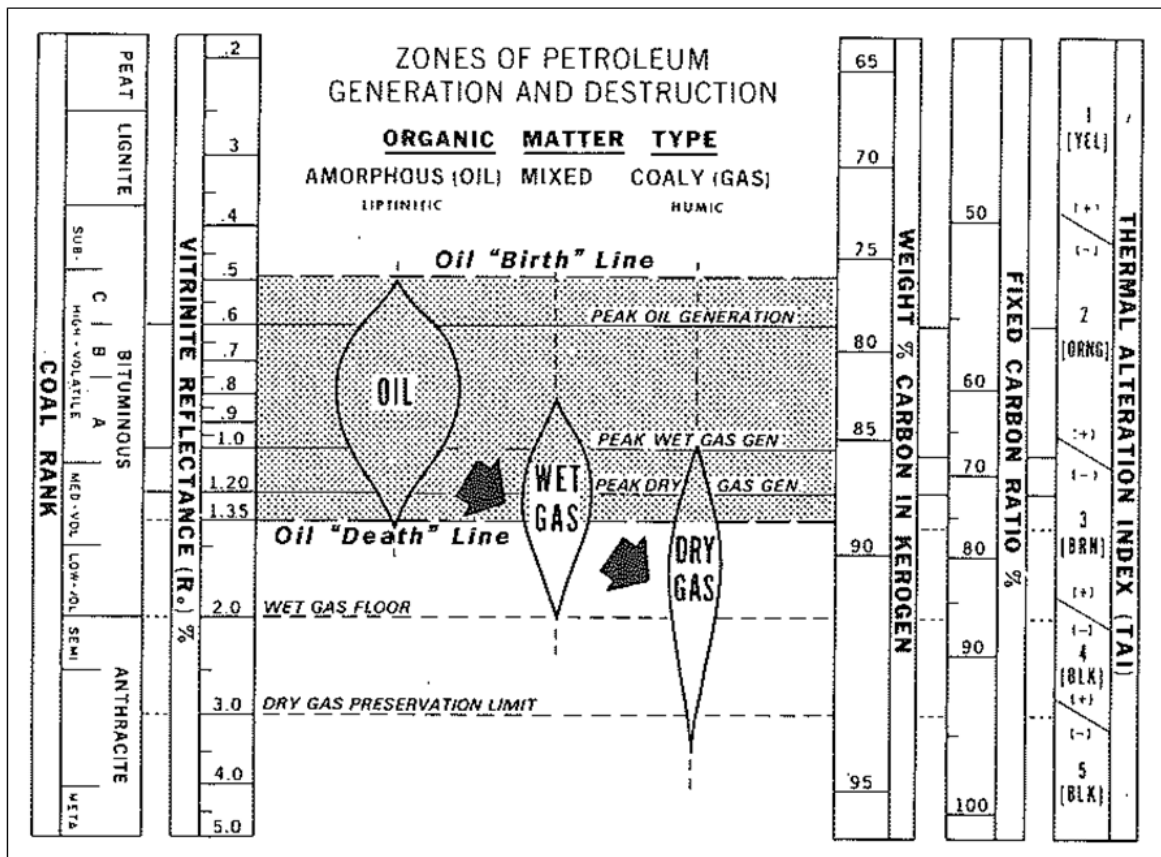
Figure 7-14. Petroleum generation chart, showing the ranges of oil, wet gas and dry gas generation (from Dow, 1977).

In addition to the average, maximum, minimum and standard deviation values measured for these samples, calculated Ro maximum and Ro equivalent values have also been computed. The Ro maximum value is calculated by the following equation from Ting (1978):

$$Ro \ maximum = (Ro \ random * 1.07)$$

This calculation approximates the Ro maximum measurement that would be obtained by using polarized light, and rotating the stage to obtain a maximum and minimum value, as is a common practice in coal petrology.

The Ro equivalent calculation was developed by Jacob (1989) to account for the fact that bitumen often has a lower reflectance than corresponding vitrinite at the same level of thermal maturity. The equation is as follows:

$$Ro \ equivalent = (Ro \ random * 0.618) + 0.4$$

7.3.3 Presentation of Results by State

7.3.3.1 Kentucky

Samples from Kentucky were obtained from two boreholes – C-361 from Pulaski County in south-central Kentucky, and C-139 from Boone County in northern Kentucky (Figure 7-15). The

organic-rich sections of these cores were few in number, but contained very abundant and large pieces of bitumen. Ro random values of 0.74 and 0.76% for C-139 and C-361, respectively, indicating thermal maturity levels in the lower to middle part of the oil window (Table 7-1).
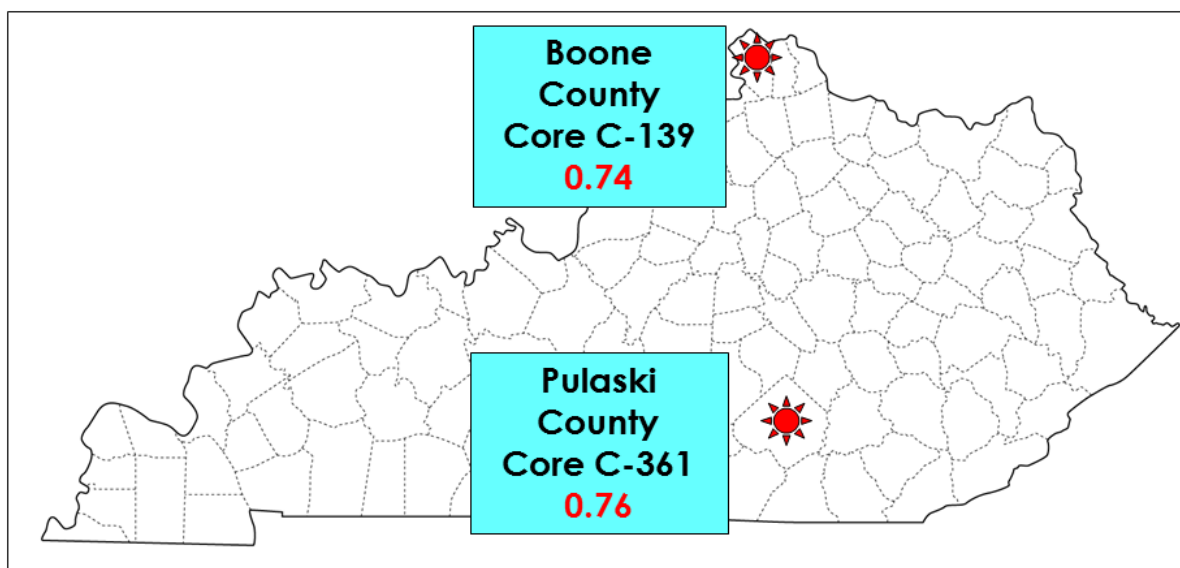
Figure 7-15. Map of Kentucky showing locations of core samples. Average Ro random values for each core are shown in red type.

Table 7-1. Reflectance data for Kentucky samples.

	Sample	Random Ro				Calculated	Calculated	No. of
Well ID	**Depth (ft)**	**Avg**	**Max**	**Min**	**Std Dev**	**Ro max**	**Ro eq**	**Observations**
C-361, Pulaski Co., KY								
	1165.8	0.74	0.81	0.67	0.04	0.79	0.86	43
C-139, Boone, Co., KY								
	215	0.76	0.86	0.64	0.06	0.81	0.87	47
	222	0.76	0.86	0.65	0.05	0.81	0.87	47
	226	0.76	0.83	0.69	0.04	0.82	0.87	47
Well Average		**0.76**	**0.85**	**0.66**	**0.05**	**0.81**	**0.87**	**47**

7.3.3.2   Ohio

Samples from 12 borehole locations in central Ohio (Figure 7-16) were analyzed. Boreholes along the western margin of the central Ohio area reported reflectance values from 0.66 to 0.71%. Borehole locations in the more central and eastern part of this area had reflectance values of 0.76 to 0.84% (Table 7-2). Collectively, the Utica/Point Pleasant in the central Ohio area has a level of thermal maturity in the lower to middle part of the oil window.
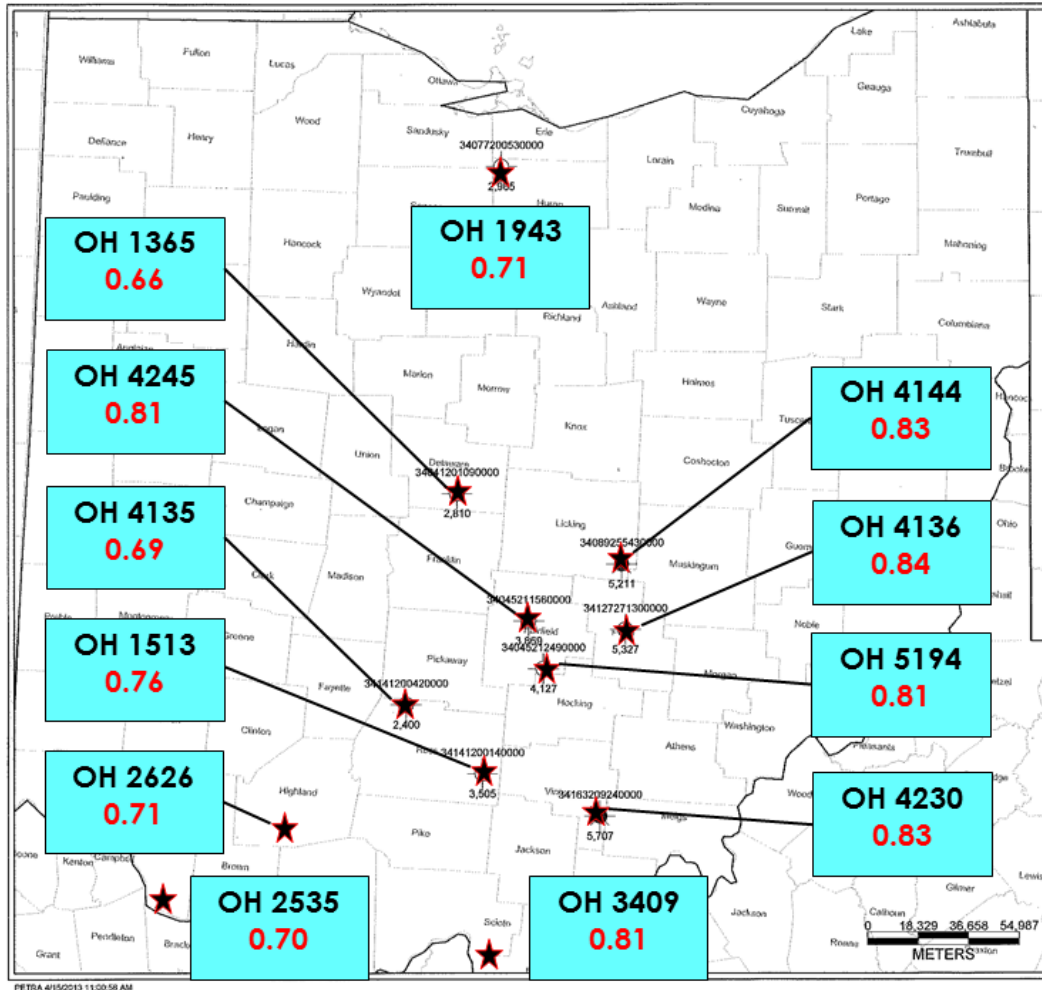
Figure 7-16. Map of Ohio showing locations of core samples. Average Ro random values for each core are shown in red type.

Table 7-2. Reflectance data for central Ohio samples.

Well ID	Sample Depth (ft)	Random Ro Avg	Max	Min	Std Dev	Calculated Ro max	Calculated Ro eq	No. of Observations
OH1365, Delaware Co., OH								
	1932	0.66	0.77	0.54	0.05	0.71	0.81	36
	1961	0.67	0.77	0.57	0.06	0.71	0.81	33
	2014	0.67	0.80	0.51	0.09	0.71	0.81	32
	2067	0.63	0.74	0.51	0.06	0.68	0.79	29
	2077	0.65	0.75	0.53	0.05	0.70	0.80	30
	2142	0.66	0.76	0.57	0.05	0.70	0.81	32
Well Average		**0.66**	**0.77**	**0.54**	**0.06**	**0.70**	**0.81**	**32**

116

Well ID	Sample Depth (ft)	Random Ro				Calculated Ro max	Calculated Ro eq	No. of Observations
		Avg	Max	Min	Std Dev			
OH1943, Huron, Co., OH								
	1948	0.71	0.80	0.60	0.05	0.77	0.84	33
	1978	0.71	0.84	0.62	0.06	0.76	0.84	32
	2070	0.70	0.81	0.60	0.06	0.75	0.84	32
	2144	0.71	0.79	0.61	0.05	0.76	0.84	32
	2195	0.71	0.81	0.61	0.05	0.76	0.84	37
	2220	0.69	0.84	0.60	0.07	0.74	0.83	32
	2250	0.70	0.80	0.60	0.05	0.75	0.83	31
Well Average		**0.71**	**0.81**	**0.61**	**0.06**	**0.76**	**0.84**	**33**
OH4144, Licking Co., OH								
	4110	0.82	0.93	0.65	0.08	0.88	0.91	21
	4120	0.86	0.93	0.78	0.05	0.92	0.93	14
	4200	0.84	0.95	0.65	0.08	0.90	0.92	32
	4250	0.86	0.99	0.76	0.06	0.92	0.93	51
	4360	0.83	0.95	0.70	0.06	0.88	0.91	27
	4390	0.83	0.94	0.66	0.08	0.89	0.91	32
	4420	0.82	0.94	0.74	0.06	0.88	0.91	27
	4450	0.83	0.96	0.70	0.06	0.88	0.91	33
Well Average		**0.84**	**0.95**	**0.71**	**0.07**	**0.89**	**0.92**	**30**
OH5194, Fairfield Co., OH								
	3170	0.78	0.84	0.70	0.04	0.84	0.88	32
	3190	0.73	0.85	0.68	0.05	0.78	0.85	28
	3210	0.77	0.86	0.65	0.05	0.83	0.88	26
	3250	0.75	0.87	0.67	0.06	0.80	0.86	33
	3290	0.77	0.84	0.70	0.04	0.83	0.88	26
	3310	0.76	0.85	0.69	0.04	0.81	0.87	27
	3330	0.76	0.85	0.68	0.05	0.82	0.87	28
Well Average		**0.76**	**0.85**	**0.68**	**0.05**	**0.81**	**0.87**	**29**
OH4230, Vinton Co., OH								
	4520	0.80	0.94	0.71	0.06	0.85	0.89	50
	4560	0.86	0.99	0.76	0.06	0.92	0.93	50
	4580	0.83	0.91	0.71	0.05	0.88	0.91	51
	4600	0.85	0.96	0.69	0.07	0.90	0.92	51
	4620	0.81	0.92	0.71	0.06	0.87	0.90	30
	4640	0.82	0.94	0.71	0.06	0.87	0.91	45
	4660	0.81	0.91	0.71	0.06	0.87	0.90	29
	4680	0.84	0.96	0.71	0.09	0.90	0.92	33
	4690	0.80	0.97	0.71	0.06	0.85	0.89	53
	4700	0.81	0.93	0.71	0.06	0.87	0.90	51
	4720	0.83	0.92	0.70	0.07	0.89	0.91	52
Well Average		**0.82**	**0.94**	**0.71**	**0.06**	**0.88**	**0.91**	**45**

Well ID	Sample Depth (ft)	Random Ro				Calculated Ro max	Calculated Ro eq	No. of Observations
		Avg	Max	Min	Std Dev			
OH4245, Fairfield Co., OH								
	2830	0.81	0.91	0.71	0.06	0.87	0.90	28
	2870	0.81	0.92	0.71	0.07	0.87	0.90	32
Well Average		**0.81**	**0.91**	**0.71**	**0.06**	**0.87**	**0.90**	**30**
OH4135, Ross Co., OH								
	2950	0.69	0.81	0.61	0.05	0.74	0.83	34
OH4136, Perry Co., OH								
	4350	0.86	0.96	0.75	0.07	0.92	0.93	31
	4410	0.83	0.92	0.71	0.06	0.89	0.91	32
	4530	0.84	0.94	0.74	0.06	0.90	0.92	36
Well Average		**0.84**	**0.94**	**0.73**	**0.06**	**0.90**	**0.92**	**33**
OH2535, Clermont Co., OH								
	67.3	0.71	0.79	0.61	0.05	0.76	0.84	34
	158	0.77	0.88	0.67	0.06	0.83	0.88	48
	178	0.75	0.84	0.59	0.08	0.80	0.86	35
	188	0.75	0.84	0.68	0.04	0.80	0.86	38
Well Average		**0.74**	**0.84**	**0.64**	**0.06**	**0.80**	**0.86**	**39**
OH2626, Highland Co., OH								
	1035	0.71	0.82	0.58	0.06	0.76	0.84	19
	1054	0.76	0.84	0.57	0.06	0.81	0.87	37
Well Average		**0.73**	**0.83**	**0.58**	**0.06**	**0.78**	**0.85**	**28**
OH1513, Ross Co., OH								
	2550	0.76	0.89	0.69	0.06	0.81	0.87	36
OH3409, Scioto Co., OH								
	2799	0.82	0.91	0.71	0.05	0.88	0.91	35
	2982	0.77	0.93	0.66	0.07	0.83	0.88	28
	3116	0.83	0.94	0.69	0.07	0.89	0.91	30
	3138	0.81	0.89	0.72	0.05	0.86	0.90	25
Well Average		**0.81**	**0.92**	**0.69**	**0.06**	**0.86**	**0.90**	**30**

Samples from 15 borehole locations in eastern Ohio (Figure 7-17) also were analyzed. Bitumen reflectance increases rapidly from 0.94% in the westernmost part of this area (location 5483, Wayne County) to 1.43% in the easternmost part of this area (location 5434 in Jefferson County, Table 7-3). Collectively, the Utica/Point Pleasant in eastern Ohio has a level of thermal maturity that includes the middle and upper portions of the oil window, the wet gas window and the lower part of the dry gas window.
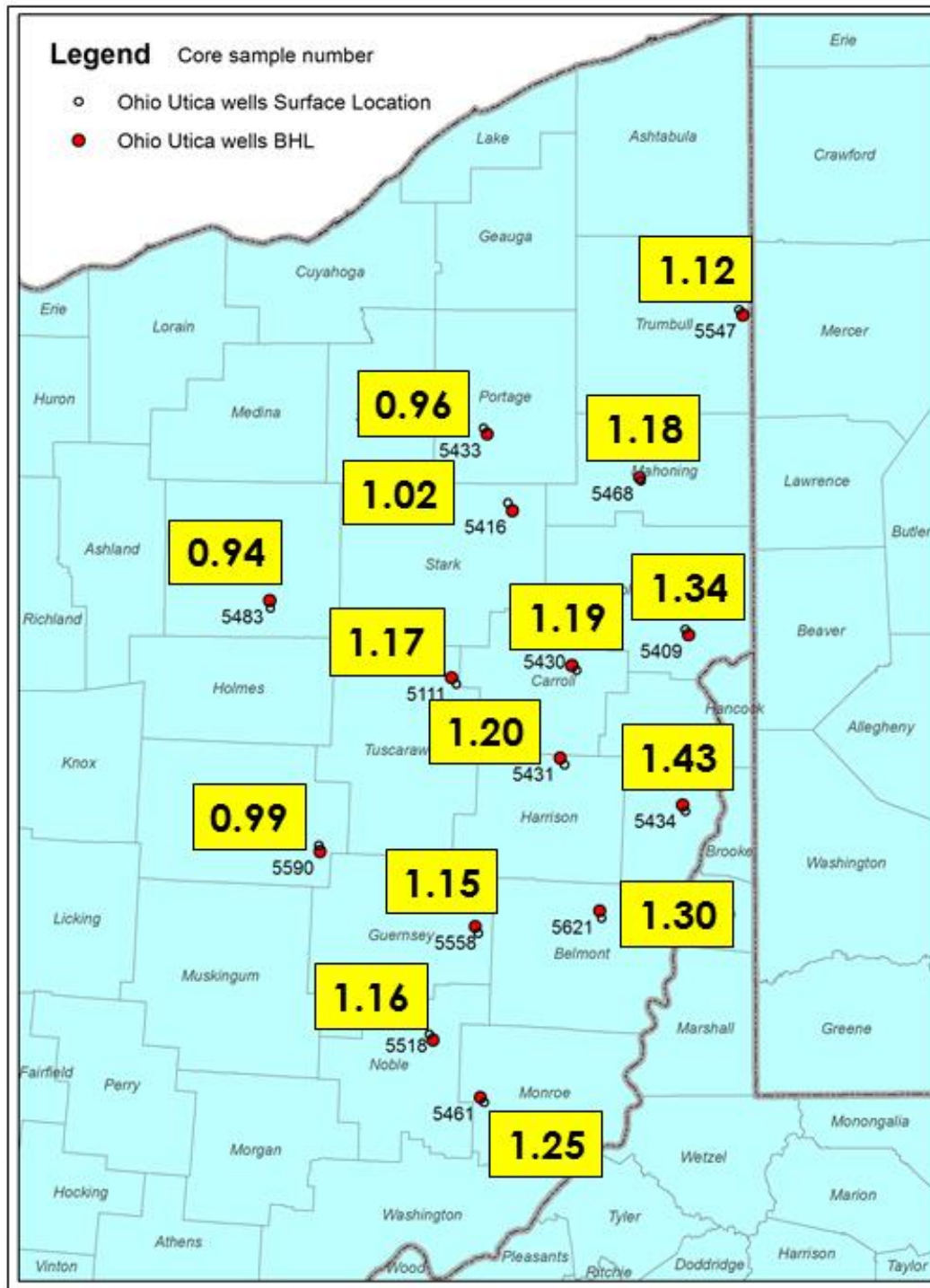
Figure 7-17. Map of eastern Ohio showing locations of core samples. Average Ro random values for each core are shown in in the yellow shaded boxes beside the core location points.

Table 7-3. Reflectance data for northeastern Ohio samples.

Well ID	Sample Depth (ft)	Random Ro				Calculated Ro max	Calculated Ro eq	No. of Observations
		Avg	Max	Min	Std Dev			
OH5558, Guernsey Co., OH								
	12,970-13,000	1.15	1.48	0.87	0.16	1.23	1.11	33
OH5547, Trumball Co., OH								
	10,880	1.12	1.42	0.90	0.11	1.20	1.09	33
OH5430, Carroll Co., OH								
	12,790-13,150	1.19	1.44	0.96	0.13	1.37	1.14	37
OH5409, Columbiana Co., OH								
	12,920-13,000	1.34	1.53	1.10	0.14	1.43	1.23	32
OH5431, Harrison Co., OH								
	13,600-13,754	1.20	1.57	0.97	0.19	1.28	1.14	35
OH5416, Stark Co., OH								
	13,480-13,510	1.02	1.29	0.81	0.16	1.09	1.03	43
OH5433, Portage Co., OH								
	10,890-10,930	0.96	1.19	0.81	0.11	1.03	0.99	40
OH5111, Tuscarawas Co., OH								
	12,260-13,342	1.17	1.39	1.00	0.11	1.25	1.12	46
OH5468, Mahoning Co., OH								
	9940-9958	1.18	1.46	0.96	0.14	1.26	1.13	45
OH5483, Wayne Co., OH								
	10,100-10,220	0.94	1.04	0.75	0.06	1.01	0.98	35
OH5590, Coshocton Co., OH								
	10,210-10,450	0.99	1.22	0.85	0.09	1.06	1.01	37
OH5621, Belmont Co., OH								
	15,210-15,300	1.30	1.55	1.10	0.12	1.39	1.20	39
OH5434, Jefferson Co., OH								
	14,970-14,990	1.43	1.61	1.17	0.12	1.54	1.29	38
OH5518, Noble Co., OH								
	12,700-12,800	1.16	1.48	0.91	0.16	1.24	1.12	47
OH5461, Monroe, Co., OH								
	8710-8800	1.25	1.51	1.12	0.11	1.34	1.17	48

7.3.3.3   Pennsylvania

Rock cuttings samples from four wells located in western Pennsylvania (Figure 7-18) were analyzed.   Samples from the Kardosh No. 1 in Crawford County were the most thermally immature, with an average Ro random of 1.08%. Samples from the Martin No. 1 in Armstrong County were the most thermally mature, with an average Ro random of 2.19%. Samples from the Starvaggi No. 1 in Washington County, at a depth from 10,610 to 10,840 ft, had an average Ro random of 1.79%. Collectively, the Utica/Point Pleasant in western Pennsylvania has a level of thermal maturity that ranges from the upper part of the oil window to the top of the dry gas window (Table 7-4).
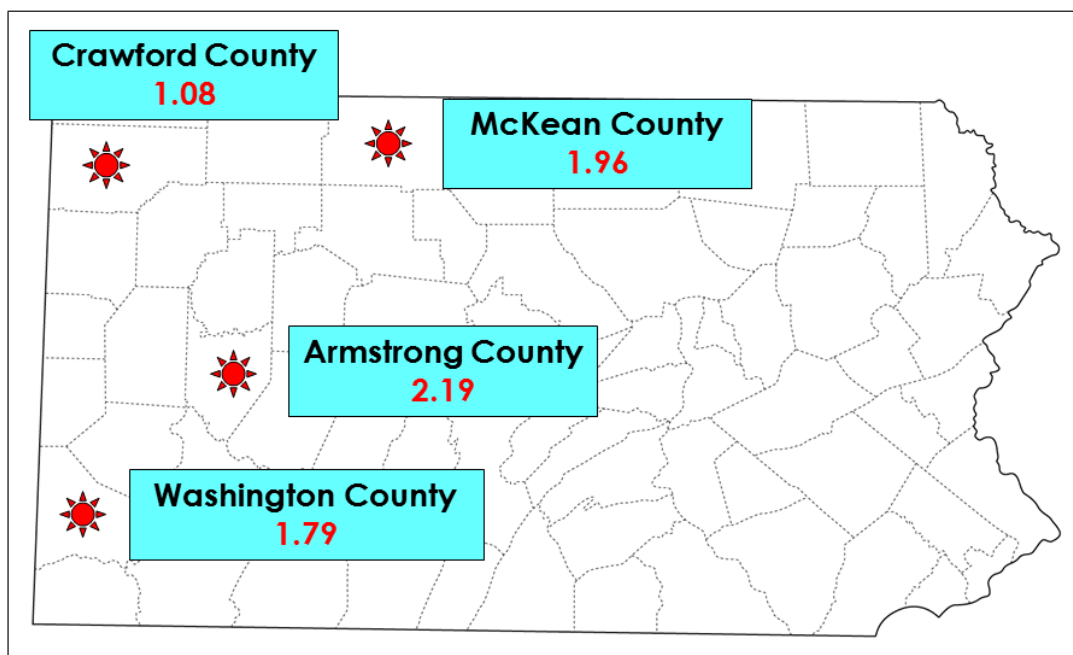
Figure 7-18. Map of Pennsylvania showing locations of well cuttings samples. Average Ro random values for each location are shown in red type.

Table 7-4. Reflectance data for Pennsylvania samples.

Well ID	Sample Depth (ft)	Random Ro				Calculated Ro max	Calculated Ro eq	No. of Observations
		Avg	Max	Min	Std Dev			
Martin No. 1, Armstrong Co., PA								
	11,860-11,870	2.22	2.60	1.81	0.22	2.37	1.77	39
	12,010-12,020	2.17	2.60	1.83	0.22	2.32	1.74	38
Well Average		**2.19**	**2.60**	**1.82**	**0.22**	**2.35**	**1.76**	**39**
Kardosh No. 1, Crawford Co., PA								
	5950-5960	1.09	1.32	0.88	0.12	1.17	1.08	35
	5990-6000	1.10	1.36	0.86	0.13	1.18	1.08	34
	6160-6170	1.06	1.25	0.90	0.09	1.13	1.05	34
Well Average		**1.08**	**1.31**	**0.88**	**0.11**	**1.16**	**1.07**	**34**
Say No. 1, McKean Co., PA								
	9070-9080	1.96	2.20	1.72	0.14	2.10	1.61	37
	9090-9100	1.97	2.22	1.72	0.16	2.11	1.62	33
	9100-9110	1.96	2.37	1.69	0.20	2.09	1.61	35
Well Average		**1.96**	**2.26**	**1.71**	**0.17**	**2.10**	**1.61**	**35**
FEI Starvaggi No. 1, Washington Co., PA								
	10,610	1.78	2.02	1.61	0.15	1.90	1.50	45
	10,730	1.81	2.08	1.50	0.17	1.94	1.52	42
	10,740	1.76	2.10	1.57	0.17	1.88	1.49	37
	10,810	1.81	2.08	1.54	0.16	1.94	1.52	32
	10,830	1.80	2.05	1.61	0.14	1.93	1.51	35
	10,840	1.79	2.09	1.57	0.15	1.92	1.51	45
Well Average		**1.79**	**2.07**	**1.57**	**0.16**	**1.92**	**1.51**	**39**

A sample of the geologically younger Marcellus Formation from Washington County (API# 3712520552), located at a depth of 6450 ft, also was analyzed for comparison purposes.   This sample reported a Ro random value of 1.39%. In addition, the Pittsburgh coal bed, which occurs within 500 ft of ground surface across Washington County, has an Ro random of 0.8 to 0.85% (Ruppert and others, 2010). Collectively, this indicates a random reflectance increase of about 1.0% over a depth range of about 10,000 ft in southwestern Pennsylvania (Figure 7-19).

Depth (ft)		Ro random
0 - 500	**Pittsburgh Coal Bed**	0.80 – 0.85
6,000 – 6,500	**Marcellus Shale**	1.30 – 1.40
10,500 – 11,000	**Utica Shale**	1.75 – 1.85
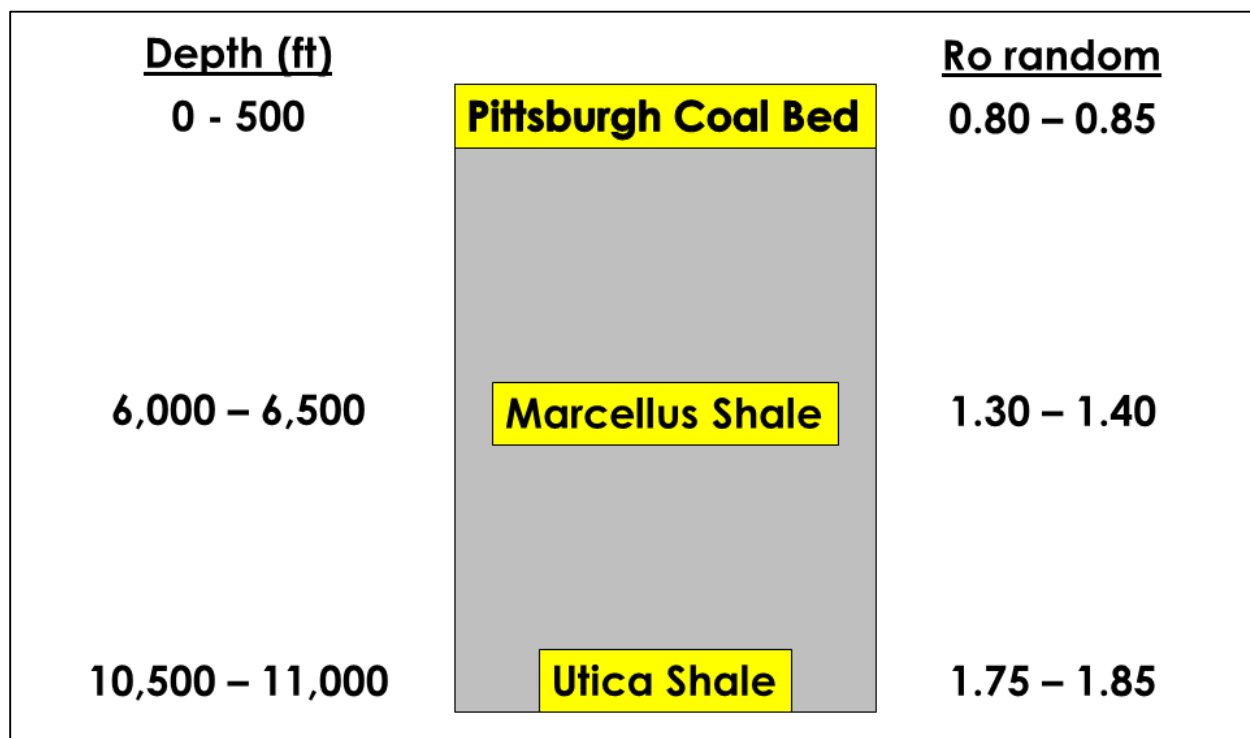
Figure 7-19.   Reflectance measurements for discrete depth intervals in Washington County, Pennsylvania, showing a change of approximately 1.0% Ro over a depth of about 10,000 ft.

7.3.4 Discussion

The organic matter composition of the Utica/Point Pleasant is uniformly dominated by amorphinite, which indicates an algal source for much, if not most, of the organic material in the rocks. Organic-rich intervals within the Utica/Point Pleasant have a greater proportion of shale in the inorganic matrix, with the organic material occurring most frequently in association with shale lithologies. Organic-poor intervals are usually carbonate-mineral dominant.

The level of thermal maturity in the Utica/Point Pleasant shows a progression in increasing bitumen reflectance from west to east, with a very steep increase occurring in eastern Ohio. This is mainly the result of a rapid increase in depth of the Utica/Point Pleasant in this area. In central Ohio, the Utica/Point Pleasant was sampled at depths from less than 100 ft in Clermont County (OH2535) to about 4800 ft in Vinton County (OH4230). Ro random values from central Ohio ranged from 0.66 to 0.84%. In eastern Ohio, sample depths ranged from 8700 ft to more than 15,000 ft, with Ro values ranging from 0.94 to 1.43%. As such, it is not surprising that the eastern Ohio area is more thermally mature. Two thermal maturity maps with isoreflectance lines (one

for central Ohio and another for eastern Ohio) are provided in Figures 7-20 and 7-21, respectively. These agree well with a previously published map for this area of the basin (ODNR, 2013).
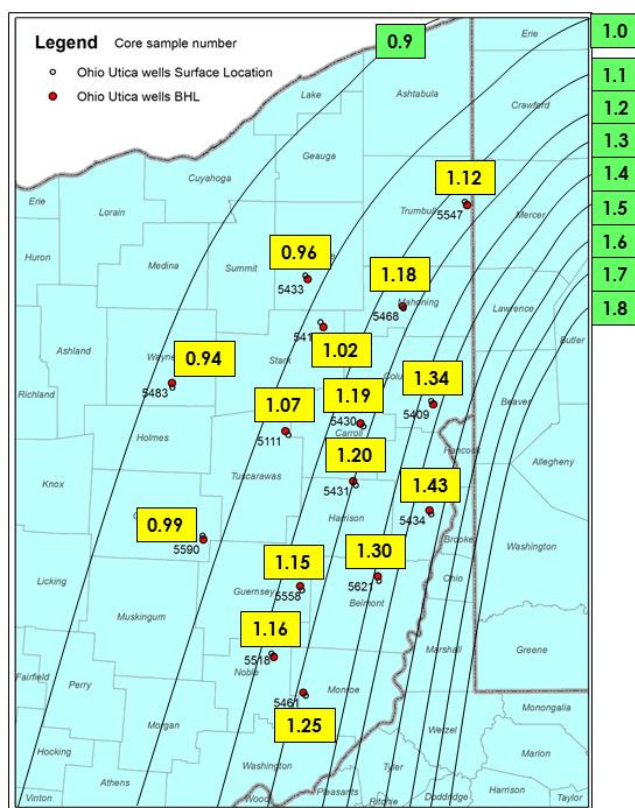
Figure 7-20. Map of eastern Ohio showing isoreflectance lines.
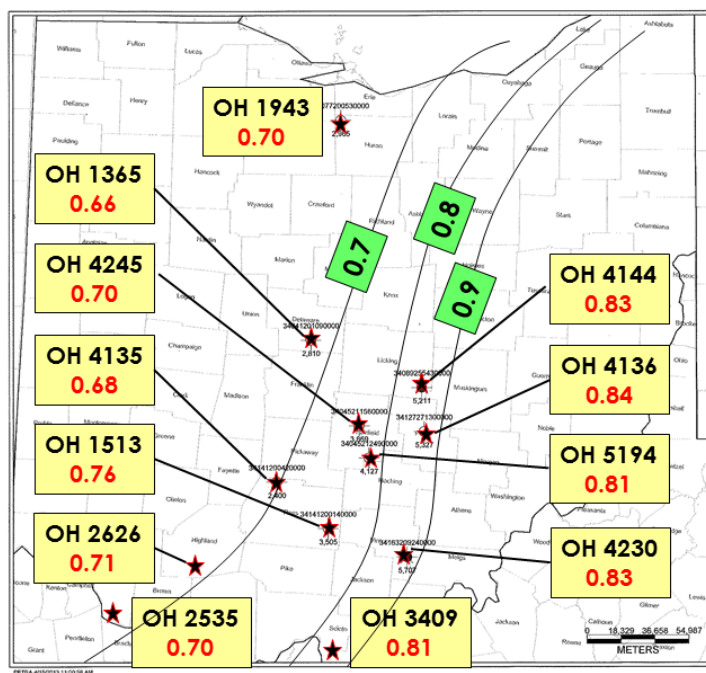
Figure 7-21. Map of Ohio showing isoreflectance lines for the central part of the state.

7.3.5 Characterizing Reservoir Quality Using Mineralogy, TOC and Bitumen Reflectance

This particular task builds on work previously conducted by Cooney (2013) regarding thermal maturity trends of the Utica Shale Play in Pennsylvania. Cooney (2013) (see Appendix 7-B) found that although mineralogy varied significantly between the Utica and Point Pleasant formations (higher carbonate in the Point Pleasant versus higher quartz and clay in the Utica), reflectance measurements collected for each interval remained very similar at most locations and did not necessarily increase with depth. Reflectance values did increase from west to east across Pennsylvania, which agrees with earlier thermal maturity studies. Since composite samples were taken in 50-ft intervals, they did not necessarily reflect small-scale variations in organic-richness that may be present within each formation, and thus, a much more detailed sample set, with formations sampled every 10-ft, was warranted for this follow-on work.

For the current task, the research team explored potential relationships among Utica and Point Pleasant mineralogy, organic content and bitumen reflectance, as well as potential trends among these parameters with well depth. Samples were collected from several wells across Pennsylvania, where thermal maturity has been shown to span from the oil window through the dry gas window.

7.3.5.1 *Materials and Methods*

Samples from several wells penetrating the Utica/Point Pleasant were collected from the PAGS rock cuttings repository for this work. In an initial study by Cooney (2013), rock cuttings from six different wells were sampled at 50-ft intervals from the top, middle and base of the Kope, Utica and Point Pleasant formations, where present (Table 7-6). Shale samples (3 to 5 g each) were collected every 10-ft along each 50-ft sampling interval, and then composited to make one representative sample for that interval. For the current Study, five additional well locations were chosen for analysis, and one well from the initial study was reexamined (Figure 7-22). For these locations, rock cuttings were sampled every 10 ft from the inorganic shale just above the Utica (i.e., Kope Formation) to the Lexington/Trenton Formation below the base of the Utica/Point Pleasant (Table 7-5).

Table 7-5. Summary of sampling intervals for preliminary work conducted by Cooney (2013) and those of the current Study.

API No.	Well Name	County	Cooney (2013)[1] Depth (ft)	Play Book Study[2] Depth (ft)
3700521201	Martin No. 1	Armstrong	10,850-11,900	NA
3702720001	Long No. 1	Centre	13,800-14,250	NA
3703920007	Kardosh No. 1	Crawford	5500-6200	NA
3704920049	PA Dept. of Forests & Waters Block 2 No. 1	Erie	NA	3715-4010
3706720001	Shade Mt. No. 1	Juniata	NA	3690-3780
3708520116	Fleck No. 1	Mercer	6930-7100	NA
3711120045	Svetz No. 1	Somerset	NA	15,000-15,160
3711320002	Dieffenbach No. 2951	Sullivan	16,200-16,350	NA
3711720181	Marshlands No. 2	Tioga	NA	11,660-12,030
3712320150	Shaw No. 1	Warren	8100-8300	8047-8362
3712522278	Starvaggi No. 1	Washington	NA	10,030-11,000

1 – 50-ft sample interval: top, middle and base of each formation
2 – 10-ft sample interval
NA – not analyzed
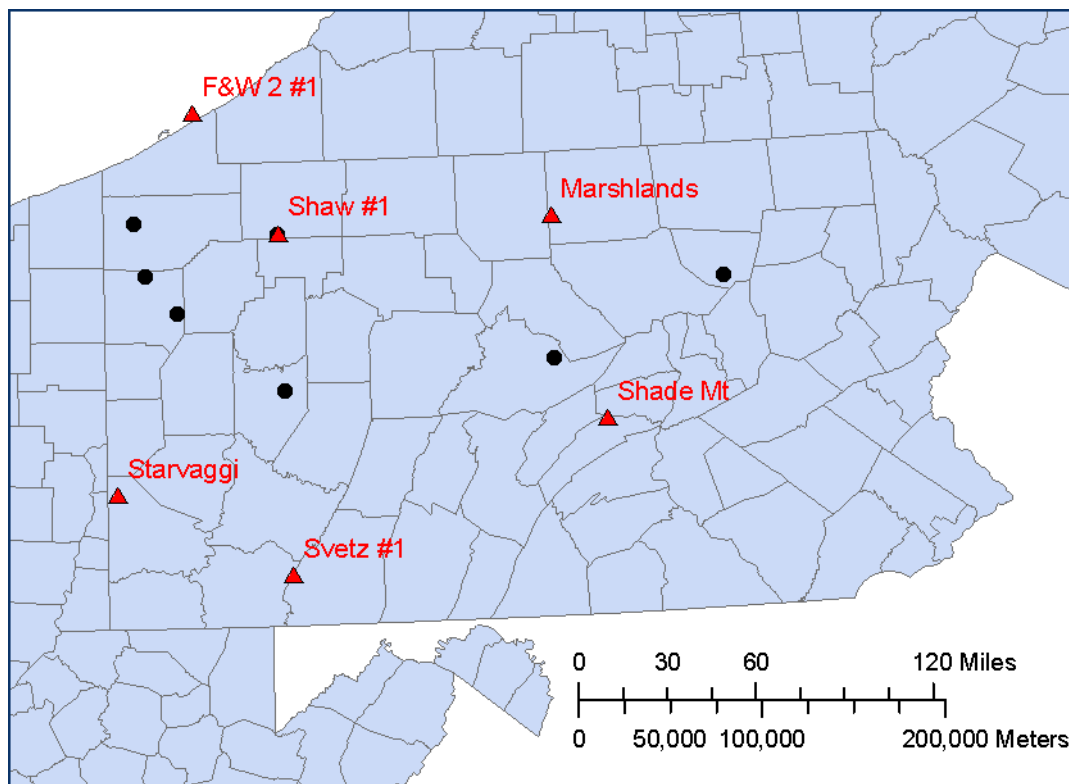
Figure 7-22.   Map of Pennsylvania showing sample locations utilized by Cooney (2013) in a preliminary study of Utica/Point Pleasant thermal maturity (black circles), and those used in the current Study (red triangles).

Each sample was ground with a mortar and pestle and sieved through a #16 sieve. Approximately 2 g of sample were added to roughly 3 g of Beuhler TransOptic powder (20-3400-080) and mixed. The sample and powder were then placed into a Beuhler Simplimet 3000 Automatic Mounting Press and run for 15.5 minutes at 4000 pounds per square inch (psi) to form solid sample plugs for reflectance analysis. After sitting overnight in a desiccator, the plugs were polished using a Beuhler Ecomet 300 and six polishing pads of varying coarseness. Each plug was analyzed using a Leica DMRX microscope which was calibrated using a (YAG) [0.901] or (GGG) [1.719] standard with MSP200V4.3 and AxioVision software. Using immersion oil and an oil objective, samples were visually assessed for bitumen using the American Society for Testing and Materials (ASTM) standard D2797. As many measurements as possible were made on macerals of sufficient size. Using the ASTM 7708 template, data were placed into a histogram that included three category divisions: coked bitumen, degraded bitumen, and homogeneous bitumen. The resulting data are provided in Appendix 7-C.

7.3.5.2 Results

PA Dept. of Forests & Waters Block 2 No.1 (API #3704920049)

Bitumen reflectance samples were collected from the PA Dept. of Forests & Waters Block 2 No. 1 well in Erie County, Pennsylvania, over a 295-ft depth range, spanning from the Kope Formation through the upper portion of the Trenton/Lexington Formation (Table 7-6). Reflectance measurements could not be made for many of these intervals due to lack of bitumen and/or insufficient maceral size. In those intervals where bitumen was present, the number of observations made was limited (Table 7-6).

Table 7-6. Mineralogy, TOC and Reflectance Data for PA Dept. of Forest & Waters Block 2 No. 1.

| Depth (ft) | Formation | Bulk Mineralogy | | | TOC (%) | Bitumen Reflectance | |
		Quartz+ (%)	Clay (%)	Carbonate (%)		Mean BRo (%)	No. of Observations (N)
3715	Kope	42	55	3	NA	1.10	1
3770	Kope	28	66	6	NA	0.98	2
3795	Kope	28	66	7	NA	1.01	2
3810	Utica	32	62	6	NA	0.96	3
3824	Utica	30	64	6	NA	1.10	5
3843	Utica	26	67	8	NA	0.94	4
3869	Utica	35	56	9	NA	1.08	2
3890	Utica	27	66	7	NA	0.92	1
3895	Utica	28	68	4	NA	1.50	4
3911	Utica	31	67	2	NA	1.58	3
3930	Utica	23	58	19	NA	1.92	1
3966	Lexington/Trenton	26	48	26	NA	1.95	1
3985	Lexington/Trenton	18	24	58	NA	2.01	1
3993	Lexington/Trenton	16	26	58	NA	1.56	1
4010	Lexington/Trenton	15	14	70	NA	2.09	1

NA – not analyzed

In general, reflectance increases with depth, with a cluster of relatively high measurements (1.5-2.0% BRo) reported near the base of the Utica Shale (3895 ft) through the top of the Lexington/Trenton Formation (4010 ft). This notable increase in measured reflectance values in

the lower Utica occurs about 50 ft shallower than any changes in mineralogy (Table 7-6). The Point Pleasant Formation is not present in this area of Pennsylvania, so the Utica and Lexington/Trenton formations are in direct, disconformable contact with one another at this location.
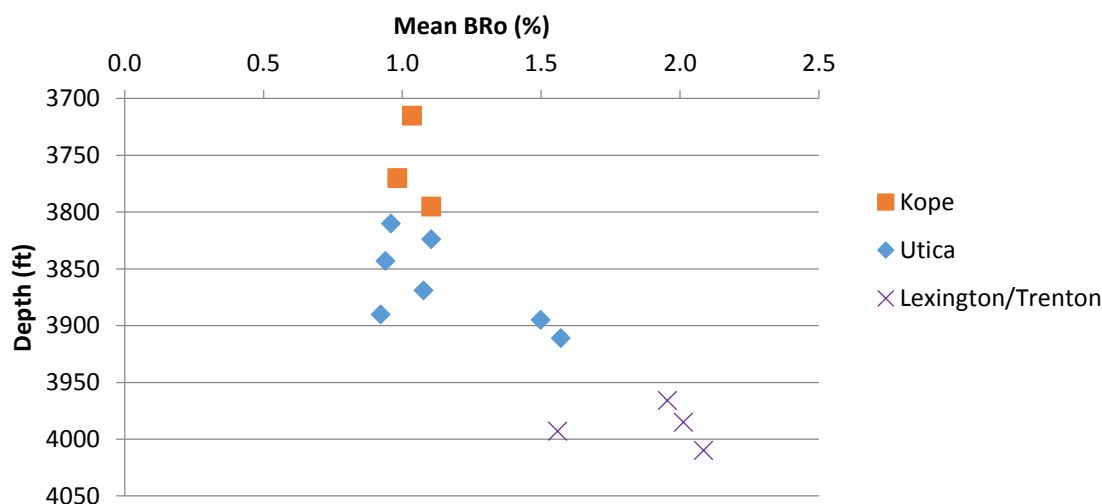
Figure 7-23. Crossplot of mean reflectance measurements (BRo%) versus depth in the PA Dept. of Forests & Waters Block 2 No. 1 well, Erie County, Pennsylvania. Reflectance generally increases with depth.

A tabular summary of the mean bitumen reflectance values (by formation) is provided in Table 7-7. The mean BRo measured in this well is 1.38%.

Table 7-7. Mean reflectance (BRo%) by formation, PA Dept. of Forests & Waters Block 2 No. 1.

Formation	Mean BRo (%)	Mean No. of Observations (N)
Kope	1.03	1.7
Utica	1.25	3.1
Lexington/Trenton	1.90	1.0
Well Mean	**1.38**	**2.1**

Shaw No.1 (API #3712320150)

Bitumen reflectance samples were collected from the Shaw No. 1 well in Warren County, Pennsylvania, over a 322-ft range spanning from the Utica Shale through the upper Lexington/Trenton Formation (Figure 7-24). The number of reflectance measurements that could be made was limited, but macerals of measureable size were more abundant in this well than in samples collected from PA Dept. of Forest & Waters Block No. 1 in neighboring Erie County. In general, intervals of high and low reflectance were found in all three formations. The most measureable macerals occurred at the bottom of the Point Pleasant Formation (8300 to 8375 ft), directly on top of the Lexington/Trenton Formation, which alludes to a relatively organic-rich zone in this part of the interval. A similar cluster of relatively higher N values is found at the bottom of the Utica Shale and into the top of the Point Pleasant.

127

There does not appear to be any correlation between intervals of higher reflectance and mineralogical variations (Table 7-8). Even so, where the highest number of measureable macerals were encountered (i.e., at the base of the Utica and Point Pleasant formations), a noticeable change in mineralogy takes place (increasing carbonate, decreasing clay). Overall, reflectance increases with depth (Table 7-8).

Table 7-8. Mineralogy, TOC and Reflectance Data for Shaw No. 1.

Depth (ft)	Formation	Bulk Mineralogy			TOC[1] (%)	Bitumen Reflectance	
		Quartz+ (%)	Clay (%)	Carbonate (%)		Mean BRo (%)	No. of Observations (N)
8047	Utica	32	62	6	NA	1.13	3
8057	Utica	31	61	8	NA	1.21	6
8066	Utica	26	67	7	NA	1.75	6
8074	Utica	30	61	10	NA	1.76	5
8087	Utica	26	61	13	NA	1.63	4
8094	Utica	28	62	10	NA	1.73	3
8108	Utica	29	64	8	NA	2.02	3
8117	Utica	28	64	8	NA	1.72	3
8120	Utica	30	63	7	NA	1.51	1
8126	Utica	30	63	7	NA	1.81	5
8136	Utica	31	65	5	NA	1.70	7
8141	Utica	32	64	4	NA	1.57	3
8146	Utica	33	57	10	NA	1.45	4
8161	Utica	29	57	14	NA	1.65	9
8168	Utica	29	52	19	NA	1.60	7
8170	Point Pleasant	24	52	24	NA	1.35	1
8197	Point Pleasant	30	49	20	NA	1.86	7
8210	Point Pleasant	35	42	23	NA	1.90	8
8220	Point Pleasant	34	36	20	NA	1.79	3
8227	Point Pleasant	30	48	22	NA	1.64	5
8240	Point Pleasant	35	43	22	NA	2.10	2
8250	Point Pleasant	31	50	20	NA	1.93	2
8263	Point Pleasant	28	46	26	NA	1.84	3
8272	Point Pleasant	27	52	21	NA	1.70	3
8282	Point Pleasant	35	37	28	NA	1.62	10
8288	Point Pleasant	31	45	24	NA	1.75	18
8296	Point Pleasant	25	51	25	NA	1.78	15
8303	Lexington/Trenton	21	49	30	NA	1.55	5
8313	Lexington/Trenton	25	20	55	NA	1.85	6
8317	Lexington/Trenton	13	7	80	NA	1.79	13
8321	Lexington/Trenton	14	5	80	NA	1.85	4
8326	Lexington/Trenton	11	81	8	NA	1.77	9
8333	Lexington/Trenton	8	20	72	NA	1.77	6
8339	Lexington/Trenton	7	6	87	NA	1.83	2
8347	Lexington/Trenton	9	6	86	NA	1.79	5
8356	Lexington/Trenton	10	8	82	NA	1.83	9
8362	Lexington/Trenton	5	4	91	NA	1.77	8
8369	Lexington/Trenton	5	5	90	NA	1.96	3

1 – TOC samples were taken from this well in 50-ft intervals by Cooney (2013). TOC results were as follows: 0.20% at 7600-7650 ft (Kope Formation); 1.20% at 8100-8150 ft (Utica Shale); and 1.54% at 8250-8300 ft (Point Pleasant Formation).
NA – not analyzed

Figure 7-24. Crossplot of mean reflectance measurements (BRo%) versus depth in the Shaw No. 1 well, Warren County, Pennsylvania. Many BRo values fall in the 1.5 to 2.0% range, regardless of formation or depth.

A tabular summary of the mean bitumen reflectance values (by formation) is provided in Table 7-9. The mean BRo measured in this well is 1.72%.

Table 7-9. Mean reflectance (BRo%) by formation, Shaw No. 1.

Formation	Mean BRo (%)	Mean No. of Observations (N)
Utica	1.62	4.6
Point Pleasant	1.77	6.4
Lexington/Trenton	1.80	6.4
Well Mean	**1.72**	**5.8**

Starvaggi No.1 (API #3712522278)

Bitumen reflectance measurements were collected from the Starvaggi No. 1 well in Washington County, Pennsylvania, over a 970-ft range that included multiple formations: the Kope, Utica, Point Pleasant and Lexington/Trenton. Generally, intervals of high reflectance are found at various depths throughout the well, but intervals with the highest numbers of measureable macerals were found in the lower Utica Shale and interspersed throughout the Point Pleasant Formation (Table 7-10). Elevated TOC values are coincident with sample intervals having the largest number of maceral observations.

Table 7-10. Mineralogy, TOC and Reflectance Data for Starvaggi No. 1.

Depth (ft)	Formation	Bulk Mineralogy			TOC (%)	Bitumen Reflectance	
		Quartz+ (%)	Clay (%)	Carbonate (%)		Mean BRo (%)[1]	No. of Observations (N)
10030	Kope	35	48	17	0.48	0.67	1
10060	Kope	25	48	27	0.41	0.59	2
10100	Kope	30	51	19	0.39	0.91	3
10200	Kope	30	63	7	0.31	1.12	1
10210	Kope	25	66	9	0.36	0.86	7
10230	Kope	32	54	14	0.38	1.06	3
10240	Kope	30	55	15	0.41	1.03	3
10260	Kope	32	53	16	0.37	1.36	1
10270	Kope	29	60	12	0.38	1.10	20
10300	Kope	27	56	17	0.39	1.11	2
10310	Kope	32	49	19	0.47	1.00	4
10320	Kope	26	61	12	0.41	0.91	2
10330	Kope	26	61	13	0.45	0.73	1
10340	Kope	29	58	13	0.46	0.85	2
10350	Kope	36	48	15	0.47	0.92	2
10360	Kope	27	64	9	0.50	0.71	1
10370	Utica	29	59	12	0.48	0.93	7
10380	Utica	29	61	10	0.55	0.99	6
10390	Utica	27	64	9	0.62	1.01	10
10400	Utica	27	62	11	0.53	1.06	3
10410	Utica	27	63	10	0.61	1.01	4
10420	Utica	30	62	8	0.53	1.21	5
10430	Utica	38	51	11	0.47	1.09	3
10440	Utica	31	59	10	0.61	0.97	5
10450	Utica	34	54	13	0.67	1.06	10
10460	Utica	29	61	9	0.62	1.22	13
10470	Utica	27	65	8	0.50	0.93	7
10480	Utica	31	58	12	0.55	0.84	1
10490	Utica	30	61	9	0.55	NA	
10500	Utica	32	57	12	0.55	1.02	3
10510	Utica	24	62	14	0.85	0.89	3
10520	Utica	28	62	11	0.64	0.95	11
10530	Utica	25	62	12	0.94	1.08	1
10540	Utica	29	59	12	1.49	1.00	24
10550	Utica	27	60	13	1.65	0.97	25
10560	Utica	28	60	12	1.98	0.98	14
10570	Utica	28	58	14	1.96	1.06	11
10580	Utica	27	60	14	2.18	1.10	16
10590	Utica	29	54	18	1.32	1.06	21
10600	Utica	27	61	12	1.32	1.04	10
10610	Utica	26	60	14	1.57	0.96	3
10620	Utica	30	53	17	1.43	1.16	1
10630	Utica	25	57	18	1.61	1.14	6
10640	Utica	31	53	16	0.99	1.11	6
10650	Utica	30	57	13	1.25	1.31	4
10660	Utica	28	58	13	1.21	1.20	3
10680	Utica	24	64	12	1.11	0.90	5
10690	Utica	25	62	13	1.77	1.06	26

Depth (ft)	Formation	Bulk Mineralogy			TOC (%)	Bitumen Reflectance	
		Quartz+ (%)	Clay (%)	Carbonate (%)		Mean BRo (%)[1]	No. of Observations (N)
10700	Utica	28	53	20	2.31	1.07	8
10710	Utica	24	47	29	2.20	1.00	12
10720	Utica	21	40	39	2.93	1.10	14
10730	Utica	20	34	46	3.71	1.00	30
10740	Utica	23	32	46	3.46	0.97	13
10750	Utica	21	28	51	4.11	0.97	20
10760	Point Pleasant	30	14	56	3.95	1.07	24
10770	Point Pleasant	33	12	55	4.19	0.94	38
10780	Point Pleasant	28	10	62	3.67	1.00	39
10790	Point Pleasant	20	5	75	3.34	1.00	35
10800	Point Pleasant	18	8	74	2.70	0.99	8
10810	Point Pleasant	13	9	78	3.04	1.06	13
10820	Point Pleasant	16	7	78	2.88	1.04	5
10830	Point Pleasant	12	6	82	3.52	0.96	23
10840	Point Pleasant	18	6	77	3.39	1.01	8
10850	Point Pleasant	16	9	75	1.51	0.97	13
10860	Lexington/Trenton	5	5	90	0.94	0.94	4
10900	Lexington/Trenton	24	0	75	1.02	0.95	16
10920	Lexington/Trenton	23	6	71	1.61	1.01	32
10950	Lexington/Trenton	19	8	73	0.65	1.04	6
10960	Lexington/Trenton	21	9	70	0.95	0.94	25
10970	Lexington/Trenton	22	2	75	0.79	0.99	27
10980	Lexington/Trenton	19	5	76	0.85	1.09	29
10990	Lexington/Trenton	24	2	74	0.88	1.03	27
11000	Lexington/Trenton	12	7	82	1.20	1.05	41

1 – BRo measurements reported for this well are suspect, based on review of other measurements prepared by this Study. See Section 7.3.5.3 below.
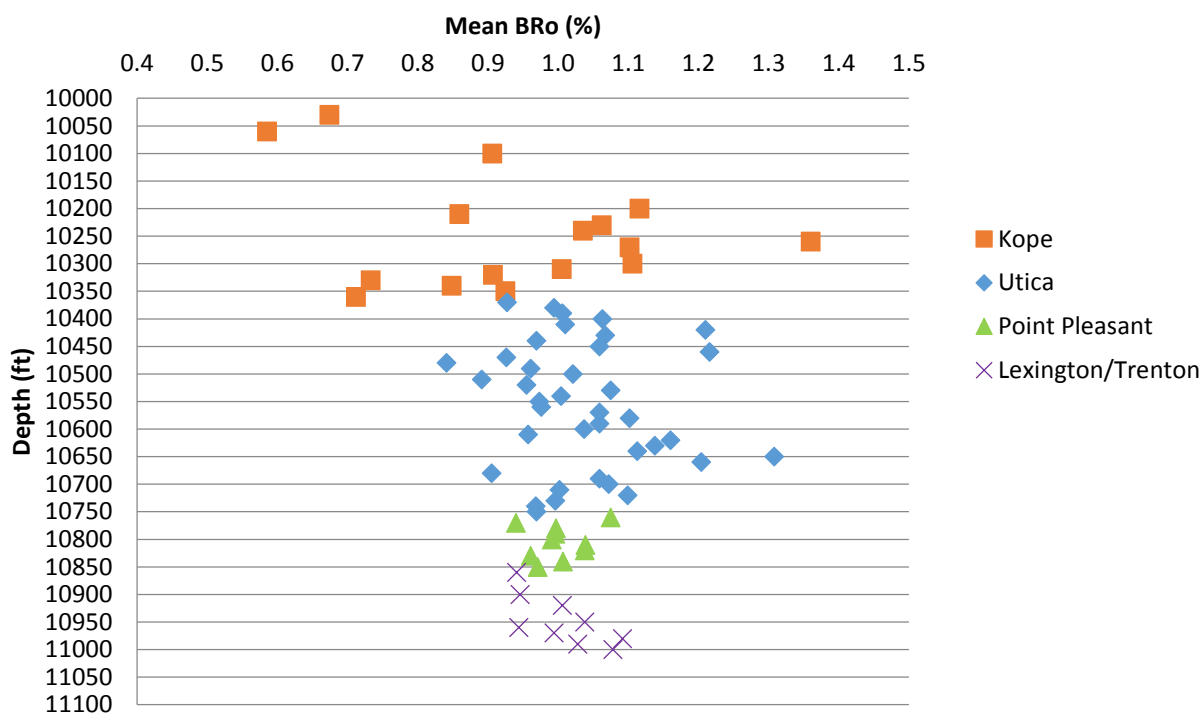
Figure 7-25. Crossplot of mean reflectance measurements (BRo%) versus depth in the Starvaggi No. 1 well, Washington County, Pennsylvania. Many BRo values fall in the 0.8 to 1.2% range, regardless of formation or depth.

A tabular summary of the mean bitumen reflectance values (by formation) is provided in Table 7-11. The mean BRo measured in this well is 1.01%.

Table 7-11. Mean reflectance (BRo%) by formation, Starvaggi No. 1.

Formation	Mean BRo (%)	Mean No. of Observations (N)
Kope	0.93	3.4
Utica	1.04	9.7
Point Pleasant	1.00	20.6
Lexington/Trenton	1.00	23
Well Mean	**1.01**	**11.5**

Marshlands No. 2 (API #3711720181)

Bitumen reflectance measurements were collected from the Marshlands No. 2 well in Tioga County, Pennsylvania, over a 370-ft interval that includes the Utica Shale and Point Pleasant Formation. Reflectance gradually increases with depth in the Utica Shale, and decreases at the top of the Point Pleasant Formation. The sharp increase in reflectance values in the lower Utica (11,900 ft) directly coincides with a significant change in mineralogy, where carbonate increases and clay and quartz minerals begin to decrease (Table 7-12).

132

Table 7-12. Mineralogy, TOC and Reflectance Data for Marshlands No. 2.

Depth (ft)	Formation	Bulk Mineralogy			TOC (%)	Bitumen Reflectance	
		Quartz+ (%)	Clay (%)	Carbonate (%)		Mean BRo (%)	No. of Observations (N)
11660	Utica	38	55	6	NA	1.75	48
11670	Utica	43	51	6	NA	1.72	16
11680	Utica	38	57	5	NA	1.71	12
11690	Utica	40	57	2	NA	1.43	1
11700	Utica	39	57	4	NA	1.80	36
11710	Utica	39	58	3	NA	1.87	50
11720	Utica	44	53	4	NA	1.85	117
11730	Utica	33	63	5	NA	1.80	43
11750	Utica	32	63	5	NA	1.86	14
11760	Utica	40	59	2	NA	1.83	11
11770	Utica	35	62	3	NA	1.86	31
11790	Utica	35	63	2	NA	1.90	3
11800	Utica	35	63	2	NA	1.97	6
11810	Utica	30	60	9	NA	2.01	11
11830	Utica	34	64	3	NA	1.73	4
11840	Utica	35	63	2	NA	1.73	1
11890	Utica	33	46	21	NA	1.65	2
11900	Utica	30	49	21	NA	2.15	10
11910	Utica	26	55	19	NA	2.28	1
11920	Utica	31	48	22	NA	2.09	6
12010	Point Pleasant	25	45	31	NA	1.61	3
12020	Point Pleasant	36	18	46	NA	1.80	1
12030	Point Pleasant	28	30	42	NA	1.54	3

NA – not analyzed
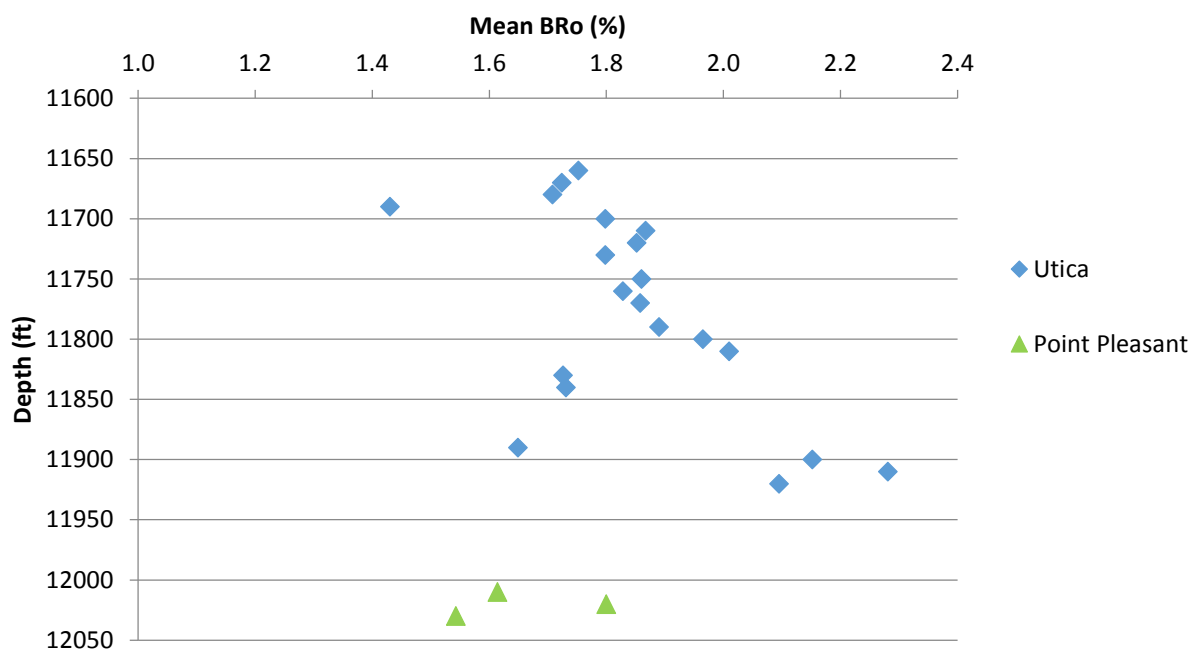
Figure 7-26. Crossplot of mean reflectance measurements (BRo%) versus depth in the Marshlands No. 2 well, Tioga County, Pennsylvania. A majority of measurements for both the Utica and Point Pleasant intervals fall in the 1.5 to 2.0% range.

A tabular summary of the mean bitumen reflectance values (by formation) is provided in Table 7-13. The mean BRo measured in this well is 1.82%.

Table 7-13. Mean reflectance (BRo%) by formation, Marshlands No. 2.

Formation	Mean BRo (%)	Mean No. of Observations (N)
Utica	1.85	21.1
Point Pleasant	1.65	2.3
Well Mean	**1.82**	**18.5**

Shade Mt. No.1 (API #3706720001)

Bitumen reflectance measurements were collected from the Shade Mt. No. 1 in Juniata County, Pennsylvania, over a 90-ft depth range comprised exclusively of the Point Pleasant Formation. Some intervals were excluded from analysis due to lack of bitumen macerals and/or insufficient maceral size. In this well, the Point Pleasant Formation exhibits a steady increase in bitumen reflectance with depth (Table 7-14).

Table 7-14. Mineralogy, TOC and Reflectance Data for Shade Mt. No. 1.

Depth (ft)	Formation	Bulk Mineralogy			TOC (%)	Bitumen Reflectance	
		Quartz+ (%)	Clay (%)	Carbonate (%)		Mean BRo (%)	No. of Observations (N)
3690	Point Pleasant	33.2	9.9	55.9	NA	0.86	22
3700	Point Pleasant	35.6	9.7	54.8	NA	0.81	16
3710	Point Pleasant	35.6	6.9	57.2	NA	0.78	3
3720	Point Pleasant	39.4	6	54.6	NA	0.96	22
3730	Point Pleasant	40.8	5.9	52.8	NA	0.99	20
3740	Point Pleasant	51.6	6.7	41.6	NA	0.89	31
3750	Point Pleasant	48.4	14.4	37.6	NA	0.85	12
3760	Point Pleasant	48.3	14.1	37.7	NA	0.89	10
3770	Point Pleasant	51.3	19	29.8	NA	1.05	31
3780	Point Pleasant	64.2	20.3	15.5	NA	1.08	18

NA – not analyzed
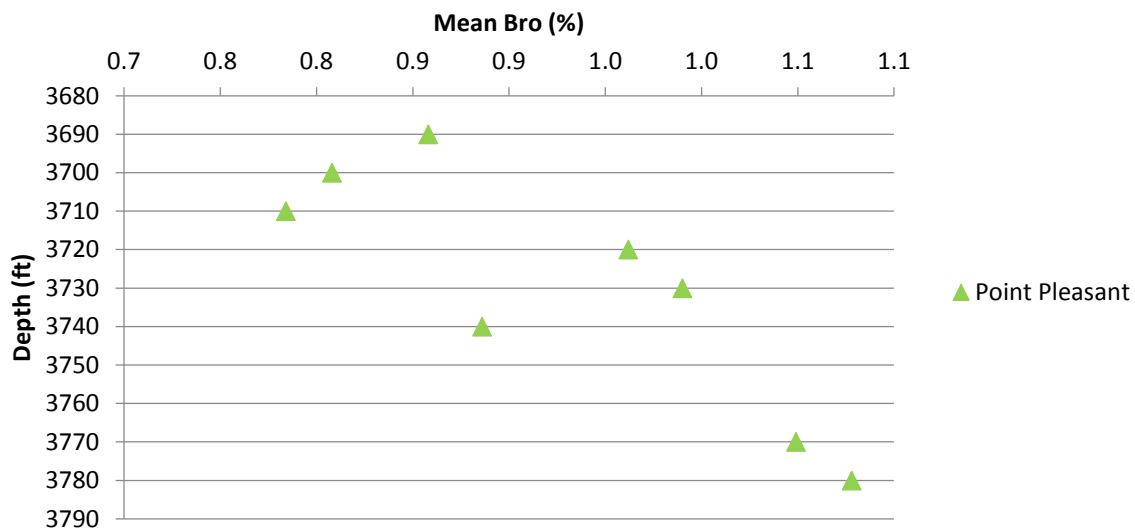
Figure 7-27. Crossplot of mean reflectance measurements (BRo%) versus depth in the Shade Mt. No. 1, Juniata County, Pennsylvania. Reflectance generally increases with depth.

A tabular summary of the mean bitumen reflectance values (by formation) is provided in Table 7-15. The mean BRo measured in this well is 0.92%.

Table 7-15. Mean reflectance (BRo%) by formation, Shade Mt. No. 1.

Formation	Mean BRo (%)	Mean No. of Observations (N)
Point Pleasant	0.92	18.5
Well Mean	**0.92**	**18.5**

Svetz No. 1 (API #3711120045)

Bitumen reflectance measurements were collected from the Svetz No. 1 in Somerset County, Pennsylvania, over a depth range of 140 ft comprised exclusively of the Utica Shale. Many of the depth intervals sampled in this well lack reflectance measurements due to an insufficient number of observations (i.e., the number and size of bitumen macerals were limited) (Table 7-16). Reflectance values range from 1.95 to 3.2% BRo, and no particular trends are noted with depth.

Table 7-16. Mineralogy, TOC and Reflectance Data for Svetz No. 1.

Depth (ft)	Formation	Bulk Mineralogy			TOC (%)	Bitumen Reflectance	
		Quartz+ (%)	Clay (%)	Carbonate (%)		Mean BRo (%)	No. of Observations (N)
15,000	Utica	36	56	9	1.29^1	1.95	1
15,020	Utica	32	58	10	1.29^1	3.19	1
15,070	Utica	39	44	17	NA	2.64	3
15,090	Utica	39	47	15	NA	3.05	3
15,130	Utica	30	55	15	NA	3.27	4
15,140	Utica	31	55	14	NA	2.46	1

1 – Legacy TOC data reported by Laughrey and others (2009) for sample collected at 14,980-15,040 ft.
NA – not analyzed
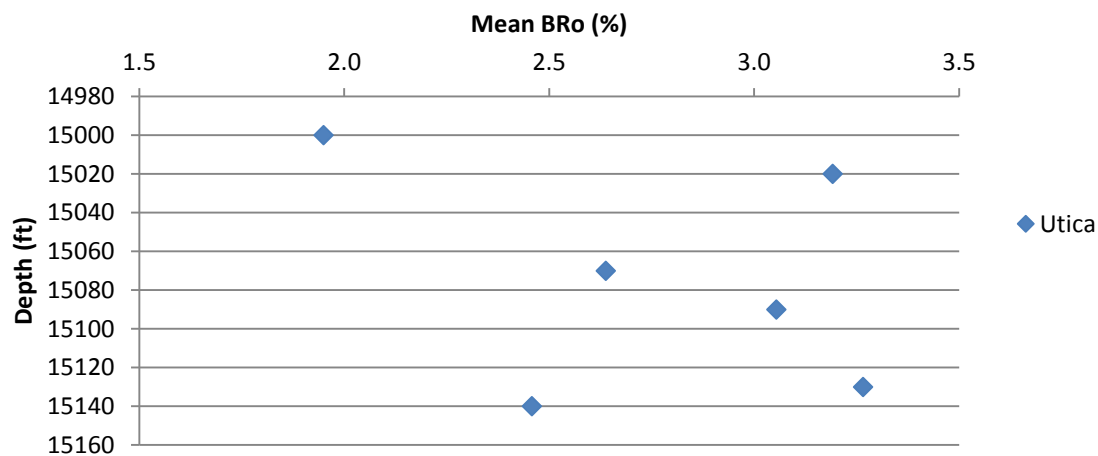
Figure 7-28. Crossplot of mean reflectance measurements (BRo%) versus depth in the Svetz No. 1 well, Somerset County, Pennsylvania.

A tabular summary of the mean bitumen reflectance values (by formation) is provided in Table 7-17. The mean BRo measured in this well is 2.76%.

Table 7-17. Mean reflectance (BRo%) by formation, Svetz No. 1.

Formation	Mean BRo (%)	Mean No. of Observations (N)
Utica	2.76	2.2
Well Mean	**2.76**	**2.2**

136

7.3.5.3 Bitumen Reflectance to Vitrinite Reflectance Equivalent Values

A correlation for transforming bitumen reflectance (BRo) measurements to vitrinite reflectance equivalent (Ro eq) values has yet to be published for the Utica Shale play. In an attempt to address this situation, we have chosen a suite of correlations developed for other organic-rich shales to transform the Pennsylvania BRo data into Ro eq values. We have selected equations by Jacob (1989), Landis and Castaño (1994) and Schoenherr (2007) for this effort. Table 7-19 summarizes the mean bitumen reflectance values (BRo%) for each well, along with representative vitrinite reflectance equivalent values (Ro eq%). An expanded discussion on this topic is provided in Appendix 7-D.

Table 7-18. Conversion of bitumen reflectance (BRo) measurements to vitrinite reflectance equivalent (Ro eq) values utilizing three different methods.

API No.	Well Name	Mean BRo (%)	Calculated Ro eq (%)		
			Jacob (1989)	Landis and Castaño (1994)	Schoenherr (2007)
3704920049	PA Dept. of Forests & Waters Block 2 No. 1	1.4	1.3	1.6	1.6
3706720001	Shade Mt. No. 1	0.9	1.0	1.2	1.1
3711120045	Svetz No. 1	2.8	2.1	2.9	2.9
3711720181	Marshlands No. 2	1.8	1.5	2.1	2.0
3712320150	Shaw No. 1	1.7	1.5	1.9	1.9
3712522278	Starvaggi No. 1	1.0	1.0	1.3	1.2

Using the correlations of Jacob (1989), Landis and Castaño (1994) and Schoenherr (2007), Ro eq values for the six Pennsylvania wells evaluated for this task range from 1.0 to 2.9% (Table 7-19). The Shade Mt. No. 1 has Ro eq values ranging from 1.0 to 1.2%, which would place it in the oil to early gas window. The PA Dept. of Forests & Waters Block 2 No. 1 (Ro eq – 1.3 to 1.6%), the Shaw No. 1 (Ro eq – 1.5 to 1.9%) and the Marshlands No. 2 (Ro eq – 1.5 to 2.1%) have values that would place these wells in the dry gas window. The Svetz No. 1 has Ro eq values ranging from 2.1 to 2.9%, which would place it in the dry gas to overmature window.

Using these correlations on the Starvaggi No. 1 well yields Ro eq values ranging from 1.0 to 1.3% (Table 7-18), which would place it in the peak oil to gas window. However, this particular well (the most recently completed well in this dataset) is known to have produced only dry gas, which is more consistent with reflectance results reported for this location by Cortland Eble (i.e., mean BRo of 1.79% and calculated Ro eq of 1.51%; see Section 7.3.3.3). To address this discrepancy, we have reviewed all bitumen reflectance data collected as part of this current work against those reported by Eble for his Pennsylvania dataset (Section 7.3.3.3), as well as those collected by Cooney (2013). Based on this review, we see consistent well-by-well results (where duplicate analyses were performed) and general agreement in thermal maturity trends across the state for all reflectance data but those of the Starvaggi No. 1. A review of our laboratory log books suggest that the discrepancy observed in BRo (and therefore, Ro eq) values for this particular location may be due to an unsatisfactory calibration of the petrographic microscope at the time the Starvaggi No. 1 samples were analyzed.

7.3.5.4   Discussion

Geographic Trends

Excluding the Shade Mt. No. 1 and adjusting the Starvaggi No. 1 to fall within the dry gas window, the calculated Ro eq values and associated Utica thermal maturities increase from west to east in Pennsylvania (Figure 7-29). Although many more data points would be required to delineate specific areas of thermal maturity, this pattern generally fits with previously published thermal maturity maps for the state (e.g., Repetski and others, 2008). This means that moving eastward toward the structural front in central Pennsylvania, one could expect to find more thermally mature rocks, capable of producing natural gas, whereas relatively immature rocks in the northwest may produce oil and/or condensate.
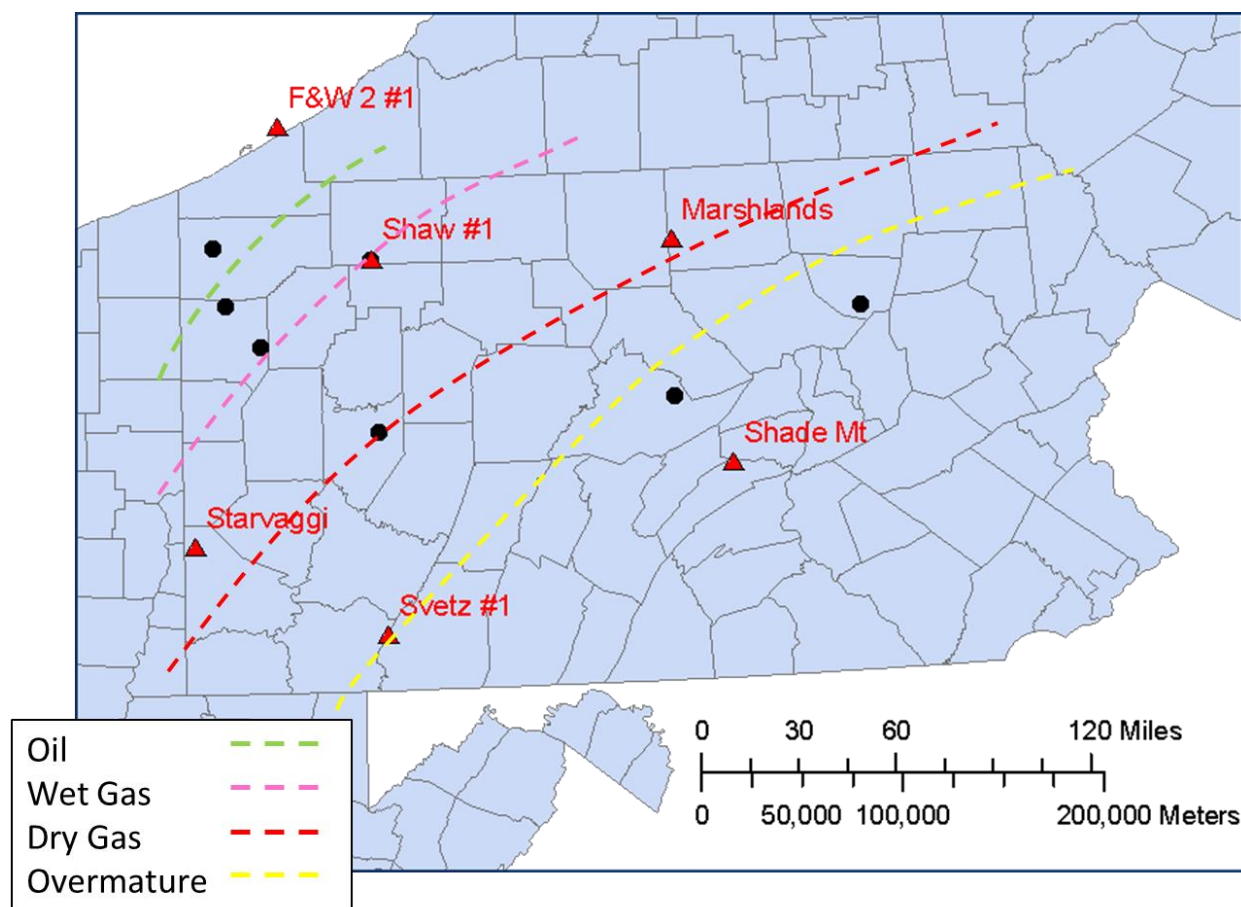
Figure 7-29. Map of Pennsylvania showing approximate thermal maturity boundaries for the Utica Shale play, based on Ro eq values calculated as part of this Study.

Thermal Maturity with Depth

Overall, we observed a general trend of increasing reflectance with depth of formation. While the relationship between depth and BRo% was not exactly linear, in most cases mean BRo% for each formation increased from the Kope to Utica, Utica to Point Pleasant and Point Pleasant to Lexington/Trenton. For some locations (i.e., Shaw No. 1 and Starvaggi No. 1), we observed a "funnel" pattern in the BRo% data when plotted against depth – in other words, a wide range in

138

BRo% values was recorded in shallower formations, and more similar BRo% values were measured in deeper formations. The large range of values in shallow formations seems to artificially raise the mean BRo% values in some wells, causing shallower formations to appear more mature than deeper formations.

Correlation of Bitumen Reflectance with Other Data

We observe no strong correlation between bitumen reflectance and mineralogy, GR log signatures and/or TOC analyses. In some wells, variations in reflectance coincide with changes in one or more of these parameters, but in others there does not appear to be any relationship among the data. In the PA Dept. of Forest & Waters Block 2 No. 1 (Erie County, Pennsylvania), the highest reflectance values occur near the Utica-Lexington/Trenton contact and do not coincide with any mineralogical changes. By contrast, in the Shade Mt. No. 1 (Juniata County, Pennsylvania), the highest reflectance values occur in the Point Pleasant, near its contact with the Lexington/Trenton Formation, and coincide with increasing quartz and clay, and decreasing carbonate. In the Marshland Unit No. 2 (Tioga County, Pennsylvania), the opposite phenomenon occurs; here, increasing BRo% coincides with a notable increase in carbonates and a decrease in quartz and clay. In two locations (the Shaw No. 1 of Warren County and Starvaggi No. 1 of Washington County), we observed intervals of higher and lower reflectance scattered throughout the entirety of the sampled intervals. In both wells, the number of measureable macerals (N) increases near the Utica-Point Pleasant contact and even more dramatically at the Point Pleasant-Lexington/Trenton contact. In the Starvaggi No. 1, where TOC data were collected, this increase in N coincides with an increase in TOC.

Sources of Error

Various sources of error can impact bitumen reflectance analyses. Bitumen can be altered by weathering to produce a mixture of less optically unaltered migrabitumen (i.e., solid oil bitumen), minerals and coke from bitumen (Jacob, 1989), making reflectance analysis increasingly difficult. Additionally, as maturity increases, more or less intense optical anisotropy and mosaic texture may develop (Jacob, 1989). For this reason, some studies (Jacob, 1989; Landis and Castaño, 1994) use only the lowest reflectance distribution when assessing the relationship between vitrinite and bitumen reflectance values. Landis and Castaño (1994) distinguish among the three optical forms of hydrocarbon, illustrating how histograms can be convoluted if the distinction is not made among the types. Further, Landis and Castaño (1994) derive "errors" in previous reports of correlation (Jacob, 1989; Riediger, 1993) between BRo and Ro studies due to a lack of indigenous virtinite, mixing of locally derived and migrated solid hydrocarbon, mixing of morphological types, limited maturation range and use of suppressed vitrinite data.

Thermal maturity analysis by way of reflectance microscopy requires a sufficient number of measurements on organic macerals to provide reliable data (~50) (Schoenherr, 2007). In most cases, however, the Utica/Point Pleasant rock cuttings available for this task provided less than 30 macerals of sufficient size per sample.

7.4   CAI Data

Conodont Alteration Index (CAI) is a well-known technique used to evaluate the level of thermal maturation in source rocks. CAI is based on color changes seen in microscopic-sized fossil teeth from the remains of eel-shaped chordates. These fossils are highly resistant to weathering and metamorphic temperature regimes and contain trace amounts of organic matter. Their color alteration is both time- and temperature-dependent and is a progressive, irreversible condition, making them ideal for correlating to maximum temperatures (Tmax). The CAI can be determined by comparing samples against a set of conodont color standards. Using CAI thermal maturation indices, the oil and gas windows are in a gradational boundary. The onset of oil generation is placed between 1.0 and 1.5, and the limit of oil generation is between 2.0 and 2.5 (Harris, 1979). Dry gas is generally associated with CAI values in excess of 2.5.

The CAI data presented in Figure 7-30 is based upon a published report by Repetski and others (2008), as well as measurements for 10 additional wells collected as part of this Study (Table 7-19). These data illustrate an increased maturity basinward, similar to the isoreflectance maps of Figure 7-20 and 7-21.

Table 7-19. Conodont Alteration Index (CAI) measurements performed by the USGS for this Study.

API No.	County	Cuttings/Core No.	Sample Type	CAI Measurement
34041201090000	Delaware	1365	Cuttings	1.5
34041202530000	Delaware	1595	Cuttings	1 to 1+
34073232830000	Hocking	4005	Cuttings	1.5
34077200280000	Huron	1234	Cuttings	1+ to 1.5
34077200530000	Huron	1943	Cuttings	1.5
34089255430000	Licking	4144	Cuttings	1.5
34089260650000	Licking	5089	Cuttings	1+ to 1.5
34127271300000	Perry	4136	Cuttings	1.5
34145601410000	Scioto	3409	Core	1 to 1+
34163209240000	Vinton	4230	Core	1+ to 1.5
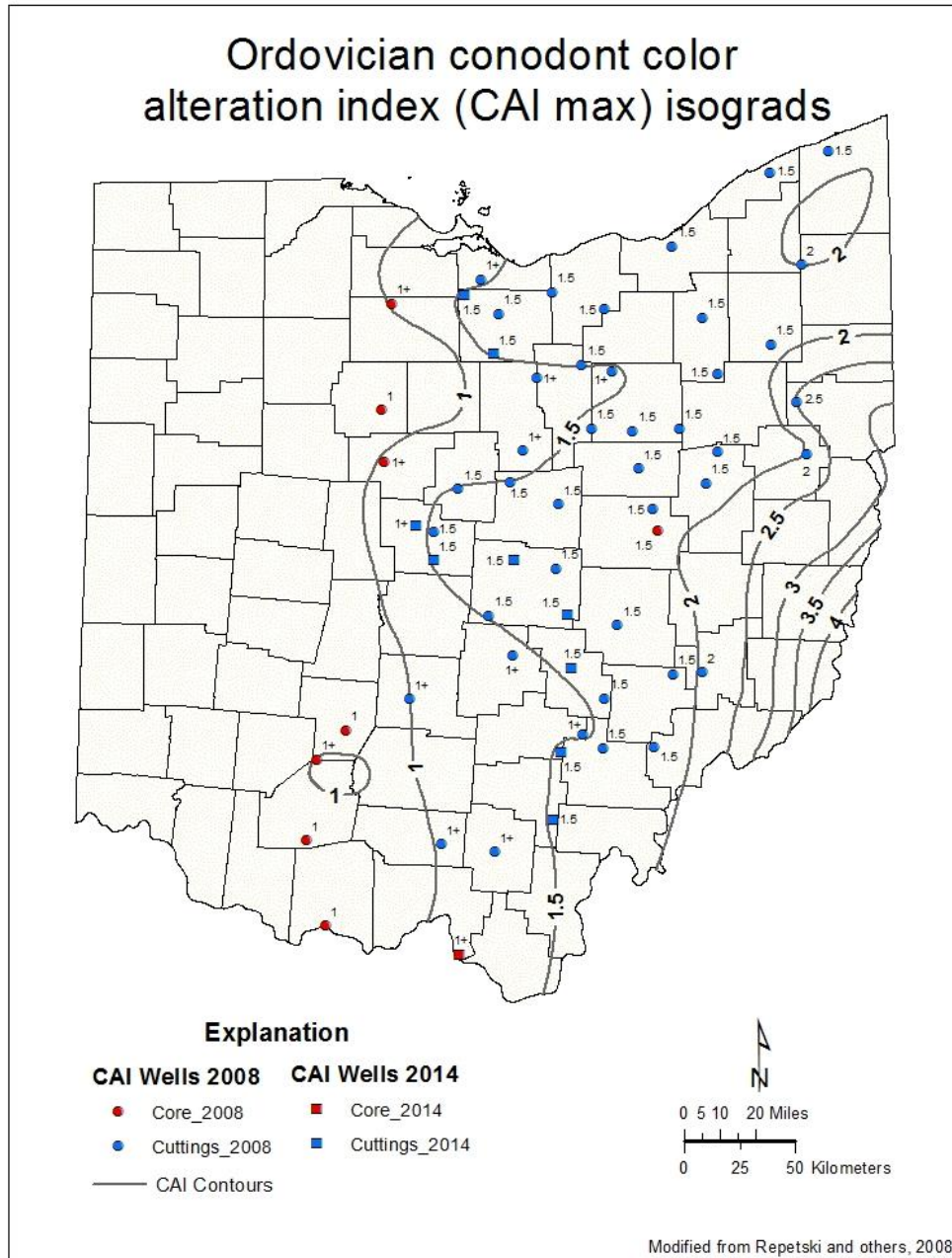
Figure 7-30. Map of CAI data for the Upper Ordovician shale in Ohio (modified from Repetski and others, 2008).

8.0 RESERVOIR POROSITY AND PERMEABILITY

The porosity and permeability data reported for the Study represent a compilation of both legacy and newly-generated data for Utica/Point Pleasant rock samples collected in the basin. The research team utilized scanning electron microscopy (SEM) and X-ray Computed Axial Tomography (CT X-ray) techniques to visualize and describe the pore space characteristics of

these reservoir rocks. We also have included laboratory-derived porosity and permeability data derived from other earlier research activities in the Study area (mainly Ohio samples).

8.1 Pore Imaging

Pore imaging work conducted as part of this Study included the application of SEM techniques (with both standard and ion-milled samples) to rock core and cuttings samples. PAGS was the team lead for pore imaging work conducted for this Study, and was assisted by research team members from Smith Stratigraphic LLC.

A certain amount of legacy SEM data (i.e., approximately 150 SEM photomicrographs from the Fred Barth No. 3 (API#3403122838) were provided by ODGS during the first year of the project. This suite of images represents three sample depths (5661, 5678 and 5684 ft) throughout the Point Pleasant Formation at various magnifications (from 140x to 100,000x). Several images show what appear to be significant organic matter pores in the samples (Figure 8-1). Others are backscatter images showing clays and calcite with bright spots that represent pyrite or other highly reflective heavy minerals (Figure 8-2). All legacy SEM images for the Barth well are available on the Consortium website.
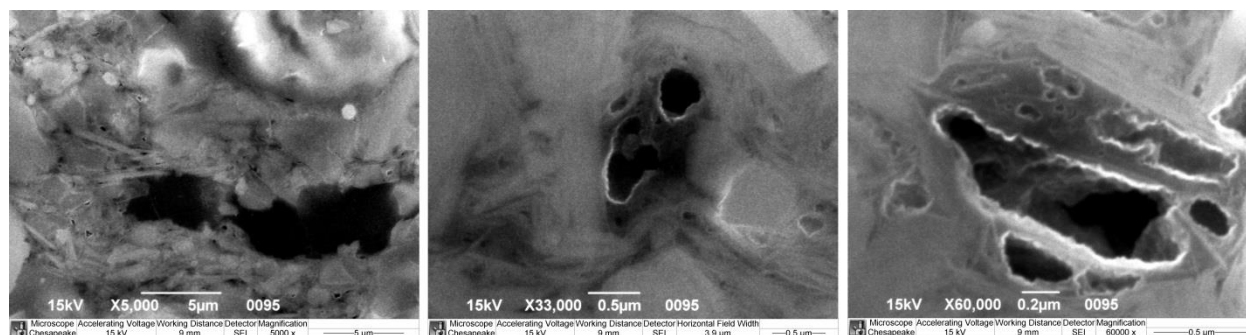
Figure 8-1. Selected SEM photomicrographs of organic matter and pores observed in the Point Pleasant Formation of the Fred Barth No. 3 well, Coshocton County, Ohio.
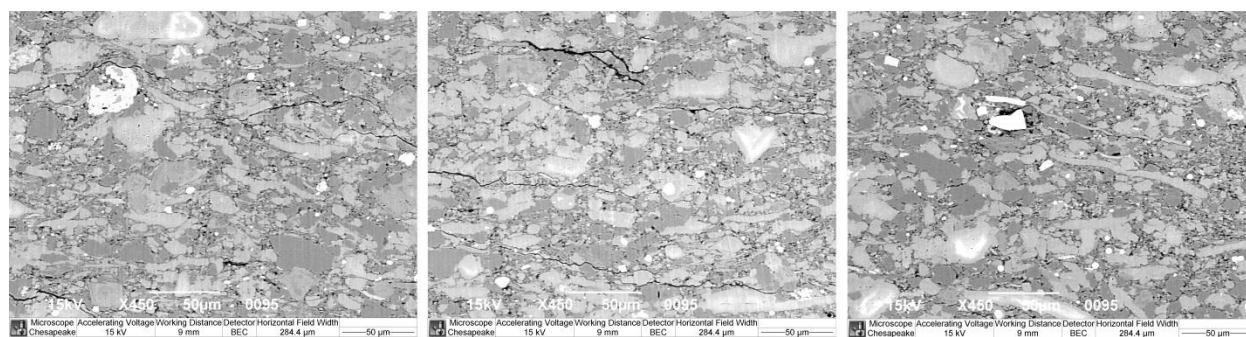
Figure 8-2. Selected backscatter SEM photomicrographs of the Point Pleasant Formation in the Fred Barth No. 3 well, Coshocton County, Ohio.

Standard SEM analyses of Utica/Point Pleasant rock samples were performed by John Barnes at the Middletown office of the PAGS. PAGS evaluated a total of 12 samples, consisting of well cuttings and outcrop samples from various Pennsylvania locations (Table 8-1).

Table 8-1. Pennsylvania samples analyzed using standard SEM techniques.

API No.	County	Location/Well Name	Sample Depths (ft)	Formation/Member	No. of Samples	Figure No.
NA	Mifflin	Utica Shale in outcrop	NA	Utica	3	8-3A
3701990063	Butler	Hockenberry No. 1	8504-8795	Kope Utica	4	8-3B
3706720001	Juniata	Shade Mt. No. 1	3720-3810	Point Pleasant Lexington/Trenton	4	8-3C
3710320003	Pike	Commonwealth of PA Tr. 163 No. C-1	13,440-13,450	Point Pleasant	1	8-3D

NA – not applicable

Figure 8-3 includes selected photomicrographs for each of the samples listed in Table 8-1, and Appendix 8-A includes the entire suite of photomicrographs for samples analyzed for this work. The scale of these images is on the order of tens of μm, and they illustrate the tight nature of the shale matrix in these samples. At this scale, mineral grains are clearly visible, but true pore space (whether phyllosilicate framework, dissolution or organic matter pores) cannot be resolved. In the case of the Utica outcrop samples (Figure 8-3), pyrite grains plucked from some samples (due to either handling during sample collection or weathering at the outcrop) have left polygonal-shaped voids (pop-out holes).

Figure 8-3. Photomicrographs of selected specimens analyzed by PAGS using standard SEM techniques. A - S12-061-003, Utica Shale outcrop, Reedsville exit ramp, Mifflin County, Pennsylvania; B - S13-013-001, top Utica Shale (8504-8513 ft), Hockenberry No. 1 (API#3701990063), Butler County, Pennsylvania; C - S13-014-003, Point Pleasant Formation (3750-3760 ft), Shade Mt. No. 1 (API#3706720001), Juniata County, Pennsylvania; D - S13-015-001, Point Pleasant Formation (13,440-13,450 ft), PA Tr. 163 No. C-1 (API#3710320003), Pike County, Pennsylvania.

PAGS also prepared rock cuttings samples from seven Pennsylvania well locations for preparation by ion milling techniques prior to SEM imaging. These particular samples, along with a continuous core sample from New York, were milled and examined by Juergen Schieber of Indiana University (Table 8-2).

Table 8-2. Samples analyzed using ion milling and SEM techniques.

API No.	County/State	Location/Well Name	Sample Depth (ft)	Formation/Member	Figure No.
3700920034	Bedford/PA	Schellsburg Unit No. 1	7690	Lexington/Trenton	8-4A
3703520276	Clinton/PA	Commonwealth of PA Tr. 285 No. 1	14,480	Lexington/Trenton	8-4B
3704920049	Erie/PA	PA Dept. of Forests & Waters Block 2 No. 1	4096	Lexington/Trenton	8-4C
3706720001	Juniata/PA	Shade Mt. No. 1	3750	Point Pleasant	8-4D
3708720002	Mifflin/PA	Commonwealth of PA Tr. 377 No. 1	5230	Lexington/Trenton	8-4E
3710320003	Pike/PA	Commonwealth of PA Tr. 163 No. C-1	13,580	Lexington/Trenton	8-4F
3712522278	Washington/PA	Starvaggi No. 1	10,040	Kope	8-4G
NA	Herkimer/NY	74NY5 Mineral Core	170 - 730	Point Pleasant Logana	8-5

NA – not applicable

Figures 8-4 and 8-5 include selected photomicrographs for these samples and illustrate various pore types and sizes. Pore types include phyllosilicate framework pores (due to presence of clay mineral platelets in various orientations or state of compaction), dissolution pores (from the dissolution of carbonate minerals) and organic matter pores (resulting from out-migration of hydrocarbons). Pores vary in size, and from location to location, but generally range from tens or hundreds of nm to as much as 1 μm or more. As SEM imaging has shown that matrix porosity is minor to non-existent in these rocks, it is the organic matter pores that are the major contributor to hydrocarbon production in the Utica/Point Pleasant play.
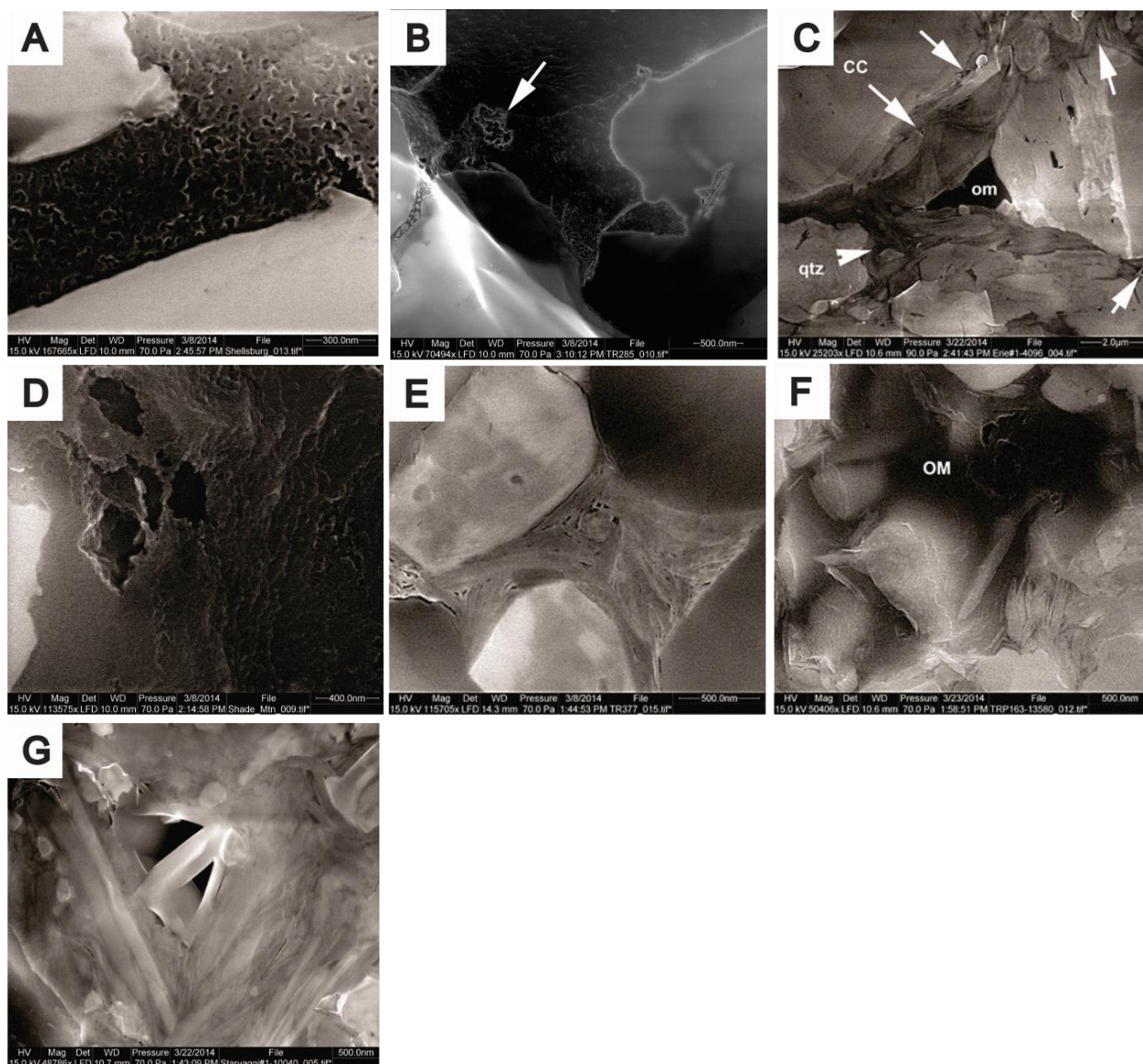
Figure 8-4. Photomicrographs of selected Pennsylvania specimens, analyzed by Juergen Schieber using ion milling and SEM imaging techniques. OM=organic matter, qtz=quartz, CC=calcite. A – Schellsburg Unit No. 1 (API#3700920034), Bedford County; B - Commonwealth of PA Tr. 285 No. 1 (API#3703520276), Clinton County: arrow points to minor pore development; C - PA Dept. of Forests & Waters Block 2 No. 1 (API#3704920049), Erie County: arrows point to triangular-shaped phyllosilicate framework pores; D - Shade Mt. No. 1 (API#3706720001), Juniata County; E - Commonwealth of PA Tr. 377 No. 1 (API#3708720002), Mifflin County; F - Commonwealth of PA Tr. 163 No. C-1 (API#3710320003), Pike County; G - Starvaggi No. 1 (API#3712522278), Washington County.

145
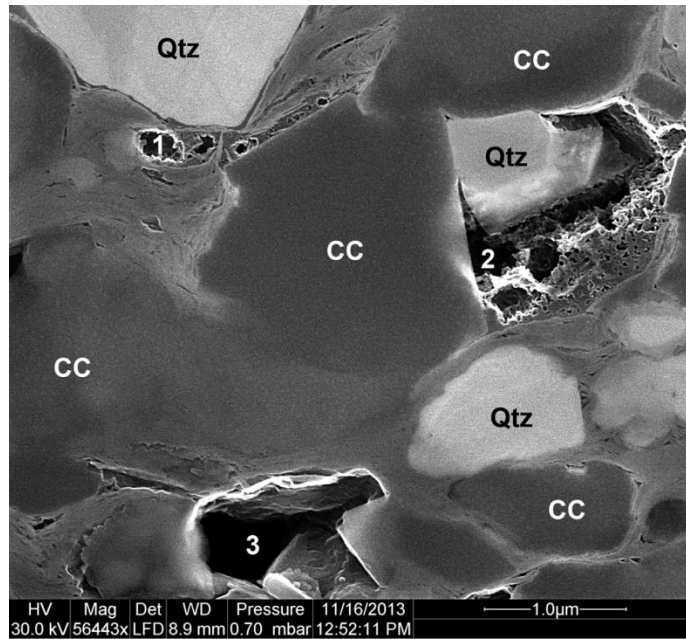
Figure 8-5. Photomicrograph of specimen from a depth of 566 ft in 74NY5 Mineral Core, Herkimer County, New York, analyzed by Juergen Schieber using ion milling and SEM imaging techniques. Qtz=quartz, CC=calcite. Area 1 shows development of large bubble pores in organic matter; Area 2 shows development of bubble pores into deep, connected channels/tubes; Area 3 shows a completely open framework pore defined by calcite grains. One could envision progressive development of organic matter pores from foam to bubbles to tubes in the organic matter, and finally completely emptying of framework pore spaces due to out-migration of liquid hydrocarbons.

Appendix 8-B provides Juergen Schieber's summary reports for each sample imaged, as well as all images captured during his analyses. The reports provide information on sample mineralogy, detailed descriptions of pore types, sizes and distribution, as well as his observations regarding porosity development and potential for hydrocarbon exploitation.

8.2   CT X-ray Analysis

Rock cores from two different regions of the Study area were made available for examination and analysis by X-ray Computed Axial Tomography (CT X-ray). WVGES provided access to three surficial rock cores, collected as geotechnical samples from the Lost River dam site in the eastern panhandle of West Virginia (Hardy County) (Figure 8-6). These cores, cut in 1977, are 2.5-in round (unslabbed) and comprise the Martinsburg Formation, a shale and limestone that are partially equivalent to the Kope Formation and Utica Shale (see Figure 2-1). In addition, ODGS provided core from the Fred Barth No. 3 (API#3403122838), drilled in Coshocton County, Ohio, in 1976. This core comprises the more typical open marine, organic-rich, calcareous black shale associated with the Point Pleasant Formation (Figure 8-6). As one of the few publicly available Utica/Point Pleasant cores in Ohio, the Barth also has been heavily sampled, plugged and cut.

The Lost River cores were used to demonstrate proof-of-concept for the CT X-ray analyses performed by U.S. DOE NETL. As part of this work, the lithology and core features were described by DOE geoscience interns following protocols developed by the predecessor of the U.S. DOE for the Eastern Gas Shales Project (EGSP) in the late 1970s. The cores were then scanned through a Multi Sensor Core Logger (MSCL) for magnetic susceptibility, p-wave

velocity, natural GR, and elemental composition by X-ray Fluorescence (XRF). Selected intervals were then analyzed by CT X-ray analysis. Following this proof-of-concept effort, the Fred Barth No. 3 core was also evaluated.
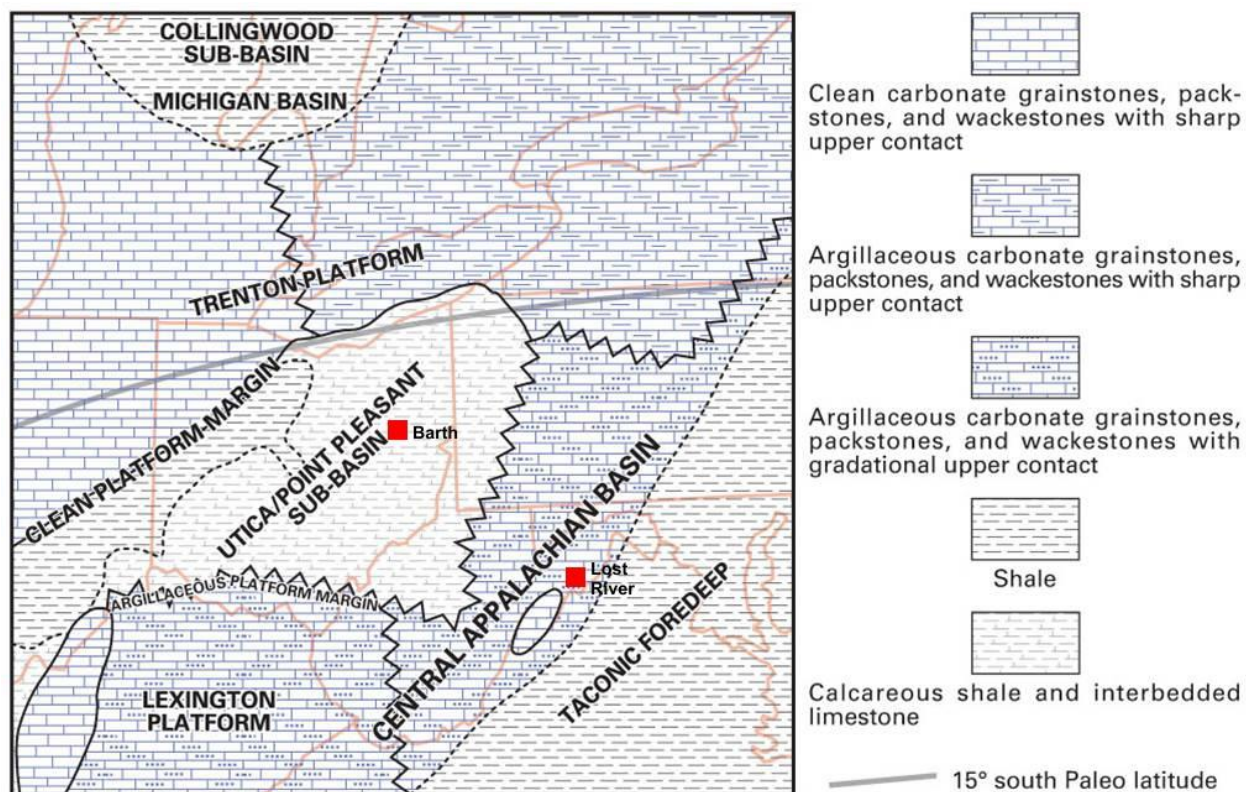
Figure 8-6. Map of the Study area showing generalized locations of the Barth and Lost River cores, superimposed on a facies map of Trenton/Point Pleasant time from the Trenton-Black River study (modified after Wickstrom and others, 2012).

8.2.1 Overview

X-ray Computed Axial Tomography, commonly known as a CT scan or "CAT" scan, produces images by measuring the contrast in transmission as X-rays pass through areas of different density within a sample. The "computed" part of the process is a software-based, three-dimensional digital reconstruction of the scanned object from numerous two-dimensional radiographs collected at multiple angles around an object (Rodriguez and others, 2014).

The first application of this technology in the 1970s was for medical use to non-invasively visualize the inside of the human body. The petroleum industry quickly recognized the applications of CT scanning for characterizing the internal structure of rock cores, and readily adopted it, along with the similar technology of Magnetic Resonance Imaging (MRI).

The configuration of the machines can vary widely, but in general, a CT scanner will have an X-ray source located opposite an X-ray detector. The sample to be imaged is placed between the two, and axial images are generated by rotating either the X-ray components or the sample, typically through a full 360° rotation.

The density, thickness and material composition of the sample determine what percentage of X-rays pass through to the detector. The linear attenuation coefficient μ at each point in the two-dimensional radiograph is measured by the CT detector. The μ is defined by Beer's law (Karacan, 2003),

$$\frac{I}{I_o} = exp(-\mu h)$$

where *Io* is the incident X-ray intensity and *I* is the intensity remaining after the X-ray passes through a thickness, h, of the sample. At X-ray energy levels below 200 kilovolts (kV), attenuation of X-rays is known to be primarily dependent on photoelectric adsorption, which is a function of the material density and the atomic number of the material, and Compton scattering, which is a function of electron density (Karacan, 2003). In general, however, high-density, thick and higher atomic number materials block a greater portion of the X-rays than lower-density, thinner or lower atomic number materials (Rodriguez, and others, 2014).

The spatial variation in μ is detected at each angle and results in a single two-dimensional radiograph of the sample. Data from radiographs are reconstructed using machine- and manufacturer-specific algorithms into a three-dimensional volume where each volume-pixel (voxel) of data is represented by a 16-bit grayscale value. Voxel dimensions are a function of the scan geometry, i.e., the distance between the X-ray source, the detector, and the object being scanned. The grayscale values are a function of the μ value, referred to as the CT Number (CTN). CTN values are often displayed with a grayscale color coding scheme such that low CTN are dark and high CTN are bright. Generally speaking, low-density materials are dark, and high-density materials are bright. It is important to keep this in mind if X-ray images are compared with SEM photomicrographs or other images. The X-ray is essentially a "negative" image, with dense materials such as pyrite appearing white, and low density areas such as fractures appearing black. Post-processing of the CTN values can result in a wide range of color schemes applied to reconstructed CT scans. An example of a reconstruction is shown in Figure 8-7.
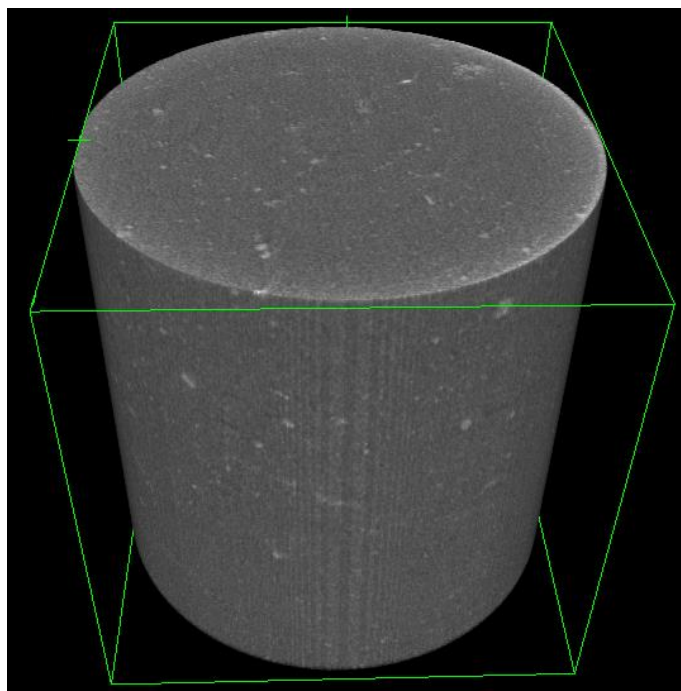
Figure 8-7. A 3-D image reconstruction of a Marcellus Shale core from the NETL CT scanner (Rodriguez and others, 2014).

8.2.2 Instrument Resolution

CT scanners have different image resolutions depending on their design. When applying these instruments to fine-grained rocks such as shale, it is important to recognize the limitations of the technology. In general, the maximum image resolution of a particular instrument and the maximum sample size are inversely proportional. For example, a scanner that can show features as small as a few microns will typically only be able to handle a sample the size of a pencil eraser. Scanners that can visualize an entire human body may only be able to show features as fine as a few mm. CT scanners in use at NETL include three types – medical, industrial and ultra-high resolution (micro- and/or nano-CT) – and are described in turn below.

Medical scanners are designed so that the X-ray source and detector rotate around the subject, such as a human body. Many modern medical CT scanners use fan beams of X-rays and multiple banks of detectors to capture multiple radiograph slices quickly, thus reducing the time of the scan and the amount of radiation to which a patient may be subjected. The "medical" scanner in use at NETL actually employs a higher-power X-ray source compared to standard units found in hospitals. This achieves greater penetration of rock samples, some of which are confined in pressure vessels or have fluid moving through the pore space. That said, it is not safe for scanning human body parts.

The NETL medical scanner, similar to the unit shown in Figure 8-8, was used for whole-core analysis of the Lost River and Barth cores. The geometry of the scanner and the rapid scanning process produced images with a resolution of a few tenths of a millimeter. Despite the relatively low resolution, it was ideal for scanning bulk core samples and identifying features for study on the higher resolution CT scanning units available at NETL. An example of a medical CT scan on

149

a 3-ft segment of Martinsburg Formation from the Lost River core is shown as a two-dimensional image in Figure 8-9.

Figure 8-8. A 16-slice Aquillion medical CT scanner, similar to the unit in use at NETL.
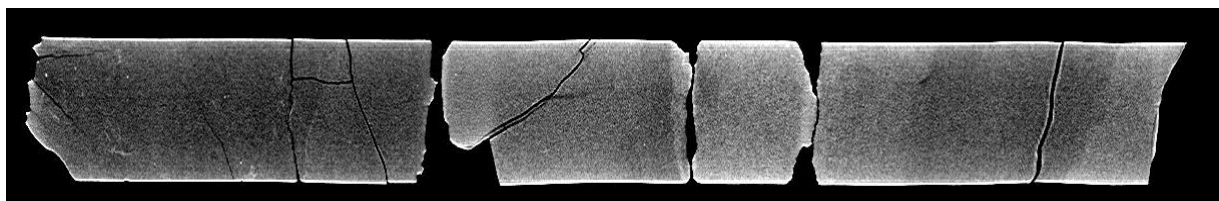
Figure 8-9. CT scan of a 2-D slice through the center of a 3-ft long segment of the Martinsburg Formation from the Lost River core. Darker (less dense) bands generally correlate with regions of higher organic matter content; lighter zones represent denser carbonate. Fine, dark traces delineate fractures.

The industrial CT scanner was designed primarily for quality control of manufactured parts. Larger systems, for quality control on fully assembled vehicles for instance, have fully independent articulating arms that enable the CT source and detector to move around the sample. Within the geosciences, smaller systems are typically used that employ a rotating sample stage with a fixed X-ray source and detector placed on either side of the subject. The NETL unit uses a stage that rotates about a vertical axis, and the distance between the source and detector can be adjusted. The ability to scan geologic samples using high powered X-rays results in higher resolution scans than medical CT scanners can provide. This is especially effective if the X-ray source is brought in close to the object, and the detector is relatively far away. However, the scans typically take much longer than medical units, sometimes requiring overnight to build up an image.

Two photographs of the NorthStar Imaging M-5000 industrial CT scanner at NETL are shown in Figure 8-10, with the detector on the left and the X-ray source on the right. In both images, the same four-inch diameter sandstone core is shown on the rotating sample stage. An example of the scan quality from this type of scanner is provided in Figure 8-11.
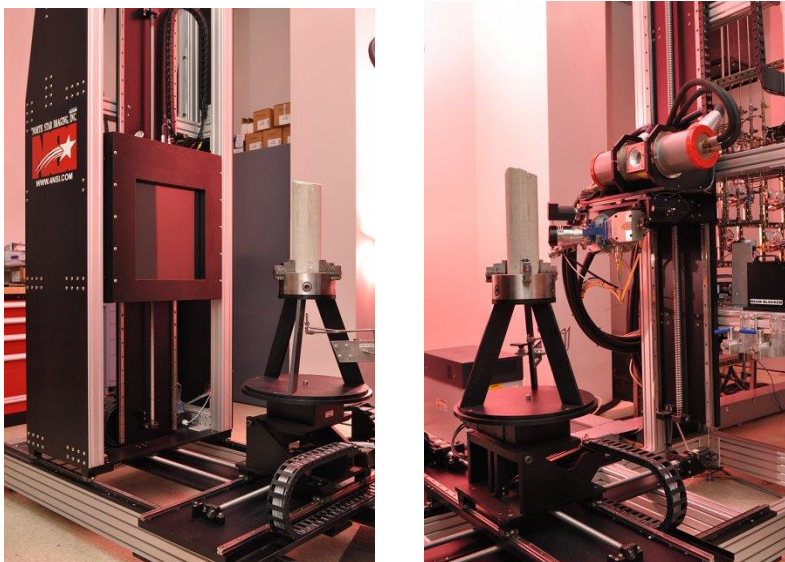
Figure 8-10.   NorthStar Imaging M-5000 industrial CT scanner at NETL. Left: X-ray detector with vertical sandstone core. Right: X-ray source with vertical sandstone core.
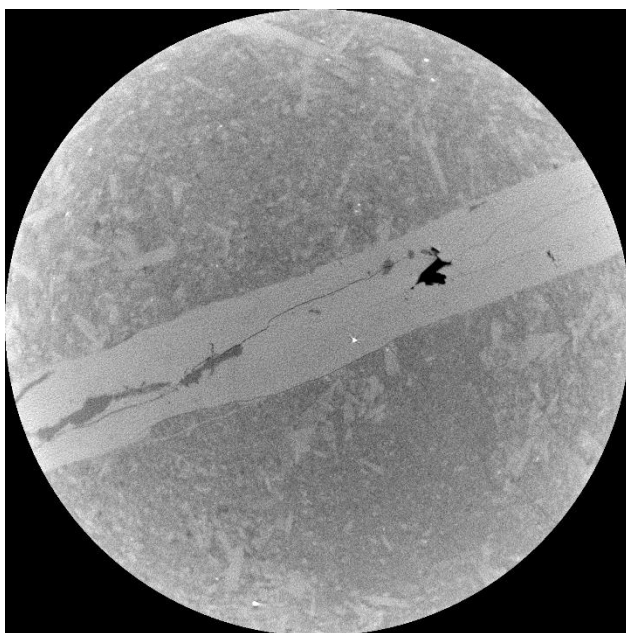
Figure 8-11. Scanned image of single layer of data along an XY plane through a one-in diameter sample of Marcellus Shale containing a mineralized fracture. Data obtained from the NETL industrial scanner.

Ultra-high resolution micro-CT and nano-CT scanners are high-precision instruments that enable samples to be scanned extremely close to the X-ray source for unprecedented detail in the resulting images. These systems are generally constructed inside of enclosures to enable their use in laboratories without the need for additional radiation shielding. The micro-CT at NETL utilizes samples a few mm in diameter (roughly the diameter of a pencil). Nano-CT scanners, available at several of the universities associated with NETL, use samples that are approximately the size of a sand grain. Scanning takes many hours, and for the largest samples capable of being analyzed, the scanning effort may literally require days. Tiny samples coupled with high-resolution scanning

151

can result in reconstructed images with a voxel volume of less than 1 cubic μm. Attempting to translate these small volumes back to the scale of a geologic reservoir can be challenging.

Figure 8-12. The micro-CT scanner at NETL. Source is on the left, rotating stage is the pedestal in the center, and detector is on the right.
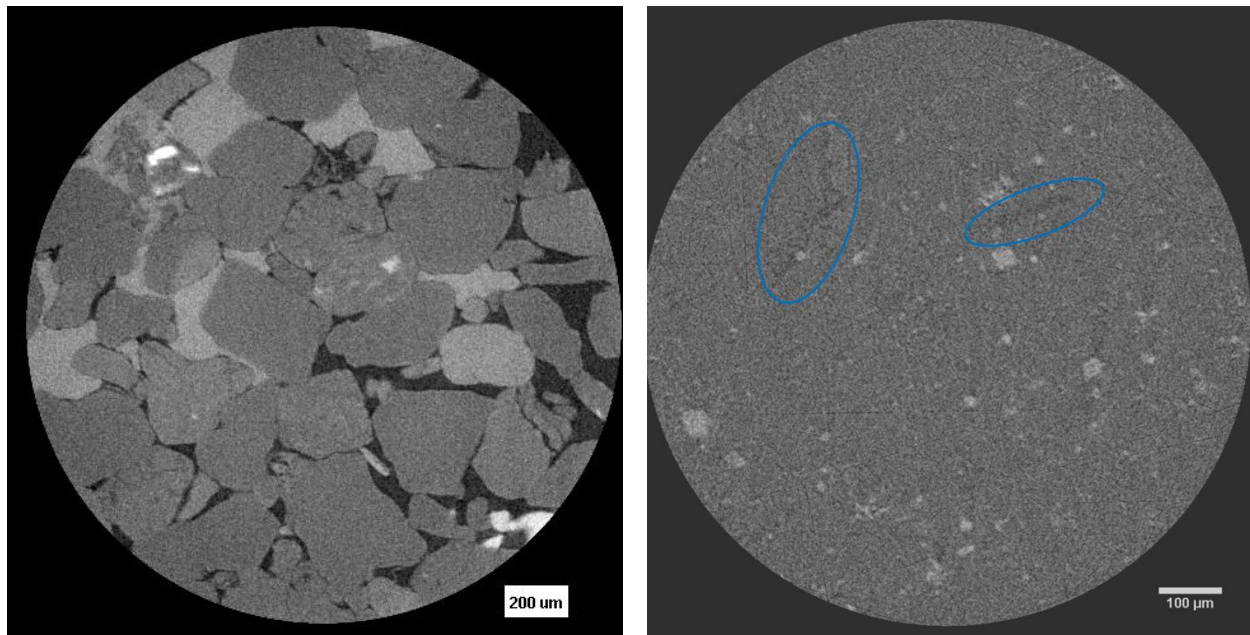
Figure 8-13. Micro-CT images of core samples. Left: 6-mm diameter sample of calcite-cemented sandstone. Right: 4-mm diameter sample of Marcellus Shale. The blue ellipses outline organic matter.

8.2.3 Results

8.2.3.1 Lost River Core

Proof-of-concept analysis of the Lost River cores began with macroscopic characterization and petrophysical logging followed by X-ray CT analysis. Core lithology logging techniques

developed by the U.S. DOE and Cliffs Minerals for the EGSP were adapted for use on these samples. Descriptions included rock type, color, bedding, fractures, and notable geologic features (Figure 8-14).

Figure 8-14. Photograph of a box of Lost River core. Note color variations (light gray to gray) that suggest relatively high carbonate and low organic content in this sampling of the Martinsburg Formation. (Image: U.S. DOE).

Core measurements were made using a Geotek© MSCL on intact segments of Lost River core samples (Figure 8-15). Measured parameters included magnetic susceptibility, acoustic impendence via P-wave velocity measurements, gamma density using a Cesium-137 source, and elemental composition via XRF spectrometry (Figure 8-16).

Figure 8-15. The GeoTek Multi-Sensor Core Logger (MSCL) scanning Lost River core at NETL. Photograph by Karl Jarvis.
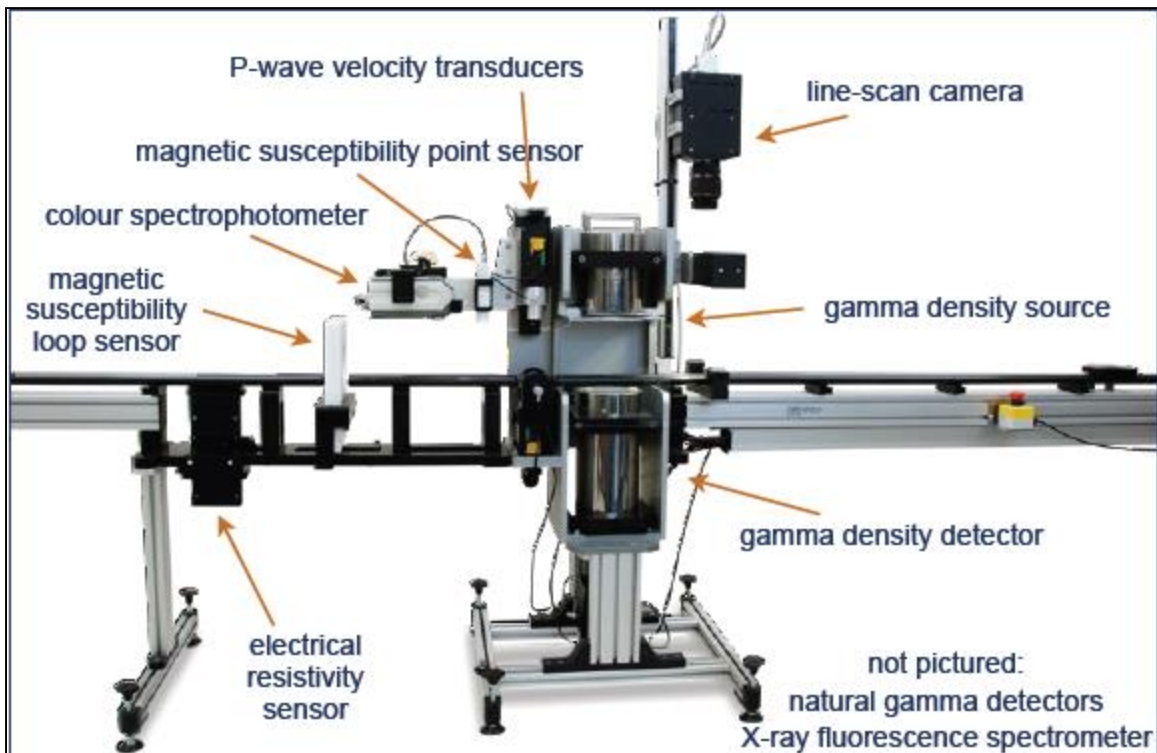
Figure 8-16. Components of the Geotek MSCL (Geotek Ltd., *Geotek Multi-Sensor Core Logger Flyer*. **Daventry, UK, 2009)**

The Lost River core data were assembled into spreadsheets for side-by-side comparison using a software program called Strater™. This software allows multiple data streams to be combined into one easy-to-read log for each core. It uses a standard input file format that includes the proper headers, empty lines for missing data sections, and different tabs for different data sets. Core analytical results and data files were imported into a Strater™ template (Figure 8-17), and compiled to create the log files included in Appendix 8-C.
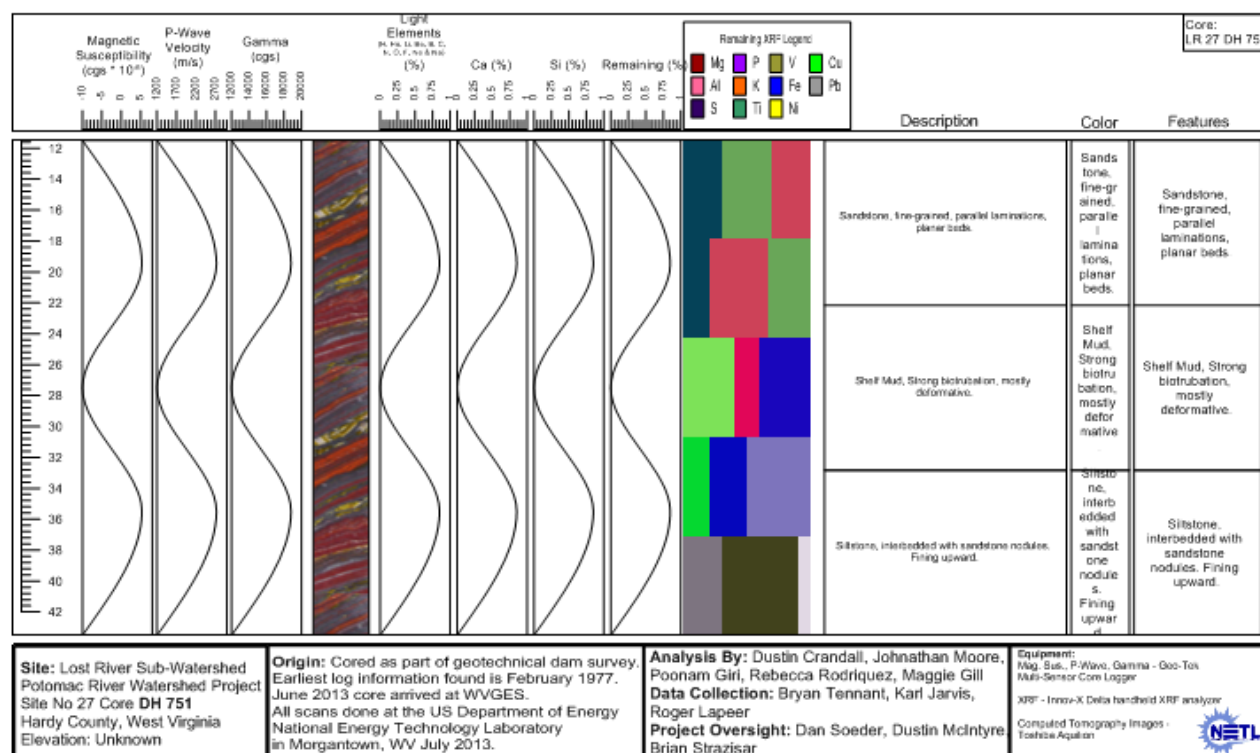
Figure 8-17. An example of the template from the Strater™ software used to display core data.

Once the macroscopic and petrophysical testing of these core samples was complete, the Lost River samples were subjected to X-ray CT analysis. Three-dimensional reconstructions from X-ray CT imaging can be evaluated quantitatively to determine surface areas, pore volume/porosity, mineral volumes, pore size distribution, relative permeability, or variations in any of these properties. Such calculations are often performed with the aid of image analysis software (such as the open-source program *ImageJ* or *Avizo Fire*). Since the pixel values in these images represent relative density or composition, thresholding (i.e., selecting specific pixel values), along with cluster analysis, can isolate a desired volume from the rest of the rock volume. This can then be used to determine bulk composition, porosity, or changes in either. A 3-D reconstruction of an industrial X-ray CT scan of the Martinsburg Formation from the Lost River core is provided in Figure 8-18, where minerals and voids have been isolated. More extensive analysis can yield connected porosity, disconnected porosity, pore size distribution, permeability and relative permeability.

The Martinsburg Formation, a generally fine-grained, micritic limestone with shell beds and interbedded, organic-rich argillaceous units, was characterized in detail using the lithologic description procedures, MSCL, and CT-scanning technologies available at NETL. The methodology has applications across the Utica and in other shale formations.

155
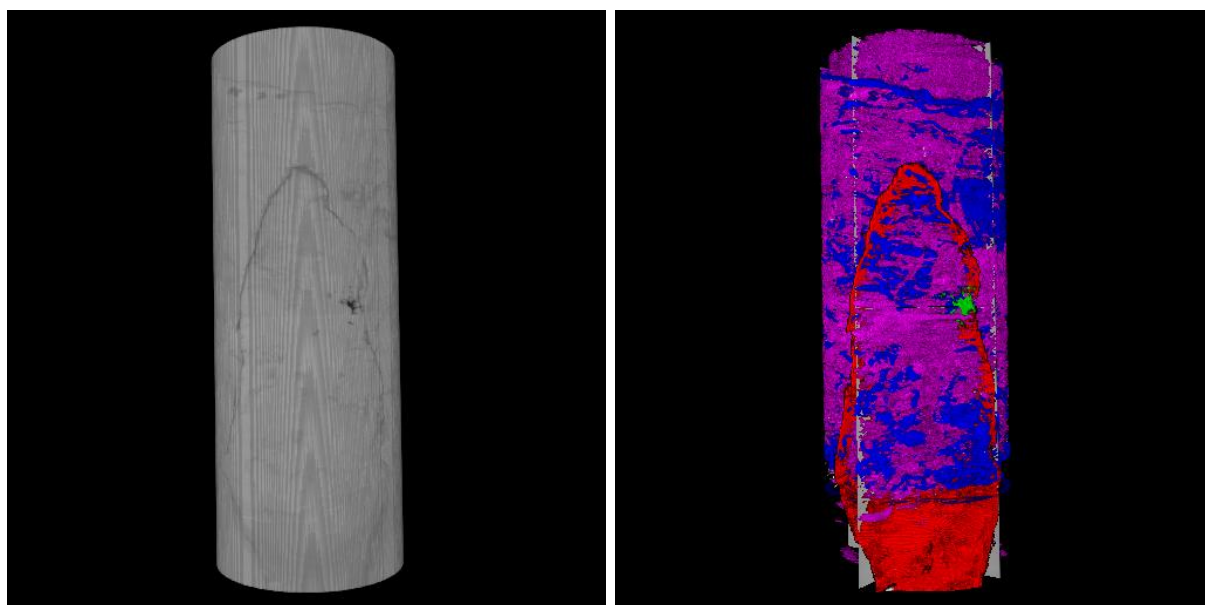
Figure 8-18. Images of Martinsburg Formation core scanned in industrial X-ray CT. Left: 3D view of original reconstruction. Right: Core segmented by density and clustering. Red: fracture volume. Blue: organic matter. Pink: carbonate. Green: porosity. (Image: U.S. DOE).

8.2.3.2 *Fred Barth No. 3*

Five sections of relatively intact Fred Barth No. 3 core samples were scanned with the NETL industrial CT-Scanner, and data for each sample are in the form of a .tiff stack. The images were delineated via best-edge approximation and un-tilting of the core sample. An example of the horizontal slices imaged through a core is provided below as a montage (Figure 8-19). X & Y planar slices lengthwise down the core also were created for each data set to represent the true variability in the core samples. One of these lengthwise images is shown next to the montage. All of the Fred Barth No. 3 scans are included in Appendix 8-D.

The MSCL was not employed on the Fred Barth No. 3 core because of the extensive plugging, slabbing and sample removal from the Point Pleasant interval (see Figure 8-20 below). The MSCL requires whole core samples to produce accurate data, and these were simply not available in this core. Lithologic descriptions had already been prepared for this core, as had porosity and permeability measurements, RockEval, porosimetry, petrography and a host of other analyses as described below. It seemed redundant to repeat these measurements, especially on core that had been so thoroughly cut, plugged and aged.

The CT scans indicate that the Barth core, while still calcareous, is much more argillaceous and clastic in origin than the Martinsburg Formation from the Lost River core. The organic matter content is considerably higher, and the core contains fewer natural fractures than the Lost River samples. The Utica/Point Pleasant Formation in the Fred Barth No. 3 core displays many of the characteristics that producers seek when developing this shale for natural gas and NGLs.
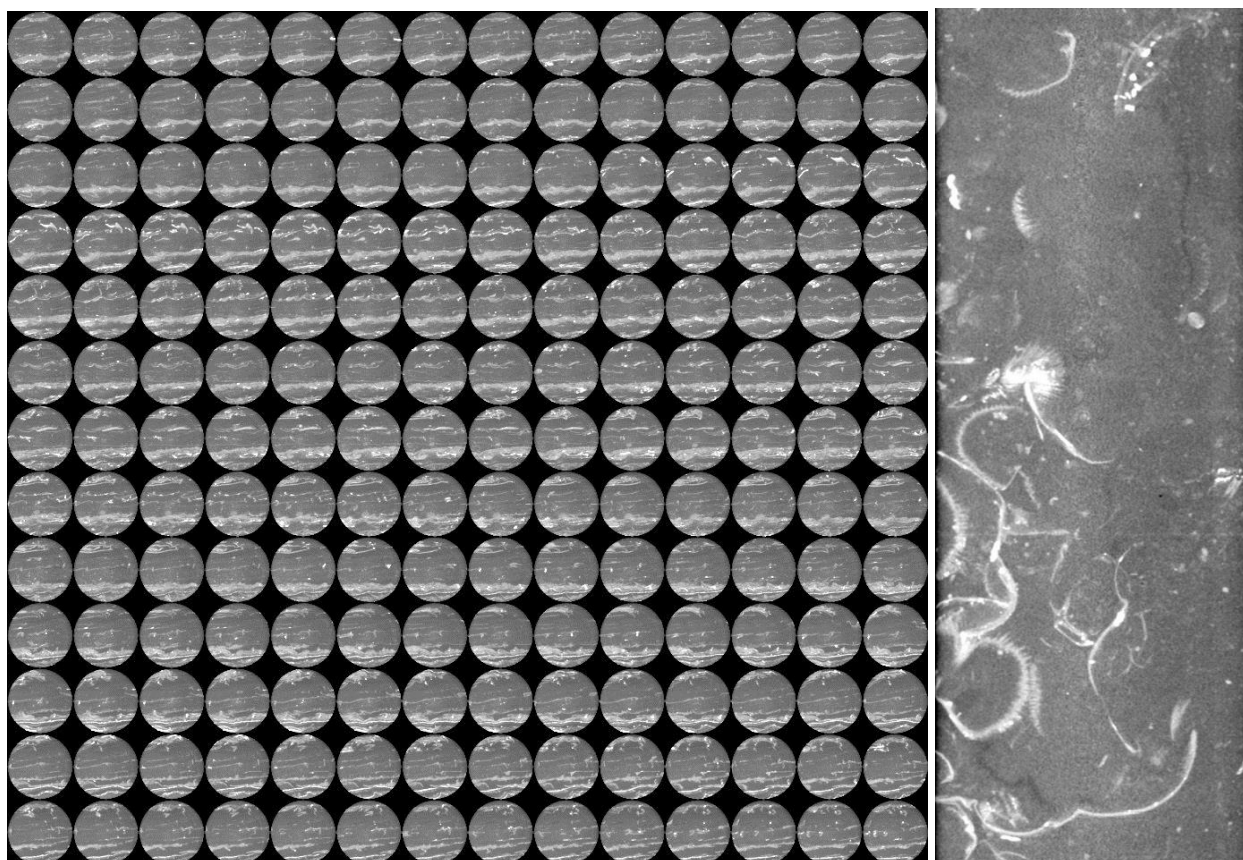
Figure 8-19. Images of Utica/Point Pleasant interval at 5672 ft (Fred Barth No. 3). Left: horizontal sample subcored along bedding planes (1700 slices at a resolution of 42 µm). Montage of 182 slices through core on Z axis; Right: middle Y-axis slice along length of core plug showing abundant shells.

8.3   Porosity and Permeability Measurements

Porosity and permeability analyses were not performed on either the Barth or Lost River samples as part of the current Study because both were too old to provide reliable core analytical results. In addition, the removal of numerous samples and plugs from the Barth core left little material behind for fresh samples. Core analysis experiments on Devonian shale cores from EGSP, which were collected around the same time as the Lost River and Barth cores, demonstrated that old shale cores contain abundant microfractures and produce permeabilities that are not representative of in-situ conditions. Nevertheless, a considerable amount of legacy core analysis data does exist on the Barth core, which can be used to provide insights into the rock's petrophysical properties.

8.3.1 Results

8.3.1.1   Fred Barth No. 3

Fairly soon after the Barth core was cut, a standard suite of core analyses were performed in 1976 by Oilfield Research, Inc., along with physical and chemical testing that same year by Halliburton. In 2009, as the Utica Shale play was gaining interest in Ohio, multiple studies on the Barth core were commissioned by members of industry. This wealth of data includes RockEval, thermal maturity, TOC via pyrolysis, crushed core pulse permeability testing, rock mechanics,

mercury porosimetry, XRD, XRF, thin section examination, and even some exotic analyses such as Rare Earth Elements, palynology, trace metals, and others. The report containing these data is identified by ODGS as Core Record #3003 (Appendix 8-E).

Figure 8-20. Photograph of the Point Pleasant interval in the Fred Barth No. 3 (API#3403122838), 5660-5670 ft. Note the significant number of plugged and slabbed segments.

The results from the 1976-era testing on the Barth core may be considered the most valid, especially for state variables like water saturation, oil content and permeability, all of which would be expected to change as the core aged, dried and oxidized. The measured gas porosity range of Barth samples was approximately 2 to 8%, with most samples around 4 to 5%. The average

porosity across the entire interval tested was 5.6%. The measurement limit for dry gas permeability back in 1976 was 0.1 millidarcy (md). Most of the Barth samples were below this limit, and therefore were reported as "non-detects" (<0.10 md). "Non-detect" also was given as the average permeability value across all core intervals sampled. A few intervals reported permeabilities as high as 0.2 to 0.25 md; however, given that typical shale permeabilities are in the sub-microdarcy to nanodarcy range (Soeder, 1988), especially when liquid phases are present, hairline or micro-cracks in the core plug may have been the cause for these unusually high results. Oil saturations measured in the Barth core in 1976 varied from about 20 to 60% of pore volume, which is a fairly wide range. The average oil saturation across the core interval tested was 40.6%. Water saturations in this core had a narrower range than oil, typically between 30 and 50%. The average water saturation across the core interval tested was 35.2%.

8.3.1.2   Legacy Data

In addition to legacy data on the Barth core, comparable petrophysical data were available from ODGS for other Utica wells in Ohio. Porosity and permeability data found in the ODGS archives are summarized in Table 8-3.

Table 8-3. Legacy porosity and permeability data for selected Ohio wells.

API No.	Well Identification	No. Samples	He φ (%)	Hg φ (%)	Hg k (md)
34101201960000	Prudential 1A	7		0.03-1.31	1.0E-7 to 1.0E-6
34157253340000	OGS CO2-1	2		0.64-1.25	1.2E-6 to 5.1E-6
34139206780000	Copper Shelby	3		0.85-3.34	2.3E-6 to 1.93E-3
34133208670000	K Vasbinder	4		0.11-0.89	1.0E-7 to 2.9E-6
34151254750000	PSR1	3		0.29-1.01	4.0E-7 to 3.1E-6
34167286660000	Strass 1	2		0.37-0.55	1.0E-7 to 6.0E-7
34169248500000	Davis View 1	2		0.26-1.08	3.0E-7 to 3.5E-6
34005241600000	Eichelberger	25	2.2-8.2	0.03-1.31	1.0E-7 to 1.0E-6

Porosity – φ, measured in percent (%) using He (helium pycnometry) or Hg (mercury injection) techniques
Permeability – k, measured in md

9.0   UTICA PLAY RESOURCE ASSESSMENT

The Utica Play resource assessment was conducted to estimate: (1) remaining recoverable hydrocarbon resources and (2) original hydrocarbon resources in-place. Remaining technically recoverable resources were determined using a probabilistic approach following an outline developed by the USGS. Original hydrocarbon-in-place resources were determined using a volumetric approach. Both approaches evaluate roughly the same play area (Figure 9-1).
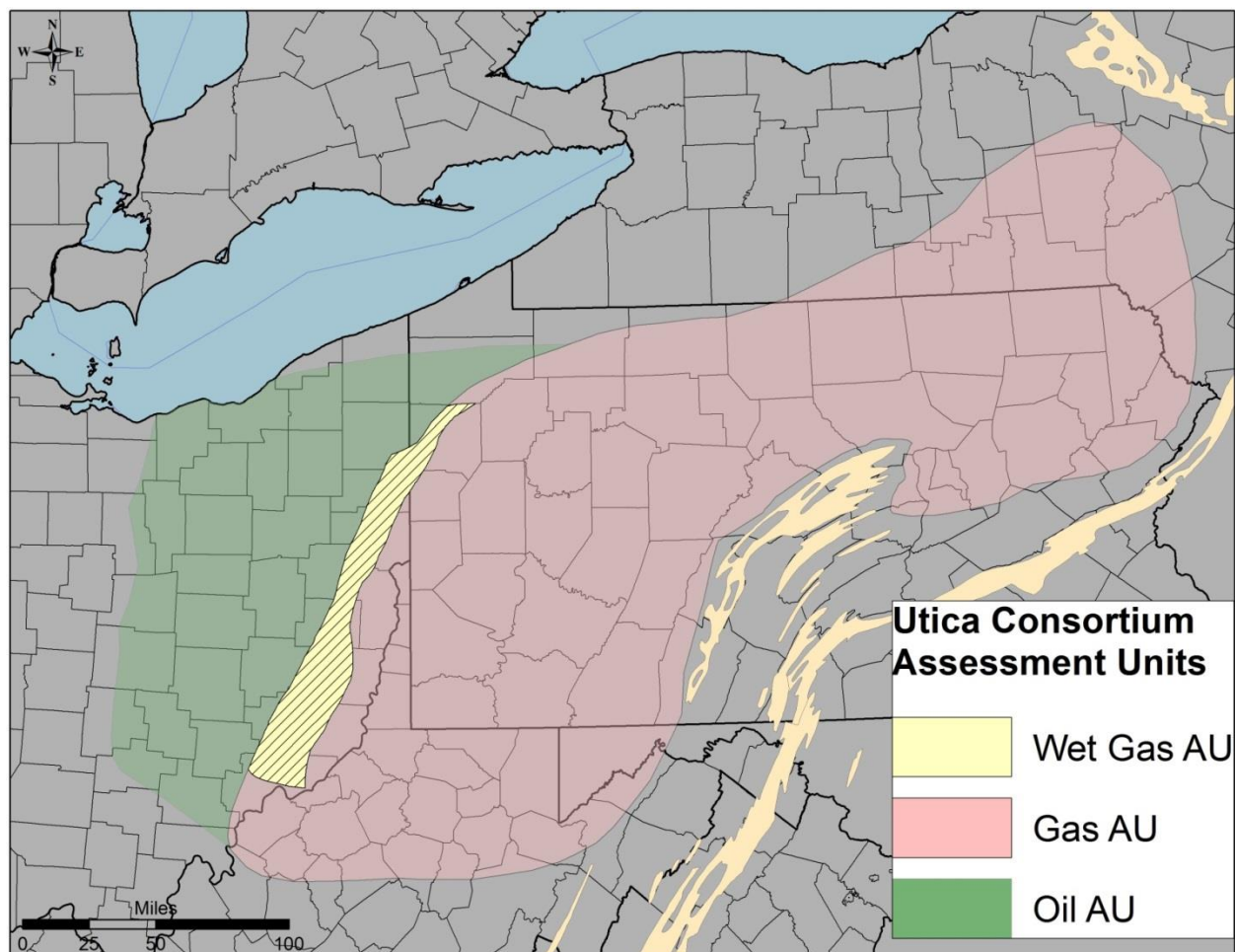
Figure 9-1. Play area used for both resource assessments performed as part of this Study. The green area highlights the oil assessment unit; the red area highlights the gas assessment unit.

9.1   Remaining Recoverable Resources

The first portion of the resource assessment task followed the probabilistic approach developed by the USGS and used in a 2012 assessment of undiscovered oil and gas resources of the Utica Shale (Kirschbaum and others, 2012). With this approach, the geologist defines the geographic limits of an Assessment Unit (AU), which is an area with expected oil or gas resources with generally the same or similar thermal maturity, organic content, lithology, source rock and trapping mechanism.

Input parameters for calculating the resource are AU area, drainage area per well, percentage of the unit untested, percentage of untested area in sweet spots, success ratios and estimated ultimate recoveries (EURs) for both sweet spot and non-sweet spot area, and co-product ratios (gas-to-oil and NGLs-to-gas ratios within oil accumulations, and liquids-to-gas ratio for gas accumulations). For each of these parameters, the geologist does not specify a single number, but rather estimates of expected minimum, maximum and average or mode, thus defining a distribution. The actual resource assessment calculations take place through a Monte Carlo

procedure, that is, through repeated sampling of the distributions through a large number of trials (1000 or more). These independent trials are used to calculate the F5, F50 (Median), F95 and average volumes of oil and gas in the AU. The procedure is described in more detail in Charpentier and Cook (2010). Calculations are made through a spreadsheet available for download from the USGS, which requires the commercial package @Risk™ to do the Monte Carlo computations.

9.1.1 Definition of Assessment Unit Sweet Spot Areas

Within each assessment unit, we calculated percentage of the undiscovered area lying within sweet spots from maps of well locations, cumulative production from each well and geographic trends in thermal maturity. Thermal maturity data collected during this project were combined with published data from the USGS, converted to vitrinite reflectance equivalent through a regression equation and mapped (Figure 9-2). We were particularly interested in delineating a gas prone region, an oil-prone region and the primary area of wet gas. Two indicator variables were created, the first by setting all reflectance values greater than 1.1 to "1" and those less to "0", and the second by setting values greater than 1.4 to "1" and the balance to "0", these two thresholds being the generally-accepted ones for defining the oil, wet gas and dry gas windows of maturity. Kriging of these two indicator variables provides local probabilities that an observed reflectance will exceed the respective threshold (Figure 9-3). Overlaying the contoured probability of exceeding the 1.1 threshold with a map of oil cumulative production (Figure 9-5), we drew a map of minimum and maximum sweet spot (Figure 9-5).
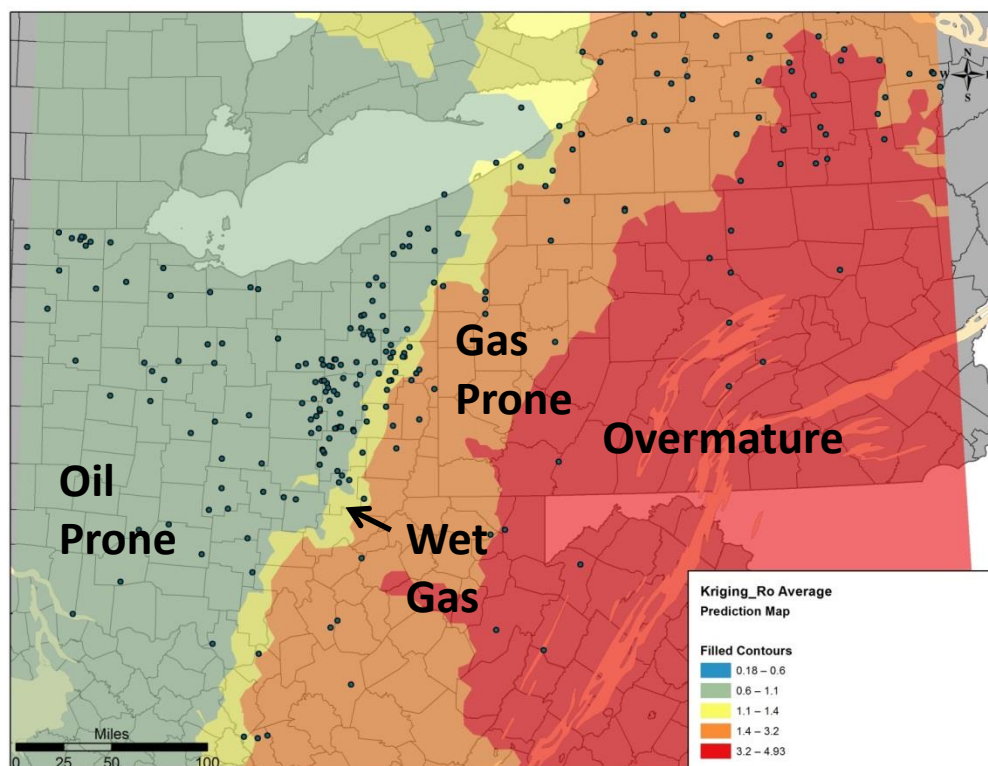
Figure 9-2. Contour map of vitrinite reflectance calculated from conodont alteration index, pyrolysis and bitumen reflectance data.
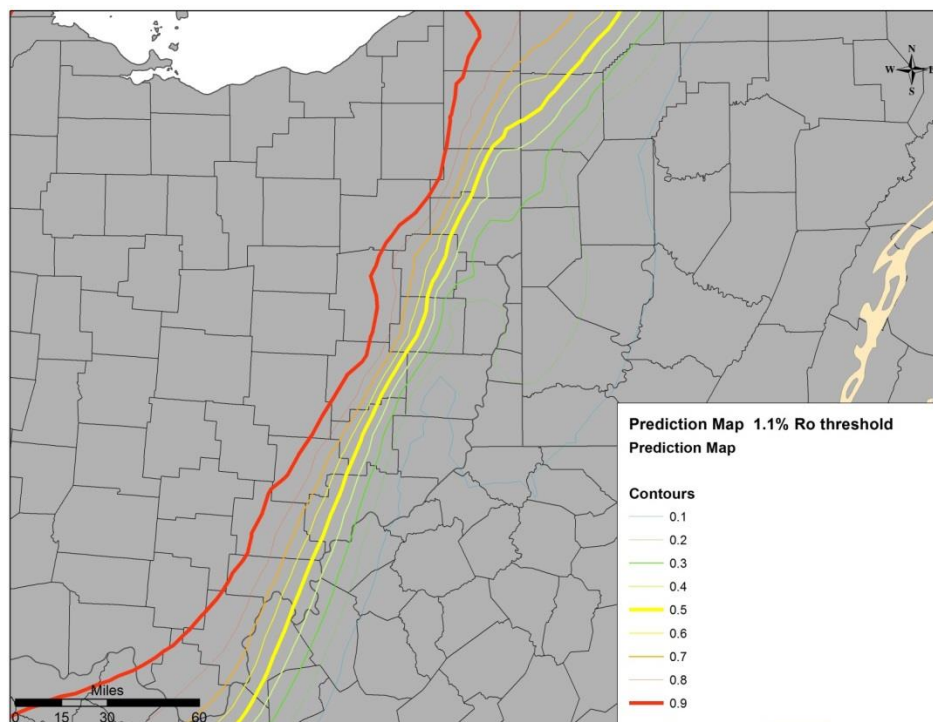
Figure 9-3. Contour map of probability that calculated vitrinite reflectance exceeds 1.1.
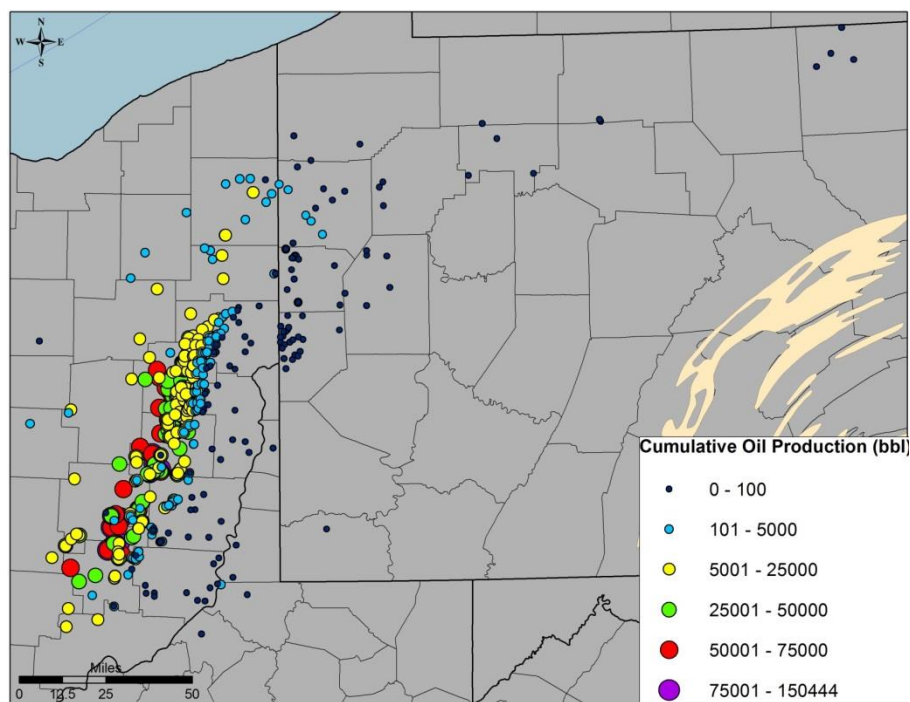
Figure 9-4. Producing oil wells by total cumulative production.

162
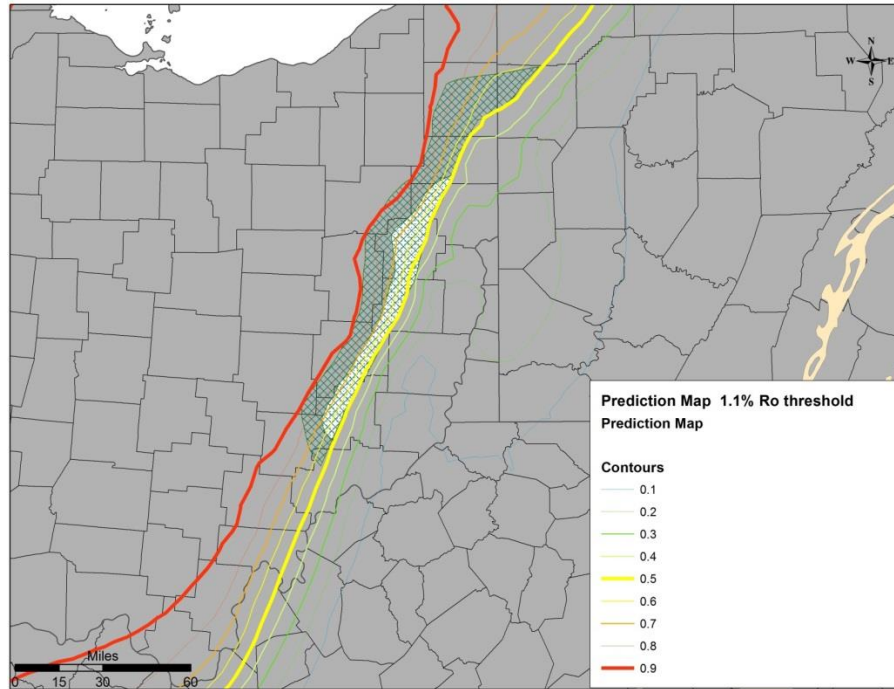
Figure 9-5. **Geographic extent of minimum and maximum Oil AU sweet spot used in resource assessment.**
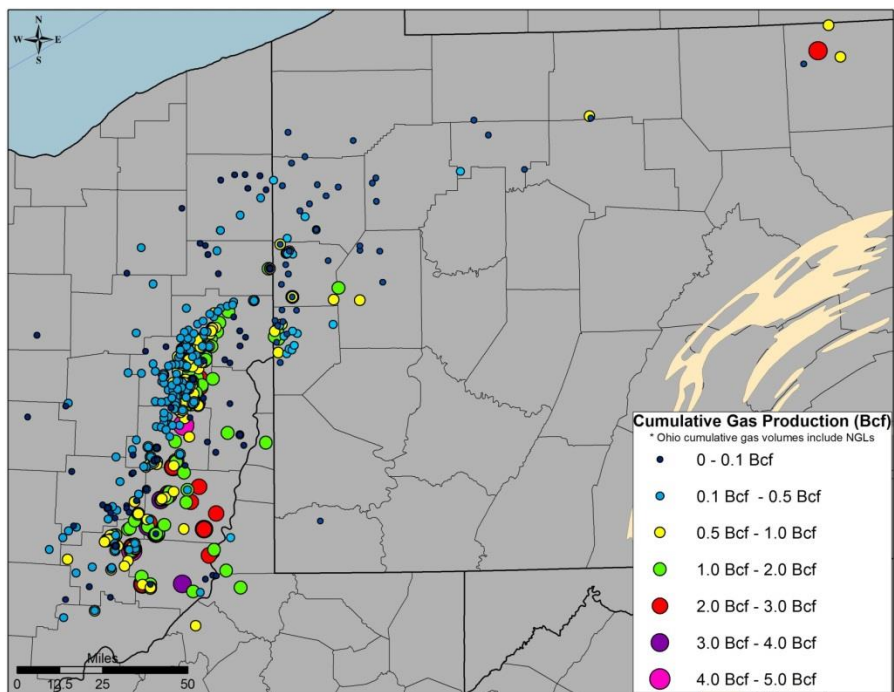
Figure 9-6. Producing gas wells by total cumulative production.
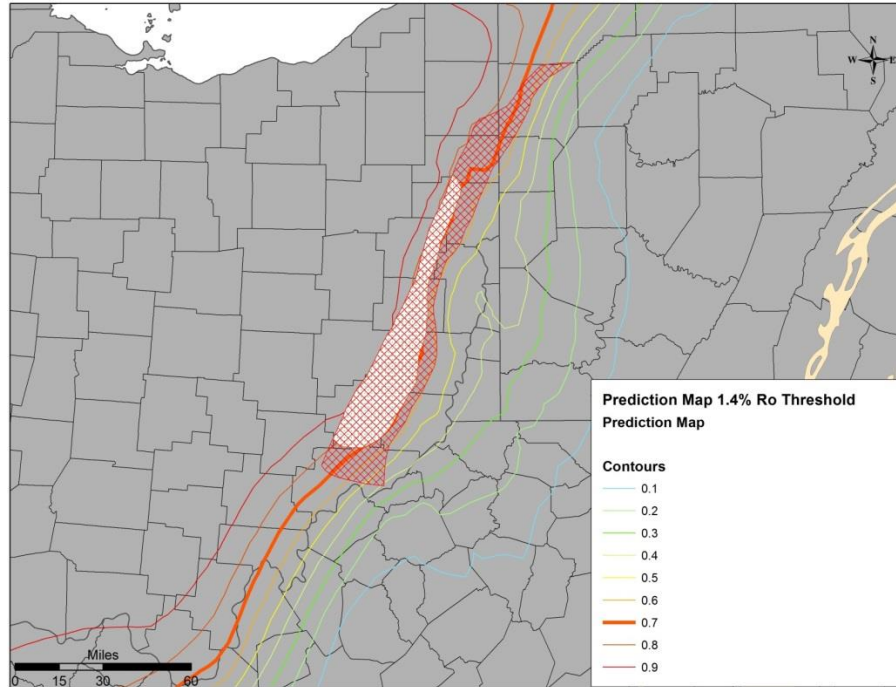
Figure 9-7. Geographic extent of minimum and maximum Wet Gas AU sweet spot used in resource assessment.

Similarly, contoured probability of exceeding the 1.4 reflectance threshold and with maps of oil (Figure 9-4) and gas production (Figure 9-6) were used to delineate extents of the minimum and maximum wet gas sweet spots, as well as the extent of the wet gas AU as a whole (Figure 9-7). Because natural gas liquids were not split out from gas in data available to us from Ohio, we could not map wet gas trends directly.

Minimum and maximum extents of the gas sweet spot for the purpose of the resource assessment were based on locations of producing gas wells in the gas prone region. Areas for each of the assessment units and respective sweet spots were calculated from the resulting map shown in Figure 9-8.
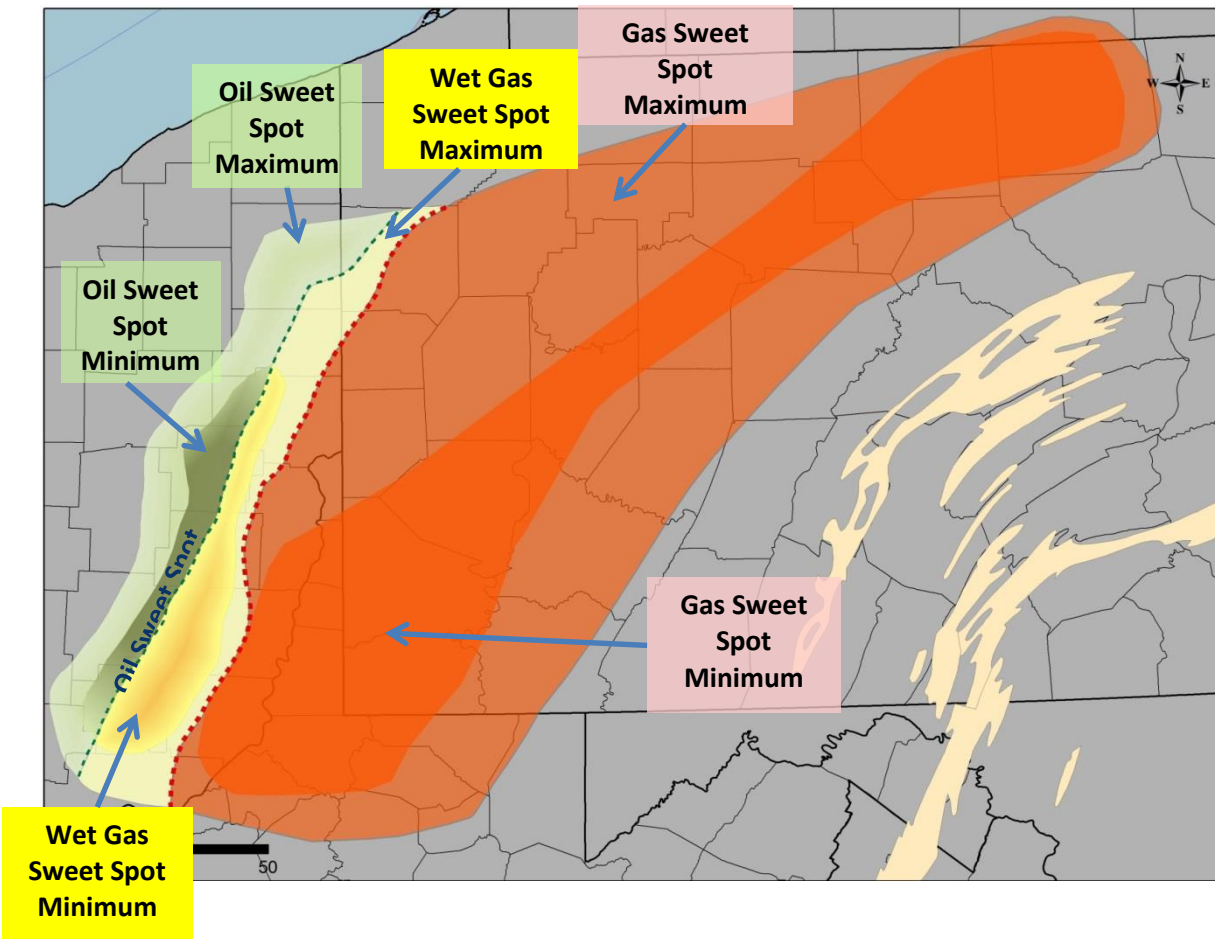
Figure 9-8. Geographic extent of minimum and maximum sweet spots used in resource assessment.

9.1.2 Estimated Ultimate Recovery

Annual production data for 2011-2014 from Pennsylvania and Ohio graphed by year in production (1st, 2nd, 3rd and 4th) showed a lot of variation with no consistent trend in medians (for example, Figure 9-9). As the play develops, one can expect an increase in productivity as the best areas are discovered and well completion strategy improves. For instance, wells with four years of data were the earliest drilled and can be expected to have below average performance compared with wells drilled in subsequent year, for which less data are available. Therefore, we examined subsets of wells based on the number of years of data available (i.e., grouped by year of completion), giving us four sets of medians for fitting a model. Note that medians for wells completed in 2012, 2013 and 2014 were shifted six months toward the origin to reflect the average number of months online, and medians for wells completed in 2011 were adjusted downward nine months because the average period of production for these wells was about three months.

A harmonic model of decline was fitted using the curve for wells completed in 2011 as a guide to shape and median production from wells completed in 2014 as an indicator of median production to expect (Figure 9-10). The model was used to compute cumulative production out to forty years as an EUR. The fifth percentile of production for wells completed in 2014 was used as a minimum within the sweet spot, and a maximum was fitted by eye from the range of outcomes

for wells in their first and second year of production. Final results expressed as median resource were relatively insensitive to changes in the maximum EUR compared with changes in median EUR, offsetting the relatively high uncertainty in maximum EUR to expect.
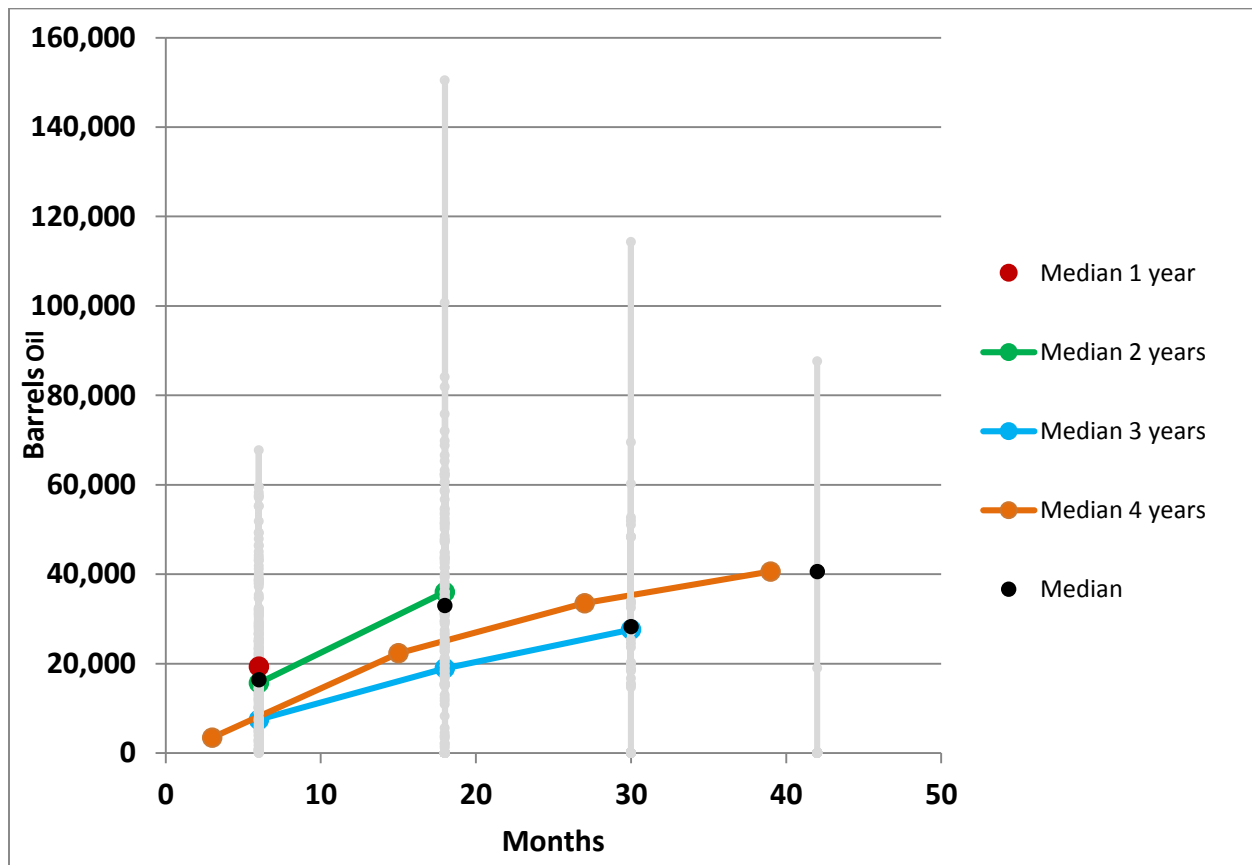
Figure 9-9. Cumulative production by months online (light gray dots), median values (black filled circles) and medians for wells in the oil sweet spot grouped by number of years of production data available ranging from 1 to 4 years.
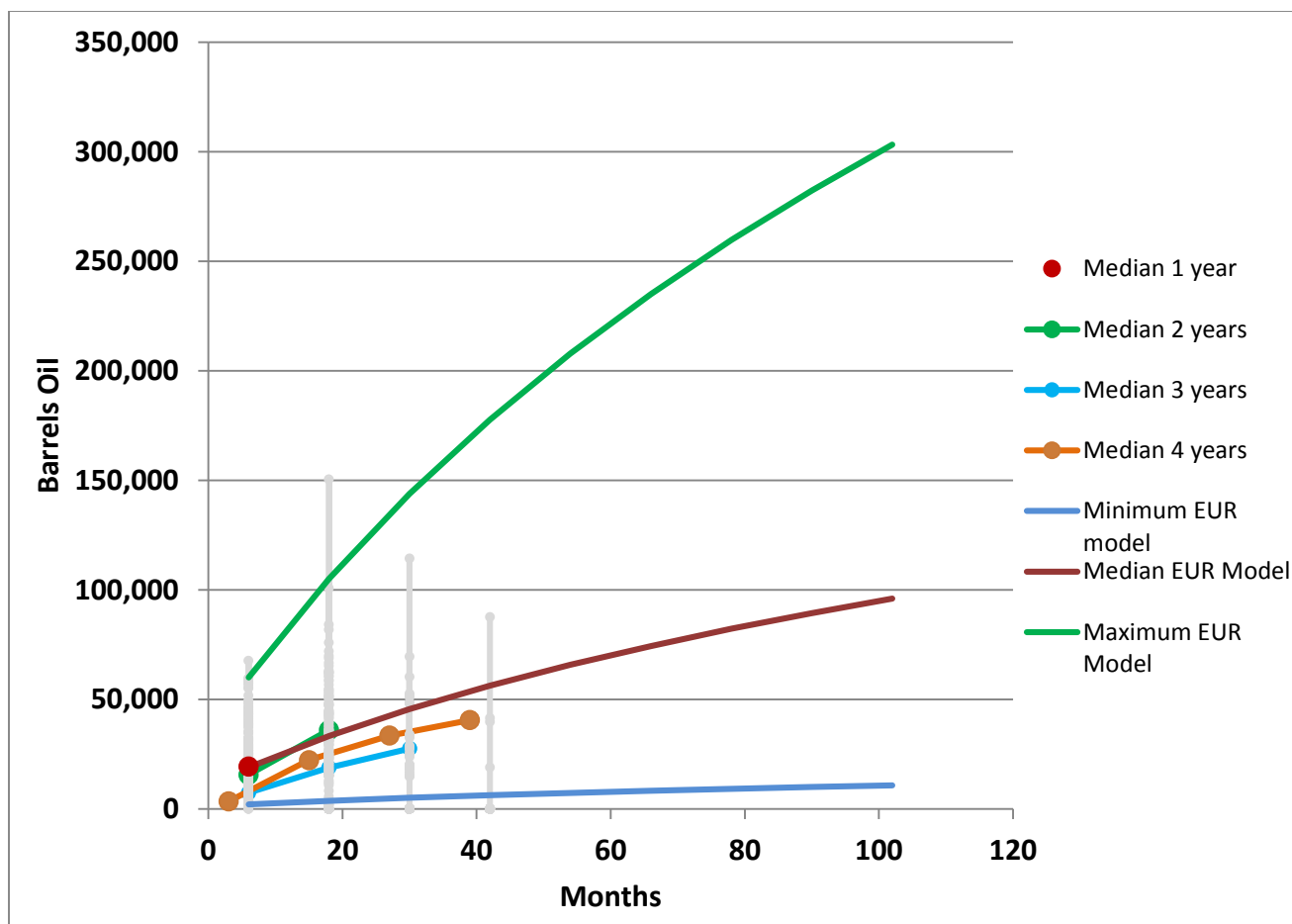
Figure 9-10. Cumulative production by months online (light gray dots) and medians for wells in the oil sweet spot grouped by number of years of production data available ranging from 1 to 4 years, and fitted models for calculating minimum, median and maximum estimated ultimate recovery.

The same procedure was followed for the oil, wet gas and gas assessment unit sweet spots (Table 9-1 to 9-3). For areas outside the sweet spots in each assessment unit, the median EUR was set at the value corresponding to the lowest five percentile of production from wells that went online in 2014, the minimum at the value corresponding to the minimum production in these wells and the maximum at the value of EUR obtained for the well at the tenth percentile.

Table 9-1. Parameters for estimated ultimate recovery used in resource assessment of Oil Assessment Unit.

Oil AU (MMbo)	Min	Med	Max
Sweet Spot	0.022	0.199	0.022
Non Sweet Spot	0.002	0.022	0.049

Table 9-2. Parameters for estimated ultimate recovery used in resource assessment of Wet Gas Assessment Unit.

Wet Gas AU (Bcf)	Min	Med	Max
Sweet Spot	0.64	5.76	18.84
Non Sweet Spot	0.20	0.64	1.19

Table 9-3. Parameters for estimated ultimate recovery used in resource assessment of Gas Assessment Unit.

Gas AU (Bcf)	Min	Med	Max
Sweet Spot	0.19	7.09	30.37
Non Sweet Spot	0.039	0.19	0.32

9.1.3 Success Ratios and Co-Product Ratios

Success ratios were defined, where possible, by examination of well performance (wells with zero production over several years, plugged wells, areas of numerous cancelled permits). Success ratios in sweet spots were set at the same values across assessment units: minimum of 90%, mode of 95% and maximum of 99%. They were set very low outside the sweet spot for the Oil Assessment Unit: minimum of 1%, mode of 5% and maximum of 10%, whereas these parameters for the Gas and the Wet Gas Assessment Units were set at 5, 10 and 40% respectively.

Co-product ratios were calculated from public records and used only for the oil assessment unit. The largest source of production data was the public database from the state of Ohio. In Ohio's way of recordkeeping, production data report NGLs and gas as a single number. Therefore, calculation of the gas resource in both the gas and wet gas assessment units includes a significant percentage of natural gas liquids which could not be separated from these totals and/or evaluated individually. For this reason, we did not include NGLs in the liquids-to-gas ratio for the gas AU or a NGLs-to-gas ratio for the oil AU. Parameters used for the gas-to-oil ratio distribution in the Oil Assessment Unit were 900 scfg/bo minimum, 3600 scfg/bo mode and 8000 scfg/bo maximum.

9.1.4 Results

The results of the probabilistic resource assessment are provided in Table 9-4. Because total oil and gas resources tend to follow a logarithmic distribution, means assessment values are higher than the medians. Total mean gas resource, which includes wet gas equivalent in the Wet Gas and Oil assessments units, sums to 782,171 Bcf. Total oil resource is 1960 MMbo.

Table 9-4: Summary of recoverable oil and gas remaining.

Oil Assessment Unit	Oil (MMbo)				Gas (Bcf)			
	F95	F50	F5	Mean	F95	F50	F5	Mean
Sweet Spot	733	1677	3744	1908	2231	6636	17,722	7949
NonSweet Spot	23	49	91	52	69	191	446	216
Total	791	1728	3788	1960	2370	6858	17,960	8165

Wet Gas Assessment Unit	Oil (MMbo)				Gas (Bcf)			
	F95	F50	F5	Mean	F95	F50	F5	Mean
Sweet Spot					23,840	49,601	106,550	55,980
NonSweet Spot					99	379	1023	447
Total					24,484	50,037	106,852	56,427

Gas Assessment Unit	Oil (MMbo)				Gas (Bcf)			
	F95	F50	F5	Mean	F95	F50	F5	Mean
Sweet Spot					220,473	590,680	1,542,873	710,341
NonSweet Spot					2862	6584	13,835	7238
Total					228,478	598,026	1,549,586	717,579

MMbo=million barrels of oil
Bcf=billion cubic feet of gas

9.2 Original In-Place Resources

A second resource assessment method was used to determine original hydrocarbon-in-place following a volumetric approach. The volumetric approach provides a means to assess resource potential from fundamental geologic data in a manner that is independent of development practice, well performance, economics and the limited geographic extent of exploratory activity that often characterizes the early development of a hydrocarbon play. Basic geologic and reservoir data are used to define characteristics of selected stratigraphic units and to calculate hydrocarbon volumes. Original in-place resources were estimated for three separate units within the Utica Shale play: the Utica Shale, Point Pleasant Formation and Logana Member of the Trenton Limestone. A summary of the methodology, input data and results is given below.

9.2.1 Methodology

The calculation for original hydrocarbon-in-place (HIP) includes separate determination of free and adsorbed hydrocarbon volumes. The basic equation to calculate original hydrocarbon-in-place is:

$$HIP_{total} = HIP_{free} + HIP_{adsrb} \tag{1}$$

To derive all required parameters, additional equations and a substantial amount of data were necessary. The derivation of each parameter is described in more detail below. For this particular assessment, the stratigraphic units were separated into two regions: one to address in-place oil resources in the western portion of the Utica Shale play and another to address the in-place gas resources to the north and east. For each region, a single phase (either oil or gas) was presumed to exist in the reservoir. Calculations were performed for selected wells at every one-half foot of thickness within the well. Data were gridded to interpolate between and extrapolate beyond wells. Petra®, ArcGIS and internally-developed software were used to manage, manipulate and analyze data.

9.2.1.1 Free Original Hydrocarbon-In-Place

Free hydrocarbon-in-place was determined using Equations 2 through 7.

$$\mathbf{GIP_{free}} = (\phi_{eff} * (1 - S_w) * (1 - Q_{nc}) * H_{fm} * A_r * 4.356 * 10^{-5}) / B_g \qquad (2)$$

$$\mathbf{OIP_{free}} = (\phi_{eff} * (1 - S_w) * H_{fm} * A_r * 7758) / B_o \qquad (3)$$

GIP_{free} = free gas (Bcf)

OIP_{free} = free oil (bbl)

ϕ_{eff} = effective porosity (fractional)

S_w = water saturation (fractional)

Q_{nc} = non-combustible gas (fractional)

H_{fm} = reservoir thickness (feet)

A_r = reservoir area (ac)

B_g = gas formation volume factor (fractional)

B_o = oil formation volume factor (fractional) (modified from Crain, 2013a)

$$\boldsymbol{\phi_{eff}} = ((\phi_n - (V_{sh} * \phi_{nsh}) - (V_{ker} * \phi_{nker})) + (\phi_d - (V_{sh} * \phi_{dsh}) - (V_{ker} * ((2650 - \rho_{ker}) / 1650)))) / 2 \quad (4)$$

ϕ_{eff} = effective porosity (fractional)

ϕ_n = neutron porosity (fractional)

V_{sh} = shale volume (fractional)

ϕ_{nsh} = shale neutron porosity (fractional)

V_{ker} = kerogen volume fraction (unitless)

ϕ_{nker} = kerogen neutron porosity (fractional)

ϕ_d = density porosity (fractional)

ϕ_{dsh} = shale density porosity (fractional)

ρ_{ker} = kerogen density (g/cc) (modified from Crain, 2013a; Crain, 2013b)

Note: Effective porosity equation (4) used for wells without porosity data from core or other samples; equation adjusted depending on relationship between log-derived and core-derived porosity.

$$\mathbf{S_w} = (((((1 - V_{sh}) * A * (R_W@FT) / (\phi_{eff}{}^M)) * V_{sh} / (2 * R_{sh}))^2 + (((1 - V_{sh}) * A * (R_W@FT) /$$
$$(\phi_{eff}{}^M)) / R_{fmd}))^{0.5} - (((1 - V_{sh}) * A * (R_W@FT) / (\phi_{eff}{}^M)) * V_{sh} / (2 * R_{sh})))^{(2/N)} \qquad (5)$$

S_w = water saturation (fractional)

V_{sh} = shale volume (fractional)

A = tortuosity exponent (fractional)

R_w = formation water resistivity (ohm-m)

ϕ_{eff} = effective porosity (fractional)

M = cementation exponent (fractional)

R_{sh} = shale resistivity (ohm-m)

R_{fmd} = formation resistivity, deep reading (ohm-m)

N = saturation exponent (fractional) (modified from Crain, 2013c)

$$B_g = (P_s * (T_f + 460)) / (P_{fm} * (T_s + 460)) * Z_{fg} \qquad (6)$$

$$B_o = 1.4, 1.2, \text{ or } 1 \text{ dependent on } D_{fm} \qquad (7)$$

B_g = gas formation volume factor (fractional)

B_o = oil formation volume factor (fractional)

P_s = surface pressure (psi)

T_f = formation temperature (°F)

P_{fm} = formation pressure (psi)

T_s = surface temperature (°F)

Z_{fg} = gas compressibility factor (fractional)

D_{fm} = formation depth (ft) (modified from Crain, 2013a)

9.2.1.2   *Adsorbed Original Hydrocarbon-In-Place*

Adsorbed hydrocarbon-in-place is determined using Equations 8 through 10.

$$GIP_{adsrb} = G_c * \rho_{fm} * H_{fm} * A_r * 1.3597*10^{-6} \qquad (8)$$

$$OIP_{adsrb} = S2 * 0.001 * \rho_{fm} * H_{fm} * A_r * 7758 \qquad (9)$$

GIP_{adsrb} = gas in place (Bcf)

OIP_{adsrb} = oil in place (bbl)

G_c = gas content (scf/ton)

S2 = oil content (mg/g)

ρ_{fm} = density (g/cc)

H_{fm} = reservoir thickness (feet)

A_r = spacing unit area (ac) (modified from Crain, 2013a; Holmes, 2013)

Note: Adsorbed oil, equation (9) as proposed by Holmes, was calculated but not included in final results.

$$G_c = TOC * G_p \qquad (10)$$

G_c = gas content (scf/ton)

TOC = total organic carbon (weight %)

G_p = gas parameter (modified from Crain, 2013a)

9.2.2 Study Wells and Data

Digital petrophysical data, supplied by Utica Consortium partners, provided the foundation for the Study. Wells with gamma-ray, density/porosity and resistivity well log data (at minimum) were selected preferentially (Figure 9-11). Additional well selection factors considered included well orientation (vertical wells only), structural complexity (lack of faulting), stratigraphic unit depth (only wells with top of the Utica Shale play greater than 2500-3000 ft), geographic

distribution and proximity to other wells. Depending on the particular stratigraphic unit, up to approximately 60 wells were selected for analysis (Figure 9-12).
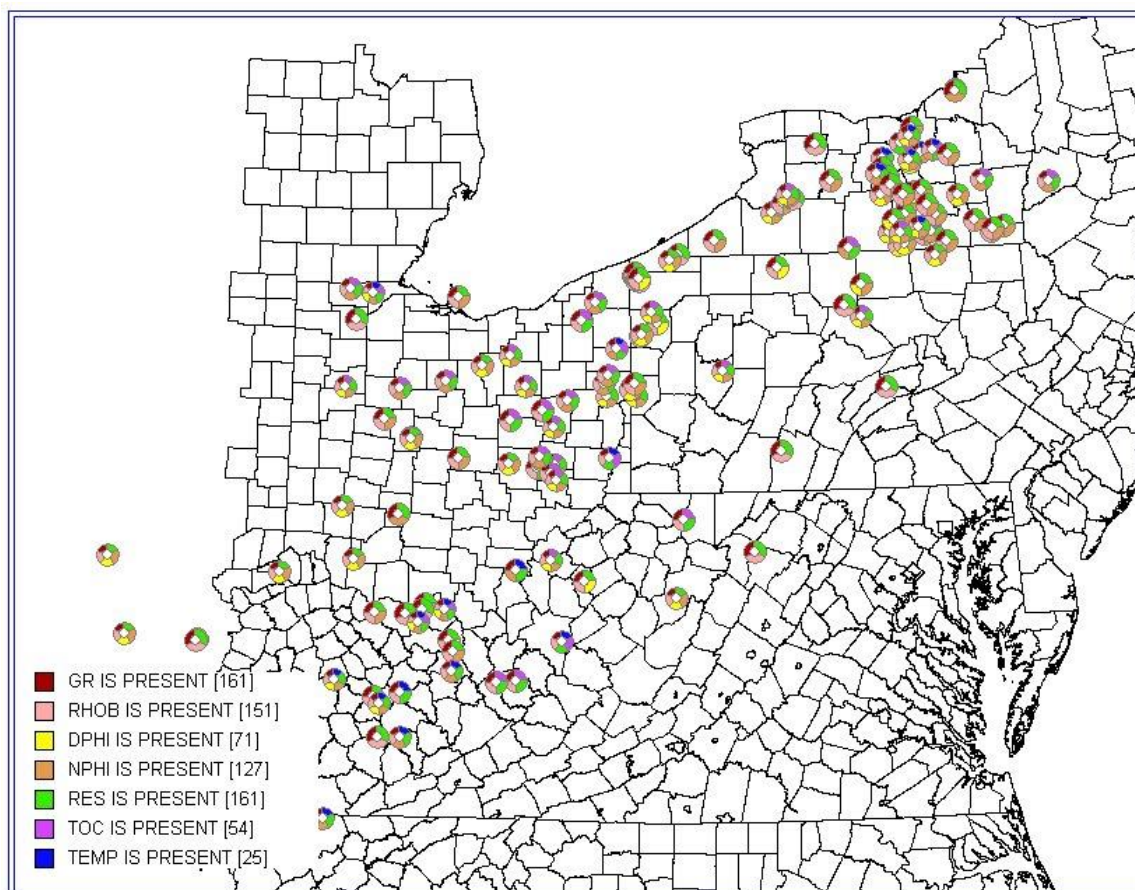
Figure 9-11. Wells with a full suite of digital logs for the Utica Shale, Point Pleasant Formation and/or Logana Member of the Trenton Limestone in the Consortium data set and with a top depth greater than 2500 feet (colors indicate well log availability through a unit of interest; red=gamma-ray (GR), pink=bulk density (RHOB), yellow=density porosity (DPHI), orange=neutron porosity (NPHI), green=resistivity (RES), purple=total organic carbon (TOC), and blue=temperature (TEMP)).

To augment digital log data, reservoir-specific input included or encompassed: thermal maturity, TOC, gas content, pressure and temperature. As detailed in "Definition of Assessment Unit Sweet Spot Areas," thermal maturity was determined for each study well from a map developed using equivalent %Ro values (Figure 9-12). TOC was available for individual wells or extracted from stratigraphic-specific TOC maps constructed for the in-place assessment (Figures 9-13 to 9-15). Stratigraphic-specific TOC maps were generated from individual wells with TOC data using the mean TOC value for a particular stratigraphic unit. Gas content, pressure and temperature were taken largely from publicly-available data, although some data were available for individual wells. In general, gas content was determined from methane isotherms given TOC and pressure (Figures 9-16 to 9-17). Reservoir pressure data were based on limited well data for West Virginia and Ohio, Consortium partner input and publicly-available data (Table 9-5). Temperature gradients were determined from a map generated from data gathered for the National Geothermal Data System (Figure 9-18).
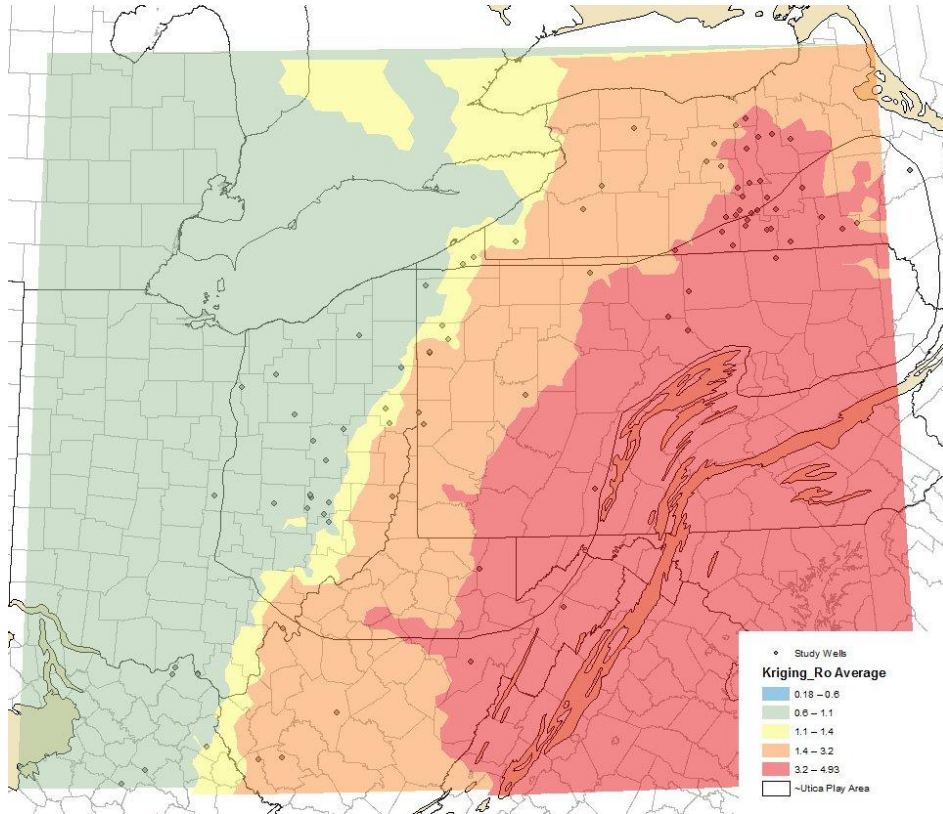
Figure 9-12. Thermal maturity as determined from equivalent %Ro; map used to determine maturity of study wells (green=oil prone, yellow=wet gas prone, orange=gas prone, pink=overmature).
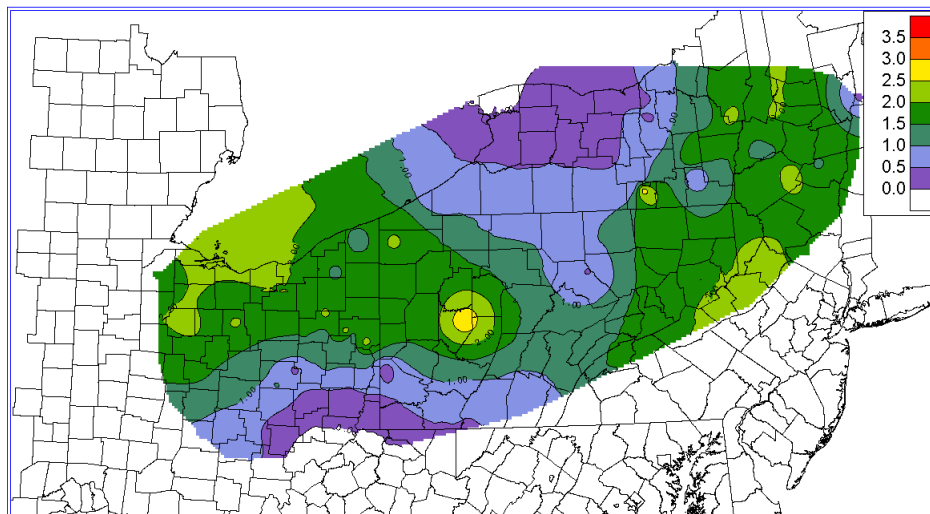
Figure 9-13. Mean total organic carbon (TOC%) for Utica Shale as derived from Consortium analytical data (purple=lower TOC, green to yellow=higher TOC).
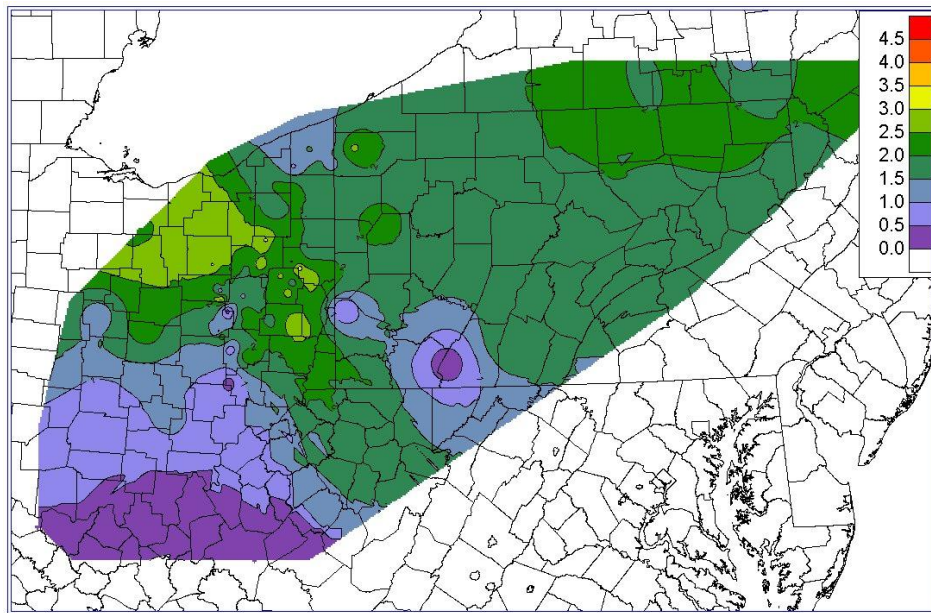
Figure 9-14. Mean total organic carbon (TOC%) for Point Pleasant Formation as derived from Consortium analytical data (purple=lower TOC, green=higher TOC).
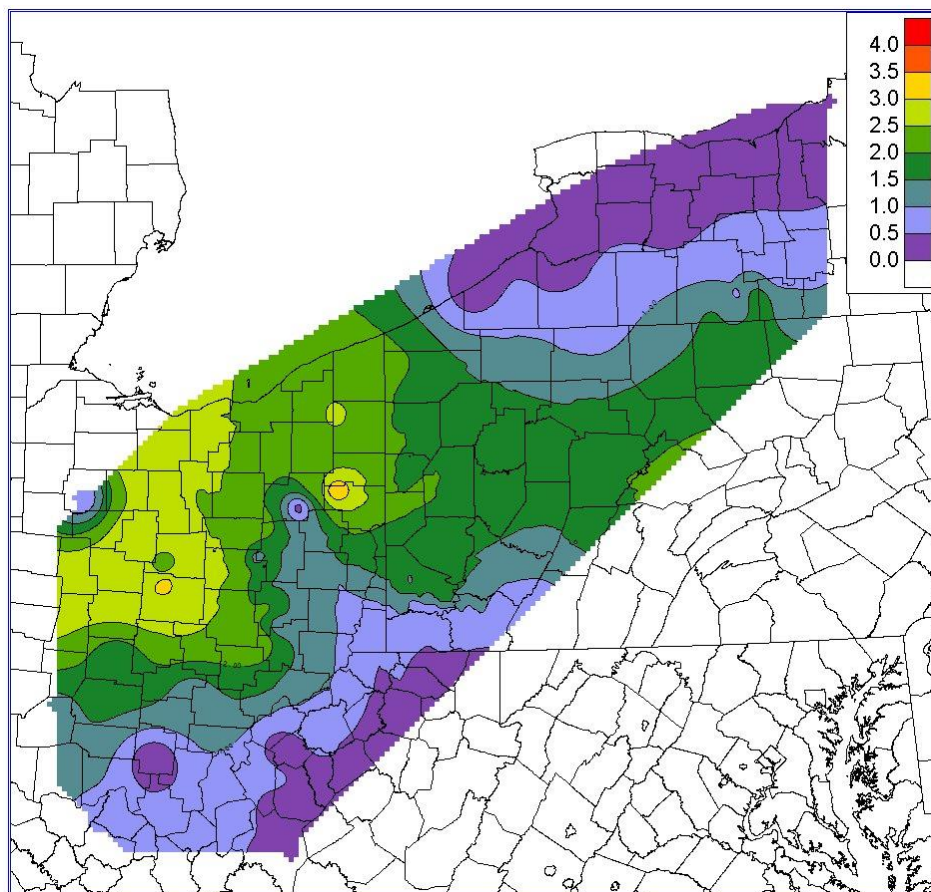
Figure 9-15. Mean total organic carbon (TOC%) for Logana Member of Trenton Limestone as derived from Consortium analytical data (purple=lower TOC, green to yellow=higher TOC).

174
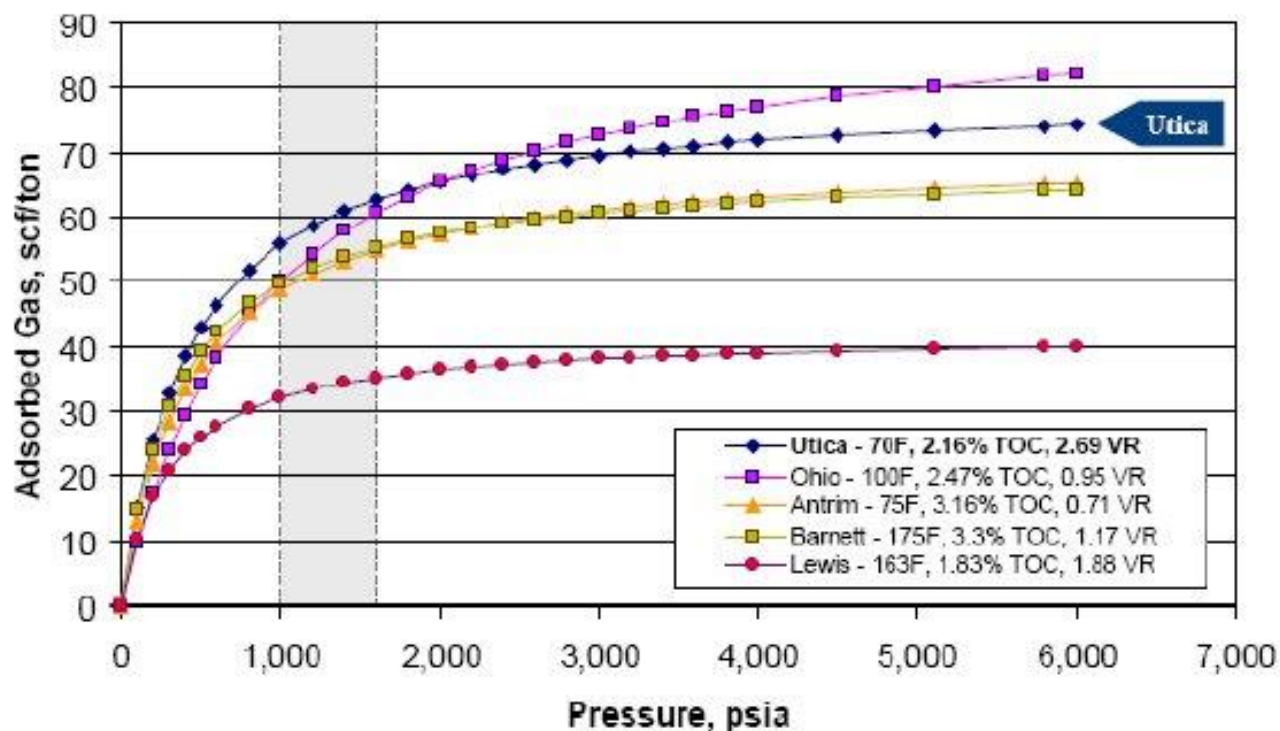
Figure 9-16. Methane isotherms for New York (Advanced Resources International, Inc., 2008). New York Utica isotherm used for New York, majority of Pennsylvania and West Virginia.
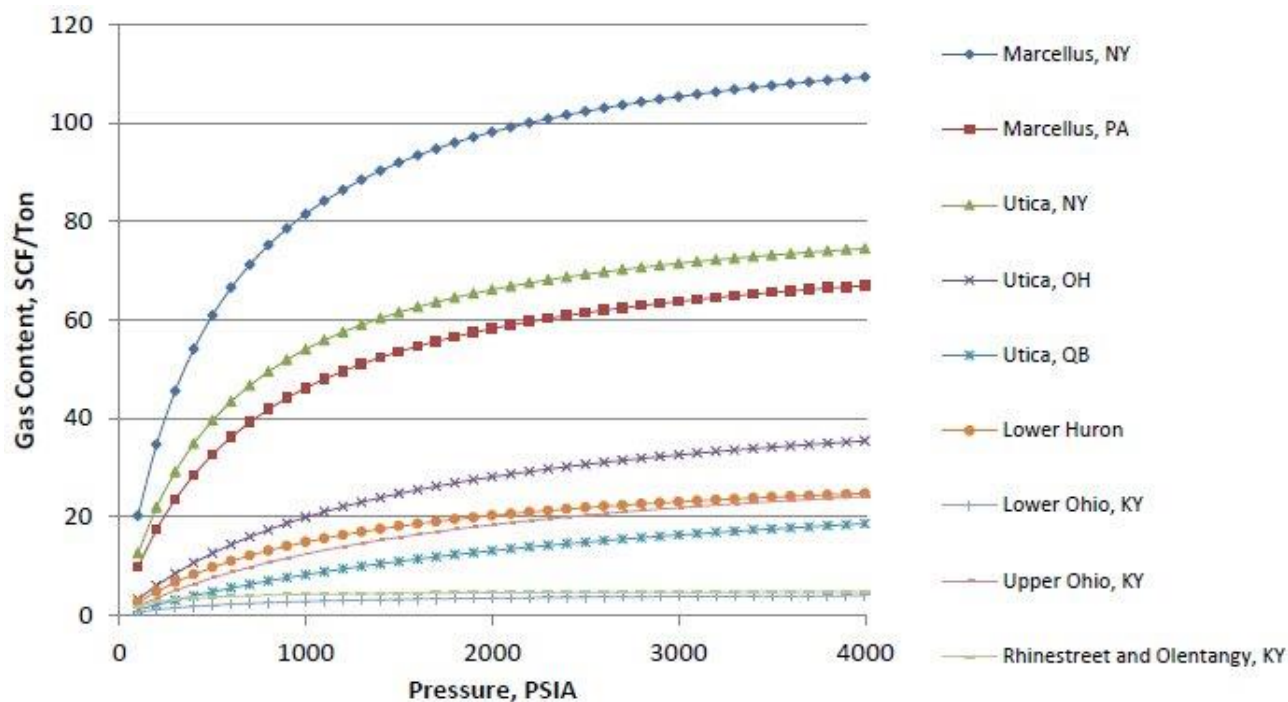
Figure 9-17. Methane isotherms for various states (Advanced Resources International, Inc., 2012). Ohio Utica isotherm used for Ohio; New York and Ohio Utica isotherms used for northwestern corner of Pennsylvania.

Table 9-5. Pressure gradient (psi/ft) as assumed given limited formation-specific well data for West Virginia and Ohio, Consortium partner input and publicly-available data.

State	Pressure Gradient (psi/ft)		Note(s)
	Low	**High**	
New York (NY)	0.433	0.5	0.433 for most of NY; 0.5 for very small portion of southern NY
Ohio (OH)	0.6	0.9	0.6 for most of OH; 0.7-0.9 for narrow region in east central OH
Pennsylvania (PA)	0.6	0.9	0.6 for most of PA; 0.7 in small portion of central PA; 0.7-0.9 in southwestern PA
West Virginia (WV)	0.6	0.9	0.6 for most of WV; 0.7-0.9 for northern WV panhandle
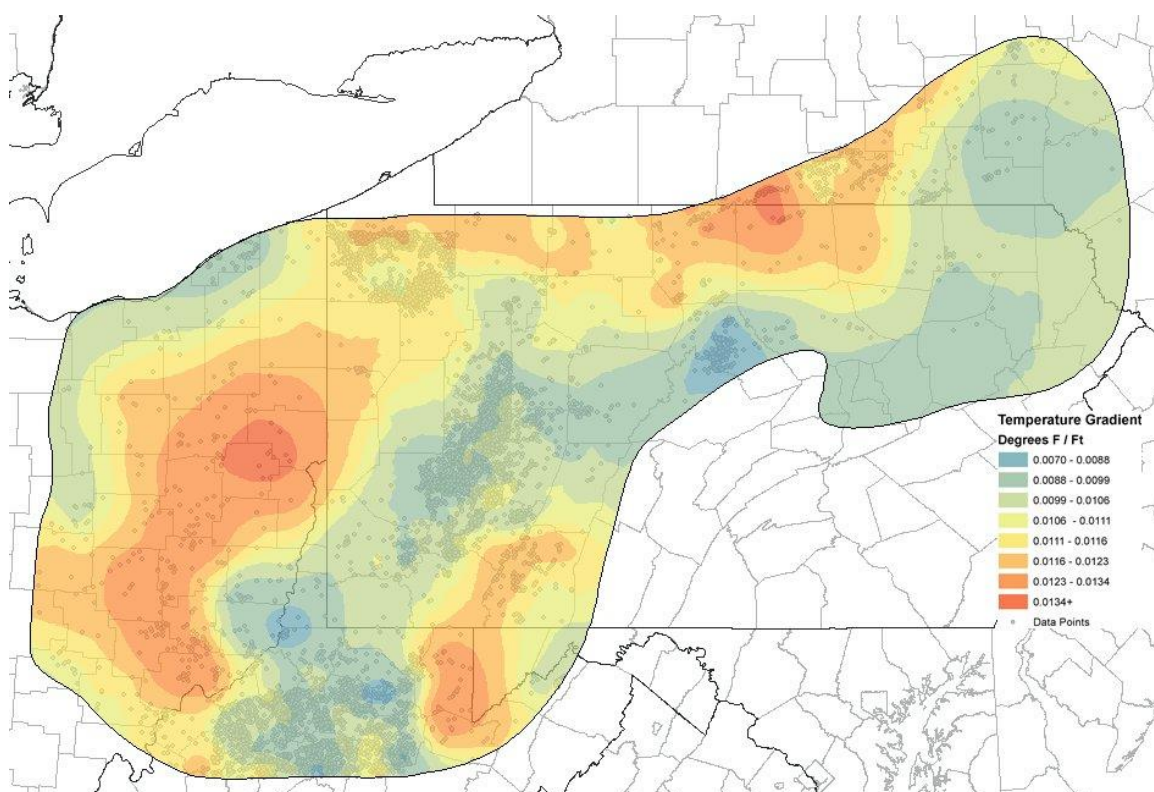
Figure 9-18. Temperature gradient (°F/ft) as derived from data obtained from the National Geothermal Data System (blue=lower gradient; orange=higher gradient).

A summary of all data and sources used to estimate original in-place free and adsorbed hydrocarbon resources are provided in Tables 9-6 and 9-7, respectively. Items marked with an asterisk (*) indicate those items obtained or derived, primarily or in full, from the results of this Study.

*Table 9-6. Data items and general data source(s) for free hydrocarbon-in-place. Data items in bold type are values that are calculated from parameters listed below the item. *= from this Study.*

Data Item	General Data Source(s)
Free Gas-In-Place (GIP$_{free}$)	calculation (Equation 2)
Free Oil-in-Place (OIP$_{free}$)	calculation (Equation 3)
Effective Porosity (ϕ_{eff})	calculation (Equation 4)
Water Saturation (S$_w$)	calculation (Equation 5)
Non-combustible Gas (Q$_{nc}$)	assumption
Reservoir Thickness (H$_{fm}$)	well logs*, maps*
Reservoir Area (A)	well logs*, maps*, reports
Gas Formation Volume Factor (B$_g$)	calculation (Equation 6)
Oil Formation Volume Factor (B$_o$)	calculation (Equation 7)
Effective Porosity (ϕ_{eff})	calculation (Equation 4)
Neutron Porosity (ϕ_n)	well logs*
Shale Volume (V$_{sh}$)	well logs*, analytical data*
Shale Neutron Porosity (ϕ_{nsh})	well logs*
Kerogen Volume (V$_{ker}$)	analytical data*, calculation
Kerogen Neutron Porosity (ϕ_{nker})	assumption
Density Porosity (ϕ_d)	well logs*
Shale Density Porosity (ϕ_{dsh})	well logs*
Kerogen Density (ρ_{ker})	assumption
Water Saturation (S$_w$)	calculation (Equation 5)
Shale Volume (V$_{sh}$)	well logs*, analytical data*
Tortuosity Exponent (A)	assumption
Formation Water Resistivity (R$_w$)	well logs*, assumption
Effective Porosity (ϕ_{eff})	calculation (Equation 4)
Cementation Exponent (M)	assumption
Shale Resistivity (R$_{sh}$)	well logs*
Formation Resistivity (R$_{fmd}$)	well logs*
Saturation Exponent (N)	assumption
Gas Formation Volume Factor (B$_g$)	calculation (Equation 6)
Oil Formation Volume Factor (B$_o$)	determination (Equation 7)
Surface Pressure (P$_s$)	assumption
Formation Temperature (T$_f$)	well logs*, published datasets
Formation Pressure (P$_{fm}$)	assumption
Surface Temperature (T$_s$)	maps, assumption
Gas Compressibility Factor (Z$_{fg}$)	assumption
Formation Depth (D$_{fm}$)	well logs*

Table 9-7. Data items and general data source(s) for adsorbed hydrocarbon-in-place. Data items in bold type are values that are calculated from parameters listed below the item. *= from this Study.

Data Item	General Data Source(s)
Adsorbed Gas-In-Place (GIP$_{adsrb}$)	calculation (Equation 8)
Adsorbed Oil-In-Place (OIP$_{adsrb}$)	calculation (Equation 9)
Gas Content (G$_c$)	calculation (Equation 10), literature
S2 (mg/g)	analytical data*
Density (ρ_{fm})	well logs*
Reservoir Thickness (H$_{fm}$)	well logs*, maps*
Spacing Unit Area (A$_r$)	well logs*, maps*, reports
Gas Content (G$_c$)	calculation (Equation 10), literature
Total Organic Carbon (TOC)	analytical data*
Gas Parameter (G$_p$)	calculation, assumption

9.2.3 In-Place Assessment Results

Tables 9-8 and 9-9 provide summary results for each stratigraphic unit evaluated using the volumetric approach. Well log data in particular were limited especially for Pennsylvania and West Virginia; and therefore, the original in-place resource estimates might change if additional data were to become available thus results should be considered preliminary. Given the data that were provided for the Study, it is estimated that original oil-in-place is approximately 39.6 MMbo/mi^2 within the sweet spot area as defined in "Definition of Assessment Unit Sweet Areas" (Figure 9-8) while the original gas-in-place is approximately 155.6 Bcf/mi^2.

Table 9-8. Estimated original in-place oil and gas resources (volumes per unit area) as determined from data provided by the Consortium partners.

Stratigraphic Unit	Original In-Place Resources, Average Volumes Per Unit Area	
	Oil (MMbo/mi^2)*	Gas (Bcf/mi^2)*
Utica Shale	20.8	53.5
Point Pleasant Formation	15.8	85.1
Logana Member of Trenton Limestone	3.0	17.0
Total for Utica Shale Play Selected Stratigraphic Units	39.6	155.6

* = average volume per square mile in the sweet spot area; sweet spot area is as defined to estimate remaining recoverable resources (Figure 9-8); MMbo=million barrels of oil and Bcf=billion cubic feet of gas

Similarly given the data that were provided for the Study, it is estimated that original oil-in-place is approximately 82,903 MMbo within the sweet spot area (Figure 9-8) while the original gas-in-place is approximately 3,192,398 Bcf or 3192.4 Tcf.

Table 9-9. Estimated original in-place oil and gas resources (total volumes) as determined from data provided by the Consortium partners.

Stratigraphic Unit	Original In-Place Resources, Total Volumes	
	Oil (MMbo)*	Gas (Bcf)*
Utica Shale	43,508	1,098,119
Point Pleasant Formation	33,050	1,745,803
Logana Member of Trenton Limestone	6345	348,476
Total for Utica Shale Play Selected Stratigraphic Units	82,903	3,192,398

* = estimated volume in the sweet spot area; sweet spot area is as defined to estimate remaining recoverable resources (Figure 9-8); MMbo=million barrels of oil and Bcf=billion cubic feet of gas

9.3 Comparison of Recoverable and Original In-Place Resources

Table 9-10. Approximate current recovery factors based on recoverable and in-place resource estimates.

Resources	Oil (MMbo)*	Gas (Bcf)*
Recoverable Resources	2611	889,972
Original In-Place Resources	82,903	3,192,398
Current Recovery Factors	3%	28%

* = estimated volume in the sweet spot area; sweet spot area is as defined to estimate remaining recoverable resources (Figure 9-8); MMbo=million barrels of oil and Bcf=billion cubic feet of gas

Based on the resource assessments to determine remaining recoverable resources and original hydrocarbon-in-place, it is expected that given current technology the play-wide oil recovery factor will be approximately 3% and the gas recovery factor will be approximately 28% in the "sweet spot" areas (Figure 9-8).

10.0 CONCLUSIONS AND IMPLICATIONS FOR PLAY DEVELOPMENT

The purpose of this chapter is to synopsize the research team's findings and provide insight as to how the Utica Shale play may be developed in the future. Perhaps the most overarching conclusion is that this play is really neither "Utica" nor "shale," based on the multi-disciplinary approach to reservoir characterization used in this Study. Evaluation of bulk mineralogy, TOC, carbonate content and thermal maturity data all point to an interbedded limestone and organic-rich shale interval in the Point Pleasant Formation as the preferred drilling target – a finding that is consistent with current drilling and production activity, especially in Ohio. The other particularly interesting finding is that reservoir porosity is comprised mostly of nm- to μm-scale pores that developed in organic matter during thermal maturation. Matrix porosity is minor to non-existent in these reservoir rocks.

The remainder of this chapter summarizes the results of research team's findings and interpretations regarding lithostratigraphy, depositional environment, core studies, TOC and thermal maturity, reservoir porosity, production data and trends, and resource assessments.

10.1 Lithostratigraphy

The research team adopted the following stratigraphic nomenclature for early Late Ordovician strata evaluated by the Study – the Kope Formation, Utica Shale, Point Pleasant Formation and Lexington/Trenton Formation. Trenton and Lexington are both formal formation names that have been applied to the same interval of rock. Therefore, in keeping with the previously published Trenton/Black River study (Patchen and others, 2006), we have designated this stratigraphic interval the Lexington/Trenton Formation. In some parts of the Study area, it is possible to differentiate individual members of the Lexington/Trenton based on their organic-rich or carbonate-rich but organic-poor characteristics. Formal names have been applied to these members in Kentucky – the Curdsville Member (organic-poor) and Logana Member (organic-rich) above. The section between the Logana Member and the Point Pleasant Formation is referred to informally herein as the upper member of the Lexington/Trenton Formation. Of all these strata, the most productive hydrocarbon source rocks tend to be the Point Pleasant Formation and the upper and Logana members of the Lexington/Trenton Formation.

10.2 Depositional Environment

The Upper Ordovician shale interval contains many sedimentary features, including burrowing, laminations, scour surfaces, apparent unconformities and abundant fossil assemblages. Burrows are common throughout much of the Devon Energy cores from eastern Ohio. The abundance of fossils indicates an environment that was well oxygenated much of the time. There are delicate trilobites and articulated ostracods that could not have been transported any significant distance. There also are beds composed almost entirely of strophomenid brachiopods, and this sort of monospecific accumulations of fossils is not likely to have been redistributed from some distant area.

Laminations are present throughout almost all of the organic-rich shales, as well as in the clay-rich, organic-poor shales. The laminations were probably produced by moving currents rather than variations in suspended load.

Scour surfaces are present throughout the studied interval from the Kope Formation to the Curdsville Member. They typically occur on top of finer shale facies and below coarser, grainier beds. These scour surfaces are surfaces of erosion that form due to an increase in energy. Given their frequency (mm- to cm-scale), they probably are evidence of a storm-dominated shelf environment. This means that the organic-rich faces were being deposited and preserved in an environment that was being hit with frequent storms.

There are several horizons within the cored intervals that appear to be unconformities. Two can be recognized in core by the presence of undulose surfaces: one is at the top of the upper Lexington/Trenton Formation, which is in the middle of the organic-rich zone, and the other is at the top of the Point Pleasant Formation. There also are two log markers that look like sequence boundaries at the top of the lower, organic-poor Utica that can be recognized on logs and correlated for long distances.

The depositional environment of the Point Pleasant Formation, upper Lexington/Trenton Formation, and Logana Member is a relatively shallow, probably <100 ft (<30 m) deep, storm-dominated, carbonate shelf that experienced frequent algal blooms. The organic matter in Upper Ordovician shales is mostly comprised of amorphinite, which indicates an algal source for the organic material in Utica and equivalent rocks. Cross-sections show that there was not much difference in water depth between the organic-rich and organic-poor areas of deposition. The fossils present in the limestone suggest water that was at times shallow, exposed to sunlight and well oxygenated. The storm-bedding throughout suggests something well above storm wave base. The environment may have been subject to seasonal anoxia due to the frequent algal blooms. A similar depositional model may be invoked for rocks deposited in New York and Pennsylvania, although these were not studied in the same detail.

10.3   Core Studies

A key element for potential production from shale reservoirs is TOC, and SGR core logging provides an opportunity to correlate wireline log data to TOC. As an example, the Devonian Marcellus Shale exhibits a good correlation among GR, uranium signature and TOC measurements. Unfortunately, the Upper Ordovician shales in the Study area did not exhibit this same relationship. The GR intensity for Utica/Point Pleasant rocks is dominated by the presence of potassium, and there is no correlation of GR intensity with the amount of organic matter. Our work demonstrates that TOC does not directly correlate to any radioactive material in the Utica-Point Pleasant interval.

Core studies of Ohio samples indicate show that GR tracks well with carbonate content, and regional log analyses and mapping efforts note a correlation between TOC and RHOB. Therefore, insoluble-residue analyses, RHOB log correlation, and/or petrographic techniques (as performed in this Study) may be better methods for predicting TOC in Ordovician shales.

10.4   TOC and Thermal Maturity

The TOC content of Utica/Point Pleasant and equivalent rocks is not identifiable by visual inspection (i.e., the "darkness" of samples does not correlate to the organic richness of samples). Many dark-colored shaly beds reported lower TOC than relatively light colored, limestone-rich beds within the same well and stratigraphic unit. In addition, because of the interlayered limestone/shale nature of these Ordovician formations, all have at least some nonorganic beds.

The Point Pleasant Formation – the drilling target in most of the wells completed to date – is an organic-rich calcareous shale with some limestone beds. The organic-rich units have roughly 40-60% carbonate content with TOC up to 4 or 5%. The organic matter composition is uniformly dominated by amorphinite, which indicates an algal source for much, if not most, of the organic material in these rocks.

The level of thermal maturity in the Utica/Point Pleasant shows a progression in increasing bitumen reflectance from west to east, with a very steep increase occurring in eastern Ohio. This is mainly the result of a rapid increase in depth of the Utica/Point Pleasant in this area. Ro random values from central Ohio ranged from 0.66 to 0.84%. In eastern Ohio, values range from 0.94 to 1.43%. Collectively, the Upper Ordovician shale in central Ohio has a level of thermal maturity in the lower to middle part of the oil window. In northeastern Ohio, the Upper Ordovician shale

has a level of thermal maturity that includes the middle and upper portions of the oil window, the wet gas window and the lower part of the dry gas window. The Utica/Point Pleasant in western Pennsylvania has a level of thermal maturity that increases basinward, ranging from the upper part of the oil window to the top of the dry gas window.

CAI analyses were prepared for samples from 10 wells in Ohio. These results were used in conjunction with those of Repetski and others (2008) to prepare an updated CAI map for Upper Ordovician shales in Ohio. CAI values range from 1 to 2.5, with a trend of increasing maturity basinward.

10.5   Reservoir Porosity

Petrographic studies indicate there is little to no matrix porosity in Utica/Point Pleasant rocks, and standard SEM imaging has confirmed the tight nature of the shale matrix in these rocks. SEM analyses of ion-milled samples, however, illustrate various pore types and sizes. Pore types include phyllosilicate framework pores (due to presence of clay mineral platelets in various orientations or state of compaction), dissolution pores (from the dissolution of carbonate minerals) and organic matter pores (resulting from out-migration of hydrocarbons). Pores vary in size, and from location to location, but generally range from tens or hundreds of nm to as much as 1 µm or more. Based on these observations, we interpret the organic matter pores to be the dominant contributor to hydrocarbon production in the Utica/Point Pleasant play.

10.6   Production Data and Trends

Since the Utica Shale play began in 2011, a significant drilling and production increase has occurred. By May 2014, approximately 1470 permits have been issued to drill horizontal wells to the Upper Ordovician Utica/Point Pleasant horizon, mainly in Ohio, but with approximately 245 in western Pennsylvania and 11 in the northern panhandle counties of West Virginia. In 2013 over 3.6 MMBbl oil and 100 Bcf gas were produced from 352 wells. These volumes represent 45% of the total oil and 58% of the total gas produced in Ohio, underscoring the importance and magnitude of this play. The total reported cumulative production for the Utica/Point Pleasant from 2011 through 2013 in Ohio was approximately 4.3 MMbbl oil and 115.3 Bcf gas from 352 wells.

A northeast-southwest trend of higher production is seen extending through Columbiana, Carroll, Harrison, Belmont, Noble and Monroe counties in the liquids-rich area. The 10 best producing wells were in Harrison, Belmont, Noble and Monroe counties. Results have been less encouraging to the north and west of these areas. Trumbull County has shown lower producing rates, consistent with recent announcements by BP and Halcon that they are terminating Utica drilling in this area. Thus far, drilling farther west in the updip portion of the oil window also has produced less encouraging results, as evidenced by nonproductive Devon wells drilled in Coshocton, Knox, Medina, Wayne and Ashland counties. A northeast-southwest trend separating the oil window from the gas window is visible from GOR mapping of quarterly production data.

10.7   Resource Assessments

Using a probabilistic (USGS-style) method, we have calculated the Utica Shale play to contain mean, technically recoverable resources of 1960 MMbo and 782.2 Tcf gas. Using a volumetric method, it was determined that original oil-in-place is approximately 82,903 MMbo while the

original gas-in-place is approximately 3192.4 Tcf. Based on the results of both assessment methods, it is expected that given current technology the play-wide oil recovery factor will be approximately 3% and the gas recovery factor will be approximately 28% in the "sweet spot" areas (Figure 9-8).

11.0   REFERENCES CITED

Note: Links are considered live as of access date; some links may become disabled after time

Advanced Resources International, Inc., 2008, Optimal Development of Utica Shale Wells: Arlington, Virginia, 29 p.

Advanced Resources International, Inc., 2012, Coal and Shale Property Database: Arlington, Virginia, Report Number DE-FE0001560-6, Task 6.7 (DE-FE0001560), 18 p.

Antero Resources, 2013, Antero press release: [http://investors.anteroresources.com/files/doc_news/2013/Antero-Resources-Reports-Second-Quarter-2013-Financial-Results_v001_i03b3o.pdf], 16 p., accessed April 30, 2014.

Boggs, Sam, Jr., 2006, Principals of sedimentology and stratigraphy (4th ed.): Upper Saddle River, New Jersey, Pearson Prentice Hall - Pearson Education, Inc., 662 p.

Bohacs, K.M., 1998, Contrasting expressions of depositional sequences in mudrocks from marine to non marine environs, *in* J. Schieber, W. Zimmerle, and P. Sethi, eds., Shales and mudstones, Vol. 1 – Basin studies, sedimentology, and paleontology: Stuttgart, E. Schweizerbart'sche Verlagsbuchhandlung, p. 33-78.

Camp, W.K., Diaz, Elizabeth, and Barry Wawak, eds., 2013, Electron Microscopy of Shale Hydrocarbon Reservoirs, Memoir 102: Tulsa, Oklahoma, American Association of Petroleum Geologists, 260 p.

Charpentier, R.R., and T.A. Cook, 2010, Improved USGS methodology for assessing continuous petroleum resources, version 2: U.S. Geological Survey Data Series 547, 22 p. and program.

Chesapeake presentation, 2013, Investor presentation: [http://www.chk.com/investors/documents/Latest_IR_Presentation.pdf], 23 p., accessed May 7, 2014.

Clendening, J.A., and M.W. McCown, 1999, Swan Creek field: Potential giant develops in Tennessee: Oil & Gas Journal, April 19, 1999, p. 95-99.

Cluff, Robert, and Michael Holmes, 2013, Petrophysics of unconventional resources [course handbook]: PTTC Technology Connections, Rocky Mountain Region [workshop], Colorado School of Mines, January 31-February 1, 2013.

Cooney, M.L., 2013, The Utica Shale in Pennsylvania: A characterization of the Reedsville, Antes, Utica and Point Pleasant formations: Undergraduate Thesis, Allegheny College, Meadville, PA, 64 p.

Crain, E.R., 2013a, Special cases – Gas Shales, *in* Crain's Petrophysical Handbook: http://www.spec2000.net/17-specshgas.htm, accessed October 14, 2013.

Crain, E.R., 2013b, Shale volume from neutron density crossplot model, *in* Crain's Petrophysical Handbook: http://www.spec2000.net/11-vshnd.htm, accessed November 17, 2013.

Crain, E.R., 2013c, Water saturation from Simandoux method, *in* Crain's Petrophysical Handbook: http://www.spec2000.net/14-sws.htm, accessed November 17, 2013.

Dow, W.G., 1977, Kerogen studies and geologic interpretations: Journal of Geochemical Exploration, v. 7, p.79-99.

Finnegan, Seth, Bergmann, Kristin, Eiler, J.M., Jones, D.S., Fike, D.A., Eisenman, Ian, Hughes, N.C., Tripati, A.K., and W.W. Fischer, 2011, The magnitude and duration of Late Ordovician–Early Silurian glaciation: Science, v. 331, p. 903-906.

Gulfport Energy Corporation, 2013, Investor presentation: [http://files.shareholder.com/downloads/GPOR/2162620688x0x661649/42586D2E-22EB-43C7-B961-5034A1D28470/GPOR_InvestorPres_GPOR_InvestorPres_3Q2013.pdf], 51 p., accessed November 1, 2013.

Gulfport Energy Corporation, 2014, Investor presentation: [http://files.shareholder.com/downloads/GPOR/2162620688x0x661649/42586D2E-22EB-43C7-B961-5034A1D28470/GPOR_InvestorPres_GPOR_InvestorPres_4Q2013.pdf], 43 p., accessed April 30, 2014.

Harris, A.G., 1979, Conodont color alteration, an organo-mineral metamorphic index, and its application to Appalachian Basin geology, *in* Scholle, P.A., and P.R. Schluger, eds., Aspects of diagenesis: Society of Paleontologists and Mineralogists Special Publication 26, p. 3-16.

Herron, S.L., 1991, In situ evaluation of potential source rocks by wireline logs, *in* R.K. Merrill, ed., Treatise of petroleum geology: Handbook of petroleum geology, source and migration processes and evaluation techniques, American Association of Petroleum Geologists, p.127-134.

Hess Corporation, 2014, Howard Weil 42nd Annual Energy Conference presentation, March 24, 2014: [http://phx.corporate-ir.net/phoenix.zhtml?c=101801&p=irol-presentations], 25 p., accessed April 30, 2014.

Holmes, Michael, 2013, A petrophysical model to analyze unconventional shale gas and shale oil reservoirs: Petrophysics of unconventional reservoirs [workshop], February 1, 2013.

Jacob, H., 1976, Petrologie, Nomenklatur, und Genesis naturlicher fester Erdolbitumina: Comp. Ergazungsband Erdol u. Kohle 76, p. 36-49.

Jacob, H., 1989, Classification, structure, genesis, and practical importance of natural solid bitumen ("migrabitumen"): International Journal of Coal Geology, v.11(1), p.65-79.

Jacob, H., 1993, Nomenclature, classification, characterization, and genesis of natural solid bitumen ("migrabitumen"), *in* J. Parnell, H. Kucha, P. Landais, eds., Bitumens in ore deposits: Special Publication No. 9 of the Society for Geology Applied Mineral Deposits: Springer-Verlag, p. 11-27.

Jarvie, D.M., 1991, Chapter 11: Total organic carbon (TOC) analysis: Geochemical methods and exploration, source and migration processes and evaluation techniques: American Association of Petroleum Geologists, p. 113-118.

Jarvie, D.M., Claxton, B.L., Henk, F., and J.T. Breyer, 2001, Oil and shale gas from the Barnett Shale, Fort Worth basin, Texas: AAPG Annual Meeting, Program and Abstracts, p. A100.

Karacan, C. Özgen, 2003, Heterogeneous sorption and swelling in a confined and stressed coal during CO_2 injection: Energy & Fuels, v. 17, no. 6, p. 1595-1608.

Kirschbaum, M.A., Schenk, C.J., Cook, T.A., Ryder, R.T., Charpentier, R.R., Klett, T.R., Gaswirth, S.B., Tennyson, M.E., and K.J. Whidden, 2012 (rev. November 2012), Assessment of undiscovered oil and gas resources of the Ordovician Utica Shale of the Appalachian Basin Province, 2012: U.S. Geological Survey Fact Sheet 2012–3116, 6 p.

Kolata, D.R., Huff, W.D., and Bergström, S.M., 2001, The Ordovician Sebree trough: an oceanic passage to the Midcontinent United States: Geological Society of America Bulletin, v. 113, no. 8, p. 1067-1078.

Kump, L.R., and M.A. Arthur, 1999, Interpreting carbon-isotope excursions: carbonates and organic matter: Chemical Geology, v. 161, p. 181-198.

Landis, C.R., and J.R. Castaño, 1994, Maturation and bulk chemical properties of a suite of solid hydrocarbons: Organic Geochemistry, v. 22, p. 137-149.

Luft, S.J., 1972, Geologic map of the Butler quadrangle, Pendleton and Campbell counties, Kentucky: U.S. Geological Survey Geologic Quadrangle Map GQ-982, scale 1: 24,000.

Lunig, Sebastian, and S. Kolonic, 2003, Uranium spectral gamma-ray response as a proxy for organic richness in black shales – Applications and limitations: Journal of Petroleum Geology, v. 26, no. 2, p. 153-174.

MacQuaker, J.H.S., Keller, M.A., and S.J. Davies, 2010, Algal blooms and "marine snow": mechanisms that enhance preservation of organic carbon in ancient fine-grained sediments: Journal of Sedimentary Research, v.80, p.934-942.

MacQuown, W.C., 1967, Factors controlling porosity and permeability in the Curdsville Member of the Lexington Limestone: Lexington, Kentucky, Water Resources Institute, University of Kentucky, Research Report No. 7.

Magnum Hunter Resources Corporation, 2014, IPAA Oil & Gas Investment Symposium New York presentation, April 2014: [http://magnumhunterresources.com/Magnum-Hunter-Resources.pdf], 56 p., accessed April 30, 2014.

McDowell, R.C., ed., 1986, The Geology of Kentucky-A text to accompany the geologic map of Kentucky: Washington, U.S. Geological Survey Professional Paper 1151-H, 76 p.

Metzger, J.G., and D.A. Fike, 2013, Techniques for assessing spatial heterogeneity of carbonate $\delta^{13}C$ values: Implications for craton-wide isotope gradients: Sedimentology, v. 60, p.1405-1431.

Metzger, J.G., Fike, D.A., and L.B. Smith, in press, Applying C-isotope stratigraphy using well cuttings for high-resolution chemostratigraphic correlation of the subsurface, *in* L.B. Smith, ed., AAPG Bulletin Special Volume in Honor of Fred Read.

Meyer, B.L., and M.H. Nederlof, 1984, Identification of source rocks on wireline logs by density/resistivity and sonic transit time/resistivity crossplots: AAPG Bulletin, v. 68, no. 2, p. 121-129.

Ohio Department of Natural Resources, Division of Geologic Survey, 2013, Calculated % Ro average per well of the Upper Ordovician shale interval in Ohio (includes "Utica", "Point Pleasant", "Lexington", and "Logana": [www.ohiodnr.com/portals/geosurvey/energy/utica/ordov-shale_Ro_average_03-2013], 1 plate, accessed July 2, 2014.

Passey, Q.R., Creaney, S., Kulla, J.B., Moretti, F.J., and J.D. Stroud, 1990, A practical model for organic richness from porosity and resistivity logs: AAPG Bulletin, v. 74, no. 12, p. 1777-1794.

Patchen, D.G., and others, 2006, A geologic play book for Trenton-Black River Appalachian basin exploration: U.S. Department of Energy, Final Report, Contract No. DE-FC26-03NT41856, 582 p.

PDC Energy, 2014, Analyst Day presentation, New York, April 17, 2014: [http://files.shareholder.com/downloads/PETD/2762178579x0x744853/11BE17C5-86D9-4D38-8FB2-4CBE738DFC3D/2014_04_17_Analyst_Day_-_Final6.pdf], 96 p., accessed April 30, 2014.

Peters, K.E., 1986, Guidelines for evaluating petroleum source rock using programmed pyrolysis: AAPG Bulletin, v. 70, no. 3, p. 318-329.

Repetski, J.E., Ryder, R.T., Weary, D.J., Harris, A.G., and M.H. Trippi, 2008, Thermal maturity patterns (CAI and %Ro) in Upper Ordovician and Devonian rocks of the Appalachian basin: A major revision of USGS Map I–917–E using new subsurface collections: U.S. Geological Survey Scientific Investigations Map 3006, one CD-ROM.

Rex Energy, 2014, Corporate presentation: [http://files.shareholder.com/downloads/REXX/3079288293x0x744435/57e634ab-6cd7-41d1-a508-577cf54d8cab/Rex%20Energy%20Corporate%20Presentation%20-%20April%202014.pdf], 54 p., accessed April 30, 2014.

Riediger, C.L., 1993, Solid bitumen reflectance and Rock-Eval Tmax as maturation indices: an example from the "Nordegg member", western Canada sedimentary basin: International Journal of Coal Geology, v. 22, p. 295-315.

Riley, R.A., Erenpreiss, M.S., and J.G. Wells, 2011, Data compilation and source rock mapping of the Upper Ordovician black shale interval in Ohio: Ohio Department of Natural Resources, Division of Geological Survey, final report for the U.S. Geological Survey, U.S Geological Survey Cooperative Agreement No. 0020003512, 17 p.

Rodriguez, R., Crandall, D., Song, X., Verba, C., and D.J. Soeder, in press, Imaging techniques for analyzing shale pores and minerals; NETL-TRS-XX-2014; Technical Report Series; U.S. Department of Energy, National Energy Technology Laboratory: Morgantown, WV.

Ruppert, L.F., Hower, J.C., Ryder, R.T., Levine, J.R., Trippi, M.H., and W.C. Grady, 2010, Geologic controls on thermal maturity patterns in Pennsylvanian coal-bearing rocks in the Appalachian basin: International Journal of Coal Geology, v. 81, p. 69-181.

Schieber, Juergen, Southard, J.B., and K. Thaisen, 2007, Accretion of mudstone beds from migrating floccule ripples, Science, v.318, p. 1760-1763.

Schlumberger, 1997, Logging tool response in sedimentary minerals, Appendix B *in* Log interpretation charts: Houston, Texas, Schlumberger Wireline and Testing, p. B5-B6.

Schmoker, J.W., 1993, Use of formation-density logs to determine organic-carbon content in Devonian shales of the western Appalachian basin and an additional example based on the Bakken Formation of the Williston basin, *in* Roen, J.B., and R.C. Kepferle, eds., Petroleum geology of the Devonian and Mississippian black shale of eastern North America: U.S. Geological Survey Bulletin 1909, p. J1-J14.

Schoenherr, J., Littke, R., Urai, J.L., Kukla, P.A., and Z. Rawahi, 2007, Polyphase thermal evolution in the Infra-Cambrian Ara Group (South Oman salt basin) as deduced by maturity of solid reservoir bitumen: Organic Geochemistry, v. 38, p. 1293-1318.

Schumacher, G.A., Mott, B.E., and M.P. Angle, 2013, Ohio's geology in core and outcrop – A field guide for citizens and environmental and geotechnical investigators: Ohio Department of Natural Resources, Division of Geological Survey Information Circular 63, p. 182-186.

Senftle, J.T., Brown, J.H., and S.R. Larter, 1987, Refinement of organic petrographic methods for kerogen characterization: International Journal of Coal Geology, v. 7, p. 105-117.

Smith, L.B., 2013, Shallow transgressive onlap model for Ordovician and Devonian organic-rich shales, New York State: Unconventional Resources Technology Conference, Denver, CO, Unconventional Resources Technology Conference (URTEC).

Soeder, D.J., 1988, Porosity and permeability of eastern Devonian gas shale: SPE Formation Evaluation, DOI 10.2118/15213-PA, v. 3, no. 1, p. 116-124.

Swanson, V.E., 1960, Oil yield and uranium content of black shales: U.S. Geological Survey Professional Paper 356-A, 44 p.

Ting, F.T.C., 1978, Petrographic techniques in coal analysis, *in* C. Karr, Jr., ed., Analytical Methods for Coal and Coal Products: New York, Academic Press, v.1, p. 3-26.

Wickstrom, L.H., Erenpreiss, M.S., Riley, R.A., Perry, Christopher, and Dean Martin, 2012, Geology and Activity Update of the Ohio Utica-Point Pleasant Play, presentation by Ohio Department of Natural Resources, Division of Geological Survey at Ohio Oil & Gas Association Meeting, March 16, 2012.

Young, S. A., Saltzman, M.R., and S.M. Bergström, 2005, Upper Ordovician (Mohawkian) carbon isotope ($\delta13C$) stratigraphy in eastern and central North America: Regional expression of a perturbation of the global carbon cycle: Palaeogeography, Palaeoclimatology, Palaeoecology, v. 222, p. 53-76.

Utica Shale Play Book

The AONGRC's Utica Shale Appalachian Basin Exploration Consortium includes the following members:

Research Team:
WVU National Research Center for Coal and Energy, Washington University,
Kentucky Geological Survey, Ohio Geological Survey, Pennsylvania Geological Survey,
West Virginia Geological and Economic Survey, U.S. Geological Survey,
Smith Stratigraphic, and U.S. DOE National Energy Technology Laboratory.

Sponsorship:
Anadarko, Chevron, CNX, ConocoPhillips, Devon, EnerVest, EOG Resources,
EQT, Hess, NETL Strategic Center for Natural Gas and Oil, Range Resources,
Seneca Resources, Shell, Southwestern Energy, and Tracker Resources.

Coordinated by:
Appalachian Oil & Natural Gas Research Consortium at **West Virginia University**